Delta and fan morphologies on Mars as climate indicators

Utrecht Studies in Earth Sciences

ISSN 2211-4335

Utrecht Studies in Earth Sciences 042

Delta and fan morphologies on Mars as climate indicators

Germari de Villiers

Utrecht 2013

Faculty of Geosciences – Utrecht University

Examination committee
Prof. dr. Alexander Densmore
Faculty of Geography
Durham University, United Kingdom

Prof dr. Ernst Hauber
Institute of Planetary Research
German Aerospace Center (DLR), Germany

Prof. dr. Hans Middelkoop
Faculty of Geosciences
Utrecht University, The Netherlands

Prof. dr. Gian Gabriele Ori
International Research School of Planetary Sciences (IRSPS)
University of Annunzio, Italy

Dr. Tanja Zegers
European Space Research and Technology Centre (ESTEC)
European Space Agency, The Netherlands

These investigations were supported by the Netherlands Space Office (SRON/ALW) with the financial support from the Netherlands Organisation for Scientific Research (NWO).

ISBN 978 90 6266 336 1

Print and Layout by Proefschriftmaken.nl || Uitgeverij BOXPress

Delta and fan morphologies on Mars as climate indicators

De morfologie van deltas en puinwaaiers en klimaatreconstructie op Mars

(met een samenvatting in het Nederlands)

PROEFSCHRIFT

ter verkrijging van de graad van doctor aan de Universiteit Utrecht
op gezag van de rector magnificus, prof.dr. G.J. van der Zwaan,
ingevolge het besluit van het college voor promoties
in het openbaar te verdedigen

op donderdag 21 november 2013 des ochtends te 10.30 uur

door

Germari de Villiers

geboren op *28 februari 1983 te Pretoria, Zuid Afrika*

Promotoren
Prof.dr. S.M. de Jong
Prof.dr. P.L. de Boer

Co-promotoren
Dr. M.G. Kleinhans
Dr. G. Postma

Dedicated to Larry T. Taunton in loving memory

Contents

Summary

The surface of planet Earth has partly been shaped by water, but this is not the only planet in the solar system where this is the case: Mars also had liquid water early in its geologic history and perhaps also more recently. The exploration of Mars has been ongoing for over a century, but a major question remains - is there life? Discovering habitable conditions beyond our planet is an ancient idea that could perhaps be seen as more philosophical that scientific, but the significance of the discovery of life beyond the bounds of Earth is unquantifiable. This thesis approaches the fundamental question of life on Mars indirectly by investigating an important necessary condition: the presence of liquid water on the surface of the planet throughout its history.

The presence, duration and quantity of water on Mars remains an important research topic in planetary science. Large valley networks, regional outflow channels, and small-scale gullies confirm the presence of water on the surface during certain time periods in the past. However, the climatic history and evolution is poorly understood because reconstruction of the early climate is still uncertain. The overall objective of this thesis is to improve our knowledge and understanding of the quantity of water and its spatial and temporal extent on the surface.

Different landforms, including mainly deltas and other fan-shaped sedimentary deposits, as well as shallow-marine impact craters, are investigated in order to infer climate conditions at the time that these features were formed. By studying the geomorphology of landforms on Mars and comparing them to the geomorphology of similar landforms on Earth and in the laboratory, important features such as length of time of formation, initial water level (if any), and upstream conditions can be deduced; all of which may be used to interpret the climate history of the planet.

This thesis includes research on a) satellite observations of shallow-marine impact craters and of fan-shaped sedimentary deposits (the equivalent of 'field-work' on Mars), b) descriptions of terrestrial analogues for Martian alluvial fans in the Atacama Desert (real field-work on Earth), c) experimental laboratory work with emphasis on the creation of different types of deltas in crater lakes and with some terrestrial application to the study of river-morphodynamics during dam removal, and d) numerical modelling of sediment transport and formative processes for delta deposits on Mars, in order to deduce the length of time required to form these deposits and ultimately, to infer the climate conditions at the time of formation. The Martian surface was studied using remote sensing satellite data from ESA (European Space Agency) and NASA (National Aeronautics and Space Administration).

From the satellite observations of shallow-marine impact craters in selected regions, it is suggested that the duration of extensive oceans may have been limited. From the satellite observations of all fan-shaped sedimentary deposits on Mars, it is observed that distinctly different classes of deposits exist and that most of these deposits have morphologies indicating short formation times. From the description of terrestrial analogues for alluvial fans, it is proposed that Martian alluvial fans may have been formed predominantly by debris-flow events instead of by run-off. From the laboratory experiments in combination with numerical modelling, the author concludes that most delta morphologies on Mars were likely constructed by single, catastrophic flow events in which large quantities of water

flowed over the surface in short periods of time and created temporary hydrological cycles. This water was likely released from the permanent frozen ice layer beneath the surface by trigger mechanisms such as magmatism, volcanism and impact cratering, frequent events especially during early Mars history.

This thesis concludes that even though water has played a crucial role in shaping the landscape of Mars, there is limited evidence of a long-duration, stable hydrological cycle that could have supported long-lived oceans. The author favours a predominately cold and dry climatic history for the planet Mars, with intermitted pulses of hydrological activity that are capable of producing the observed fluvial landforms.

Samenvatting

Het oppervlak van de Aarde is in belangrijke mate gevormd door de werking van stromend water. De Aarde is niet de enige planeet in het zonnestelsel waar dat gebeurde; ook planeet Mars had vloeibaar water in zijn vroegste geologische periode en wellicht ook later. Mars wordt al meer dan een eeuw bestudeerd, maar een belangrijke vraag – was er leven – blijft vooralsnog onbeantwoord. Aan het huidige oppervlak van Mars zijn veel landvormen te zien ontstaan door stromend water. Deze landvormen zijn duidelijk zichtbaar op satellietbeelden van ESA (European Space Agency) en NASA (National Aeronautics and Space Administration). Delta's, puinwaaiers, rivierdalen en andere geulen op het oppervlak van Mars zijn tekenen dat er ooit water stroomde. Van het klimaat op Mars in het verleden is echter nog veel onduidelijk, met name wanneer er water stroomde, hoeveel, en hoe wijd verbreid.

Het doel van dit proefschrift is om inzicht te krijgen in de hydrologische geschiedenis van Mars. Hiervoor werden satellietbeelden gebruikt van inslagkraters in ondiepe zeeën en van delta's en andere waaiervormige afzettingen en deze werden vergeleken met onder andere aardse puinwaaiers in de Atacamawoestijn die model kunnen staan voor Martiaanse puinwaaiers. Door deze sedimentaire landvormen na te bootsen in het laboratorium en met simpele numerieke computermodellen door te rekenen werden de waterdiepte, levensduur en bovenstroomse condities afgeleid.

Uit dit proefschrift blijkt dat water weliswaar een belangrijke rol speelde in de vorming van deze Martiaanse landschappen, maar dat er nauwelijks bewijs is voor een langdurig actieve hydrologische cyclus. Daarentegen steunt dit proefschrift de hypothese dat de planeet Mars vooral een koud en droog klimaat had met sporadische hydrologische activiteit die de sedimentaire landvormen veroorzaakten die nu vanuit de ruimte te zien zijn.

"What is a geographer?" asked the little prince. "A geographer is a scholar who knows the location of all the seas, rivers, towns, mountains, and deserts. But he is not an explorer. It is not the geographer who goes out to count the towns, the rivers, the mountains, the seas, the oceans, and the deserts."

1 General Introduction

The study of planetary morphology began in 1609 when Galileo Galilei turned his telescope to the Moon. His first major discovery was that the Moon's surface is covered by mountains, and is not a perfect sphere as had been previously assumed. This discovery and the many to follow changed the world's perspective of the universe, and became the foundation upon which planetary science is built. Planetary science, and in particular planetary geology and geography, is the study of landforms and surface features on other bodies in our solar system. Mountains, valleys, impact craters, volcanoes, and many other morphological features have been identified on the surfaces of the Moon, Mercury, Venus, Mars, Titan, and also on other moons, dwarf planets, and asteroids. These morphological features have been studied on Earth for centuries, and by applying our understanding of landscape evolution on Earth, we can understand the evolution of the planetary surfaces of our neighbours in space. Likewise, by studying these morphological features on other planetary surfaces, we also improve our understanding of our own planet and the processes that have created, shaped, and modified its surface through time.

Numerous features that indicate the presence of water on the surface at certain points in time have been identified on Mars. However, the climate evolution and history are still poorly understood and reconstruction of the early climate is still uncertain, and most importantly, the quantity of water and its spatial and temporal extent on the surface is still unknown. The Martian surface is host to a large variety of landforms that are studied with the use of remote sensing satellite data, predominately from ESA (European Space Agency) and NASA (US National Aeronautics and Space Administration). In this dissertation, different landforms are investigated, including mainly deltas and other fan-shaped sedimentary deposits, and also including impact craters, in order to reconstruct the climate conditions when these features were formed. By investigating the geomorphology of landforms on Mars and comparing them to the geomorphology of similar landforms on Earth, in the laboratory, and in numerical modelling, important parameters that yield insight into the conditions at the time of formation of these landforms, can be deduced and used to interpret the climate history of the planet.

In the following sub-sections the remote-sensing techniques that enable surface studies of this kind are introduced. Next, a brief history of Martian geology and climate is given, including descriptions of some of the most common fluvial features that prove that water once flowed on the surface. This section provides background for the discussion about spatial and temporal quantity of water on Mars, which is the topic of this study. Following that, the two categories of surface landforms that are investigated in this dissertation are introduced. This includes shallow-marine impact craters and fan-shaped sedimentary deposits. Lastly, a short synopsis is given, illustrating the specific topics that are covered in the following chapters.

1.1 Remote sensing

Obtaining information about an object without making physical contact is referred to as remote sensing (Lillisand *et al.* 2007). Humans have not been to Mars yet, making traditional scientific methods such as field observations and measurements fairly challenging. Information on the surface morphology and minerals (Christensen *et al.* 2003; Neukum *et al.* 2004a; Jaumann *et al.* 2005; Yen *et al.* 2005; Carter *et al.* 2013), the atmosphere (Withers *et al.* 2012; Mahaffy *et al.* 2013), and even the sub-surface (e.g. Plaut *et al.* 2007; Watters *et al.* 2007; Beuthe *et al.* 2012) of Mars has been obtained through remote sensing with the use of robotic spacecraft such as orbiters and landers. Over forty robotic spacecraft have been sent to Mars in the last five decades and the majority of Martian data comes from instruments mounted on these platforms, both robotic ground-based spacecraft as well as orbiting satellites that continuously photograph and monitor the planet (Jaumann *et al.* 2002; 2007 and references therein). Roughly two-thirds of all spacecraft destined for Mars have failed without completing their missions. Some data are acquired with large telescopes from Earth and from orbit around Earth, but the resolution of these datasets is not feasible for comprehensive studies of the surface. Besides traditional visual photography and infrared spectrometry (product of passive sensors), other datasets are obtained through radar (radio detection and ranging) and lidar (light detection and ranging) instruments such as laser altimeters, usually by means of emitting electromagnetic radiation at different wavelengths (active sensors). Spacecraft that have successfully been sent to Mars by space agencies from different countries and regions include the pioneering Mariner spacecraft; the two Viking landers; the first rover, Pathfinder; the twin rovers Spirit and Opportunity; the Phoenix lander and more recently, Mars Science Laboratory; and a host of orbiters with different instruments designed to globally map the planet. At present, five missions are operating on the surface of or in orbit around Mars (Fig. 1.1).

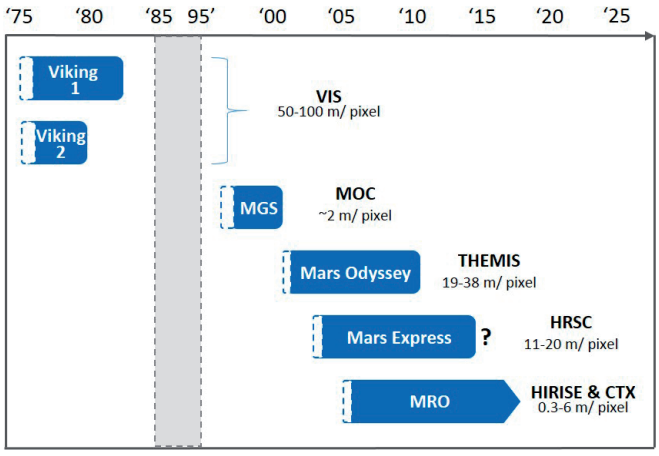

Figure 1.1: History of orbital exploration of Mars. Currently three orbital spacecraft are still operational.

The datasets used in this dissertation are primarily from the High Resolution Stereo Camera (HRSC), an instrument on board ESA's Mars Express spacecraft which has been in orbit

around Mars since December 2003 (Neukum *et al.* 2004b; Jaumann *et al.* 2007) and is still functioning to date. The datasets are available through the Planetary Science Archive (PSA), maintained by ESA and through the Planetary Data System (PDS), maintained by NASA. Other datasets used in this study include visual images from the Mars Orbiter Camera (MOC) on board NASA's Mars Global Surveyor spacecraft, the Thermal Emission Imaging System (THEMIS) on board NASA's Mars Odyssey spacecraft and the Context Camera (CTX) as well as the High Resolution Imaging Science Experiment (HiRISE) on board NASA's Mars Reconnaissance Orbiter spacecraft.

HRSC is a multi-sensor instrument comprising multiple line sensors, mounted in parallel to capture high-resolution stereo images of the surface. The average spatial resolution is 10 m per pixel and some selected areas are photographed at 2.3 m per pixel with the Super Resolution Channel (Neukum *et al.* 2004b; Jaumann *et al.* 2007). MOC is a narrow-angle camera that obtained high-resolution images (with a spatial resolution of typically 1.5 to 12 m per pixel) and a wide-angle camera for lower resolution context images (240 m per pixel) and global images (7.5 km per pixel; Malin *et al.* 2010). THEMIS is a multi-wavelength camera with a 5-wavelength visual imaging system (up to 18 m per pixel) and a 9-wavelength infrared imaging system (100 m per pixel; Christensen *et al.* 2004). CTX is a visual context camera with a 0.35 m focal length telescope (6 m per pixel) and HiRISE is visual high-resolution camera with a 0.5 m reflecting telescope (0.3 m per pixel resolution from 300 km height) with a higher resolution than most sensors that orbit the Earth. The data points that are provided on the surface by landers, and sometimes by their rovers, are useful for providing a source of ground truth with which to compare and evaluate the quality of the satellite data. Typically there is a very good agreement between surface measurements and observations from orbit. Ground truth is used for sensor design, calibration and validation.

Terrestrial observation of surface morphology is becoming increasingly more popular with the greater availability of easily accessible, high-quality satellite imagery through online geographical information programs such as Google Earth. The resolution of the imagery is generally around 15 m per pixel, depending on the quality of the satellite data, which comes from a variety of sensors in orbit around the Earth, including Landsat – the oldest, ongoing Earth-observation program which was launched by NASA in the early seventies; and ASTER (Advanced Spaceborne Thermal Emission Reflection Radiometer) - a Japanese sensor on board NASA's Terra satellite launched into orbit in 1999. NASA's Shuttle Radar Topography Mission (SRTM) provides topographic data with a vertical resolution of 10-16 m (Falorni *et al.* 2005). The study of geomorphological features on other planetary bodies would not be possible without the ability to describe, measure, and document landforms from a distance. The various remote sensing techniques are key to our observation and understanding of planetary surfaces.

1.2 Martian history

Mars has a complex climate history that is not completely defined, and reconstructions of the climate on early Mars are uncertain at best (e.g. Baker 2001; Carr and Head 2010; Lasue *et al.* 2012). The current climate on Mars is cold and dry, but the question is whether this has been the case throughout the history of the planet. Mars was formed along with the rest

of our solar system at around 4.6 Ga b.p. (before present) and is thus believed to be of the same age as the Earth. Based on crater density, three geological time periods, characterized by different dominant processes, have been defined: the Noachian Period – named after type location Noachis Terra and ranging from ~4.1 to ~3.7 Ga, the Hesperian Period – named after Hesperia Planum and ranging from ~3.7 to ~3.0 Ga (the end of the Hesperian is somewhat disputed based on different crater counting methods), and the Amazonian Period – named after Amazonis Planitia and ranging from ~3.0 Ga to present (Fig. 1.2; Hartmann and Neukum 2001; Carr and Head 2010). Scientists assume that comets and asteroids strike all regions of a planetary body at approximately the same rate over a given time span and thus the crater density of a planetary surface indirectly indicates the relative age of that surface (Hartmann 1977). If a planet (or moon) is geologically active or has an atmosphere or hydrosphere, then processes such as volcanism, tectonics, weathering and erosion will partially or completely erase craters. The time it takes for a crater to be completely erased from the surface is referred to as the crater retention age (Hartmann 1966). On Earth the crater retention age is much shorter than on Mars due to the many active erosion processes on Earth. The Noachian Period follows the Pre-Noachian (of which very little is known, much like the terrestrial Hadean Eon; Fig. 1.2) and is associated with the Late Heavy Bombardment which has also been documented on the Moon and other planetary surfaces. Heavy resurfacing due to volcanic activity characterized the Hesperian Period, and the Amazonian Period is generally believed to have been largely geologically inactive, preserving numerous landforms on the Martian surface.

At present, surficial and near-surface water is present on Mars (Haberle *et al.* 2001; Solomon *et al.* 2005; McSween 2006; Kereszturi and Rivera-Valentin 2012). However, water in liquid form is not stable on the surface mainly due to the low pressure but also due to the low temperatures. The atmospheric pressure on Mars at present is significantly lower than that on the Earth (< 1% of mean sea level pressure) but this may not always have been the case. The loss of a primordial atmosphere has been described as resulting from loss of atmospheric particles due to impact processes (Melosh and Vickery 1989; Jakosky and Phillips 2001); neutron loss due to the weak gravitational field (Molina-Cuberos *et al.* 2001); or scouring by solar wind after the loss of the protective magnetic field that was present on early Mars (e.g. Russell 1978; Jakosky *et al.* 1994; Molina-Cuberos *et al.* 2001). A magnetic field would deflect most energetic solar radiation, preventing erosion and scouring of the upper atmosphere (Russell 1978; Jakosky and Phillips 2001). The Martian dynamo (responsible for the formation of the magnetic field) is believed to have ceased abruptly during the early Noachian (Lillis *et al.* 2008; Kuang *et al.* 2008; Fassett and Head 2011) exposing the atmosphere to being stripped away by a more active solar wind due to no protection from a global magnetic field (Jakosky *et al.* 1994). Both the impact frequency and the Martian dynamo activity ceased early in Martian history, and aqueous-features have been formed since, suggesting that Mars was able to retain part of its atmosphere despite these events.

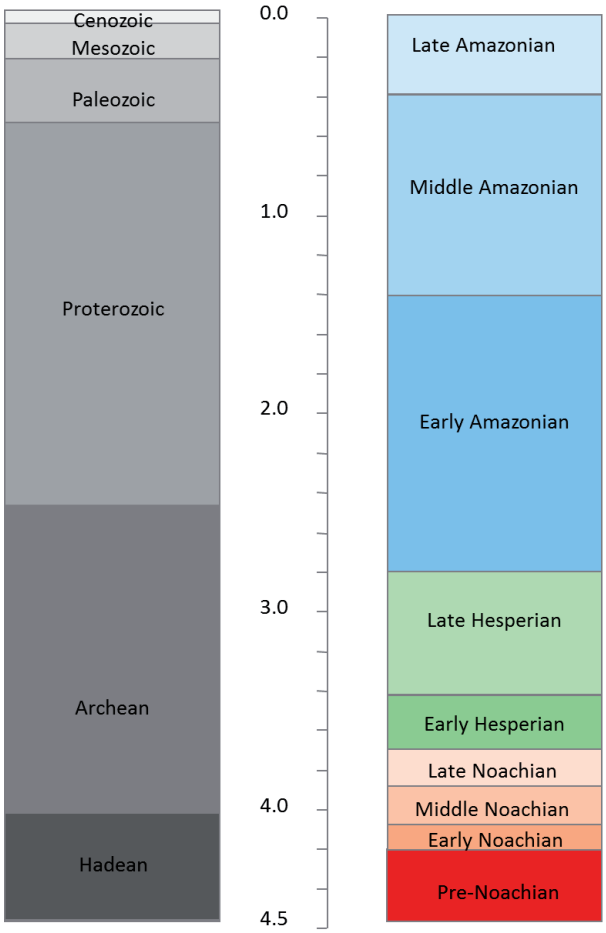

Figure 1.2: Martian chronostratigraphy (right) in comparison with that of the Earth (left). Age is given in Ga.

Water mainly occurs in a frozen state at the poles and right below the surface. It may be present as liquid groundwater further underneath the surface due to the Martian equivalent of geothermal heat flux (Baker *et al.* 2005). Water vapour in the thin Martian atmosphere largely escapes as a result of the low gravity field. At least four indicators of water on the surface have been described: a) the fluvial geomorphology and landforms that are produced during aqueous activity (Baker 2006); b) altered and evaporite minerals such as sulphates and haematite (Squyres *et al.* 2004; Paige 2005; Poulet *et al.* 2005; Wyatt and McSween 2006); c) the composition of Martian meteorites, containing traces of water-precipitated minerals such as carbonates and sulphates, most likely precipitated from saline liquid water (Gooding 1992; Leshin and Vicenzi 2006); and lastly, d) evidence of subsurface ice can be found in the presence of glacial landforms and unusual crater ejecta shapes caused by fluidization of ice and other subsurface volatiles (Wohletz and Sheridan 1983; Barlow and Perez 2003; Neukum *et al.* 2004a; Barlow 2005).

Geomorphological indicators of water include valleys, channels, gullies, alluvial fans, and deltas (Solomon *et al.* 2005; Baker 2006). Extensive valley networks formed during the

Noachian, regional outflow channels during the Hesperian, and small, local-scale gullies as recently as the Amazonian. Therefore it is certain that water has played an important role in the sedimentary history of the planet (Baker 1982; Carr 1983). Even though other options have been considered for the formation of valleys and channels on Mars (e.g. Sagan *et al.* 1973; Hoffman 2000; Leverington and Maxwell 2004; Leverington 2004; 2006), liquid water is still the most convincing in most cases (Carr 1983; Grant and Parker 2002). Indicators of flowing water are found all over the surface of the planet, but valleys and channels are more prevalent in the mid-latitude regions. This distribution was suggested to indicate that water might have once flowed from the higher southern latitudes to the lower northern latitudes, forming an ocean in the northern plains (e.g. Parker *et al.* 1989; Baker *et al.* 1991; Head *et al.* 1999; Fairén *et al.* 2003; Luo and Stepinski 2009; Fig. 1.3).

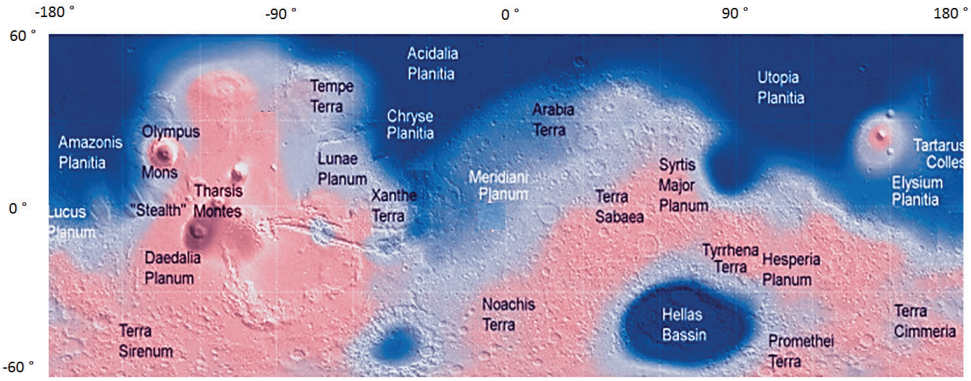

Figure 1.3: Geographic distribution of features and regions mentioned in the text. Type locations Noachis Terra, Hesperia Planum and Amazonis Planitia are also shown. The background shows the global topography over a MGS-MOLA shaded relief map with high altitudes in red and low altitudes in blue. [Image Source: Gasnault et al. 2010]

1.2.1 Valley networks

Extensive networks of valleys, originally termed run-off channels, cover the ancient, heavily cratered, southern highlands of Mars (Pieri 1980; Baker 1982; Carr 1983; Goldspiel and Squyres 2000; Gulick 2001; Luo and Stepinski 2009; Hynek *et al.* 2010). According to Solomon *et al.* (2005), there is evidence for interaction of liquid water with the Martian surface particularly during the Noachian Period, and Fassett and Head (2008) found that all valley networks in the southern, cratered highlands date from the Mid Noachian to the Early Hesperian.

These valleys are much like terrestrial ones in the sense that they have tributaries and that they start small and increase in width downstream, suggesting that the valleys formed as a result of erosion by streams (Carr 1983; Irwin *et al.* 2005). However, it has been shown that the drainage densities of the Martian valleys are much lower than those observed for terrestrial valleys (Baker 2001; Aharonson *et al.* 2002; Irwin *et al.* 2005), the drainage basins are small, suggesting that the system did not have time to become mature (Carr 1983); and the topographies of the drainage basins are immature and likely not constructed by

regular rainfall-fed overland flow (Aharonson *et al.* 2002). Based on morphology, it has been suggested by Pieri (1980) and others (e.g. Goldspiel and Squyres 2000; Baker 2001; Gulick. 2001; Aharonson *et al.* 2002) that groundwater sapping instead of overland flow was responsible for the formation of the valleys and that this may have been a regional instead of global process. Through numerical modelling based on terrestrial analogues, but modified to reflect Martian conditions, Goldspiel and Squyres (2000) showed that groundwater sapping does not depend on a warmer climate, but rather on high regolith permeability in combination with high water temperatures generated by the internal heat flux, both which can also exist under the current climate conditions. A precipitation-driven hydrological cycle is not stable under the current climate conditions of low atmospheric density and temperature, and therefore would imply a warmer, wetter Mars. Based on relative ages and on a lack of modification features, the proposed warm and wet climate seems to have ended abruptly at some point during the Early Hesperian (Howard *et al.* 2005; Fassett and Head 2008).

1.2.2 Outflow channels

Outflow channels have been observed at the surface along with valley networks, although stratigraphic relationships and crater counting suggest that these channels are younger than the valleys, primarily of Hesperian age (Sharp and Malin 1975; Carr 1983; Andrews-Hanna and Phillips 2007). The largest channels delivered discharge to the low-lying northern plains (Baker 1982; 2001; 2005), likely creating a temporary or sustained northern ocean (Parker *et al.* 1989; Baker *et al.* 1991). The outflow channels start abruptly, originating from broad areas of disrupted terrain, often termed "chaos region" or from a tectonic canyon (Sharp 1973; Nummedal and Prior 1981; Andrews-Hanna and Phillips 2007). Few, if any, tributaries are observed and their enormous size (several 10's to 100's of km in length) implies immense discharge, likely related to catastrophic flooding (Sharp and Malin 1975; Carr 1983). Burr (2011) and others (Baker and Milton 1974; Masursky *et al.* 1977; Baker 2009a) have suggested that a good terrestrial analogue for the Martian outflow channels is the Channelled Scabland of western North America, where catastrophic floods have spilled over the Columbia Plateau creating similar streamlined forms as those on Mars.

Some of the mechanisms that have been suggested for the release of large amounts of water in order to form the outflow channels include: geothermal melting of ice by impacts or volcanism (Masursky *et al.* 1977; Melosh and Vickery 1989; Howard *et al.* 2005), geothermal decomposition of hydroscopic clays (Clark 1978), liquefaction of water-rich sediments (Nummedal and Prior 1981), and breakout of water from confined aquifers under high pressure (Carr 1979, 1983; Andrews-Hanna and Phillips 2007; Bargery and Wilson 2011). Modelled peak discharges of 10^6-10^7 m^3s^{-1} were obtained for an outflow channel in Ares Valles with water volumes of 600-5000 km^3 (Andrews-Hanna and Phillips 2007).

1.2.3 Gullies

Small gullies on steep slopes (Malin and Edgett 2000; Dickson *et al.* 2007, 2009; Schon *et al.* 2009; de Haas *et al.* 2013) have been identified on Mars. These gullies are young, relatively small-scale (100's of metres in radial length), and mass-flow dominated. Hypotheses about their formation suggest either dry, granular mechanisms resulting from lower particle settling

velocities (Shinbrot *et al.* 2004), or a combination of groundwater seepage (Malin and Edgett 2000; Heldmann and Mellon 2004; Solomon *et al.* 2005) and surface run-off (Head *et al.* 2008). Small gullies usually are formed in crater walls and on steep dune faces, with a clear alcove and a depositional colluvial fan (Schon *et al.* 2009). The distribution of gullies is limited to mid-high latitudes (> 30°), more frequently in the southern than the northern hemisphere (Dickson *et al.* 2007).

The majority of gullies on Mars are difficult to date because the areas of individual gully deposits are too small for obtaining accurate ages on the basis of crater size-frequency distributions, but some have been dated at 1.25 Ma (Schon *et al.* 2009). Additionally, repeated satellite imagery of the same locations shows seasonal gully activity on present-day Mars (Diniega *et al.* 2010; Dundas *et al.* 2010) as modelled by Heldmann *et al.* (2005). Interpretations of gully formation include fluvial processes driven by melt water in the previous obliquity cycle (>400 ka) and by seasonal cycles of freezing and thawing of carbon dioxide in present-day climates (Hoffman 2002; Diniega *et al.* 2010; Dundas *et al.* 2010; Fassett and Head 2011).

In summary, the evidence for water on Mars is unequivocal. Aqueous activity was, and to some extent still is, present on Mars. The question is not if water was present on the surface but rather when exactly water was present and for what quantity, frequency, and duration. This question can be addressed by focusing on other Martian surface features indicative of water, such as shallow-marine impact craters and fan-shaped sedimentary deposits, as discussed in the sections to follow.

1.3 Shallow-marine impact craters

The formation of impact craters is one of the most common physical processes on solid planetary surfaces in the solar system and one of the most important physical features from which the evolution and composition of planetary surfaces can be deduced. Preserved craters are relatively rare on Earth, because weathering and other geological processes continuously obscure and remove them. Currently there are 184 confirmed impact crater structures (Earth Impact Database 2013) and approximately 550 probable and/or possible suspected impact craters (Suspected Earth Impact Sites Database 2010) on Earth. On Mars there are more than 42,000 known large crater structures (diameter greater than 5km). Due to significantly less atmosphere-surface interaction and the total absence of vegetation, the craters on Mars do not erode as fast as those on Earth. Mars is also much less geologically active than the Earth at present, and therefore it is not surprising that the crater population on Mars is much larger than that on Earth.

The physical conditions of planetary surfaces can be deduced from impact craters by looking at the morphology of these craters. A layer of water on the surface influences the shape of the final crater (Gersonde *et al.* 2002; Ormö *et al.* 2002), and thus the morphology of craters formed in sub-aerial environments differs from craters formed in sub-aqueous environments. Observations of Earth-based marine-target impacts as well as numerical modelling, show that the water column greatly influences the shape, size, and lithology of the resulting crater fill (Gersonde *et al.* 2002; Ormö *et al.* 2002, 2004; Senft and Stewart 2007). This gives impacts into sub-aqueous marine environments a substantially different

appearance from impacts into dry, sub-aerial targets. If the crater target materials are covered by a layer of water, the three-layer composition makes the morphology of the resulting crater even more specific, commonly resulting in an "inverted sombrero" shape (Collins and Wünneman 2005; Kenkmann and Schonian 2005; Horton *et al.* 2005, 2006). This inverted sombrero shape is an outer ring with a large, inward-sloping, annular surface surrounding a central uplift or central ring uplift, which may have a deeper inner crater within (Fig. 1.4).

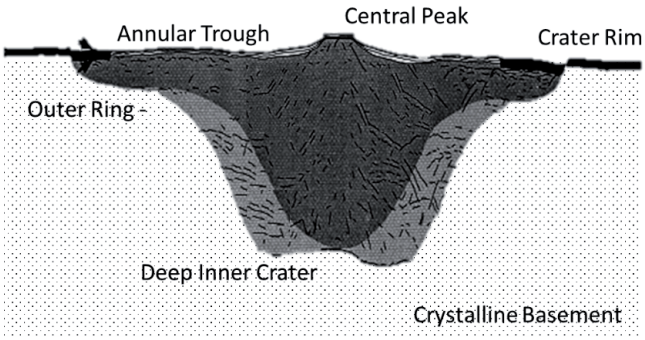

Figure 1.4: The inverted sombrero shape that is common for marine-target impact structures. It comprises an outer ring with a large, inward-sloping, annular surface surrounding a central uplift or central ring uplift, which may have a deeper inner crater within. [Image source: Tsikalas et al. (1998)]

The target rheology is also responsible for creating planes on which slump blocks can easily slide down, resulting in a larger crater with a wider annular trough (Collins and Wünneman 2005; Senft and Stewart 2007). This is the combined effect of the target being saturated and the water returning from outside the transient crater to the crater basin, either as a flow or as moving pore water exerting pressure. According to Artemieva and Shuvalov (2002), when a projectile enters an aqueous target, several events occur in the water column and on the seafloor, including a strong shock-wave, surge formation, and tsunamis. Sonett *et al.* (1991) have done both numerical and laboratory studies on impacts into ocean environments and concluded that at least two strong waves are generated upon impact, which can be responsible for the formation of surge and resurge waves as well as tsunamis. These events, combined with the stages of crater formation (contact and compression, excavation, and modification (Melosh 1980)), were used to formulate an idea of which morphologies could be expected for candidate shallow-marine craters on Mars (Ormö *et al.* 2004).

Regions on Mars where shallow-marine impact craters can be expected, include areas that fall roughly along the dichotomy (the sharp contrast between the rugged southern highlands and the relatively smooth northern plains), or more specifically along the shorelines proposed by Parker (1989), Head *et al.* (1999), Clifford and Parker (2001), and Fairén *et al.* (2003). Specifically, Arabia Terra, which is a broad, extensive plain through which two of the three proposed shorelines run (Parker 1989; Parker and Currey 2001) and where subaqueous sedimentary deposits have been proposed (Edgett and Parker 1997), is an ideal area to search for these features. Figure 1.5 shows the locations of shorelines of oceans early in Mars' history as proposed by Head *et al.* (1999) and Fairén *et al.* (2003).

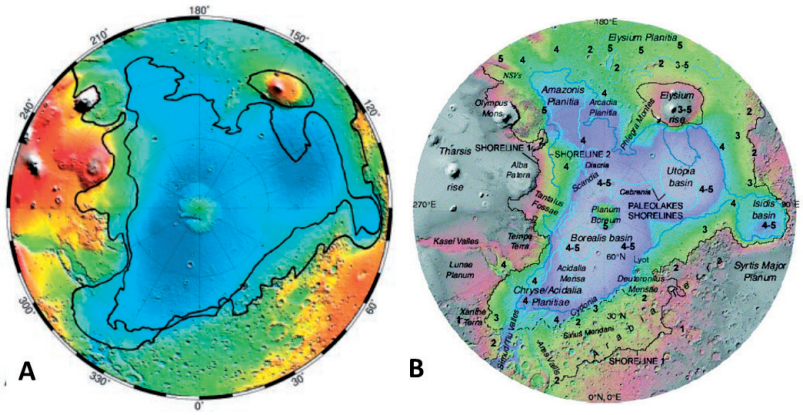

Figure 1.5: Locations of shorelines proposed by Head et al. (199) and Fairén et al. (2003) as viewed from the North Pole. Contact 1/Shoreline 1/Meridiani shoreline is indicated by the outer line, and Contact 2/Shoreline 2/ Deuteronilus is the inner line. [Image source: Head et al. (1999) and Fairén et al. (2003); MGS-MOLA]

In summary, if oceans existed for a significant period of time on the surface of Mars, there is a high probability that evidence of landforms associated with these oceans exists. If evidence of shallow-marine impact craters can be found, this may help to answer the question of how much water was present on the surface of Mars, and for how long.

1.4 Fan-shaped sedimentary deposits

Sedimentary landforms such as alluvial fans (e.g. Cabrol and Grin 1999; Howard *et al.* 2005; Moore and Howard 2005; Williams *et al.* 2006; 2011; 2013; Kraal *et al.* 2008a; Grant and Wilson 2011) and deltas (e.g. Ori *et al.* 2000; Malin and Edgett 2003; Howard *et al.* 2005; Irwin *et al.* 2005; Hauber *et al.* 2009; 2013; Di Achille and Hynek 2010) have been identified within impact craters and other basins on Mars, some of which were likely filled with water early in Mars' history (e.g. Cabrol and Grin 1999; 2001). Alluvial fans are formed where rivers enter wide plains (sub-aerially), and deltas are formed where rivers or alluvial fans enter lakes or seas (sub-aqueously), if the receiving basin environment is not able to re-distribute the sediment. Sediment thus is deposited where streams or rivers enter plains or lakes and where the gradient of the local topography changes significantly enough to decrease the velocity and sediment-carrying capacity of the stream (Bull 1968; 1977; Blair and McPherson 1994; Leeder 1999; Parker 1999). For plains and lakes much wider than the river, these deposits are fan-shaped as a result of discharge spreading out as un-channelized sheet flow or as a result of frequent radial shifts of channels avulsing over the delta plain.

1.4.1 Alluvial fans

In longitudinal profile, fans are usually concave, and in cross-sectional profile, mostly convex (Blissenbach 1954; Hooke 1967, 1987; Bull 1968, 1977; Lecce 1990; Leeder 1999). Alluvial fans are commonly found in arid and semi-arid environments, where sediment supply is fairly high. However, alluvial fans are also found in other regions such as humid, arctic, and alpine environments where sediment supply is high (Blissenbach 1954; Bull 1968, 1977;

Lecce 1990). Either sediment gravity flows or fluid gravity flows can be the dominant process on an alluvial fan, or a combination of the two (Blair and McPherson 1994; Volker *et al.* 2007). Gravity-dominated fan deposits are usually smaller, more episodic, and less well sorted than fan deposits dominated by run-off (e.g. Rachocki 1981; Blair and McPherson 1994; Collinson 1996; Leeder 1999). Fan-basin morphometric relationships show that small, steep, debris-flow fans are associated with small, rugged basins, and similarly, that large, low-gradient, fluvial-flow fans are associated with large, less rugged basins (Lecce 1990). A gradation exists between concentrated debris flows (47%–77% sediment concentration by volume), less concentrated water flows (sediment concentration <20% by volume), and hyperconcentrated flows (20%– 40% sediment concentration by volume; Costa 1988; Leeder 1999; Sohn *et al.* 2002). In mixed alluvial fans, where both processes operate, gravity flow tends to dominate in the upper parts of the fan and fluvial flow dominates in the lower parts, probably due to the greater mobility of fluvial flows (Moore and Howard 2005; Volker *et al.* 2007).

Martian alluvial fans have been identified at different scales, from short-range, sub-kilometre scale fans (e.g. in Promethei Terra, Schon *et al.* 2009; in Mojave Crater, Williams and Malin 2008) to long-range, multi-kilometre scale fans (as described by e.g. Moore and Howard 2005; Kraal *et al.* 2008a). Alluvial fans on Mars show gradients and morphometric relationships to their source basins (as observed from satellite imagery and/or calculated from digital elevation models) that are comparable to those of terrestrial alluvial fans (Garvin and Frawley 1998; Howard *et al.* 2005; Kraal *et al.* 2008a). Most alluvial fans exhibit a classical cone-shaped morphology with superposed ridges, oriented radially over the surface, and these fans have short and steep, or altogether absent feeder channels.

1.4.2. Deltas

Deltas differ from alluvial fans in that they commonly do not have prominent lobes in any direction and that their morphology reflects their partially sub-aqueous formation (Postma 2001). Deltas vary greatly in size, shape, and sediment type (Postma 1990) and based on these variables, Postma (1990) divided deltas into two types: coarse-grained, gravely fans, commonly referred to as fan deltas, and fine-grained, sandy to silty/clayey fans, referred to as river deltas. Fan deltas differ from river deltas mainly with regard to grain size and gradient (from these two variables it is possible to calculate discharge), and often also in size. Both fan deltas and river deltas form into standing water such as oceans and lakes, although fan deltas are usually more coarse-grained, steeper, and less extensive than river deltas (Leeder 1999). A major difference is that fan deltas are commonly fed by alluvial fans, whereas river deltas are fed by (large) rivers (Postma 1990). Gilbert-type deltas, as described by Gilbert (1890) in Lake Bonneville, have characteristic profiles with smooth delta plains and steep delta fronts, a clear indicator of the more or less stable water level and quiet conditions in the receiving basin. According to Postma (1990), a universal delta classification system should consider the nature of the feeder system, the depth of the water in the receiving basin, the processes at the river-mouth, and the diffusive modification processes driven by tidal, wave, and gravitational energy. Deltas on Earth can be classified into three groups based on the dominant processes (fluvial, tidal, and wave-related) in the system (Galloway 1975).

However, for deltas in crater lakes on Mars, the influence of wave-related (Kraal *et al.* 2006) and tidal processes (Moore *et al.* 2003; Weitz *et al.* 2006) should be minimal, and therefore we consider only the fluvial processes.

Martian deltas exhibit steep peripheral scarps at their outer margins (Irwin *et al.* 2005) and show architectural elements similar to terrestrial deltas, e.g. delta lobes, terraces in incised valleys, convex/concave delta-plain gradients, and incised delta fronts (Hauber *et al.* 2009). Undoubtedly, scarp deposits can also be erosional in nature and thus their occurrence alone cannot be used to infer formative processes. Obvious delta deposits on Mars are located where incised valleys occur directly upstream, suggesting once more that they formed in the same time period as (or merely slightly later than) the incised valleys, which have been dated as Late Noachian or Hesperian (Howard *et al.* 2005; Irwin *et al.* 2005; Mangold *et al.* 2012; Hauber *et al.* 2013). No clear distinction has been made as yet between fan deltas and river deltas on Mars, as has been done on Earth. All deltas on Mars are thus far assumed to be fan deltas.

1.4.3 Classification

Classification of Martian fan-shaped deposits is challenging due to the fact that similar fan-shaped deposits on Earth do not have a single, widely accepted, genetic classification system. Perhaps this is due to the many local variations in different parts of the planet, or perhaps due to the difficulty in observing and preserving structures related to vegetation and erosion on Earth. A broad classification system should ideally be based on the primary processes that are responsible for fan formation. However, fan morphology is usually not only affected by the primary processes that are involved in their formation, making it difficult to discern the primary processes from the secondary modification processes. The most important secondary processes that can modify the shape of the fan after deposition are groundwater, aeolian and fluvial reworking (Blair and McPherson 1994; Leeder 1999; Ventra *et al.* 2013). Due to the great amount of terrestrial deposits that have been modified by these secondary processes, it is challenging to design a simple classification system. Martian deltas, like Martian alluvial fans, exhibit no post-formation dissection such as expected from a decrease in run-off or a decrease in the basin water level (Howard *et al.* 2005; Irwin *et al.* 2005). Very few signs of post-formation modification are observed, and of course, no interference by vegetation cover. This makes Mars the ideal surface for drawing inspiration for a classification system for fan-shaped sedimentary deposits.

In summary, the fan-shaped deposits on Mars hold information about the climate conditions at the time of their formation. The volume of water and its spatial and temporal extent necessary for the formation of deltas differs from that which is needed to form alluvial fans. Even more importantly, the formation of a delta can only occur if the sedimentary system ends in a body of water. Thus, the scientific basis of this study is that the presence or absence of deltas is crucial in the understanding of palaeoclimate and climate change, and therefore it is important not only to understand the formation of fan-shaped deposits on the Martian surface, but also to determine whether they are alluvial fan or delta deposits. Three outstanding questions are to be answered for all fan-shaped deposits on Mars: a) whether the deposit is an alluvial fan or a delta; b) if it is an alluvial fan, whether it is dominated by

run-off or by debris-flow processes; c) whether deposition occurred as a single, catastrophic and short-lived event, or during multiple episodes as part of a continuous and long-lasting occurrence. A schematic flow-chart illustrates these three questions (Fig. 1.6).

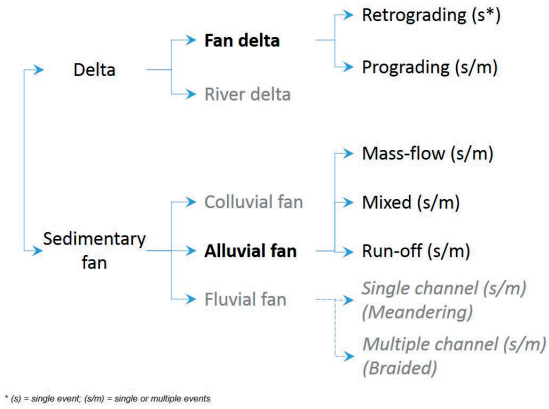

Figure 1.6: Tree diagram of all fan-shaped deposits, with highlights on those that are covered in this dissertation.

1.5 Synopsis

Valley networks, channels, gullies, alluvial fans, deltas, and other fluvial features on Mars clearly indicate the presence of surface water in the past. These and other geomorphological features contain information about the evolution of the planetary landscape, about the environmental conditions at the time of their formation, and about the quantity and quality of surface water that formed these features.

Specifically, we investigate Martian shallow-marine impact craters by comparing their morphologies to those of terrestrial shallow-marine impact craters, and we investigate Martian deltas and alluvial fans by looking at terrestrial alluvial fans in the field and deltas modelled in the laboratory and by addressing their formation in physics-based, numerical models.

The central objective of the study presented in this dissertation is to investigate the presence of water on Mars and to provide novel constraints on climate conditions at the time of formation: when and for how long water was present, to what extent water was present on a spatial scale, what geomorphologic forms were created as a direct result of its presence, and whether these forms are similar to geomorphologic features on Earth. An answer to this question is deduced from a) remote sensing and satellite observations of candidate shallow-marine impact craters and of fan-shaped sedimentary deposits, b) experimental laboratory work with emphasis on the creation of deltas in crater lakes and with terrestrial application to the study of river-morphodynamics during dam breaching or removal, c) numerical modelling of sediment transport and formative processes for fan-shaped sedimentary deposits, and d) descriptions of terrestrial analogues of alluvial fans and direct comparison to the morphologies found on Mars. The specific objectives per chapter are presented below.

Chapter 2 shows the work that has been done on the description and inventory of shallow-marine impact crater morphologies on Mars. In this chapter, the aim is to analyse

evidence of a northern ocean by comparing impact morphologies in Arabia Terra, an area on the crustal dichotomy, where ancient shorelines may have existed, to both other impact craters in the southern highlands on Mars as well as to terrestrial analogues such as the shallow-marine impact craters in Wetumpka, Alabama and Chesapeake Bay, Virginia (Poag 1997; King *et al.* 2002; 2006; Horton *et al.* 2006).

In chapter 3, the variety and spatial distribution of fan-shaped deposits on Mars is examined, using primarily the unique remote sensing data by Mars Express–HRSC to qualify and quantify the relations between different morphological parameters on the surface of fan and fan delta deposits as well as in the upstream and downstream areas immediately adjacent to the deposit. These features contain information about the duration and magnitude of surface water activity and about distinctive relationships between morphology and the conditions at the time of formation.

Chapter 4 systematically explores the relation of Martian delta morphologies with formative conditions in flume experiments in the Eurotank, a large laboratory basin equipped with photogrammetry producing high-quality DEMs for quantitative analysis. In particular, the focus is on how much water was released, whether the flow was episodic or sustained, and what the influence of the water level is on the delta morphology. Results are verified against terrestrial systems and the scaling between experiment and large-scale systems is addressed using verified models correcting for gravity by using non-dimensionless equations and by correctly scaling the flow parameters. Numerical models are used to explore the different scenarios for delta formation.

Chapter 5 describes a set of terrestrial coastal alluvial fans in the Atacama Desert with apparent similarities to some of the Martian alluvial fans based on satellite imagery. Surface morphology, sedimentology and stratigraphy are described, and this ground truth forms the basis of our interpretations of Martian alluvial fan formation. Early in this chapter a simplified, process-based classification is proposed, in order to facilitate the comparison between Martian fan-shaped depositional systems and their terrestrial analogues. Most importantly, this chapter aims to provide an alternative hypothesis for the formation of Martian alluvial fans, involving less run-off and more debris flows.

In chapter 6, the similarity of process between delta and fan creation and modification in closed or open (breached) basin lakes on Mars and dam creation and removal in active river systems on Earth is discussed. Sedimentary deposits in wide reservoir lakes record the sediment transport capacity of the upstream river and past water levels in the downstream basin, much like fan deltas on Mars. Results show that dam breaching or removal at wide lakes may lead to an inverse relation between discharge and erosion of the deposit, which has consequences for the subsequent sediment pulse magnitude, which in turn directly affects downstream construction and ecology. Even though the experimental work is already discussed in detail in Chapter 4, this chapter highlights the terrestrial application of these experiments and their significance in settings that are somewhat closer to home.

Finally, chapter 7 provides a synthesis in the form of a general discussion and summary of the work in this dissertation, with conclusions from our observations, implications for other observations, and emphasis on the open-ended questions.

“What a queer planet!” he thought. “It is altogether dry, and altogether pointed, and altogether harsh and forbidding.”

2 Candidate Marine-Target Impact Craters on Mars

Based on:
de Villiers, G., King, D. T., & Marzen, L. J. (2010). A study of candidate marine-target impact craters in Arabia Terra, Mars. *Meteoritics & Planetary Science*, 45(6), 947–964, doi: 10.1111/j.1945-5100.2010.01068.x.

Abstract - Previous workers have proposed that a northern ocean existed early during Martian geological history and the shorelines of that ocean would coincide roughly with the crustal dichotomy that divides the smooth, northern lowlands with the cratered, southern highlands. Arabia Terra is a region on Mars that straddles the crustal dichotomy and several proposed shorelines are located in the area. Shallow-marine impact craters on Mars likely would exhibit features like those on Earth, including characteristic morphological features that are distinctly different from that of craters formed on land. Common attributes of terrestrial marine impact craters include features of wet mass movement such as gravity slumps and debris flows; radial gullies leading into the crater depression; resurge deposits and blocks of dislocated materials; crater rim collapse or breaching of the crater wall; a central peak terrace or peak ring terrace; and subdued topography (an indicator of both age and possible flood inundation immediately following impact). In this paper, these features have been used to evaluate craters on Mars as to a possible marine origin. This study used a simple quantification system to approximately judge and rank shallow-marine impact crater candidates based on features observed in terrestrial analogues. Based on the quantification system, 77 potential shallow-marine impact craters were found within an area bounded by 20°N and 40°N as well as 20°W and 20°E. Nine exemplary candidates were ranked with total scores of 70% or more. In a second, smaller study area, impact craters of approximately similar size and age were evaluated as a comparison and average total scores are 35%, indicating that there is some morphological difference between craters inside and outside the proposed shorelines. Results of this type of study are useful in helping develop a general means of classification and characterization of potential marine craters.

2.1 Introduction

Impact craters are the most common physical features on most solid planetary surfaces in the solar system and are one of the most important physical features from which the evolutionary history and composition of these surfaces can be deduced. Crater studies can provide important information about the geological history of planetary bodies in our solar system, and play a large role in understanding the properties of the target surfaces, their ages, and the physical conditions at the time of impact.

The physical conditions of planetary surfaces can be deduced from impact craters by looking at the morphology of these craters. One type of physical condition that is particularly important is surface water cover. A layer of water on the surface influences the shape of the final crater (Gersonde *et al.* 2002; Ormö *et al.* 2002), and thus the morphology of craters formed in sub-aerial environments differs from that of craters formed in sub-marine environments. This study explored the surface in an area on Mars previously suggested to have been a shallow continental shelf environment (e.g. Parker *et al.* 1989; Edgett and Parker 1997; Clifford and Parker 2001; Fairén *et al.* 2003; Ormö *et al.* 2004) by investigating Martian craters in that area, which may have formed in such a shallow-marine environment. Although it is believed that marine-target craters should exist on Mars and some craters have been identified previously as potential shallow-marine impact craters (Ormö *et al.* 2004), as yet there still is no catalogue of potential marine-crater candidates and large areas of continental shelf environment lie unexplored.

The influence of the target material composition is a common topic of research in impact studies and it may even be more important in shape determination than the properties of the projectile (Melosh 1989). Observations of Earth-based marine-target impacts as well as numerically modelling, show that the water column greatly influences the shape, size, and lithology of the resulting crater fill (Gersonde *et al.* 2002; Ormö *et al.* 2002; 2004; Senft and Stewart 2007). This gives impacts into marine environments a substantially different appearance from impacts into dry, sub-aerial targets. Impacts into sedimentary targets where sediments overlie basement rock generally exhibital two-fold rheology: a weak, volatile-rich upper layer, and a hard, crystalline lower layer. Impacts into soft, layered targets, such as unconsolidated sands, yield craters that are commonly larger, than impacts into solid targets such as crystalline bedrock, due to the differences in strength of the various layers that are present in the target material (Ormö and Lindström 2000; Ormö *et al.* 2002; Kenkmann and Schonian 2005; Senft and Stewart 2007). However, if the crater target materials are in turn overlain by a layer of water, the three-layer composition makes the morphology of the resulting crater even more specific, commonly resulting in an "inverted sombrero" shape (Collins and Wünneman 2005; Kenkmann and Schonian 2005; Horton *et al.* 2005; Horton *et al.* 2006). This inverted sombrero shape is an outer ring with a large, inward-sloping, annular surface surrounding a central uplift or central ring uplift, which may have a deeper inner crater within. In this scenario, the target rheology is also responsible for creating planes on which slump blocks can easily slide down, resulting in a larger crater with a wider annular trough (Collins and Wünneman 2005; Senft and Stewart 2007). This is a combined effect of the target being saturated and the water returning (either as a flow or as moving pore water exerting pressure).

Even though few marine impact craters are identified on Earth, it should be noted that exceptional preservation is required to confirm a marine origin. When seafloor craters are formed, their post-modification shapes are usually better preserved in aqueous environments due to rapid sediment burial preserving the shape of the crater (Ormö and Lindström 2000; Dypvik *et al.* 2004), hence most confirmed marine impacts are well-preserved examples. Table 2.1 lists the locations, diameters, and ages of 17 confirmed marine impact craters on Earth. This study focused on craters within a size range of 10 to 100 kilometres (km) in diameter. The spatial resolution of the topographic data determined the lower limit, whereas the upper limit is really an arbitrary cut-off. Note that most of the terrestrial analogues for shallow-marine impact craters fall within this range.

Table 2.1: Marine impact craters on Earth. Modified from Ormö and Lindström (2000) and Dypvik and Jansa (2003). The five impact craters that are primarily used as analogues in this study are printed in italics.

Crater	Locality	Diameter (km)	Age (Ma)
Avak	Alaska, USA	12	> 95
Chesapeake Bay	*Virginia, USA*	*85*	*35.5 +/- 0.3*
Chixulub	*Yucatan, Mexico*	*~180*	*64.98 +/- 0.05*
Eltanin	South Pacific	?	2 to 15
Gusev	Donets, Russia	3	49.0 +/- 0.2
Granby	Linköping, Sweden	3	470
Kaluga	Kaluga, Russia	15	380 +/- 5
Kamensk	Donets, Russia	25	49.0 +/- 0.2
Kara	Kara Sea, Russia	65	70.3 +/- 0.3
Kärdla	Hiiumaa, Estonia	4	455
Karikkoselkä	Läsi-Suomi, Finland	1.3	440 to 445
Lockne	*Östersund, Sweden*	*13.5*	*455*
Mjølnir	*Barents Sea, Norway*	*40*	*142 +/- 2.6*
Montagnais	Nova Scotia, Canada	45	50.5 +/- 0.76
Neugrund	Gulf of Finland, Estonia	20	535
Ust Kara	Kara Sea, Russia	25	70.3 +/- 2.2
Wetumpka	*Alabama, USA*	*7.6*	*81.0 +/- 1.5*

The selected area of study on Mars falls largely within north-western Arabia Terra with small sections in Acidalia Planitia and Chryse Planitia. The study area lies just above the equator on the central meridian line and is bounded by the 20°N and 40°N latitude lines as well as the 340°E and 20°E longitude lines. Arabia Terra is a large, flat region that straddles the crustal dichotomy. Average elevation is approximately 1 to 2 km below mean surface level. The study area comprises mainly the Noachis Terra geological unit which is Noachian in age (Tanaka *et al.* 2005). Two smaller geological units, Nepenthes Mensae (of Early Hesperian to Early Noachian age) and Vastitas Borealis (of Amazonian age) are also present within the study area (Tanaka *et al.* 2005). However, the fact that Arabia Terra is covered by a thin layer of fine-grained sand or silt, does not mean that it had to have been covered by water. It could have been volcanic (e.g. Hynek *et al.* 2003) or aeolian (e.g. Fassett and Head 2007). For the purpose of this study, assuming that a large sea once covered the northern lowlands early in its history (e.g. Parker *et al.* 1989; Clifford and Parker 2001; Fairén *et al.* 2003), water would have covered all areas north of the dichotomy, thus creating a shallow-water, continental shelf environment of varying width all along the dichotomy, maybe on more than

one occasion. On Earth, a continental shelf is an ideal setting for the preservation of shallow-marine impact craters because a seafloor crater is more likely to form in shallow water and in this setting rapid sedimentation is more likely to keep further erosional processes from destroying the crater geomorphology. Therefore, north-western Arabia Terra, which arguably could once have been part of a continental shelf, makes a suitable study area for shallow-marine impact craters.

2.2 Background

According to Artemieva and Shuvalov (2002), when a projectile enters an aqueous target there are numerous events that occur in the water column and on the seafloor, including a strong shock-wave, surge formation, and tsunamis. Sonett *et al.* (1991) have done both numerical and laboratory studies on impacts into oceanic environments and conclude that there are at least two strong waves generated upon impact, which can be responsible for surge and resurge formation as well as tsunamis. These events, combined with the stages of crater formation (contact and compression, excavation, and modification (Melosh 1980)), are used to formulate an idea of which target morphologies can be expected in shallow-marine craters.

Good terrestrial analogues formed in a continental shelf environment show well-preserved structures and features that are commonly preserved in detail. Some analogues were particularly useful in this study, and they include the large Chesapeake Bay (Horton *et al.* 2006) and Chicxulub (Collins *et al.* 2002) craters, the medium Lockne (von Dalwigk and Ormö 2001) and Mjølnir (Gudlaugsson 1993; Dypvik *et al.* 1996) craters, as well as the small Wetumpka impact crater (King *et al.* 2002; Tab. 2.1).

The Chesapeake Bay impact structure, currently buried beneath 150 to 400 m of post-impact sediments (Horton *et al.* 2006), is very well preserved but not visible from the surface. Collins and Wünneman (2005) modelled the Chesapeake impact event and concluded that the main factor responsible for the morphology of the crater is the variation in strength of the layers present in the target. Without this variation in strength amongst the layers, it is likely that the diameter of the Chesapeake structure would have been only half of the actual 85 km determined through seismic profiling (Collins and Wünneman 2005). Chesapeake Bay impact structure exhibits “inverted sombrero” morphology and the rim has been subject to large-scale collapse and slumping resulting in crater-wall failure (Poag 1997; Horton *et al.* 2006). Numerous extensional collapse structures are observed in the seismic profiles, resulting in radial enlargement of the crater (Poag 1997; Horton *et al.* 2006). Chicxulub is a well-preserved crater beneath a layer of sediments and the surge deposits are particularly well-preserved, including deposits of massive sands, debris flows, and collapse of the central peak into a peak ring (Dypvik *et al.* 2004; Kring 2005). Lockne impact crater contains very good examples of resurge gullies that have been associated with large-scale resurge flows (von Dalwigk and Ormö 2001). Four gullies, as well as several debris-flow units, have been described and the rim has been classified as breached in more than one location (von Dalwigk and Ormö 2001). Mjølnir impact crater is not exposed at the surface, but instead is located on the seafloor and presently covered by ~350 m of water and 50 to 400 m of sediments (Gudlaugsson 1993; Dypvik *et al.* 1996; Dypvik and Jansa 2003). The Mjølnir crater rim is characterized by terraces that are bordered by faults and possible gullies (Dypvik and Jansa

2003). This crater also exhibits the classic inverted sombrero morphology with inner and outer zones (Dypvik and Jansa 2003) and rotated fault blocks are found in the annular trough (Ormö and Lindström 2000). Wetumpka impact crater exhibits signs of intra- and extra-crater resurge deposits as well as a partially collapsed rim (King *et al.* 2002; 2006), which provided an avenue of marine resurge into the crater.

Based on the morphological characteristics observed in the terrestrial analogues mentioned above, several indicative characteristics that can be associated with shallow-marine impact craters have been identified. These include features indicative of wet mass movement (Dypvik *et al.* 2004), radial gullies (von Dalwigk and Ormö 2001), resurge deposits, collapsed rims, central terraces, and subdued topography (see de Villiers *et al.* 2007). These features are visible in high resolution orbital images and could therefore be used as key characteristics in the identification of Martian shallow-marine impact craters.

Wet Mass Movement (WMM) - Wet mass movement occurs when saturated sediment is mobilized, either in a brittle or ductile manner (Dypvik and Jansa 2003). Mass movement can occur at various rates, but most important in this study is the rapid movement of unconsolidated sediment as a result of weakness induced by saturation. Two types of mass movement are particularly important: slides, where the movement occurs in a well-defined plane; and flows, where the movement is more fluid in behaviour and of which the deposit shape is more rounded and continuous. A slump is a brittle slide where material moves downward as a parcel or unit, often with a backward rotation on a curved displacement surface (Kennett 1982). Listric and normal faults form as the result of this displacement. A debris flow is a ductile flow where particles chaotically move downslope in water-saturated sediment slurries while supported by cohesion strength (Kennett 1982). Slumps, or block collapse of rim material into the crater are indicative of weak or unconsolidated target material (Dypvik and Jansa 2003). Slump blocks are present in both Mjølnir and Chesapeake Bay crater structures, (Ormö and Lindström 2000) and slump flows, have been observed in both Chicxulub (Kring 2005) and Lockne (von Dalwigk and Ormö 2001) craters.

Radial Gullies (RG) - Resurge channels carved by sediment-loaded waters induced by violent floods are common in marine-target craters (Ormö and Muinonen 2000; von Dalwigk and Ormö 2001). Radial gullies have been observed in both the Lockne (Lindström *et al.* 1996) and Kamensk (Ormö and Lindström 2000) craters. Even though resurge gullies are expected to be one of the most distinctive characteristics of marine impact craters, they tend to occur only in deeper water where the water depth exceeds the projectile diameter (Ormö *et al.* 2002), hence are not expected to be that common in Arabia Terra, unless the shorelines were much higher than currently envisaged. The water depth at the time of impact for Lockne has been estimated at 1000 m (Ormö *et al.* 2002) and for Kamensk at 100 to 200 m (Ormö and Lindström 2000). Clearly very shallow water depths limit the potential for the formation of radial gullies.

Resurge Deposits (RD) - Deposits related to surge or resurge flows may form inside or outside of the crater, depending on the depth of the target water, the strength of the target material, and possibly the location of the crater with respect to the main direction of surge flow (Ormö

et al. 2007). Intra-crater terrain is the evidence of surge in the form of avalanches, slides, and slumps of mixed blocks inside the crater (Dypvik and Jansa 2003). Extra-crater terrain is the evidence of surge in the form of resurge sediments and mixed blocks outside the crater (Dypvik and Jansa 2003). As discussed by King *et al.* (2006), the "extra-structure terrain" observed at Wetumpka is likely a product of collapse of the rim in response to flow. Resurge deposits are more often water-rich debris flows and not slump blocks. Resurge deposits on Earth have been confirmed through drilling and fieldwork in combination with subsequent sedimentological description (von Dalwigk and Ormö 2001; King *et al.* 2006), but may be difficult to discern from satellite imagery. Due to the directional relationship between these two types of deposits and their depositional agents, they are kept in the same category and not grouped with features of wet mass movement.

Rim Collapse (RC) - Crater rims are usually tough features formed from crystalline bedrock. When craters form in sedimentary environments, the rims are not as pronounced or as strong. Often no remnant of a rim is visible due to large amounts of inward slumping (Dypvik and Jansa 2003). This is sometimes also referred to as structural rim failure. Structural rim failure may be due to instability of the rim or due to resurge activity (King *et al.* 2006). In fact, collapsed rims are usually associated with wet mass movement and resurge (Dypvik and Jansa 2003). However, wet mass movement can occur without a breach in the rim and is also observed without the presence of identifiable gullies.

Central Terrace (CT) - A central peak terrace or a peak ring terrace is a large structure in the centre of the crater, sometimes associated with equally flattened concentric rings (Dypvik and Jansa 2003). In smaller craters, a central pit (most likely the summit pit-type) may be present instead of a peak ring (Barlow 2010). Development of flat-topped central uplifts has been predicted by some studies (Gault and Sonett 1982) and could be an indication of a marine origin and that the structure has been buried under water for some time. Central terraces indicate long-standing water, potentially spanning from right after formation until the end of the oceanic phase (Gault and Sonett 1982; Dypvik and Jansa 2003).

Subdued Topography (ST) - Craters that exhibit subdued topography have little to no elevation of the rim above the surrounding topography. Subdued topography is indicative of the amount of erosion that has taken place since formation, and thus the amount of time that has passed. As erosion is often induced by water, it could also indicate that large amounts of water were present on the surface for an extended period of time (Ormö and Lindström 2000). If an ocean once existed in the northern lowlands on Mars, it could have occurred during the late Noachian, very early in Mars's history (Parker *et al.* 1989; Fairén *et al.* 2003), leaving plenty of time for the craters to become degraded and the surrounding topography to become subdued. Lack of an elevated rim is considered by Dypvik and Jansa (2003) to be one of the most distinctive features of marine impacts, yet it could also merely indicate age.

Note that none of the characteristics listed above can be used with certainty to imply a marine origin. Other processes may be responsible for generating similar features in different locations; for example, complex craters on Earth often show signs of slumping without

having formed in marine environments. Only evidence of deposition of marine sediments before and after the impact event, or drill cores proving the existence of resurge deposits, is conclusive evidence. However, if more than two of these geomorphic characteristics are observed, it is more likely that a marine origin can be implied.

2.3 Methods

This study employed datasets gathered by three different instruments: a) Mars Orbiter Laser Altimeter (MOLA) and b) Mars Orbital Camera (MOC), which were on board the Mars Global Surveyor (MGS) spacecraft, and c) Thermal Emission Imaging System (THEMIS) on board the Mars Odyssey spacecraft. The spatial resolutions of these datasets are substantially better than that of the Viking images, which previously were used in geomorphological studies of this nature. MOC images are generally at 2-10 meter/pixel resolutions when taken with the narrow angle camera (Malin *et al.* 1992) and THEMIS visual images generally have resolutions of around 20 meter/pixel (Christensen *et al.* 2002). For topography, a MOLA 128 meter/pixel base map from the Planetary Data System (PDS) was used.

All the expected characteristics listed above were observed, including: a) evidence of wet mass movement; b) radial gullies entering the crater from one or more locations on the crater rim; c) resurge deposits; d) evidence of rim collapse; e) central terraces; and f) subdued topography (examples shown in Fig. 2.1). From these observed features, six categories were constructed in a database of potential marine-target craters, including wet mass movement (WMM); radial gullies (RG); resurge deposits (RD); rim collapse (RC); central terraces (CT); and subdued topography (ST). These categories were weighted to reflect the relative importance of various characteristic features. Wet mass movement is an important, relatively indicative factor, and as such comprises 40% of the score. This includes 20% for evidence of slumping and 20% for evidence of debris flows. Radial gullies, though not as common

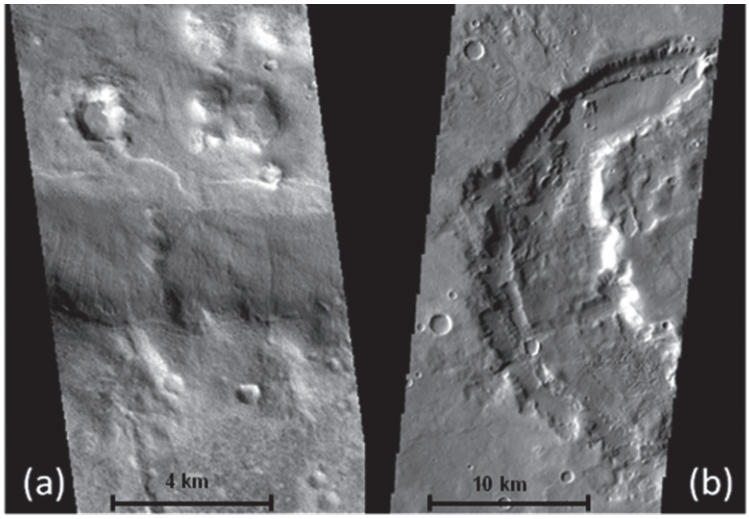

Figure 2.1: Examples of subdued topography and no elevated rim (a) (MOC image E0600102 located at 39°N; 359°E); as well as a central terrace and possible resurge deposits (b) (THEMIS image V12594005 located at 39°N; 11°E).

in shallow water as in deeper water, are also indicative and therefore comprise a further 20% of the score (one gully is 10%, and two or more gullies is 20%). Resurge deposits are more difficult to discern from orbital imagery, resulting in the factor only comprising 10% of the score. Rim collapse, central terrace, and subdued topography are all factors that are less indicative of a marine origin, or not necessarily related to a marine origin, and thus make up only 10% each of the total score. Wet mass movement is likely the most important characteristic, however, it should be noted that there are numerous ways of forming wet mass movement features and that these features do not only occur in shallow-marine environments.

This system makes it possible to approximately quantify the features observed and to rate each crater based on properties associated with terrestrial marine craters. Each candidate crater is assigned a total score and these values are used to rank and classify shallow-marine crater candidates.

2.4 Results

Four sets of analyses were done: a) a pilot analysis on earlier identified candidates to act as reference for subsequent sets; b) an initial analysis based on available MOC imagery for

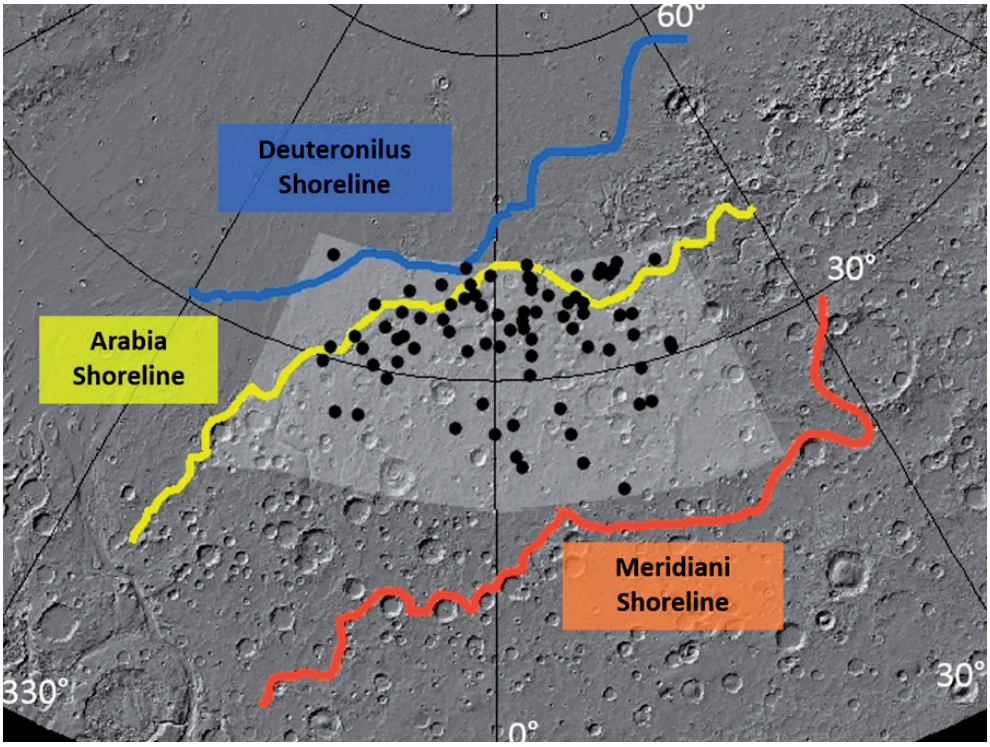

Figure 2.2: Locations of all potential shallow-marine impact craters of this study in relation to the three shorelines proposed by Parker et al. (1989) as well as Edgett and Parker (1997). Shorelines are labelled, and Meridiani shoreline is shown in light grey, Arabia shoreline is shown in white, and Deuteronilus shoreline is shown in dark grey. North polar projection hill-shade base map is from the USGS and is based on MOLA topographic data. Study area is indicated by the light grey quadrangle.

the study area (set A); c) a second analysis based on MOLA topography (set B); and d) a comparative analysis in an area slightly southeast of the Arabia Terra study area. The pilot analysis was done on the potential craters proposed by Ormö *et al.* (2004). All the results of the ratings for the first three sets are given in Table 2.2. Results of the comparative analysis are given in Table 2.3. All the crater candidate sites fall north of (within) the Meridiani shoreline (shown in light grey on Fig. 2.2) proposed by Edgett and Parker (1997) and discussed by Fairén *et al.* (2003), and only a few fall north of (within) the Noachian Arabia shoreline (original Contact 2 – shown in white; Parker *et al.* 1989; Fairén *et al.* 2003). The Deuteronilus shoreline (Parker *et al.* 1989; Fairén *et al.* 2003) is likely the result of a smaller, more recent Hesperian ocean and is indicated in dark grey. The location of this shoreline is largely outside the study area, which is indicated by the grey rectangle and can be seen to encompass a large part of the Arabia Terra continental shelf.

2.4.1 Ormö *et al.*'s candidate crater results

The four craters proposed by Ormö *et al.* (2004) as potential shallow-marine impact craters were rated first in the quantification system. The assigned total value is a number ranging from 0.0 to 1.0, reflecting the percentage confidence that a particular crater is of marine origin. A stacked histogram is plotted with all the variables shown as individual blocks (Fig. 2.3). Total scores range from 0.5 to 0.8 as even these prime examples do not exhibit all possible characteristics. Crater D is the most likely of the marine impact crater candidates proposed by Ormö *et al.* (2004) to be a shallow-marine impact crater with an assigned total score of 0.8. Five of six categories have features present in Crater D, and both slumps and flows are observed.

2.4.2 Results from Set A

In the database of MOC images in Arabia Terra there are 868 images that were taken during the period September 1997 to September 2005. Through thorough screening, 51 images of 40 candidate craters were identified as useful. Pertinent THEMIS images were subsequently downloaded for the 40 candidate sites to serve as context images.

Fifteen of the candidate craters were found to be too small (diameters <10 km) to fall within the population for this study and were thus discarded. The 25 remaining craters were divided into three groups based on size. These divisions were created because the size of the crater could affect the morphology of the crater (Dypvik and Jansa 2003), and as such an effective assessment of craters can only be done if similar craters are compared with each other. Small craters have diameters of 10 to 30 km, medium craters have diameters from 30 to 50 km, and large craters have diameters 50 to 100 km. These 25 shallow-marine crater candidates were rated for shallow-marine origin and plotted in Figure 2.3, with the craters clustered based on size. The first twenty craters are small (D = 10 to 30 km), the next four are medium size (D = 30 to 50 km), and the last one is large (D = 50 to100 km). It is evident from the data that the population is skewed to the smaller sizes. This occurrence is addressed in the next section. Scores range from 0.2 to 0.95 with an average of 0.52. The three highest ranked craters are Crater 6, Crater 17, and Crater 24, and all are small.

Table 2.2: Locations and total scores for all evaluated crater sites within the study area, including those of Ormö et al. (2004), as well as Set A and Set B.

Set	Crater	Location	Score	Set	Crater	Location	Score
Pilot	A	39°N 11°E	0.50	Set B	41	37°N 9°E	0.55
	B	39°N 11°E	0.60		42	38°N 14°E	0.50
	C	39°N 11°E	0.50		43	38°N 13°E	0.30
	D	39°N 359°E	0.80		44	38°N 10°E	0.40
Set A	1	39°N 4°E	0.60		45	36°N 8°E	0.70
	2	26°N 6°E	0.65		46	34°N 15°E	0.40
	3	34°N 8°E	0.65		47	32°N 14°E	0.60
	5	31°N 17°E	0.40		48	33°N 4°E	0.50
	6	35°N 9°E	0.70		49	36°N 1°E	0.40
	7	35°N 1°E	0.45		50	33°N 1°E	0.40
	8	35°N 3°E	0.50		51	36°N 3°E	0.60
	9	36°N 4°E	0.50		52	40°N 4°E	0.65
	12	35°N 13°E	0.40		53	34°N 355°E	0.45
	14	32°N 11°E	0.30		54	35°N 355°E	0.70
	15	31°N 3°E	0.60		55	36°N 359°E	0.70
	16	33°N 9°E	0.50		56	27°N 13°E	0.55
	17	37°N 6°E	0.70		57	23°N 7°E	0.30
	18	35°N 7°E	0.60		58	27°N 6°E	0.75
	19	39°N 4°E	0.55		60	31°N 351°E	0.30
	24	38°N 354°E	0.95		61	35°N 350°E	0.45
	25	39°N 341°E	0.55		62	35°N 352°E	0.20
	26	40°N 357°E	0.50		64	26°N 348°E	0.55
	27	33°N 357°E	0.40		65	37°N 357°E	0.50
	30	33°N 350°E	0.30		66	38°N 358°E	0.70
	32	37°N 350°E	0.40		68	26°N 346°E	0.40
	35	27°N 14°E	0.30		69	34°N 349°E	0.60
	37	30°N 14°E	0.30		70	31°N 347°E	0.30
	38	30°N 344°E	0.55		72	32°N 346°E	0.20
	40	32°N 4°E	0.60		73	24°N 2°E	0.10
					75	21°N 10°E	0.40
					77	38°N 18°E	0.50
					78	31°N 17°E	0.20
					79	26°N 2°E	0.10
					80	29°N 350°E	0.20
					81	33°N 359°E	0.40
					82	37°N 358°E	0.15
					83	36°N 355°E	0.20
					84	38°N 4°E	0.45
					85	28°N 359°E	0.35
					86	33°N 351°E	0.30
					87	32°N 352°E	0.55
					88	30°N 349°E	0.65
					89	26°N 0°E	0.10
					90	36°N 10°E	0.60
					91	34°N 3°E	0.30
					92	26°N 357°E	0.20
					93	35°N 347°E	0.50
					94	40°N 1°E	0.40

2.4.3 Results from Set B

Due to the high resolution of the MOC imagery and smaller field of view, much of the larger picture and context of the images are lost as the entire image footprint often lies within the crater. Candidates within the initial database are all relatively small, mostly ranging from 10 to 30 km in diameter. To expand this population a second search was completed, this time only by looking at the MOLA base map, which shows a larger regional context. From the second search, 48 additional potential candidates were identified. Candidate craters from Set B are larger in size and more similar to the potential candidates identified by Ormö *et al.* (2004).

Table 2.3: Locations and total scores for some crater sites further southwest of the study area (outside the proposed shorelines), evaluated as comparison to those that fall within the shorelines.

Crater	Location	Score
1	08.18°N 001.36°E	0.40
2	08.67°N 001.92°E	0.25
3	03.60°N 003.46°E	0.40
4	09.51°N 004.50°E	0.10
5	09.60°N 005.08°E	0.40
6	05.24°N 005.81°E	0.40
7	07.20°N 006.90°E	0.45
8	10.00°N 008.25°E	0.50
9	05.56°N 008.55°E	0.30
10	08.20°N 008.70°E	0.35
11	03.69°N 009.64°E	0.45
12	07.53°N 010.00°E	0.20
13	02.15°N 010.60°E	0.30
14	08.80°N 011.10°E	0.50
15	06.75°N 011.80°E	0.30
16	06.73°N 014.35°E	0.40
17	05.06°N 016.30°E	0.50
18	06.01°N 016.60°E	0.30
19	05.36°N 016.75°E	0.20
20	08.30°N 018.60°E	0.40

High-resolution datasets (both MOC and THEMIS) were downloaded for the new potential sites (165 images in total). The candidates in the second set were judged by the same system of quantification as those in the first and the results are shown in Figure 2.3. From Set B there are four small craters (D = 10 to 30 km), twenty-nine medium craters (D = 30 to 50 km), and fifteen large craters (D = 50 to 100 km). Total scores range from 0.1 to 0.75 with an average of 0.42. The highest ranked crater is Crater 58, with four craters (Crater 45, 54, 55, and 66) following closely. Crater 58 is large, but the other four top-rated craters are all medium in size.

The scale of the MOLA imagery and the large sizes of the craters made judging the second set of potential candidates challenging. The regional scale of the imagery means that the resolution is too low to judge individual features such as slumps and flows. In addition, for larger craters only small parts of the crater are covered by a single image, hence entire features cannot be seen and the context of features is lost. Available imagery does not sufficiently cover the potential sites to assign total scores with certainty, and therefore the average total scores are lower for the second set than for the first.

2.4.4 Exemplary candidates

From the 77 craters in the database, nine were chosen for further discussion based on ranking. Craters D, 6, 17, 24, 45, 54, 55, 58, and 66 have total scores of 0.7 or higher, and were the highest-ranking examples in this study. Most of these crater sites are discussed in more detail in the next section. All of these craters exhibit signs of slumping, rim collapse and subdued topography. Furthermore, 77% of these show signs of debris flows and resurge deposits, and 66% have radial gullies and/or central terraces. Pie-charts for the characteristics observed

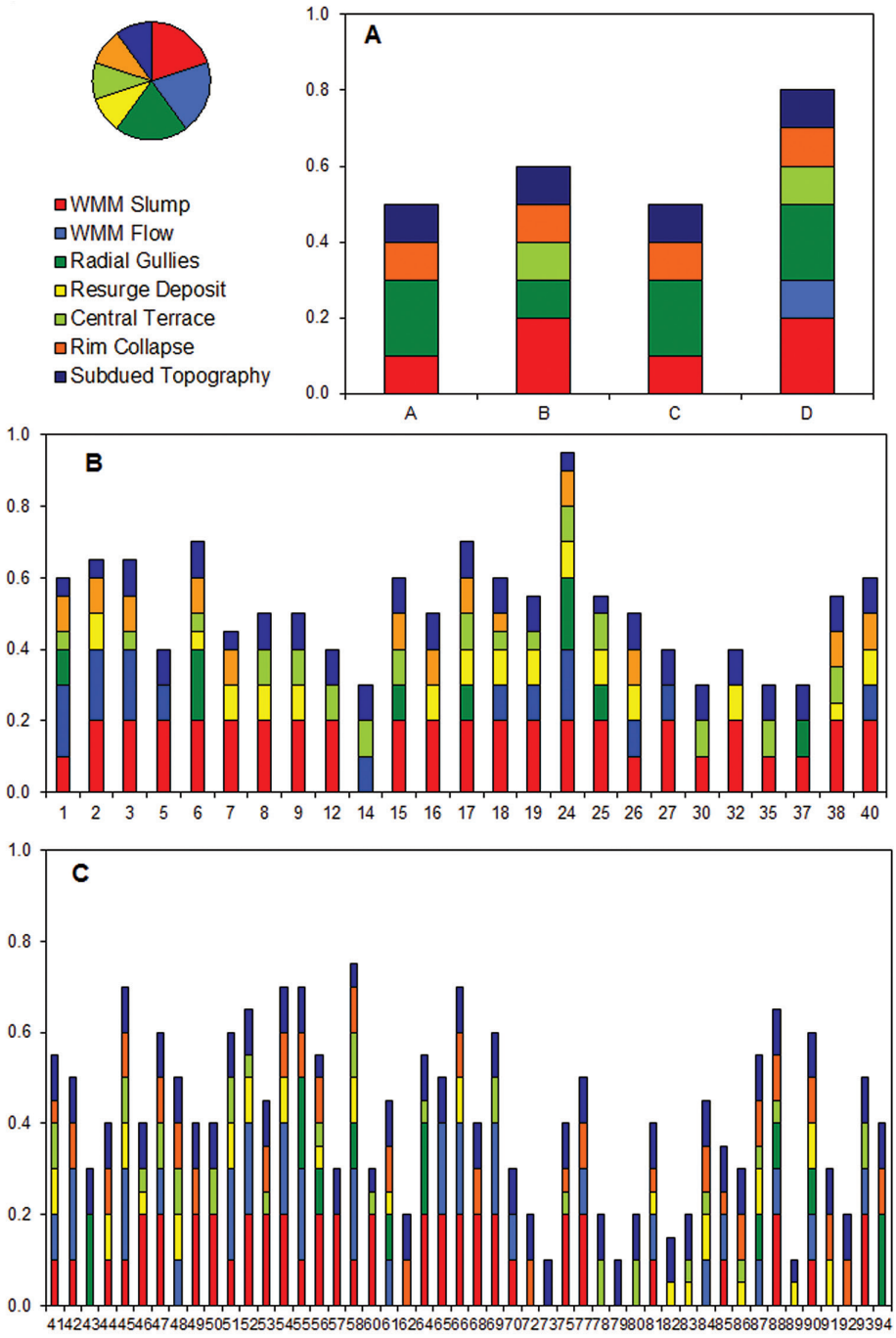

Figure 2.3: Stacked columns with individual contributions to the overall ranking or total value for (a) the four candidate Martian marine craters proposed by Ormö et al. (2004), (b) Set A craters, and (c) Set B craters. Note the weighted distribution of the six classes of shallow-marine crater characteristics including: wet mass movement (WMM), radial gullies (RG), resurge deposits (RD), rim collapse (RC), central terrace (CT) and subdued topography (ST). Wet mass movement is split into two sub-categories; slump (S) and flow (F).

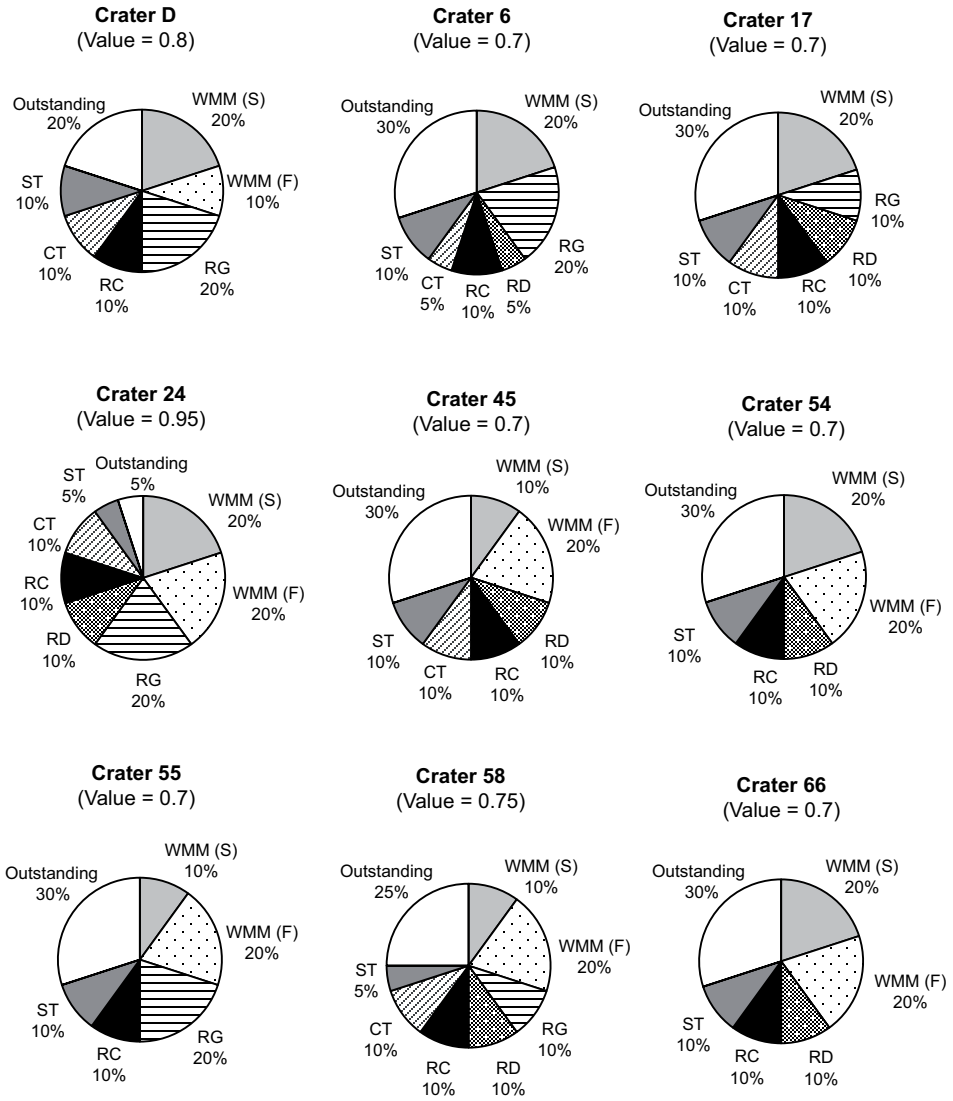

Figure 2.4: Breakdown of characteristics present in exemplary candidates. Total values are the sums of the percentages of present characteristics and are shaded or hatched. Outstanding values are the sums of absent characteristics and are shown in white.

in these craters are drawn in Figure 2.4. Wet mass movement is divided into two categories: slump (WMM-S) and flow (WMM-F). The sizes of the exemplary candidates range from 20 to 60 km in diameter, with most of the craters falling in the medium (30-50 km diameter) range. The average total score for Set A is 0.52 ± 0.15; whereas the average total score for Set B is 0.42 ± 0.18. Again, total scores within Set B are slightly lower than those in Set A due to the lower resolution of the MOLA data. The standard deviations for both sets are less than 0.2, indicating a grouping of total scores around the average values.

In impact crater studies, several physical parameters are used to describe impact craters, including the rim diameter and crater depth, two of the most important morphologic

elements of an impact crater (Stewart and Valiant 2006; Boyce and Garbeil 2007). The depth to diameter ratio is often a reliable indicator of the type of crater (i.e., the environment in which it was formed) and the extent of crater modification (Garvin *et al.* 2000; Aharonson *et al.* 2001; Boyce *et al.* 2005). Diameter may not change much during crater modification and can be used as a good estimate of original crater size, but in contrast, surface processes significantly influence crater depth over time (Boyce *et al.* 2005; Stewart and Valiant 2006; Boyce and Garbeil 2007).

Depths, diameters, and depth-diameter relationships were measured in this study. Common depth-diameter ratios for simple, terrestrial craters range from one-third to one-fifth, depending on the nature of the target material (Melosh 1989; Ormö and Lindström 2000). More particularly, $d = 0.29D^{0.93}$ for simple terrestrial craters, and $d = 0.15D^{0.43}$ for complex terrestrial craters (Grieve 1987) where d is the depth of the crater from the rim, and D is the rim-to-rim diameter, both in kilometres. Notice that complex craters are shallower than simple craters. While the transition between simple and complex craters on Earth is around 4 km, on Mars it occurs at around 7 km (Garvin *et al.* 2000). Garvin *et al.* (2000) found depth-diameter relationships for Martian polar and non-polar craters to be $d = 0.03D^{1.04}$ and $d = 0.19D^{0.55}$ respectively. For fresh, complex craters on Mars, this relationship has been defined as $d = 0.33D^{0.53}$ (Smith *et al.* 2001) or $d = 0.381^{0.52}$ (Boyce and Garbeil 2007) and ranging from roughly $d = 0.2D^{1.0}$ to roughly $d = 0.5D^{0.25}$ (Stewart and Valiant 2006). Depth-diameter ratios for Martian craters seem to decrease with an increase in latitude due to an increase in sub-surface volatiles and ice (Barlow 1993; Barlow 1995). Craters in Arabia Terra have a d/D ratio ranging from 0.07 to 0.09 (Barlow 1993; Barlow 1995). Modelling experiments suggest that marine-target craters should be wider than craters formed on land under similar conditions (Gault and Sonnett 1982) due to radial enlargement (Dypvik and Jansa 2003). Some processes have been suggested to be responsible for the widening of the crater, of which the most common are rim failures due to resurge or erosion by water currents or due to sediment instability. Boyce *et al.* (2005) concluded that low depth-diameter ratios suggest subsequent infilling by sedimentary deposits, thus supporting the theory of a large ocean depositing the Vastitas Borealis Formation (VBF) during the Late Hesperian/early Amazonian.

The accuracy with which these parameters are measured depends directly on the resolution of the MOLA data. Depths were measured by subtracting the average height of the crater floor (d_c) from the average height of the crater rim (d_r). MOLA topography is not continuous and the use of this dataset is prone to errors; however, four measurements were taken on the rim and another four just inside of it and these measurements were averaged to yield the best number. Table 2.4 lists the depths, diameters, and depth-diameter ratios (d/D ratios) as measured and calculated (predicted) for the exemplary candidates. Note that the d/D ratios range from approximately 0.01 to 0.03, which is much lower than the ratios of 0.07 to 0.09 measured for craters in Arabia Terra by Barlow (1993; 1995). Low depth-diameter (d/D) ratios could be an indication of age since older craters have rims that have been more eroded and crater shapes that are shallower due to sediment infilling (Craddock *et al.* 1997), or it could be a result of the difference in topographic data used for the measurements (Viking as opposed to MOLA). However, resurge deposits and post-impact sedimentation from the water column would fill the crater faster than craters on land, and could therefore

also be responsible for the low crater depths. Using the depth-diameter relationships defined by Garvin *et al.* (2000), one can estimate the depth by substituting the diameter (shown in Tab. 2.4). Crater D stands out as potentially anomalous with nearly an order of magnitude difference between the measured value and the estimated value. The remaining depths vary consistently with a factor around two, possibly due to differences in crater populations, e.g. faster rates of infilling for craters in shallow-marine environments.

Table 2.4: Physical parameters of exemplary candidates, as measured from MOLA data. All depths are negative, or below mean surface level. The last column gives the ratio between the predicted and measured depths.

	Rim depth, d_r (m)	Crater depth, d_c (m)	Measured depth, d_m (m)	Measured diameter, D (km)	Measured d/D ratio	Predicted depth, d_p (m)	d_p/d_m ratio
D	3599	3746	147	37	0.004	1384	9
6	2325	2874	549	26	0.021	1140	2
17	2022	2394	372	23	0.016	1066	3
24	3698	4375	677	21	0.032	1014	2
45	2152	2783	631	32	0.020	1278	2
54	3468	4135	667	36	0.019	1364	2
55	3411	4155	744	36	0.021	1364	2
58	1902	3051	1148	60	0.019	1806	2
66	3642	4387	745	32	0.023	1278	2

2.4.5 Comparative analysis

As a comparative study, a small area southeast of the study area was selected and 20 craters were evaluated using the similar high-resolution THEMIS imagery and the same ranking system. The selected area is located slightly southeast of the Arabia Terra study area, within 0°N to 10°N and 0°E to 20°E (Fig. 2.5). The average total score for this new set is 0.355 ± 0.1. Total scores in the comparative set are almost 20% lower than those of Set A, and almost 10% lower than those of Set B. Remarkably, the standard deviation is much less than for Sets A and B, indicating even more of a grouping of total scores around average values. The highest ranking crater in the comparative group received a score of 0.5. This is quite a high

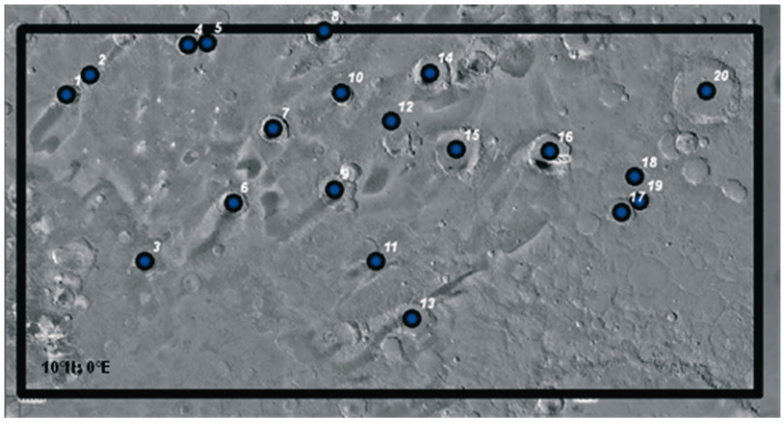

Figure 2.5: Locations of comparative craters and their spatial distribution. The study area is located from 10°N; 0°E to 20°N; 20°E.

score, since the craters in this comparative area should not have formed under water and should not exhibit shallow-marine crater features. It must thus be underlined once more that the characteristics used in our system of evaluation are not absolute and much remains to be discussed. Some features could be the result of other processes, and it is impossible to say with certainty whether certain deposits are truly resurge-related due to the lack of surface geological observations. This is merely the start of a possible way to quantitatively evaluate possible marine impact craters.

2.5 Interpretations

The shallow-marine impact crater candidate database contains the four craters identified by Ormö *et al.* (2004), 25 craters identified in Set A, and 48 craters identified in Set B. From this database, nine exemplary candidates were chosen and their locations relative to the proposed shorelines are shown in Figure 2.6. In this figure, the dark grey line represents the location of the Deuteronilus shoreline and the light grey line represents the location of the Arabia shoreline. The Meridiani shoreline runs further southeast and all candidate craters fall within its boundaries.

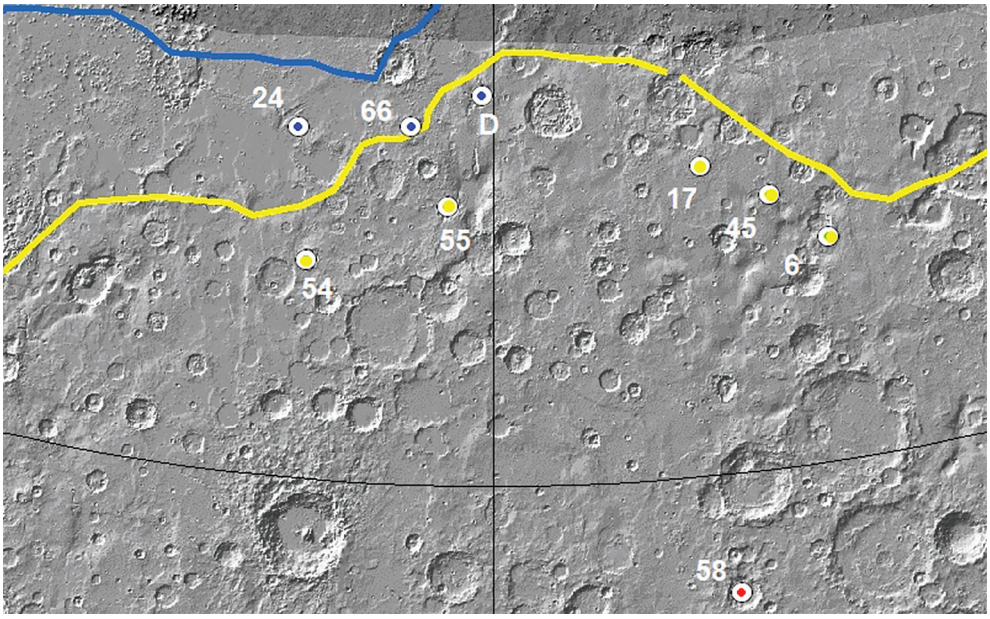

Figure 2.6: Locations of exemplary candidate craters and their spatial distribution relative to the Deuteronilus (blue) and Arabia (yellow) shorelines. Meridiani shoreline lies towards the southeast. Craters with blue dots correspond closely to the Deuteronilus shoreline and those with yellow dots correspond closely to the Arabia shoreline.

The exemplary candidate craters are divided into three classes based on total scores, sizes, and locations. Three of the nine craters fall in the type I group; a further five falls in the type II group; and one falls within the type III group. There seems to be a direct correlation between location of the crater and its rating. Type I candidates include well-developed, mostly medium-sized examples and are located in close proximity to the Arabia shoreline;

Type II candidates include typical examples of small and medium size and are located some distance away from the Arabia shoreline, in the direction of the Meridiani shoreline (Fig. 2.6). It is impossible to comment on the spatial distribution of Type III craters since there is only one large potential candidate. Based on the close proximity of the exemplary candidates to the Arabia shoreline, it seems more likely that this shoreline, instead of the Meridiani shoreline, was in fact the shoreline of an ancient Noachian Ocean. However, since the Meridiani shoreline does include all sites, it cannot be excluded as a possible shoreline at some point in Martian history. Additionally, even though most candidate sites fall outside the younger Deuteronilus shoreline, it is still possible that some marine craters may have formed in a more recent oceanic environment.

2.5.1 Type I candidates

Crater D - Ormö *et al.* (2004) originally identified Crater D as a potential marine-target crater, based on certain morphological features observed by looking at Viking imagery. Crater D is located at roughly 39.0°N and 359.0°E and well within the Meridiani shoreline as defined by Edgett and Parker (1997) and Fairén *et al.* (2003). Several MOC images draped over a MOLA base map in ArcGIS create layered, composite context images with high-resolution details. Of the potential marine craters suggested by Ormö *et al.* (2004), Crater D has the highest total score of 0.8. In Figure 2.7 (left), the radial gullies are the most remarkable features of this candidate crater (indicated by white dashed lines). One large gully enters the crater from the southwest and is likely responsible for the large resurge deposit (A) in the south-western section of the crater. Features of wet mass movement are also evident in both the form of slumping of the crater wall as well as the presence of debris flows, particularly in the southern part of the rim (B).

Crater D is roughly 37 km in diameter and hence falls in the medium class (30-50 km diameter). The depths between the surrounding topography and the bottom of the crater floor vary greatly, but average around 200 m. A north-south profile of Crater D is shown in Figure 2.8a. The d/D ratio was calculated to be 0.004, and even though low values are expected for marine craters on Mars, this value could be anomalously low considering that the average d/D ratio for the exemplary candidates is 0.02. As mentioned earlier in this chapter, low d/D ratios are indicative of old age and large amounts of sedimentation. Impacts into marine environments should exhibit more sediment infilling than impacts on land. Resurge and tsunami deposits could contribute largely to this rapid infilling; beyond regular fast rates of burial. From the profile shown in Figure 2.8a one can see the terraced central uplift and what seems to be a central ring. The subdued topography of the crater walls is clear on the northern rim. Also visible in the southern half of the profile is a terraced resurge unit, possibly deposited by a large gully entering from the southwest.

Crater 24 - Located at roughly 38.4°N and 354.0°E, and well within both the Arabia and Meridiani shorelines, Crater 24 has a total score of 0.95 – the highest ranking of all craters in the database. This crater exhibits all the characteristics, except that the topography is not as subdued as expected, casting some doubt on the age of this crater. Additionally, the presence of an ejecta blanket around the crater is indicative of a relatively young formative

age (Barlow 1990). Thus, even though the confidence rating is high, it is arguable that this crater did in fact form during the Noachian. However, due to the relatively close proximity of this crater to the younger Deutoronilus shoreline (of Hesperian age), one cannot exclude its potential marine origin.

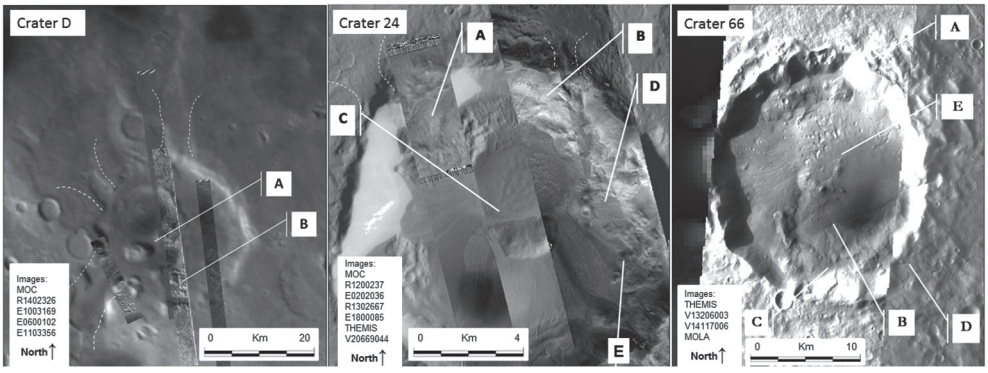

Figure 2.7: Examples of Type 1 craters. (Left) MOC narrow angle image overlay in detail for Crater D. Radial gullies are indicated by white dashed lines and resurge deposit A as well as mass movement deposit B is discussed in text. (Middle) MOC narrow angle image overlay in detail for Crater 24. Radial gullies are indicated by white dashed lines and resurge deposits (A), slump deposits (B), a central terrace (C), signs of rim collapse (D), and debris flows (E) are indicated through labels. (Right) THEMIS image overlay for Crater 66. Features A and B are slump and flow deposits, feature C is a collapsed rim, feature D is subdued topography, and feature E is a terraced central pit.

In terms of morphology, this candidate exhibits some good examples of the characteristics that are thought to be present in shallow-marine impact craters (Fig. 2.7; middle). Deposits that have a possible resurge origin are the most remarkable features of this candidate crater (A). Gullies seem to enter the crater from the northwest as well as the north-northeast (shown in white dashed lines) and are likely responsible for the large resurge deposits in both these areas. Large amounts of slumping can be seen around the crater rim (B), and though a central terrace is present in this crater (C), large amounts of post-impact sediments seem to cover most of the intra-crater terrain. In some places the rim has started to collapse (D). Debris flows dominate the eastern half of the crater (E). Some of the flows, particularly in the south-southeast, are much younger than the crater itself and are the result of subsequent draining into the crater. Large valleys can be seen in the south-southeast and these should not be confused with the flows related to the impact such as those further north.

Crater 24 is roughly 21 km in diameter (the smallest of the exemplary candidates) and hence falls in the small class (10-30 km diameter). The north-south profile of Crater 24 in Figure 2.8b shows that this crater is fairly deep and that the rim is still somewhat elevated above the surrounding areas. A thick sedimentary unit is visible in the southern half of the profile, and though it is possibly a resurge unit resulting from the gully to the south-southwest, it is impossible to exclude post-impact sedimentation from younger drainage systems. This resurge unit may be responsible for the low d/D ratio (0.03) calculated for this crater. Regardless of the fact the d/D ratio is low compared to that of other craters on Mars, it is still the highest d/D ratio measured in this study, indicating that this crater may be younger

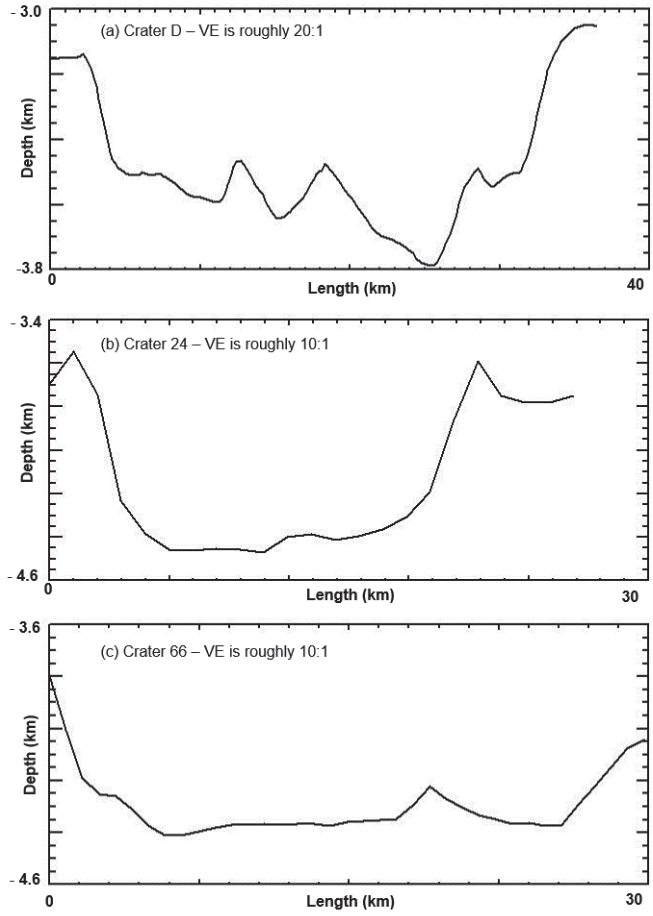

Figure 2.8: Profile views of three exemplary candidate craters (a-c) showing varying depth (km) with variation in length (km) along a profile from north (left) to south (right).

than the other exemplary craters. Again, this may indicate that Crater 24 is not of Noachian age, yet it could still be of marine origin and could have formed during the Hesperian period.

Crater 66 - Located at roughly 38.2°N and 357.5°E, Crater 66 lies within both Arabia and Meridiani shorelines, thus the probability that it formed in a marine environment is quite high. Crater 66 has a total score of 0.7. Particularly striking in Figure 2.7 (right) are the features of wet mass movement. Both slumps and flows are present, particularly near the southern and northern parts of the crater (A and B). This is in agreement with the general location of the crater in relation to the shoreline. According to paleogeography, the resurge waters would have entered the crater from the north and potentially affected the northern walls more severely than the eastern and western walls. The crater's wall has collapsed in the southernmost parts of the crater (C).

Topography in and around Crater 66 is subdued and the rim is hardly elevated above average surface height (see D in Fig. 2.7 (right)). The central pit, likely a summit pit (see

Barlow 2009; 2010), seems possibly to have been affected by resurge waters by having the entire northern half obliterated (E). Crater 66 is roughly 32 km in diameter and therefore falls in the medium class (30-50 km diameter). It has a low d/D ratio (0.02), which is average for this population of craters. A north-south profile of Crater 66 is shown in Figure 2.8c, in which slumping is evident, particularly in the northern parts of this crater. A topographic high is visible in the southern half, but this uplift is only the southern part of the eroded central pit. Resurge waters have likely completely eroded the northern part of the central pit. The sedimentary deposit directly north of this collapsed central pit could have formed as a result of water resurge from the north, leaving blocks of rim and other material on the crater floor. The location of the gully that may have dumped this sediment is uncertain, but the water may have been too shallow to allow gully formation. Depths between the surrounding topography and the bottom of the crater floor vary between 300 m in the south to 600 m in the north. This supports the observation of structural rim failure and subdued topography in the southern crater wall.

2.5.2 Type II candidates

Crater 6 - Crater 6 is located at roughly 35.3°N and 9.2°E and has a total score of 0.7. As seen in Figure 2.9 (left), slumping is evident all around the rim (A), but no debris flows are present. The central terrace is not well developed and may be covered in post impact sediments. A few small gullies are present (shown with white dashed lines), but they are not distinct and possibly even post-impact. It is mainly the rim collapse sedimentary deposit (B) in the northwest corner of the structure that indicates some resurge.

Crater 6 has a diameter of approximately 26 km and falls in the small class (10-30 km diameter). The d/D ratio for Crater 6 is approximately 0.02; around average again for the exemplary candidates. A north-south profile of Crater 6 is shown in Figure 2.10a, within which the terraced central uplift is the most prominent feature. Large slumps are present in the northern half of the structure and the subdued topography of the crater walls is clear on the southern rim.

Crater 54 - Located at roughly 34.9°N and 354.8°E, this crater has a total score of 0.7. Features of wet mass movement are evident in both the form of slumping of the crater wall (A) as well as the presence of debris-flow lobes (Fig. 2.9 (right)). A large well-developed debris-flow tongue (B) is visible in the north-northeast of the crater, and numerous smaller flows are also visible in the THEMIS images, however, some of these debris flows may be much younger than the crater itself. The crater rim is not elevated above the topography, and in some places, the rim has collapsed (C). No gullies are observed in this crater, and no central terrace is evident. Some structural blocks are found on the crater floor (D), possibly deposited as rim material being washed into the crater as the water returned.

Crater 54 is 36 km in diameter (very similar to Crater D) and hence falls in the medium class (30-50 km diameter). It is also close to Crater D in relative location. A north-south profile of this crater is drawn in Figure 2.10b. Depths between the surrounding topography and the bottom of the crater floor vary greatly, with a maximum of 1500 m. The central uplift and the subdued topography are the two features that are most evident from the profile. Some

slumping is apparent in the southern rim area and sediment fills the northern half of the crater, possibly induced by debris-flow activity.

2.5.3 Type III candidates

Crater 58 - Located at roughly 27.4°N and 6°E, Crater 58 is the farthest south of all of the exemplary candidates. It is in a class of its own because of its large size and because of its relative location to the shorelines and other candidates. It falls within the Meridiani shoreline, but is not even close to the Arabia shoreline, thus decreasing its chances of having formed in an oceanic setting. Crater 58 has a total score of 0.75. Despite its southern location, numerous indicative features are found in this structure. Figure 2.11 shows the resurge unit that enters the crater structure from the north (labelled A) and that has been subsequently modified and eroded. This is in accordance with the assumed age of the craters in this crater population. Radial gullies seem to enter the crater from a few different areas, mainly from the north (shown with white dashed lines). MOLA topography indicates a large low-lying area directly north of this crater, and the rim in this vicinity is totally collapsed. Rim collapse indicates resurge; and the relative location of the crater with respect to the proposed shorelines makes this a likely scenario. Features of wet mass movement (labelled B) are also present in both the form of slumping of the crater wall as well as debris flows, but these features are not well defined in this crater.

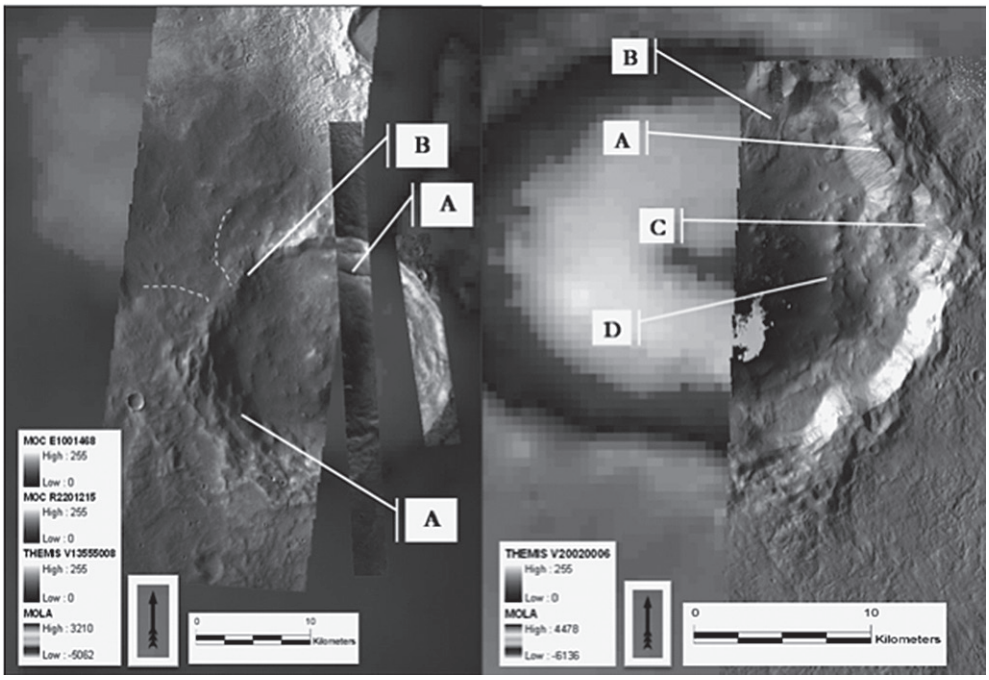

Figure 2.9: Examples of Type 2 craters. (Left) Crater 6 compiled from MOC and THEMIS image overlays. Features labelled A are slump deposits and the feature labelled B is a possible resurge deposit related to structural rim failure. (Right) Crater 54 with THEMIS image overlay. Features A and B are slumps and flows, respectively, feature C is a collapsed rim, and feature D refers to structural blocks that could be part of a resurge deposit.

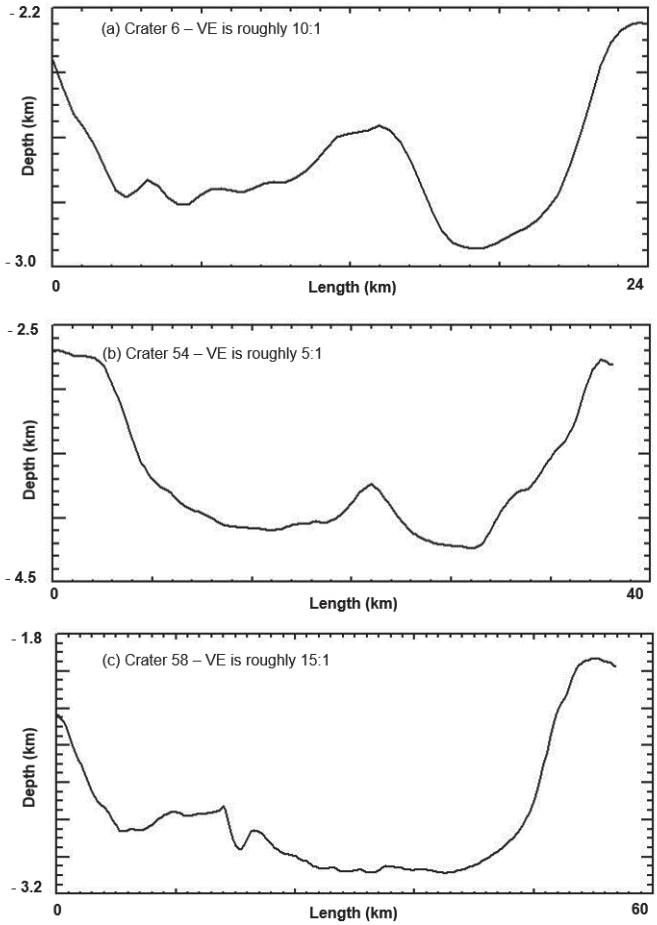

Figure 2.10: More profile views of exemplary candidate craters (a-c) showing varying depth (km) with variation in length (km) along a profile from north (left) to south (right).

Crater 58 is roughly 60 km in diameter and is the only exemplary candidate that falls in the large class (50-100 km diameter). The north-south profile view of Crater 58 (Fig. 2.10c) shows possible resurge deposits in the northern half of the crater where the rim is largely destroyed. This resurge unit could likely be responsible for the crater's low d/D ratio of around 0.02. The topography is subdued, particularly in the north.

2.5.4 Summary

Based on the quantification system designed in this study, nine craters were rated with total scores of 70% and higher and are subsequently classified as exemplary candidates. All of these craters exhibit signs of slumping, rim collapse and subdued topography. Furthermore, 77% of the exemplary candidates show signs of debris flows and resurge deposits and 66% have radial gullies and/or central terraces. Low depth-diameter ratio values were calculated for all of the exemplary candidates. The values may be anomalous, but low values are expected for such

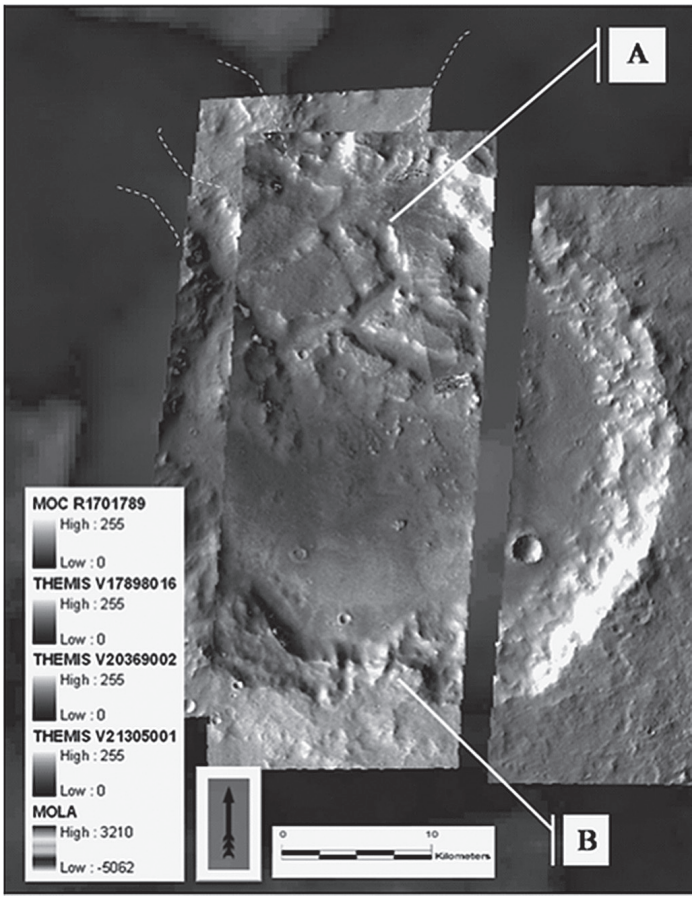

Figure 2.11: Example of a Type 3 crater (Crater 58) showing MOC and THEMIS image overlay on top of MOLA topography. Feature A is an extensive resurge deposit and feature B indicates various wet mass movement deposits. Positions of radial gullies are indicated by white dashed lines.

old craters, and even more so if a large amount of resurge deposition filled the crater shortly after formation. In a comparative study of craters in a nearby area, craters were rated with average total scores of 35.5%, indicating that some factors are clearly ambiguous; however, these scores are much lower than those for Sets A and B. This indicates that the morphology of craters inside and outside the proposed shorelines are indeed somewhat different.

2.6 Conclusions

This study found 77 impact craters in the area of Arabia Terra on Mars that potentially formed in a shallow-marine environment. These craters are identified based on high-resolution imagery data from Mars Orbiter Camera (MOC) and Thermal Emission Imaging Spectrometer (THEMIS), in combination with topographic data from Mars Orbiter Laser Altimeter (MOLA). The classification and ranking of these craters is based on the presence of certain morphological features identified from shallow-marine craters on Earth.

The exemplary candidates were classified into three groups or types. Type I includes well-developed, mostly medium-size examples located close to the Arabia shoreline; type II includes typical small and medium-size examples located closer to the Meridiani shoreline; and type III includes other large potential candidates. Based on the close proximity of more of the exemplary candidates to the Arabia shoreline, it seems more likely that this shoreline, instead of the Meridiani shoreline, was in fact the shoreline of an ancient Noachian Ocean.

The results of this study are useful in contributing to develop a general classification and characterization of potential marine craters. However, a few limitations should be considered: a) the images either show a large amount of detail with very little context, or good context but little detail; b) many of the features that have been listed as characteristics of shallow-marine impact craters can also be formed in other ways and are therefore not entirely predictive; and c) not much is known about the geomorphology of terrestrial shallow-marine impact craters, particularly from a remote-sensing point of view, and thus it is hard to compare terrestrial analogues with Martian examples.

This study concludes that some evidence for potential shallow-marine impact craters can be found on the surface of Mars as exemplified by Arabia Terra. However, initial comparative studies indicate that similar characteristics can be observed in craters that were highly likely not formed under water, further emphasizing the fact that these features only indicate a possible marine origin. The limited evidence of shallow-marine impact craters may be interpreted as the result of less temporally extensive oceans or in other words, oceans that were relatively more short-lived. Much work remains to be done on other study areas in and around the dichotomy boundary as well as in other areas where shallow-water impact events may have occurred.

2.7 Acknowledgements

Alabama Space Grant Consortium funded the majority of this study as a master's thesis through NASA's Experimental Program to Stimulate Competitive Research (EPSCoR). The authors would like to thank S. Stewart, N. Barlow, and an anonymous reviewer for much-appreciated, thorough reviews of this paper. Special acknowledgement goes to T. Hare, A. Jayakeerthy, G. de Villiers (not the author) and F. Bianchi for discussion and assistance with data processing. The thesis was published by G. de Villiers in December 2007 and is available on the internet at http://etd.auburn.edu/etd/handle/10415/1343. Authors acknowledge extensive use of MOC and THEMIS images that are available online.

“A rock pile ceases to be a rock pile the moment a single man contemplates it, bearing within him the image of a cathedral.”

3 Fan-shaped sedimentary deposits on Mars

Based on:
de Villiers, G., Hauber, E., Kleinhans, M. G., & Postma, G. (n.d.). Fan-shaped sedimentary deposits on Mars - morphology, classification, distribution, and implications for climate evolution (in preparation).

Abstract - Fan-shaped deposits on Mars have been identified in numerous studies, and being remarkably well preserved due the lower weathering rate on this planet, their morphologies can easily be mapped and quantified. They are important surface landforms that give indications of the environment in which they were formed. We suggest a simple, morphology-based classification system based on morphological parameters of the deposits and their immediate environments (upstream feeder channel and downstream depositional basin) in order to isolate the key processes that play a role during their formation. The three distinctly different groups include alluvial fans, retrograding fan deltas, and prograding fan deltas. We analyse the conditions that are responsible for their formation by addressing three factors: the amount of available discharge, by looking at the size and shape of the feeder channel; the available accommodation, by looking at the hypsometry of the basin; and the nature of the sediment supply, by looking at the global distribution, regional lithology and other factors that influence the amount and the character of the sediment. We conclude that discharge, sediment supply, and accommodation, are three factors that directly influence the morphologies of the fans and deltas. Based on morphology of the upstream feeder channel, the amount of discharge is inferred, and based on the character of sediment supply in the drainage basin, the ratio of sediment to water is inferred. The conclusions support the hypothesis that the early climate on Mars may not have been characterized by extensive and sustained hydrological activity and that catastrophic and regional (or local) trigger mechanisms may have been sufficient for the formation of the majority of the fan-shaped deposits on the surface of the planet.

3.1 Introduction

Fan-shaped sedimentary deposits are found all over the Earth in different environments and have also been identified from satellite imagery on the surface of Mars (e.g. Ori *et al.* 2000; Malin and Edgett 2003; Moore and Howard 2005; Howard *et al.* 2005; Irwin *et al.* 2005; Di Achille *et al.* 2006a,b; Pondrelli *et al.* 2008; Kraal *et al.* 2008a; Hauber *et al.* 2009, 2013; Di Achille and Hynek 2010; Grant and Wilson 2011; Williams *et al.* 2011, 2013; DiBiase *et al.* 2013). Fan-shaped deposits are formed where rivers enter plains or lakes and where the gradient changes sufficiently enough to decrease the velocity and sediment-carrying capacity of the stream (Bull 1968; Blair and McPherson 1994; Leeder 1999; Parker 1999). Fans are formed where mountainous drainage outlets enter wide plains (sub-aerially), while fan and river deltas are formed where fans and rivers, respectively, enter lakes or seas (sub-aqueously). Deltas differ morphologically from sub-aerial fans in that the first commonly exhibit relatively steep peripheral scarps at their outer margins where the sub-aerial delta plain meets the sub-aqueous delta front (e.g. Moore 1966; Irwin *et al.* 2005; van Dijk *et al.* 2012). Throughout this study, when describing morphology, the reference to fans/deltas in general include all fan-shaped sedimentary deposits (e.g. alluvial fans, fluvial fans, fan deltas and river deltas) unless specified.

Under conditions of sufficient available discharge, fan-shaped deposits form where water flow spreads out as un-channelized sheet flow or as channelized flow that frequently avulses radially across the fan surface depending on the available water discharge and sediment grain size (Whipple *et al.* 1998). These often rapidly crevassing, shallow, and unstable braided streams commonly characterize base-of-slope settings in poorly vegetated regions. Sufficient sediment input is required to build up a fan-shaped sedimentary deposit and sufficient discharge is required to distribute the sediment (Gilbert 1890; Leeder 1999). The balance between sediment supply and discharge is crucial in the formation of different types of fans and deltas, affecting in particular their sizes, shapes and gradients - morphological parameters that can be measured from remote sensing satellite data if the resolution is high enough.

Fans and deltas vary greatly in size, depending on the environment in which they are formed as well as on the processes that dominate during formation. The amount of deposition depends on the sediment transport rate, influenced by both sediment supply and amount of discharge (e.g. precipitation), and can therefore be highly sporadic. Different processes that operate on the fan/delta surface influence the shape of the deposit. The morphological variations in shape have been studied and include the number of visible delta fronts (single or multiple), the number of deposition lobes, the length and irregularity of the fan/delta perimeter or shoreline, the branching of channels on the fan/delta surface and their degree of incision across this surface; all variables that are addressed in this paper (e.g. Moore 1966; Wright and Coleman 1973; Geleynse *et al.* 2010; van Dijk *et al.* 2012). The slopes or longitudinal gradients of fans and deltas differ significantly due to the mode of sediment transport at the surface, which is a function of discharge, sediment supply and grain size (Kleinhans 2005a). Often fans have much steeper longitudinal gradients than both fan and river deltas. Likewise fan deltas have generally steeper longitudinal gradients than river deltas. Also the concavity of the radial profile can differ based on the formative processes – debris-flow dominated fans

tend to have more concave radial profiles whereas run-off dominated fans tend to have less concave profiles due to the distributive power of the run-off processes.

In order to qualify and quantify architectural elements of Martian fan and delta systems and to infer water and sediment discharge, our objectives are threefold. First, to compare Martian fan and delta morphologies to that of terrestrial fan and delta systems so as to categorically classify the types of Martian sedimentary deposits based on morphology. Second, to link distinct morphologies to their formative conditions and dominant sediment transport processes. Third, to reconstruct, on the basis of formative conditions, the climate conditions during the history of the planet Mars.

3.2 Terrestrial fan-shaped deposits

In order to qualify and quantify architectural elements of fan-shaped sedimentary systems on Mars, we first need to look at the various types of fan-shaped sedimentary systems on Earth as well as the processes that define their character and influence sedimentation. Classification systems on Earth include schemes based on the type of feeder system, sediment properties and grain size, processes operating on the fan/delta surface, as well as basin characteristics and initial morphology (e.g. McPherson *et al.* 1987; Nemec and Steel 1988; Postma 1990; Stanistreet and McCarthy 1993).

There has been much debate about the exact definition of an alluvial fan (see McPherson *et al.* 1987; Hooke 1987; Stanistreet and McCarthy 1993; Harvey 2010; etc.). In another study, de Villiers *et al.* (submitted; Chap. 5) group the vast amount of types of sub-aerial fans into three categories: Colluvial fans (e.g. debris cones and others described by Hooke 1987; Harvey 2010; 2012; Ventra *et al.* 2013), alluvial fans ('classic' cone-shaped fans with variable gradients as described by McPherson *et al.* 1987; Hooke 1987; Harvey 2010), and fluvial fans (large, low-gradient fluvial complexes as described by Stanistreet and McCarthy 1993; Gupta 1997; Horton and DeCelles 2001; Leier *et al.* 2005; Nichols and Fisher 2007; Harvey 2010). Colluvial fans are defined as dry, granular mass flows that are primarily formed by rockfall (Ventra 2012). Alluvial fans can be defined as either mass-flow dominated, commonly debris flows, or run-off dominated, but often a combination of both processes operate on alluvial fan surfaces (Bull 1977; Hooke 1987; Volker *et al.* 2007; de Villiers *et al.* (submitted, Chap. 5)). Fluvial fans can be defined as either braided (multiple channels) or meandering (single channel), and also here some systems may have both types of processes operating on the fan surface at different moments in time (Hartley *et al.* 2010; Harvey 2010; Weissmann *et al.* 2010).

Both fan and river deltas form into similar downstream depositional environments consisting of bodies of standing water such as oceans, seas, and lakes. But the upstream feeder systems are vastly different: fan deltas are fed by alluvial or fluvial fans, whereas river deltas are fed by established rivers (e.g. McPherson *et al.* 1987; Sun *et al.* 2002). Furthermore, the morphological differences are also important: fan deltas are more coarse-grained, steeper in gradient, and usually less extensive than river deltas (Postma 1990; Leeder 1999).

For all fan-shaped sedimentary deposits, sedimentation - the result of interaction between sediment supply and accommodation - is influenced by climate (mainly temperature and precipitation: volume, duration, intensity) and tectonics (Reading and Levell 1996;

Leeder 1999). Climate conditions determine the magnitude and intensity of fluvial processes and weathering patterns, which in turn affect the water and sediment supply (Lecce 1990; Reading and Levell 1996). Accommodation, which is usually related to tectonics or simply to basin size, plays a large role in the formation of sedimentary deposits. Additionally, lithology in the hinterland determines the amount of available sediment and the sediment grain size distribution (Bull 1964; Wells and Harvey 1987; Lecce 1991; Kodama 1994; Nichols and Thompson 2005). For instance, debris-flow processes are associated with hinterlands that yield large amounts of sediment from sedimentary, low-grade metamorphic, and silica-poor igneous rocks whereas fluvial processes are more common in basins with less available sediment due to a prevalence of high-grade metamorphic and silica-rich igneous rocks with lower weathering rates (Lecce 1991; Harvey 2010; Arzani 2012). Flow discharge and grain size distribution determine dominance by debris-flow processes or by run-off, determined by the ratio between sediment and discharge (Orton and Reading 1993), which can also be inferred from the steepness of the delta front, where sediment settles on a slope with a gradient no higher than the angle of repose (Leeder 1999; van den Berg van Saparoea and Postma 2008).

From the above, and in agreement with Postma (1990), it can be deduced that the development of substantial deltas depends on at least three factors: a) sufficient discharge – there must be enough discharge to move sediment, to induce bed-load transport, and to fill the basin to create a lake for the formation of deltas; b) sufficient accommodation - there must be a basin, empty for alluvial/fluvial fans and filled (or filling) with water for a certain period of time for the formation of deltas; and c) sufficient sediment supply - there must be a source feeder sediment and sediment-influx must exceed the capacity of sediment diffusion in the lake. Three hypotheses based on these factors are considered for the deposits on Mars and discussed below.

3.3 Martian fan-shaped deposits

Catalogues of fan-shaped deposits on Mars have been compiled by authors such as Cabrol and Grin (1999; 2001), Irwin *et al.* (2005), Moore and Howard (2005), Kraal *et al.* (2008a), Di Achille and Hynek (2010). Initially, Cabrol and Grin (1999; 2001) listed and described 75 delta deposits based on morphology. Subsequently, Malin and Edgett (2003) investigated approximately 80 locations of landforms on Mars that resemble alluvial fans or deltas and concluded that they found no discernible expression of deposition in most of the cases. This may have been due to a lack of high-resolution imagery. Irwin *et al.* (2005) re-examined the sites where deltas had been reported by Cabrol and Grin (1999), and found that only three of the proposed sites contain features that resemble unmodified deltas. A further 30 valley-mouth deposits were listed by Irwin *et al.* (2005) as potential sites of delta preservation, bringing the final count to 33 valley-mouth deposits that may have formed in a lake. Irwin *et al.* (2005) classified these features as scarp-fronted deposits (no distributary network observed), scarp-fronted fans (evidence of distributaries), or stepped deposits (cone deposit with segmented scarps). Hauber *et al.* (2009) described a range of fan-shaped sedimentary deposits in Xanthe Terra, some of which have not been previously described, and Di Achille and Hynek (2010) also published a list of delta deposits that includes the majority of the Irwin *et al.* (2005)

deltas, with the addition of 15 more examples. To date, only fan deltas have been identified and described, and no clear evidence for authentic river deltas has been established as yet.

Large numbers of fan-shaped sedimentary deposits without scarp-fronted edges have also been described on Mars. These are interpreted as fans and not deltas, because the toes of these deposits typically terminate in a concordant manner with the crater floor (Irwin *et al.* 2005). Moore and Howard (2005), did an in-depth morphological study on 31 fan-shaped deposits in the equatorial highlands, all described as alluvial fans. Kraal *et al.* (2008a) published a catalogue of 65 large alluvial fans (including the ~50 published earlier by Moore and Howard (2005)); and classified all of these as fluvial fans based on the fan slopes, the lack of discrete lobes, and the apparent uniform grain size. Wilson *et al*. (2013) identified many more alluvial fan deposits and classified them based on observed channels on the fan surface. Many authors have done more in-depth studies on individual fan/delta sites with higher resolution remote sensing data (e.g. Pondrelli *et al.* 2008, 2011; Grant and Wilson 2011; El Maary *et al.* 2012; Mangold *et al.* 2012; DiBiase *et al.* 2013; Williams *et al.* 2013).

In this study we focus on large alluvial fans (lengths > 1 km), thus excluding colluvial fans (sediment-gravity-driven, dry granular systems) and large fluvial fans (100's of km in length, dominated by fluvial distributive processes) comparable to the Taquari Megafan in Brazil (Assine 2005). Comparable fluvial fans have not been unequivocally identified on Mars, although the Eberswalde and Jezero Crater deposits (Malin and Edgett 2003; Fassett and Head 2005; Pondrelli *et al.* 2008, 2011; Schon *et al.* 2012) and the Gale Crater deposit (Williams *et al.* 2013) may perhaps be considered examples in this category.

In order to classify these Martian fan-shaped sedimentary deposits, we look at terrestrial classification systems such as that of Postma (1990), which includes the nature of the feeder system, the depth of the water in the basin, the processes at the river mouth, and the diffusive modification processes driven by tidal, wave, and gravitational energy. On Mars tidal influence is minimal and waves are probably not very strong due to the insufficient fetch in the relatively small crater basins that are not larger than 100 km in diameter and due to relatively low atmospheric pressure during most of Mars` history leading to a low shear stress on the water surface (Parker and Currey 2001; Di Achille *et al.* 2006b; Kraal *et al.* 2006). We assume that in the Martian craters, accommodation is only related to basin hypsometry and to changes in water level in the basin if applicable (Muto and Steel 1997, 2001; Kleinhans *et al.* 2010a; de Villiers *et al.* 2013, Chap. 4). Due to the limited knowledge of grain sizes, water depth, and river-mouth processes at the time these deposits were formed on Mars, an extensive classification system such as that for fans and deltas on Earth cannot yet be defined, but a simple classification based on morphology is proposed in the following sections.

3.4 Methods

To best address our objectives of quantifying the architectural elements of Martian fan and delta systems, we investigate three hypotheses for relationships between elements such as feeder channel geometry, receiving basin dimensions and fan morphology. Based on the preceding discussion, these three main relationships are addressed in the results section: The relation between fan/delta and feeder channel geometry, thus addressing sufficient discharge; the relation between fan/delta and basin geometry, thus addressing sufficient accommodation;

and the relation between fan/delta and regional geology or geomorphology thus addressing sufficient sediment supply. The morphological parameters needed for the quantification of the above-mentioned geometries are measured from satellite data, described in detail below.

The data sets used in this study are primarily from the High Resolution Stereo Camera (HRSC), an instrument on board the European Space Agency (ESA) Mars Express spacecraft which has been in orbit around Mars since December 2003 and is still functioning to date (Neukum *et al.* 2004b). The datasets are available through the Planetary Science Archive (PSA), which is maintained by ESA and through the Planetary Data System (PDS), maintained by the North American Space Agency (NASA). Other data used in this study include visual images from the Mars Orbiter Camera (MOC) that was on board NASA's Mars Global Surveyor spacecraft, the Thermal Emission Imaging System (THEMIS) that is on board NASA's Mars Odyssey spacecraft and the Context Camera (CTX) as well as the High Resolution Imaging Science Experiment (HiRISE) on board NASA's Mars Reconnaissance Orbiter spacecraft.

We have drawn up a catalogue comprising established lists of fan-shaped deposits and some newly discovered sites (e.g. Weitz *et al.* 2008; Hauber *et al.* 2009; 2013; Di Achille and Hynek 2010; Wilson *et al.* 2013), bringing the total number of fan-shaped deposits to roughly 100. We limit the inclusion of large, typical alluvial fan deposits because numerous similar deposits can often be found within a certain region (frequently within the same crater).

Our catalogue includes important morphological features indicative of upstream conditions (e.g. features that are indicative of discharge and sediment properties such as the size of the feeder channel and hinterland lithology) and downstream conditions (e.g. features that are indicative of basin hypsometry, such as size and shape of the basin) at the time of formation. Our approach is to measure and interpret the morphology of Martian fans/deltas in view of literature and models of terrestrial systems as well as in view of numerical and experimental analogues (Kraal *et al.* 2008b; Kleinhans *et al.* 2010a; van Dijk *et al.* 2012; de Villiers *et al.* 2013, Chap. 4).

Morphological aspects of the selected sedimentary deposits are mapped by using the HRSC topographic data in conjunction with the available visual images. The DEM creation and image processing is done according to standard procedures with VICAR software at the DLR in Berlin (Gwinner *et al.* 2009). As far as possible, the mapping and quantification of morphologies focuses on the channelized and non-channelized areas of the upstream area (e.g. the feeder valley), the sedimentary deposit itself, and the downstream area (e.g. the basin within which the delta was formed). We determine lengths and gradients of feeder channels (if applicable); the sizes, shapes, and gradients of the sedimentary deposits; and the diameters, depths, and volumes of the basins (mainly impact craters). Average gradients for all deposits are calculated across the whole landform, from the proximal apex to the distal tip of the deposit.

3.5 Results and Discussion (Part 1)

We propose a simple morphology-based fan and delta classification system as suggested by Cabrol and Grin (2001) with added information on the feeder system (considering geometry and gradient), the fan surface processes (considering longitudinal profiles and surface

properties), and the basin (considering initial morphology and characteristics). As mentioned in the methods section, we have combined catalogues of large fan-shaped deposits that have been published by other authors (e.g. Cabrol and Grin 1999; 2001; Irwin *et al.* 2005; Moore and Howard 2005; Kraal *et al.* 2008a; Di Achille and Hynek 2010) to form a single substantial catalogue. Our list comprises more than 70 basins within which at least one large fan or delta deposit (sometimes more than one) is visibly preserved (see appendix). We use morphological parameters, size, shape and gradient as the main factors in our classification system; thus grouping the large Martian fan-shaped deposits into three classes.

Class 1 - Classic, cone-shaped alluvial fan deposits with relatively high gradients of roughly 3 degrees and lengths of 10-30 kilometres. Martian examples include those in Ostrov Crater in the southern highlands and others as listed by Moore and Howard (2005) and Kraal *et al.* (2008a) (Fig. 3.1 a-c). The relatively high gradients of the Martian alluvial fans could indicate debris-flow dominated processes (as evident from terrestrial analogues, see de Villiers *et al.* (submitted, Chap. 5)), however these deposits have previously been classified as fluvial fans based on the size and gradient (Moore and Howard 2005). These fans have short and steep, or altogether absent feeder channels and they would match approximately with the "classic" alluvial fans as described by McPherson *et al.* 1987.

Class 2 - Back-stepping or terraced retrograding fan delta deposits with an indicative shape that comprises multiple, stacked fan-shaped layers with several steep and clear foresets, sometimes frayed at the edge. Each layer is smaller than the previous in longitudinal length, resulting in a stack of semi-circular delta plains with decreasing radial sizes towards the top. The gradients range from as steep as 10 degrees to as gentle as 2 degrees. The deposits are interpreted to have formed during rising water level in the basin and longitudinal profiles of these deposits are strikingly stepped, indicating the effects of the interaction between the rising water level and the variable sediment supply on the morphology of the deposit (de Villiers *et al.* 2013, Chap. 4). Well-known Martian examples of this type are the Coprates Catena terraced deposit, formed in a rift in the vicinity of Valles Marineris, and the deposit in Tyras Vallis (Weitz *et al.* 2006; Di Achille *et al.* 2006a, 2006b; Fig. 3.1 d-f). These retrograding fan deposits have short feeder channels, as far as can be observed.

Class 3 - Common, semi-circular, prograding fan delta deposits with a single steep and clear foreset (including two sub-type deposits with or without large branching networks). The average gradient is about 1 degree and lengths are approximately 5-10 kilometres. The deposits are interpreted to have formed while the water level in the basin was more or less constant (perhaps overflowing; see de Villiers *et al.* 2013, Chap. 4) and longitudinal profiles of these deposits are usually smooth and even, evidence of the progradation that is taking place. The two sub-types that have been identified include 1) branched or bird-foot shaped deltas indicating channelized flow; and 2) unbranched or flat-topped deltas indicating un-channelized or sheet flow. Typical Martian examples of this type include the deltas in Nanedi Vallis and Aeolis Mensae (e.g. Harrison and Grimm 2005; Irwin *et al.* 2004; Hauber *et al.* 2009; 2013; Fig. 3.1 g-i). The low gradients on the sub-aerial slopes of these deposits indicate

the dominance of sheet-flow processes. These prograding fan deltas often have medium to long feeder channels, perhaps indicative of bed load transport.

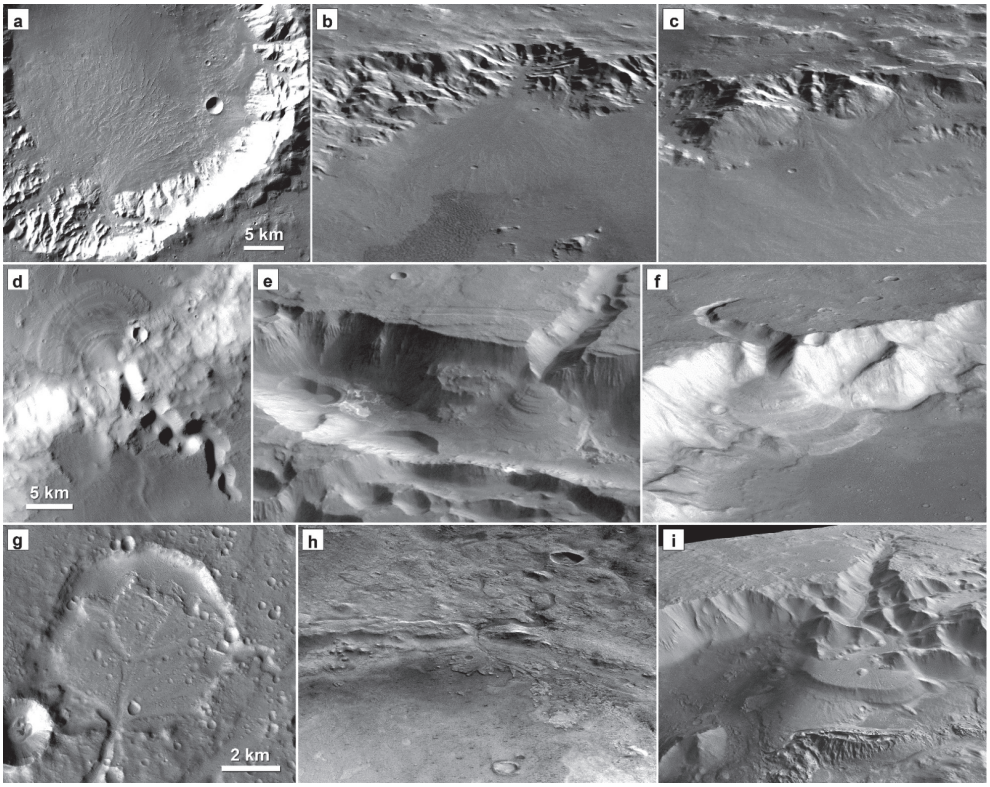

Figure 3.1: Examples of deposits in the three classes used in this study. Upper row: Alluvial fans, middle row: Retrograding deltas, lower row: prograding deltas. (a) Alluvial fan in unnamed crater at -27.88°/332.7°E in Noachis Terra (Grant and Wilson 2011). Mosaic of CTX images B01_009999_1519 and P21_009432_1520. North is up. (b) Alluvial fan in unnamed crater (Moore and Howard 2005). Perspective view looking north, derived from HRSC image h0533_0000. Fan width ~20 km. (c) Alluvial fan in Holden Crater (perspective view looking north; derived from HRSC stereo image h0511_0000). Fan width ~17 km. (d) Retrograding, stepped fan delta in Terra Sirenum (Kraal et al. 2008b). CTX image P02_001644_1713, -8.6°/200.72°E, North is up. (e) Retrograding, stepped fan delta in Coprates Catena at -15°/299.75°E (Di Achille et al. 2006a). Perspective view looking south, derived from HRSC image h1929_0000. Delta width ~9 km. (f) Retrograding, stepped fan delta in Dukhan Crater at -7.59°/321.03°E (Hauber et al. 2013). Perspective view looking south, derived from CTX images and HRSC DEM. Delta width ~7 km. (g) Prograding fan delta with distributory channels in Xanthe Terra at 8.62°/212° E (Hauber et al. 2009). CTX image P06_003407_1872, North is up. (h) Prograding fan delta in Jezero Crater at 18.5°/77.3°E (Fassett and Head 2005). Perspective view looking west, derived from HRSC image h0988_0000. Delta width ~10 km. (i) Prograding fan delta with flat surface and steep frontal scarp in Nephentes region at 2.0°/121.48°E. Perspective view looking south, derived from HRSC image h5212_0000. Delta width ~10 km.

In a different study, de Villiers *et al.* (2013; Chap. 4) report on the successful creation of morphological analogue deposits for the different types of Martian fan delta deposits described above under controlled conditions in our own laboratory set-up in the Eurotank facility in Utrecht, The Netherlands (see de Villiers *et al.* 2013, Chap. 4; Fig. 3.2). In these experiments, it has been shown that the behaviour or evolution of the water level in the

basin has the strongest influence on the morphology of the deposits. It has also shown that the majority of the Martian fan/delta morphologies can be created in single, short-duration events. Based on our experimental results, the formation of an alluvial fan is interpreted to have happened under conditions of low/short discharge, i.e. with no filling of the basin with water; the formation of a retrograding fan delta due to medium discharge, i.e. filling of the basin with water, but no constant water level; and the formation of a prograding fan delta under conditions of high/long discharge, i.e. a water-filled basin with a constant water level for some time. In other words, the behaviour of the water level within the basin (if present) is the main factor responsible for the differences between the different morphologies (de Villiers *et al.* 2013, Chap. 4).

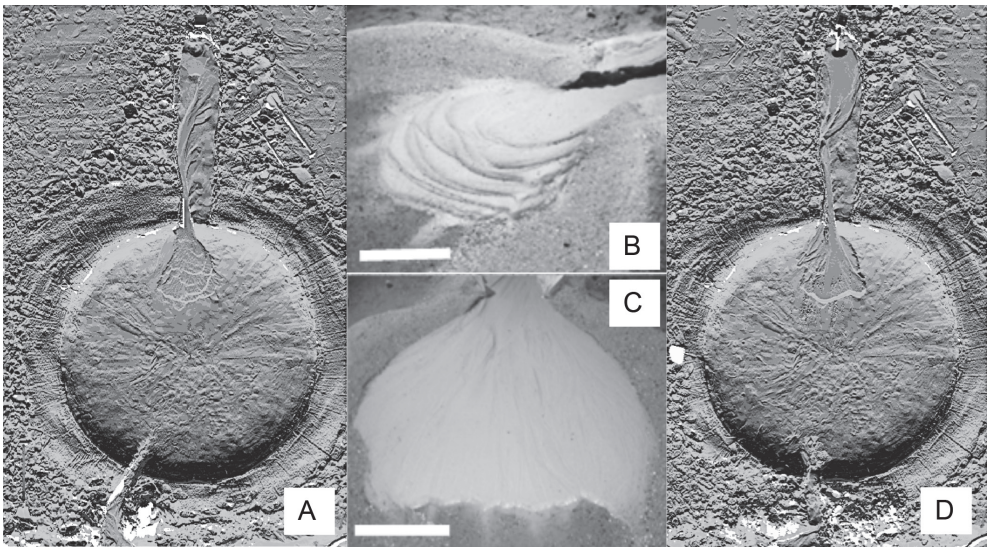

Figure 3.2: Photographs and slope maps superimposed on digital elevation maps of laboratory analogues for delta deposits on Mars, created in the Eurotank at Utrecht University in the Netherlands. For the slope maps (a & d), flow is from top of image to the bottom; crater diameter is 4m. For the photos (b & c), flow is roughly from the back of the image to the front; scale bar is 50 cm.

Analogues of these Martian alluvial fans and fan deltas occur on Earth (Fig. 3.3). Good terrestrial examples of alluvial fans are found in cold polar deserts such as on Svalbard (Norway; Hauber *et al.* 2011) and in hot hyper-arid environments such as in the Atacama Desert (northern Chile; Hartley *et al.* 2005a; Haug *et al.* 2010). Good terrestrial analogues for fan deltas are harder to find due to the large amounts of vegetation on the delta floodplains. Nonetheless, some analogues do exist, for example the Pleistocene Emme Delta in Germany, an example of a retrograding fan delta in a lacustrine environment (Winsemann *et al.* 2009; 2011), and the modern day Okavango Delta in Botswana (Stanistreet and McCarthy 1993; McCarthy 1993), an example of a prograding, branched fan delta in a lacustrine environment.

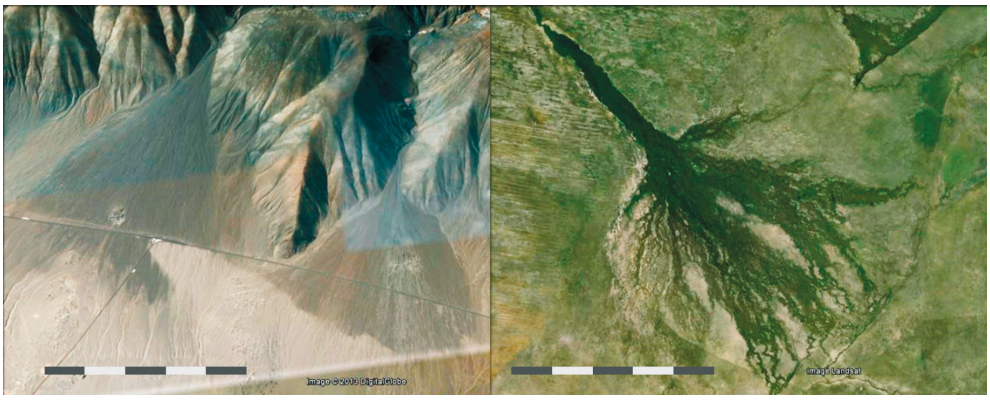

Figure 3.3: Examples of terrestrial analogues for deposits on Mars. Left: Alluvial fans in the Atacama Desert in northern Chile; scale bar is 2 km. Right: Okavango Delta in northern Botswana; scale bar is 100 km.

3.6 Results & Discussion (Part 2)

The morphological elements that we have used to classify large fan-shaped sedimentary deposits include fan/delta length (measured from apex to distal end), area and gradient; feeder channel length and gradient; and basin diameter. Fan/delta length and gradient are plotted in Figure 3.4 to show the ranges of dimensions of these morphologies. From these histograms we observe that alluvial fans (in red) tend to all have similar gradients (2-4°), despite the large variation in fan lengths (5-30 km); that retrograding fan deltas (in green) show a very narrow range of lengths (3-10 km) but a much wider range of gradients (2-10°); and that prograding fan deltas (in blue) also exhibit similar gradients within a slightly lower range than alluvial fans (0.5-3.4°) and that the range of lengths is somewhat smaller (2-20 km) than that of alluvial fans. We find that some of the retrograding fan deltas exhibit significantly high gradients, which is representative of the multiple high gradient scarps or "steps" (on Earth, the angle of repose of the sediment is typically around 30°) that are measured along with the lower gradient top sets when the whole deposit is to be considered.

A graphical representation of the analysis of profile data is shown in Figure 3.5a where it is observed that the gradient fluctuates greatly between the gently sloping top sets and steeply dipping front sets (indicative of a retrograding, stepped fan delta). Such a derivative plot is also shown for a representative simple prograding fan delta (Fig. 3.5b) as comparison, where the delta front can be observed as one steeply dipping front set, with smaller variations of the surface topography across the length of the deposit. The scatter is most likely due to local variations on the surface (micro-topography), and minimum gradient is zero or even negative in some cases due to the influence of local topography.

The maximum gradient in any of the stepped profiles across the retrograding fan deposits is around 15 degrees and in any of the profiles across the prograding fan deposits is around 18 degrees, which is not near the expected dynamic angle of repose for dry sediment. On Earth the dynamic angle of repose ranges from 25 to 35 degrees for coarse, angular and poorly-sorted sediment; on Mars it could be similar or slightly less (Atwood-Stone and McEwen 2013). This firstly supports sub-marine formation as angles of repose in sub-aqueous settings are often no more than half the reported value in sub-aerial settings (Selby 1982). It could

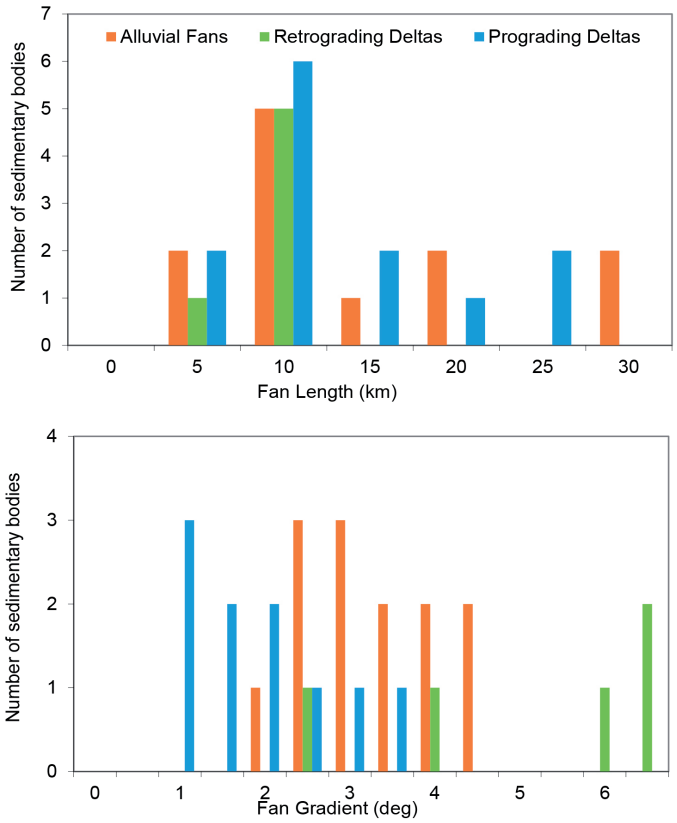

Figure 3.4: Frequency distribution of fan lengths in bin sizes of 5 km (top) and of fan gradients in bin sizes of half a degree (bottom)

also be an indicator that the angle of repose on a planet such as Mars, with a lower gravity and a less dense atmosphere, is less than the angle of repose on Earth. This argument has received some attention in work by Kleinhans *et al.* (2011) who concluded that the dynamic angle of repose may be reduced by about 10 degrees for all sediments under Martian gravity, but that would only account for some of the difference. Another plausible reason for this phenomenon could be the "smoothing effect" that comes with any DEM which would imply that the slopes that we expect to find are not accurately measured and hence not observed. Similar angles of around 10 to 15 degrees for delta fronts have been reported by Mangold and Ansan (2006) and Schon *et al.* (2012).

The relationship between fan/delta length and gradient as well as that between fan/delta length and area is shown in Figure 3.6. For all fans and fan deltas, the inverse relationship between fan length and gradient that has been documented on Earth can be observed. As expected, the plot between fan/delta length and area shows a clear relationship for both alluvial fans and prograding fan deltas, both with a wide range of values. In contrast, the retrograding fan deltas form a cluster with a much smaller range of values for both delta length and area; these fan deltas are all smaller in surface area for a given length, suggesting

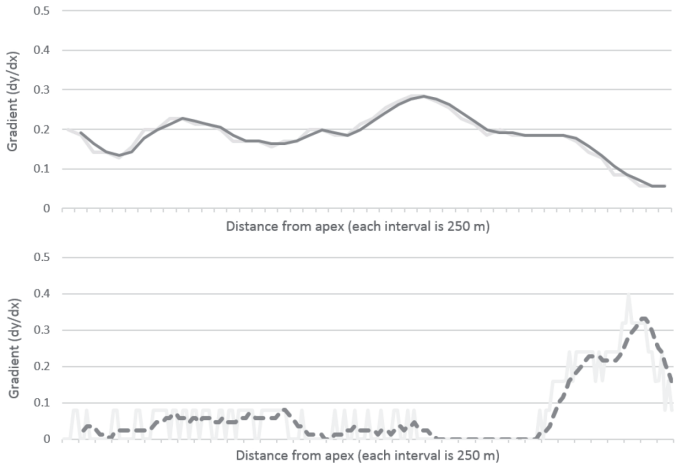

Figure 3.5: Plots of dy/dx (gradient) against distance from the apex to the distal end for two deltas. Top: retrograding fan delta in Coprates Catena (15°S/299.75°E; Di Achille 2006a) also shown in Figures 3.1e and 4.1a (solid line). Bottom: typical prograding fan delta in Aeolis Mensae (5.15°S/132.85°E; Irwin et al. 2004) also shown in Figure 4.1e (dotted line; real data plotted in light grey, moving average in dark grey).

that there is not enough time for the delta to develop substantially in lateral directions. Correlation coefficients for both linear and power relationships are given in Table 3.1.

As mentioned in the previous section, the development of substantial deltas depends on sufficient discharge, sufficient accommodation, and sufficient sediment supply; these factors are addressed in detail below by looking at the parameters related to these factors, i.e., size of the feeder channel, size of the basin, and location of sediment supply sources.

3.6.1 Discharge

The amount of discharge that feeds a system is directly related to the size of the feeder channel, i.e. a large quantity of discharge usually carves a large, wide channel and a small amount of discharge either carves a small, narrow channel or no discernable channel at all.

In Figure 3.7 (a to f) we plot the values for fan/delta lengths and gradients against channel lengths, average widths, and gradients (where available) to investigate the relationships (if any) between fan/delta and channel morphology. Our hypothesis is that a) alluvial fans should be expansive and steep initially as the deposit is draped on the crater wall, requiring only small or low discharges and thus narrow channels (i.e. in the case of mountain front alluvial fans), b) retrograding fan deltas should be relatively small and steep with medium-sized channels as discharge increases, and c) prograding fan deltas should be larger and less steep than retrograding fan deltas with large feeder channels as high discharge is maintained for at least some period of time to keep the water level in the basin stable (de Villiers *et al.* 2013, Chap. 4), a necessary condition for creation of a prograding morphology.

In Figure 3.7 (a) we observe no clear correlation, but we see that alluvial fan lengths vary while feeder channel widths are narrow or non-existent (<1 km). Retrograding fan delta lengths are more or less constant, but feeder channel widths vary somewhat and are typically wider (1-3 km) than for alluvial fans. Prograding fan delta lengths vary, and feeder channel

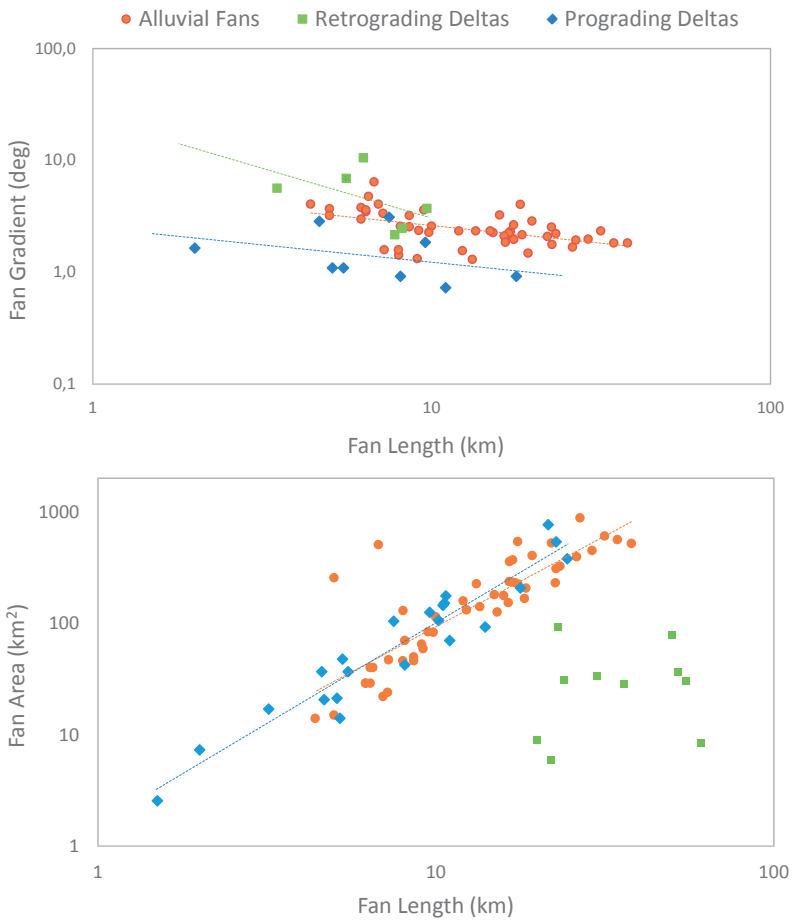

Figure 3.6: Plots of fan gradient against fan length (top) and fan area against fan length (bottom), to highlight the strong relationship between these parameters for some deposits and the lack of such strong relationship for others. Not all gradients could be accurately measured and some points are thus excluded from the top plot. Trend lines are shown when correlation is deemed strong enough (see text and Table 3.1 for elaboration).

widths show quite some variation. In Figure 3.7 (c), fan length is plotted against channel length. For alluvial fans, feeder channel lengths are consistently short or non-existent (<10 km), whereas for both retrograding and prograding fan deltas, the feeder channel lengths are more varied (5-80 km). The relationship between all fan/delta lengths and feeder channel lengths is clearer and could indicate that longer and more established channels yield longer (and possibly larger) fans/deltas. With our limited dataset it is impossible to identify with certainty any strong relationships for feeder channel gradient (Fig. 3.7e), but a possible inverse correlation between channel gradient and fan length is indicated for retrograding fans. This would imply that a system fed by a more mature, lower gradient feeder channel, will likely be a system that has had sufficient time to form a longer (and possibly larger) sedimentary deposit. In general, alluvial fans tend to have higher gradient feeder channels (consistent with the mountainous source terrain) and retrograding fan deltas tend to have much lower gradient feeder channels, both for all fan/delta lengths.

Table 3.1: Correlation coefficients for all data that is shown, showing that a power law is a better fit than a linear relationship in some cases (shown in italics in column two). The significant correlations are shown in bold, and visually represented on the graphs by trend lines (Figures 3.6, 3.7 and 3.9).

		Alluvial Fan R^2	Retrograding Delta R^2	Prograding Delta R^2
F Gradient vs F Length	Linear	0.20	0.25	0.26
	Power	0.25	0.27	0.14
F Area vs F Length	Linear	0.73	0.01	0.62
	Power	**0.70**	0.03	**0.91**
F Length vs C Width	*Linear*	0.34	0.18	0.02
	Power	0.30	0.16	0.02
F Gradient vs C Width	*Linear*	0.15	0.21	**0.79**
	Power	0.11	0.15	0.50
F Length vs C Length	Linear	0.23	0.35	0.12
	Power	**0.35**	**0.62**	**0.44**
F Gradient vs C Length	*Linear*	**0.49**	0.12	0.01
	Power	0.48	0.01	0.01
F Length vs C Gradient	*Linear*	0.15	**0.42**	0.09
	Power	0.17	0.27	0.14
F Gradient vs C Gradient	*Linear*	**0.44**	**0.61**	**0.69**
	Power	0.26	0.62	0.56
F Length vs B Diameter	*Linear*	**0.39**	**0.49**	**0.36**
	Power	0.53	0.22	0.42
F Gradient vs B Diameter	*Linear*	0.04	**0.90**	0.19
	Power	0.06	0.79	0.12

**F denotes Fan, C denotes Channel, and B denotes Basin*

When it comes to gradients, in Figure 3.7 (b and d) we observe that alluvial fan gradients as well as prograding fan delta gradients are all very similar, but that retrograding fan delta gradients are spread somewhat widely. This interesting observation invites further analysis, but could perhaps indicate the differences in magnitudes of the different events. A clear relationship between fan gradient and channel width (Fig. 3.7 b) for the retrograding stepped deltas, in other words, the tendency of steeper deltas to be associated with larger channel widths, could imply that larger discharges (wider channels) fill the basin much more rapidly and hence the retrograding fan delta has limited or no time to expand and prograde and thus is draped on the crater wall with an overall larger gradient. This relationship is not observed between fan/delta gradient and channel width for alluvial fans and prograding fan deltas, but it is expected that wider channels should result in lower gradients for these deposits due to their more normal evolutionary behaviour. In Figure 3.7 (d), the only observed correlation is a vague yet foreseeable inverse relationship between alluvial fan gradient and channel length. This is in accordance with terrestrial observations that short feeder channels usually occur in young systems with high relief in the source area and hence high gradient deposits, and that longer feeder channels are often part of established drainage systems which have deposits tending to lower gradients., and our data does not exclude this hypothesis. Finally, for channel gradient (Fig. 3.7f), we see that alluvial fan gradient is more or less constant despite variations in channel gradient, and similarly, the same seems true for prograding fan delta gradient. For retrograding fan deltas, however, the relationship is positive, indicating

higher delta gradients for deposits with higher gradient feeder channels. In Table 3.1, all correlation coefficients for the data that is shown in Figure 3.7 is given.

Since we observe distinct clustering of deposits in terms of morphological parameters, based on our interpretation of their origin as alluvial fan, retrograding fan delta and prograding fan delta, and since channel morphology can be an indicator of the amount of water that has been transported, the observation confirms our hypothesis about fan formation and discharge.

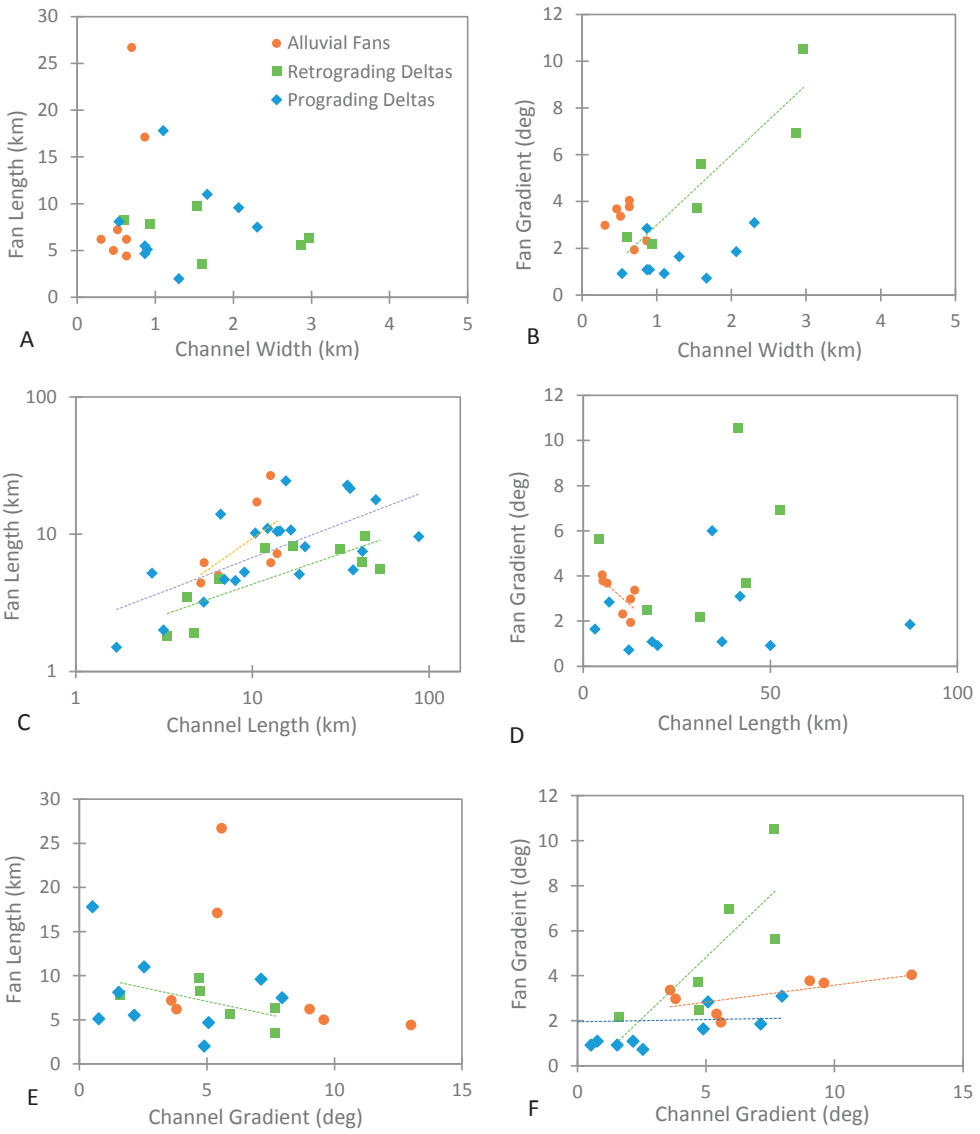

Figure 3.7: Selected graphical representations of various morphological parameters, description in text. Alluvial fans are plotted in red circles, retrograding fan deltas are plotted in green blocks, and prograding fan deltas are plotted in blue diamonds. Trend lines are shown when correlation is deemed strong enough (see Table 3.1).

3.6.2 Accommodation

The formation of alluvial fans on Mars, as common on Earth, is restricted to areas where high topographic gradients abruptly meet low gradients, such as at the rims of impact craters (where the rim is a high-gradient area that changes relatively suddenly to a more gently sloping or flat inner crater area). The formation of fan deltas is restricted to either open or closed water-filled basins. If unbreached, these closed-basin lakes are particularly well-suited to the formation of retrograding fan deltas due to the clear influence of the variation in water level on fan delta morphology (Muto and Steel 2001; Kraal *et al.* 2008a; de Villiers *et al.* 2013, Chap. 4). If breached, however, these systems become open-basin lakes (e.g. Fassett and Head 2008; Goudge *et al.* 2012), and the formation of retrograding fan deltas either precedes the breach or does not occur at all. In both cases, the availability of accommodation is crucial for the formation of a sedimentary deposit of any kind. Most of the fan-shaped sedimentary systems on Mars have sufficient accommodation due to the existence of impact basins at their downstream end. However, some basins are larger than others and as such may exhibit larger sedimentary deposits due to less influence of the crater rim as a limiting boundary to the expanding fan-shaped sediment body (as seen in experiments by de Villiers *et al.* 2013, Chap. 4). Our hypothesis is that the larger the basin (and thus the available space), the wider (or more expansive) the sedimentary deposit, for a given amount of discharge and sediment volume, thus depending on the confinement only.

In Figure 3.8 (a and b) we plot the values for fan/delta lengths and gradients against basin diameter (correlation coefficients are given in Table 3.1). We observe that the variable alluvial fan length is somewhat related to basin diameter and that fans tend to have greater lengths in larger basins (Fig. 3.8a). A similar correlation between basin size and fan/delta size was also reported by Cabrol and Grin (2001). Alluvial fan gradient is not limited to certain basin sizes and is scattered across the plot, and for prograding fan deltas the relationship is vague at best, if any (Fig 3.8b). For retrograding fan deltas, the relationship seems to be clearly inverse and indicate that higher fan gradients correspond with smaller basin sizes. This once more supports the hypothesis of rapid retrograding formation of these deltas as the basin is filling with discharge. Smaller basins will fill quicker and high gradient, draping fan deltas will form more easily than in larger basins.

3.6.3 Sediment supply

Even if there is enough discharge and ample accommodation, a sedimentary deposit will not develop if there is no sediment supply to the system. There must be some quantity of sediment available in the feeder (depending on factors such as lithology, relief, regional geomorphological processes such as volcanism and erosion) and sediment-influx must exceed the capacity of the sediment diffusion processes in the basin.

In Figure 3.9 we show the regional distribution of Martian alluvial fans and fan deltas from our catalogue. Our observations are thus only valid for these alluvial fans and fan deltas and exceptions that deviate from our generalizations may occur. We observe that there are very few deposits outside the 40 degrees north and south latitudes, and that some clusters of deposits are found in certain areas (as also discussed by Moore and Howard 2005; Kraal *et al.* 2008a; Grant and Wilson 2011). It is also evident that a large number of fan delta

deposits seem to be located approximately around the location of the crustal dichotomy (also mentioned by Di Achille and Hynek 2010), possibly related to the large change in altitude being responsible for directional water drainage in those areas. Crater rims such as that of Holden Crater in the southeast seem to provide ideal locations for large alluvial fans. In general, alluvial fans appear to have formed in the southern highlands, perhaps indicating a tendency to form in craters where a large amount of sediment is immediately available in the rim and/or there is significant relief in the source basins to promote sediment transport.

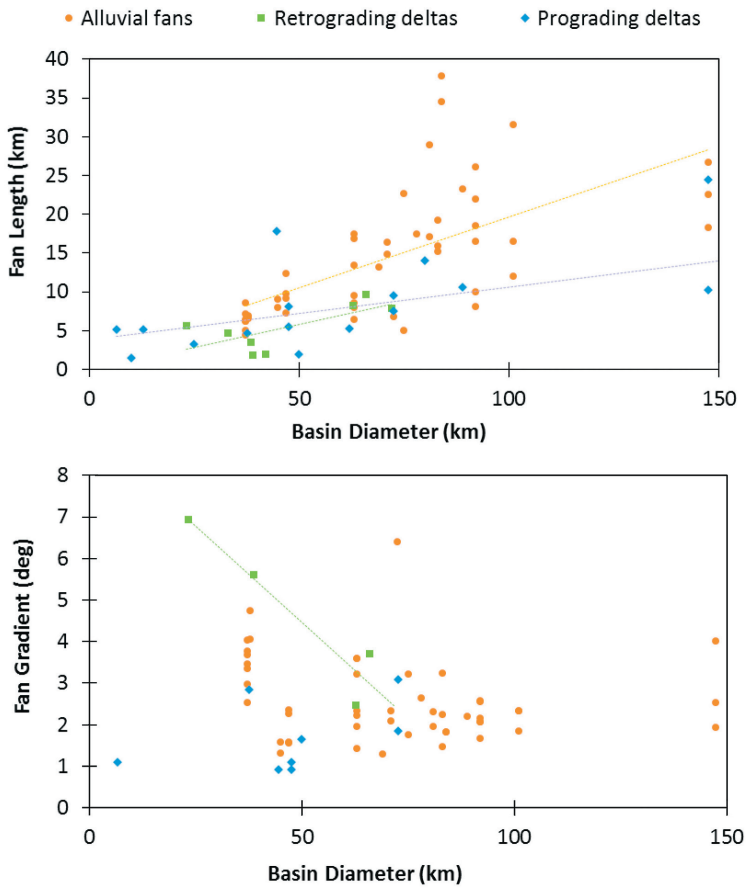

Figure 3.8: Graphical representations of the variation in fan/delta gradient (a) and fan/delta length (b) with basin diameter. Not all gradients could be accurately measured and some points are thus excluded from the top plot. Trend lines are shown when correlation is deemed strong enough (see Table 3.1)

Debris-flow processes are associated with basins that yield large quantities of sediment in areas where sedimentary and low-grade metamorphic rocks are dominant, while run-off processes are more common in basins with less available sediment due to a prevalence of high-grade metamorphic rocks (Lecce 1991; Harvey 2010; Arzani 2012). Basaltic rocks that are rich in mafic minerals, such as clinopyroxenes and plagioclase, occur throughout most of the southern highlands on Mars (Bandfield *et al.* 2000; Bibring *et al.* 2005), and have

the potential of providing large quantities of clay and fines that contribute in acquiring and maintaining cohesive strength of debris flows (Arzani 2012). Layered sedimentary rocks are also common but occur mostly in the northern hemisphere in the lowlands (e.g. Vastitas Borealis Formation) or within Valles Marineris and craters in Arabia Terra and surrounding areas. It is then not surprising to see similar associations for the occurrence of our fan-shaped sedimentary deposits in these regions, i.e. fan deltas in areas with available sediment in their source regions.

Grain size is an important parameter in deciding whether an alluvial fan is dominated by debris flows or by run-off flows (e.g. McPherson *et al.* 1987; Lecce 1991; Whipple *et al.* 1998; Nichols and Thompson 2005). Large quantities of coarse-grained sediments are more likely to produce gravity-induced debris flows than run-off flows (if there are enough available fines to act as lubrication), which in turn tend to produce smaller, steeper, less extensive fans on Earth. The availability of a bimodal sediment supply (Herkenhoff *et al.* 2004) with ample fine material is ideal for the formation of debris flows. Long debris flows have been documented when floods caused by lake-breakouts erode into volcanic ash deposits on Earth (Scott 1989; Tanaka 1999), indicating that abundant fine-grained volcanic material in combination with a coarse sediment fraction on Mars could be an excellent source for debris flows during catastrophic aqueous events.

3.7 Implications for Martian climate

Our classification system and subsequent morphometric analysis is used to infer past climate conditions from the locations and character of different fan types on the surface of Mars. In particular, we focus on how much water was released and whether the flow was episodic (related to local, pulsed trigger mechanisms) or sustained (related to a stable and persistent, global hydrological cycle).

To some authors (e.g. Malin and Edgett 2003; Irwin *et al.* 2005), the presence of a delta implies lacustrine longevity and stability as well as ineffective sediment re-distribution. However, catastrophic events of low frequency and high intensity may contribute much more sediment to fans and deltas than relatively frequent events of moderate intensity (as originally proposed by Wolman and Miller (1960)). Short-term catastrophic events can cause large changes in run-off as the sediment supply and average grain size is suddenly increased. Stream power and inertia of flood streams are much higher than during normal flow, and the erosive capability of these streams is often high enough to carry large quantities of coarse sediment (Postma 2001).

It has been shown that deltas can be created in geologically short time periods (e.g. Kraal *et al.* 2008b; Kleinhans *et al.* 2010a; de Villiers *et al.* 2013, Chap. 4). Interestingly, the manner in which the three types of classes of fan-shaped deposits have been identified on Mars, in combination with the results from de Villiers *et al.* (2013, Chap. 4), makes it possible to view them as different phases of development of the same systems, merely halted at different moments in time. Class 1 deposits (alluvial fans) are formed into basins with no ponding water; Class 2 deposits (retrograding fan deltas) are formed into basins with a rising water level; and class 3 deposits (prograding fan deltas) are formed into basins with a steady water level (constant equal input and output, perhaps overflowing). Our observation that fan/

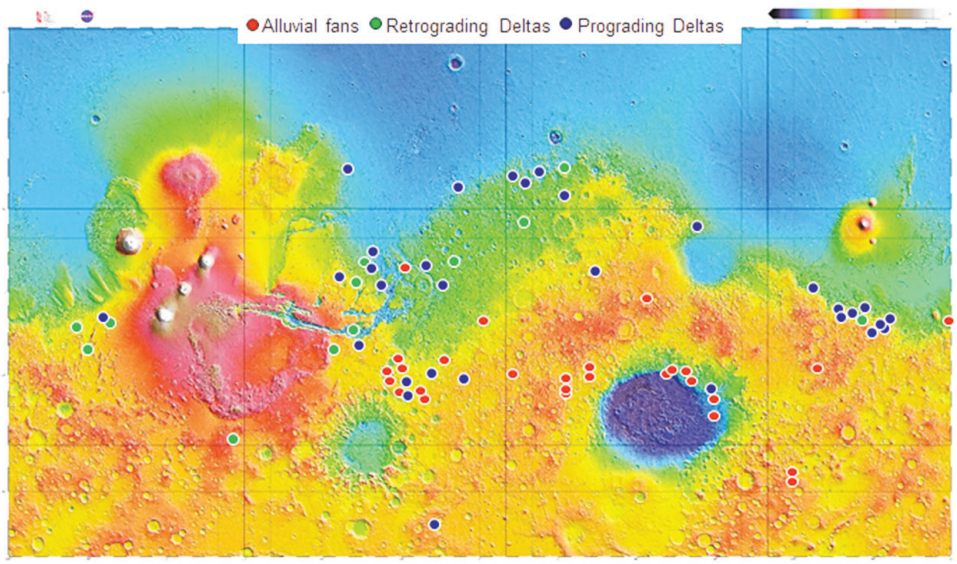

Figure 3.9: Regional distribution of large fan-shaped deposits on Mars super-imposed on a topographic DEM indicating the southern highlands in red tones and the northern lowlands in blue tones separated by the dichotomy shown in green.

delta area does not scale well with fan/delta length in cases of retrograding fan deltas (as opposed to alluvial fans and prograding deltas) indicates that there was not enough time for the deposit to develop substantially in a lateral direction, which further supports a short time-scale formation.

Our observations of feeder channel geometry, basin hypsometry and regional distribution indicate that both water discharge and character of the sediment supply are important contributors to all types of fan and delta formation and that accommodation is only an important factor for the retrograding fan deltas.

The aqueous discharge was most likely more continuous during the Noachian than during the Hesperian even though the unit of discharge per time period may have been higher during the Hesperian (as evident from the valley networks and the outflow channels). However, more continuous water supply does not necessarily imply a sustained warm and wet climate on Mars as suggested in previous studies (e.g. Craddock and Howard 2002), as supported by the fact that the valley networks have a lower drainage density than their terrestrial analogues that have been formed under hydrologically active conditions. The large discharges that were responsible for the formation of the outflow channels may have ponded in the northern lowlands creating temporary lakes and oceans (Head *et al.* 1998; 1999; Clifford and Parker 2001; Carr 2003; Fairén *et al.* 2003) but the possible occurrence of these oceans is not enough to infer a stable, hydrologically active climate with persistent rainfall, and in fact, may not have lasted all that long (de Villiers *et al.* 2010a, Chap. 2) although they may be responsible for creating short-lived rainfall episodes. Similarly, the mere occurrence of fan deltas and alluvial fans on the surface of Mars indicates that surface water was present at one point in time but these landforms may have formed in geologically short time periods,

with episodic and/or catastrophic water release, and with the discharge abruptly ending soon after formation.

Especially in the cases of the fan deltas, we can be certain that the discharge stopped abruptly as there is limited signs of further surface modification (such as erosive channels) after the initial formation of the deposits. Fan morphology on Earth is modified by secondary processes such as wind, groundwater seepage, and fluvial reworking (Blair and McPherson 1994; Leeder 1999). On Mars, the influence of chemical erosion has been far much less than on Earth and sedimentary deposits are often well preserved. Spectrographic data suggests that large parts of the Martian surface contain minerals which are easily altered by water, indicating that subsequent aqueous modification must have been local and limited to small areas or short periods of time (Yen *et al.* 2005; Bibring *et al.* 2006, Leverington 2011). This observation also agrees well with a localized occurrence of flood events that stopped as abruptly as they were initiated.

In order to form fan-shaped deposits, we may not necessarily need a globally, stable, warm and wet climate that is able to sustain rainfall for thousands of years. On the other hand, catastrophic flood scenarios on Mars may be common occurrence, or at least could have been so in the past, and could easily be responsible for most (if not all) sedimentary deposits on Mars. Trigger mechanisms that could be responsible for the melting of sub-surface ice have been suggested by other authors, including impact cratering, volcanic activity and orbital variation (Lasue *et al.* 2012). Impact cratering events were frequent at least up until 3.7 Ga (Tanaka 1986; Hartmann and Neukum 2001; Fassett and Head 2011) and undoubtedly may have served as potential triggers for large-scale heating of the sub-surface permafrost, resulting in localized floods in areas far enough away from the impact itself for the water not to be vaporised, yet close enough to experience the heat increase (Melosh 1989; Segura *et al.* 2008; Toon *et al.* 2010). Regional volcanism is another likely candidate as a trigger mechanism for a flash flood (e.g. Baker 1991; Mangold *et al.* 2012; Lasue *et al.* 2012). Especially in the smaller basins on Mars (up to 40 km in diameter), the produced run-off may be localized as not much discharge is needed to fill such a small basin. This agrees well with Postma (2001) who states that small deltas fed by small drainage basins are particularly sensitive to climate variations, especially when compared to large deltaic complexes.

3.8 Conclusions

We conclude that the majority of Martian fan-shaped sedimentary deposits can be grouped, based on morphology, into three classes: alluvial fans, retrograding fan deltas and prograding fan deltas. These three types of deposits have distinct morphologies and the relations between morphological parameters such as length or gradient differs for each category. The markedly different retrograding fan deltas show that their fan areas are much less than expected based on terrestrial observations and much less than observed for Martian alluvial fans and prograding fan deltas. This observation, in combination with the tendency of high gradient retrograding fan deltas to form in association with wide feeder channels and in small basins, strongly supports the rapid formation of retrograding fan deltas and hence supports the short formation times of fan deltas that have been predicted on the basis of models (Kleinhans *et al.* 2010).

We have seen that discharge influences fan/delta type by a) allowing the formation of alluvial fans in cases with insufficient discharge to fill the basin; b) allowing the formation of retrograding fan deltas in cases with sufficient discharge to fill the basin rapidly but not to sustain a stable water level and c) allowing the formation of prograding fan deltas in events with enough discharge to fill the basin and maintain a stable water level for some time. These filling stages of the basin can be inferred as different time-steps at which the evolution of the fan-shaped deposits is paused or stopped entirely. The amount of available accommodation does not seem to be a deciding factor in fan morphology, but the regional distribution of available sediment and the sediment character do have an influence.

Lastly, based on the limited signs of post-formation incision, we agree with the hypothesis of rapid and violent formation with an abrupt end. The wide range of ages of these deposits also indicates the possibility of formation under current, cold and dry conditions, indicating that the majority of the fan-shaped deposits on Mars were most likely products of regional or local catastrophic events.

3.9 Acknowledgements

The authors would like to acknowledge Gerhard Neukum and the entire HRSC-team as well as the hospitality of the German Aerospace Centre (DLR) in Berlin, with special thanks to Thomas Roatsch for help with the data. We thank Erin Kraal and Caleb Fassett for valuable input and fruitful discussion.

“The only things you learn are the things you tame”

4 Experimental Deltas in the Eurotank

Based on:
de Villiers, G., Kleinhans, M. G., & Postma, G. (2013). Experimental delta formation in crater lakes and implications for interpretation of Martian deltas. *Journal of Geophysical Research: Planets*, 118(4), 651–670, doi:10.1002/jgre.20069.

Abstract - The morphology of delta deposits in crater lakes on Mars is indicative of upstream (e.g. flow discharge and sediment properties) and downstream (e.g. basin characteristics) parameters, from which the hydrological conditions at the time of formation can be inferred. To investigate the influences of these parameters on delta morphology, we experimentally created deltas in crater-shaped basins by feeding a range of constant flow discharges over a feeder channel of various sand textures. We reproduced three categorically different types of deltas covering most of the examples that have been identified on Mars. basin size and hypsometry, and basin floor permeability, can explain most delta morphologies on Mars. Stepped, retrograding deltas formed during water level rise, prograding deltas formed during a stable water level, and during water level fall deltas were partially destroyed by erosion. On Mars numerous retrograding and prograding deltas have been preserved, most of them without indications of channel incisions or other fluvial modification. We conclude that the main difference between a single-foreset prograding delta and a multiple-foreset, retrograding delta is the behaviour of the water level in the basin. These simple delta morphologies cannot be reconciled with long-duration hydrological activity, because that would imply crater lake fluctuations due to inherent complex water level histories along with complex sediment delivery histories. Our experiments and numerical verifications demonstrate that such deltas preferentially form during one aqueous event, which parsimoniously argues for short-duration hydrological activity.

4.1 Introduction

The presence of water on the surface of Mars is reflected throughout its history by the occurrence of large valley networks, regional outflow channels, and small, local gullies (e.g. Carr 1983; Cabrol and Grin 2001; Gulick 2001; Baker 2001; Hynek *et al.* 2010). The occurrence of valley networks implies the possibility of rainfall in either a warm and wet surface environment (e.g. Craddock and Howard 2002), or on the other hand a cold and dry surface environment with episodic floods (e.g. Gaidos and Marion 2003). Morphologies of sediment bodies within impact craters have been identified as alluvial fans and deltas (e.g. Malin and Edgett 2003; Irwin *et al.* 2005; Kraal *et al.* 2008a; Hauber *et al.* 2009, Di Achille and Hynek 2010; Fig. 4.1), which implies that these craters were once water-filled (partially if not full) lakes early in Martian history (e.g. Cabrol and Grin 1999). As is known from Earth, delta morphologies contain information of the hydrological conditions that formed them. By analogy, Martian deltas may provide an indication of the hydrological conditions during the planet's history and contain valuable information about the magnitude and duration of fluid surface water.

Terrestrial delta morphology is determined by upstream factors such as climate, geology, and vegetation, as well as by factors in the downstream receiving basin, such as basin morphology, waves, tides, and sea level fluctuations (e.g. Postma 1990, 2001; Porebski and Steel 2006). As Martian deltas commonly formed in impact crater lakes with average diameters of around 40 km, waves were probably insignificant due to insufficient fetch and lower gravity (Kraal *et al.* 2006). Tides were most likely absent because Mars has no large satellite like the Moon is for Earth and additionally Mars is about 1.5 times further from the Sun than the Earth. With no interference by vegetation on the surface of Mars, the upstream conditions (climate and sediment texture), and downstream conditions (the dominant processes on the deltas and the behaviour of the water level) are the most important formative parameters for deltas on Mars.

Climate variation affects fluvial sedimentation on different timescales (Postma 2001) and can be a factor in both the upstream and downstream environments. Previous experiments have demonstrated that delta morphology is particularly related to flow discharge and duration, sediment texture, and water level change (Schumm *et al.* 1987; van Heijst and Postma 2001; Muto and Steel, 2004). The same factors are expected to be important also on Mars, thus we focus on these in our experiments below. In the upstream environment, source water generation can be highly sporadic thus producing large variations in runoff. This phenomenon could occur on either small or large timescales, for example short-term melting of ice or long-term stable rainfall. The amount of deposition not only depends on the amount of water but also on the sediment availability in the drainage basin, which may also depend on climate (van Heijst *et al.* 2001). In the downstream environment, the water level behaviour in a closed basin (like many of the craters on Mars) depends directly on the discharge (input rate) and partly on the rate of losses such as sub-surface percolation and evaporation.

The textural properties of the sediment, in particular grain size and grain sorting, determine the dominant transport processes and rate of delta formation. Grain size distributions are not well constrained on Mars, but Kleinhans (2005a) suggests a coarse, bimodal sediment

with D_{50} between 0.01-1 m for the gravel fraction and D_{50} between 0.1-2 mm for the sand fraction based on rock size frequencies measured in lander imagery (Golombek *et al.* 2003, Herkenhoff *et al.* 2004). Such coarse sediment would predominantly be transported as bed load (Kleinhans 2005a), which is associated specifically with steep sloping (~ 25 degrees) delta foresets characterizing Gilbert-type deltas (Postma 1990), also known as Gilbertian profiles. Deltas formed by suspended transport would have gentle (~ <1 degree) sloping foresets. The sediment on Mars is probably so poorly sorted that some of it is transported as bed load and some as suspended load, which could affect the morphology of the delta.

Martian deltas exhibit many morphological elements that are similar to those of terrestrial deltas, e.g. fan shapes; surface gradients; concave/convex profiles; and the presence of lobes and channels (Fig. 4.1 and Tab. 4.1). However, terrestrial deltas are not nearly as well-preserved or observable as deltas on Mars due to erosion and deformation, as caused by plate tectonics, climate and sea level changes as well as vegetation. Moreover, some features of Martian deltas, for example the stepped profiles, are not commonly found on Earth. Based on a few simple morphological parameters like cross-sectional geometry and delta slope, most of the Martian deltas can tentatively be grouped into two categories, i.e. 1) retrograding deltas with multiple stacked steps of steep foresets of decreasing radius, and 2) prograding

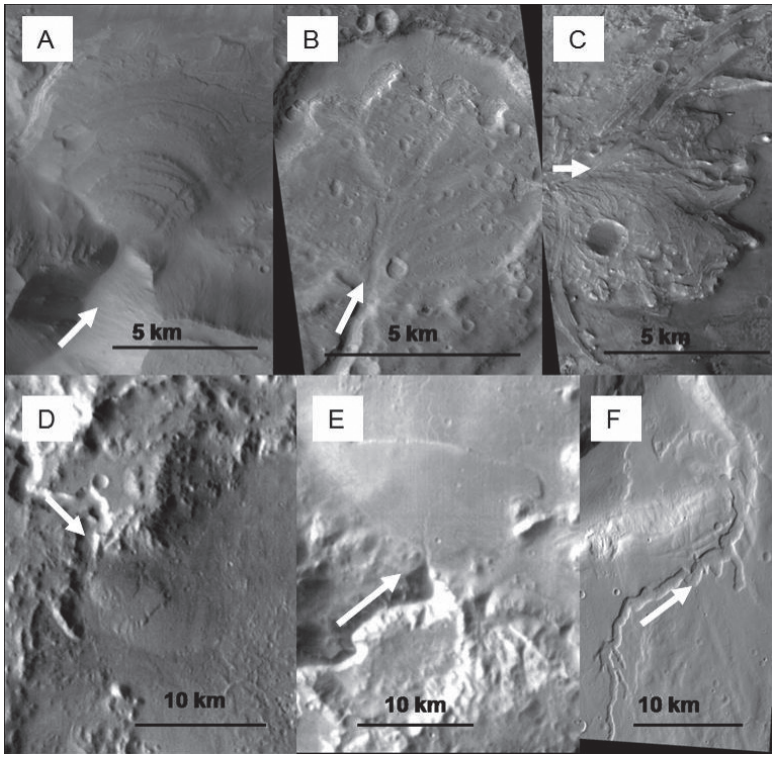

Figure 4.1: Examples of three categories of delta deposits on Mars formed in enclosed impact craters or rift basins. (a and d) Multiple-scarped, stepped, retrograding deltas (THEMIS image V17040003 and I10125008; (b and c) Single-scarped, branched, prograding delta (HiRISE image PSP_006954 and PSP_003798); (e and f) Single-scarped, smooth, prograding delta (THEMIS image I10805012 and V12581003). White arrows indicate flow direction.

deltas with single steep foresets, either flat-topped or branched (Tab. 4.1; de Villiers *et al.* 2009).

Martian deltas have been considered in terms of location and environmental context and their formative processes inferred from general morphology (Cabrol and Grin 2001). Some studies have investigated the implications of observed delta locations and morphologies for climate conditions (e.g. Di Achille and Hynek 2010), but these interpretations did not employ the full potential of laboratory experiments and numerical modelling on terrestrial and Martian deltas. Laboratory studies (e.g. Muto and Steel 2001; van Heijst and Postma 2001; van Heijst *et al.* 2001) have shown that retrograding delta morphologies can be induced by climate-related base level oscillations. Numerical modelling studies (e.g. Ritchie *et al.* 2004) have also shown that base level oscillations may produce distinct morphologies, most of which are clearly visible in both modern and ancient terrestrial deltas (e.g. Tye and Coleman 1989; van Heijst *et al.* 2001). Only one experimental study (Kraal *et al.* 2008b) and one numerical study (Kleinhans *et al.* 2010a) were applied to Martian deltas, both suggesting that these deltas were formed in a single event, which is in stark contrast with the rich formative histories underlying many terrestrial deltas.

Table 4.1: Morphological characteristics and examples of Martian delta deposits (de Villiers et al. 2009).

Approximate Shape:	Multiple foresets with Gilbertian profiles	Single foreset with Gilbertian profile
Average Delta Plain Gradient:	~ 2 degrees	~ 1 degree
Average Length:	~ 10 km	~ 7 km
Example Locations:	**-15.0 N 299.7 E**	**-5.2 N 132.9 E**
	(Di Achille *et al.* 2006a)	(Irwin *et al.* 2004)
	-10.9 N 306.6 E	**8.5 N 312.0 E**
	(Di Achille & Komatsu 2008)	(Hauber *et al.* 2009)
	8.3 N 310.7 E	**35.5 N 26.3 E**
	(Di Achille *et al.* 2006b)	(McGill 2002)

Our objective is to systematically couple the simple morphological elements in Martian delta systems (Fig. 4.1) to their formative processes and boundary conditions through laboratory experiments. We test the hypothesis that the morphology of deltas on Mars and their (dis) similarities with their counterparts on Earth and in the laboratory are indicative of upstream (e.g. discharge amount, discharge duration and sediment properties) and downstream (e.g. basin size and hypsometry) conditions at the time of formation. We focus particularly on deposits that exhibit steep peripheral scarps at their outer margins due to the interaction of the lacustrine regime and the water level in the receiving basin, which is often an impact crater. Specifically, our aims are to create various types of sedimentary deposits in the laboratory as a function of the aforementioned factors, to present both qualitative and quantitative evidence enabling us to relate formative processes and morphologies of the small-scale experimental deltas to the full-scale deltas on Mars, and to constrain the hydrological environment in which these deltas may have formed.

4.2 Experimental methods

The experimental work was carried out in the Eurotank facility at Utrecht University in the Netherlands. The Eurotank is a flume of 6.3 m wide, 11.4 m long and 1.2 deep, within

which sediment and water can be introduced to reproduce processes of erosion, transport and deposition. Water was supplied by a regulated pressure tank, controlled by valves and measured with rota-meters.

We experimentally created deltas in small crater-shaped basins (2m and 4m in diameter) carved in sand. Various causal factors were isolated as much as possible by keeping most of the boundary conditions (e.g. discharge, sediment properties) constant and the initial conditions (basin morphology) idealized. We systematically varied one boundary condition, such as flow discharge or sediment properties and investigated the effect of crater basin size and shape. For each experiment we study rising, constant, and falling water level in the basin.

The scaling approach of these landscape-sized models is the same as used by van Dijk *et al.* (2009; 2012) and Kleinhans *et al.* (2010b), where four criteria for flow and sediment transport characteristics are obeyed: 1) flow is fully turbulent, 2) flow is not above critical (Froude number ≤ 1), 3) sediment is moved as bed load and 4) the sediment must be coarse or poorly sorted enough to protrude the near-bed laminar flow layer, to ensure rough boundary conditions as to avoid the formation of small-scale ripples and unrealistic scour holes as observed in experiments by Kraal *et al.* (2008b) and van Dijk *et al.* (2009). The mobility of the sediment is determined mostly by channel gradient and depth. Depth on Mars is typically about 50 m (Kleinhans *et al.* 2010a), which would scale to 5 mm in the experiment. In order to mobilize this sediment, the gradient thus must be much larger than in nature. Bed load movement by water flows in experimental set ups like ours requires slopes that are steeper than in nature, yet sediment mobility in experiment and in natural systems are comparable so that morphology is comparable.

Our setup was similar to that of Kraal *et al.* (2008b), yet with a few modifications to both boundary and initial conditions (see Table 4.2). We constructed circular basins with diameters of 2 m (experiment numbers A-N) and 4 m (experiments O-S) with shapes comparable to those of complex impact craters. Martian complex craters have a diameter of more than 8 km and a flat crater floor (as opposed to simple, small, bowl-shaped craters; see French 1998; Melosh 2011), where the depth-diameter relation is a power function for pristine craters and where the idealized shape of the inner crater wall is also described by a power function (Garvin and Frawley 1998, Garvin *et al.* 2000, Kleinhans *et al.* 2010a). For both setups we modelled a crater of 40 km diameter without a central mound, which is the average size of Martian craters with fan-shaped deposits. For the smaller crater a two times vertical exaggeration was applied to produce more pronounced deltas, while the larger crater was scaled with natural geometry. The crater depth as measured from floor to rim was about 15 cm in all cases.

A feeder channel initially sloping 1.1º (± 0.4º) funnelled water and sediment into the basin (Fig. 4.2). Water discharge was systematically varied (Table 4.2) to obtain a range of crater filling rates and sediment mobility, as well as a range of ratios of crater diameter and self-formed channel width (which scales with discharge). In experiment J we applied the largest discharge possible with this setup. In experiment S we constructed a narrower feeder channel filled with sediment between non-erodible banks, 0.25 m apart, to investigate the influence of upstream channel dimensions on morphology.

In all but two experiments, sediment for the delta became available through cannibalization of the feeder channel that widened and deepened during delta formation.

In two experiments (F and G) sediment was added at the upstream boundary of the feeder channel. This mimics two possible sediment supply mechanisms on Mars, a supply of sediment from a large upstream drainage area (here mimicked by feeding) and sediment delivered locally by headward erosion, widening and lateral migration of the feeder channel.

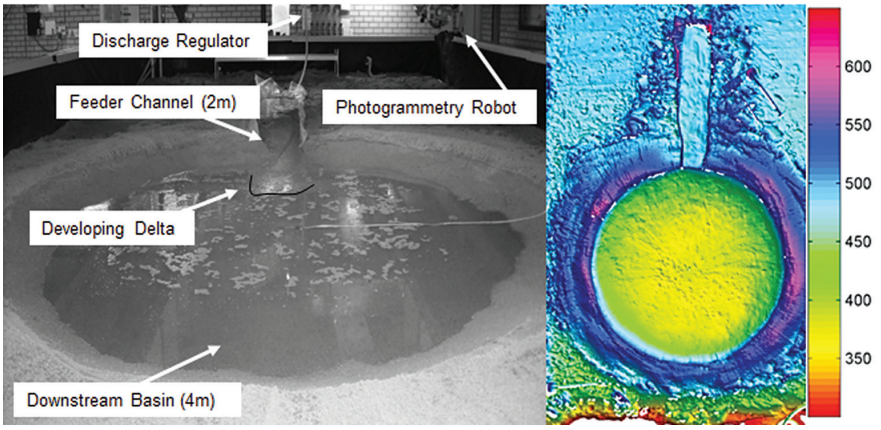

Figure 4.2: Left: Oblique photograph of the experiment set-up in the Eurotank for run O with a filling lake and developing delta (looking upstream). The feeder channel is 2 m long and the downstream basin is 4 m wide (with foam floating on the water surface). Right: Shaded DEM of the unfilled crater with scales in mm.

Four sediment grain size distributions were applied to vary sediment mobility leading to bed load or suspended load dominated sediment transport. We used three poorly sorted coarse sands (sand 1 in experiments A-C, sand 2 in experiments D-E and J-S, and sand 3 in experiments H-I; see Table 4.2 and Fig. 4.3) or uniform fine sand (sand 4 in experiments F-G). By means of dry-sieving of the coarse tail of the sediment grain size distribution, the degree of size-selective transport and resultant spatial sorting patterns and armouring tendency found in sand 1 in experiments A-C was reduced. The fraction greater than 4.7 mm was removed for experiments D and E as well as for J-S, and the fraction greater than 1.4 mm was removed for experiments H and I. The bed load to suspended load ratio was varied in experiments K-N by adding 20% or 40% by volume of silt-sized material (silica flour) in the feeder channel sediment (Table 4.2). Experiments with silica flour in concentrations higher than 40% resulted in undesired effects such as fluidized sediment transport and strong adhesive effects leading to hardening of the surface. This occurred due to complete filling of the pore spaces of the sand by the silica flour and a consequent decrease in porosity and permeability (e.g. Kleinhans *et al.* 2010b). Silica flour was also added when moulding the basin rim in some cases (experiments K-N) in order to reduce erodibility. In experiments M and N we tested the results of multiple drowning events, or in other words successive phases of filling and breaching of the crater. The only difference between M and N is that for experiment M we used full craters (craters filled with water up to the apex), whereas for experiment N we used half-full craters (craters filled only halfway before draining). This mimics a scenario where the breaching process occurs earlier (before the crater lake is filled up entirely and overflow occurs naturally) perhaps due to some inherent weakness of the crater rim. In fact, all our experiments are somewhat designed to occur like this, since we

always initiated breaching instead of waiting for overflow. Experiment N showed that even with only half-filled craters the delta morphologies remain similar.

Table 4.2: Ten sets of experiments (only first phases) to test combinations of flow discharge, particle size distributions, silt component and crater diameter. Duration, upstream channel slope and width were measured during the experiments. Delta volume was determined from DEMs and modelled volume was calculated from the predicted sediment transport (see text).

Run	Basin Diameter (m)	Fines Content (%)	Grain Size (D_{50}) (mm)	Grain Size (D_{90}) (mm)	Discharge (l/sec)	Time (H:M)	Average Slope (Dec)	Width (m)	Delta Volume (actual) (L)	Delta Volume (model) (L)
A1	2	0	0.47	2.5	0.07	04:00	n.d.	0.168	7.6	97.7
B1	2	0	0.47	2.5	0.21	00:30	n.d.	0.320	7.3	14.4
C1	2	0	0.47	2.5	0.35	00:15	0.029	0.258	22.3	5.9
D1	2	0	0.45	2.0	0.35	00:30	0.033	0.258	-	6.9
E1	2	0	0.45	2.0	0.07	03:15	0.037	0.278	-	52.5
F1	2	0	0.23	0.28	0.35	00:15	0.042	0.238	21.8	0.2
G1	2	0	0.23	0.28	0.07	03:00	0.078	0.380	35.8	7.3
H1	2	0	0.40	0.8	0.07	03:00	0.053	0.336	9.6	12.0
I1	2	0	0.40	0.8	0.35	00:15	0.045	0.400	19.1	0.9
J1	2	0	0.45	2.0	1.08	00:05	0.050	0.414	14.4	1.2
K1	2	20	0.45	2.0	0.35	00:10	0.040	0.192	4.1	2.7
L1	2	20	0.45	2.0	0.07	01:45	0.035	0.163	-	28.9
M1	2	40	0.45	2.0	0.35	00:07	0.032	0.180	-	2.5
N1	2	40	0.45	2.0	0.35	00:05	0.047	0.170	-	2.5
O1	4	0	0.45	2.0	0.28	00:45	0.023	0.182	9.0	2.2
P1	4	0	0.45	2.0	0.35	00:30	0.023	0.172	12.3	1.2
Q1	4	0	0.45	2.0	0.07	03:45	0.017	0.163	7.7	9.1
S1	4	0	0.45	2.0	0.35	00:30	0.020	0.200	15.4	48.3

**The number of the phase is shown next to the experiment letter. Only first phase results are shown here.*

Each experiment listed in Table 4.2 was performed in two phases. In phase 1, the basin was filled with water through the upstream feeder channel. While basin level rose, sediment was supplied through a sediment feeder and/or eroded from the channel banks. Delta deposits were formed while the water level in the basin rose. Some water was lost by infiltration into the crater floor and wall. Once the basin was full, or when the water level had reached the level of the feeder channel, we ended phase 1 and drained the crater to measure and photograph the delta deposit. Then we carefully filled the basin again to the former level and restarted the flow through the feeder channel before commencing with phase 2, manually breaching the crater rim locally, to simulate water loss from the lake by overflow. This led to a constant water level in cases where water supply equalled discharge lost through the breach and into the sub-surface, and otherwise to a fall in basin water level when the crater rim eroded rapidly. In every experiment discharge and sediment grain size distribution were kept constant.

Morphology before, during, and after each experiment was measured through detailed photogrammetry using an automated positioning system designed for high-resolution surface scans. Digital elevation models (DEMs) for the 2 m craters were created from stereo pairs using the dedicated software SANDPHOX. DEMs for the 4 m craters were created from laser

line scanning that was obtained after an upgrade of the laboratory equipment. DEMs were subsequently gridded and analysed with median filtering for outlier removal to produce data similar to those taken by the High Resolution Stereo Camera (HRSC) on board the Mars Express spacecraft.

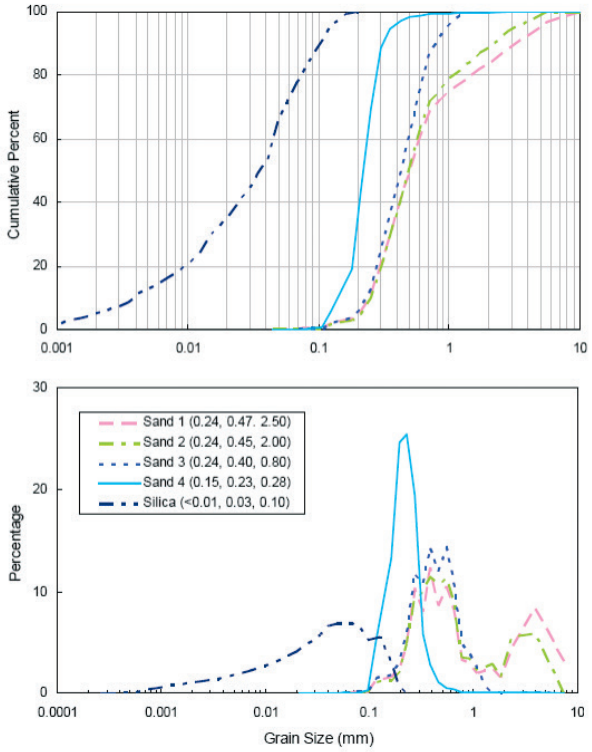

Figure 4.3: Sediment size distributions for the four different types of sediments and the silica flour used in the experiments (see full description in text). Sediment descriptions given as Sand type (D_{10}, D_{50}, D_{90}).

4.3 Results

All first phase experiments with rising water level produced retrograding or back-stepping deltas with lobes that stepped landward and did not fully cover previously deposited lobes as fan radius steadily decreased (Fig. 4.4a and 4.4c). The experiments show that delta formation occurs by a sequence of events beginning with massive flows of relatively high sediment concentration gradually decreasing to dilute flow as the slope of the feeder channel decreases with the filling of the lake. Initially, as the water reaches the basin, the water first infiltrates into the permeable crater floor before starting to fill the crater. The first stage of fan formation is likely to be initiated by a hyper-concentrated particle flow or mass flow, which deposits a fan-shaped drape on the crater wall. As water starts to pond, a retrograding delta begins to form (described in more detail below).

During the second phase the crater rim was breached manually at a point, causing water level to drop quickly as the unconsolidated rim eroded rapidly. This rapid lowering of the water level caused deep incisions in the fan surface and formed terraces and telescoping

morphologies (Fig. 4.4b). In the 4 m diameter crater with a wider rim, the outflow of water was relatively slower so that an almost-constant water level was maintained for some time. This resulted in the formation of well-developed, prograding deltas described in more detail below (Fig. 4.4d).

As a consequence of water level behaviour in the crater lake, three main types of delta morphologies developed: A) a retrograding, stepped delta morphology with multiple steep delta faces formed during rising water level (Fig. 4.4a, 4.4c and 4.5a); B) a prograding delta morphology with a single steep delta face formed during constant water level (Fig. 4d, 4.5b and 4.5c), and C) an incised delta with a telescoping morphology formed during falling water level (Fig. 4.4b). We will refer to this as large-scale or primary morphology.

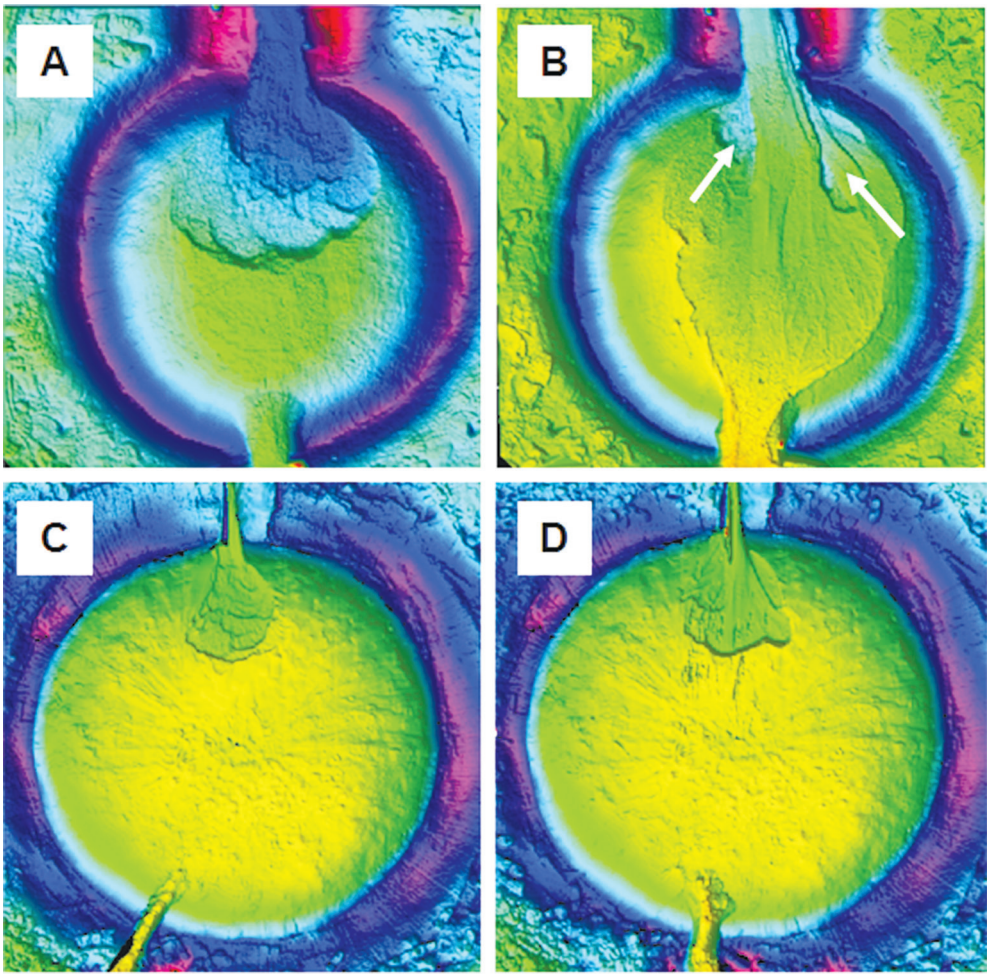

Figure 4.4: Shaded DEMs of deltas into constructed craters. A and B have a 2 m crater (run D); C and D have a 4 m crater (run P). Water and sediment enter from the top. (a and c) Retrograding, back-stepping morphology as a result of basin level rise. Note that the crater rim was breached after the experiment to empty the lake in order to measure topography. (b) Telescopic and incised prograding morphology as a result of rapid water level fall after breaching the crater wall; note terraces flanking the central channel. (d) Prograding morphology as a result of nearly constant basin level; note minor terraces flanking the central channel. See DEM colour bar in Figure 4.2.

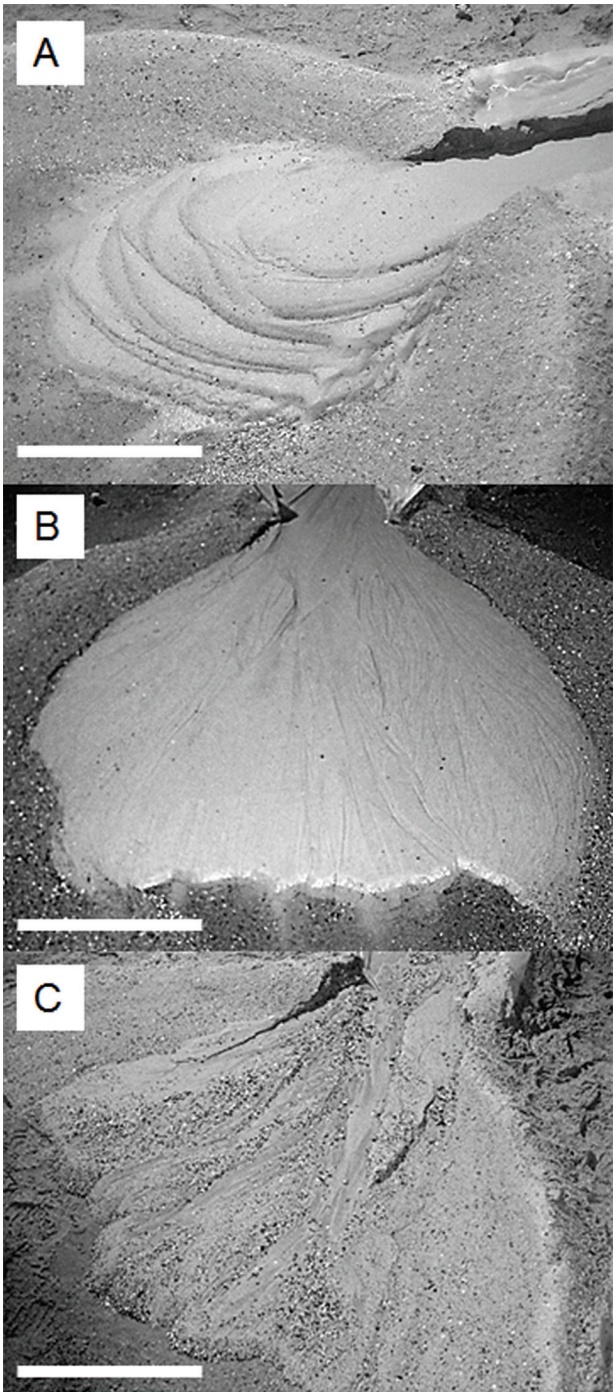

Figure 4.5: Examples of delta deposits in the laboratory. (a) Smooth, retrograding, stepped delta (run F), (b) smooth, prograding delta (run G) and (c) branched, prograding delta (run B). White line is ~50 cm.

The profiles of both the retrograding and prograding deposits (Fig. 4.6) demonstrate steep delta faces dipping about 25-27 degrees, formed as a consequence of the predominant bed load transport (e.g. Postma 1990). The retrograding deposit profiles are distinctly stair-stepped with multiple, stacked, tabular delta bodies, whereas the prograding deposit profiles show only one continuous top-set and one delta face, much like a classic Gilbert-type delta. Each main type morphology deviates in detail (which we here refer to as secondary morphology) as a consequence of differences in water discharge and sediment texture. Deltas had more lobes during low discharge conditions as well as when poorly sorted sediment was used. We refer to the occurrence of more lobes as increasing lobateness, and we describe these variations in more detail below for the two experiment phases.

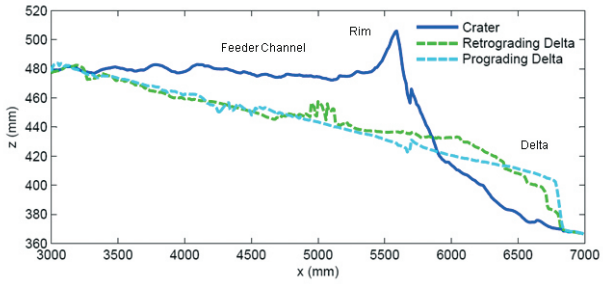

Figure 4.6: Long profiles of run P showing the difference in profiles of retrograding and prograding delta deposits. Flow is from left to right into the crater basin. The crater rim can be seen in the original topography (blue line).

4.3.1 Phase 1 - rising water level

In the initial phase of the experiment the flow rapidly cut into the intersection of the crater and the upstream channel. The primary morphology of back-stepping or retrograding deltas was created mainly by the rising water level and all our phase 1 experiments showed similar primary morphologies due to this factor. Repeated bank collapse in the upstream channel is essential for the formation of back-stepping morphology, as the collapsed sediment temporarily enlarges the sediment flux to the delta. On a smaller scale, the retrograding deltas showed large variety in secondary delta morphology. Independent variables other than water level resulted in morphological elements that are superimposed on the primary, large-scale morphology. These independent variables are 1) discharge; 2) sediment texture (grain size and sorting) and percentage of suspended material; 3) basin size and feeder channel width (Table 4.2).

High discharge (0.35 l/sec) showed much less channelization on the delta surface than low discharge (0.07 l/sec) due to the wide sheet flow that dominated in these cases, and resulted in a more evenly distributed stepped delta with smooth edges (Fig. 4.7a). On the other hand, lower discharge caused more and smaller lobes – thus creating a somewhat frayed edge for the deposit (Fig. 4.7b). Low-discharge experiments show channelization on the delta surface as the flow focused in weakly-defined channels that transported sediment to a segment of the shoreline. Nodal channel avulsion caused erratic, lobate stacking. In summary, a smaller discharge formed narrower channels that produced smaller lobes, and poorer sorting of the

sediment caused more spatial sorting patterns that enhanced channelization, which also produced lobes.

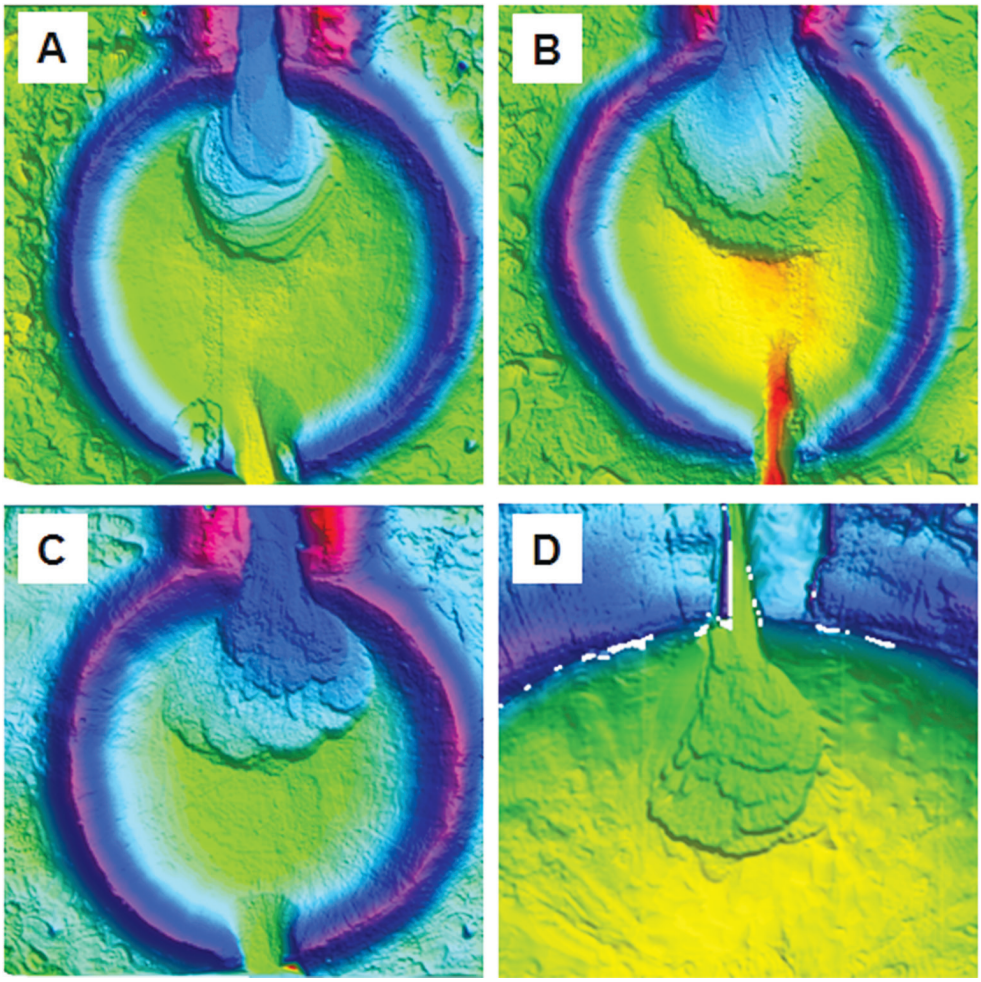

Figure 4.7: Shaded DEMs of four retrograding back-stepping deltas formed during rising base level. (a) Run F (see Table 4.1) with high discharge, well-sorted fine sand in a small basin (2 m) showing a pancake stacking of lobes; (b) Run G with low discharge, well-sorted fine sand in a small basin (2 m); (c) Run D with high discharge, moderately sorted coarse sand in a small basin (2 m); and (d) Run P with high discharge, moderately sorted coarse sand in a large basin (4 m, also shown in Fig. 4.4c). Vertical striping in A and B is a minor DEM error made visible by the shading. See DEM colour bar in Figure 4.2.

Coarser grain sizes (0.45 mm, poorly sorted) resulted in a more lobate delta shape and less well developed steps (Fig. 4.7c). Finer grain sizes (0.225 mm, well sorted) resulted in a less lobate shape and better developed steps (Fig. 4.7a; see trend in Fig. 4.8). Clear sorting patterns were observed in the delta sets that were formed from the coarse and poorly sorted sediment. The top-set was coarse and often armoured. The delta front was locally fining-upward but varied strongly spatially as each lobe and avulsion formed its own foreset. The toe-set consisted of very fine sand to silt that was deposited from suspension, only when a

significant amount of fine material was supplied to the system. This stratigraphic size-sorting is consistent with terrestrial Gilbert-type deltas. As can be expected, in the experiments with finer and well sorted sediment it was more difficult to observe clear sorting patterns. In some cases (e.g. experiment F) we observed a surprisingly regular pattern of increasingly smaller semi-circles tabularly stacked one upon another (Fig. 4.5a and 4.7a). Here we observed sheet flow rather than channelized flow, similar to the experiments of van Dijk *et al.* (2009).

Deltas in the large 4 m crater basin experienced a much slower water level rise during phase 1 and a slower fall during phase 2. Hence the steps are fewer and the foresets are more pronounced (see Fig. 4.7d) compared to those in the 2 m basins. Furthermore, as visible in Figure 4.7, the extent of the delta deposit is much less influenced by the physical crater rim boundaries for the bigger crater (Fig. 4.7d) than for the smaller crater (Fig. 4.7a to c). In the small crater the delta deposit merges with the crater rim, while in the bigger crater the delta deposit does not, demonstrating that its fan-shaped morphology is unaffected by the crater rim. Hence, the ratio between the fluvial input and the size of the receiving basin may constrain delta morphology.

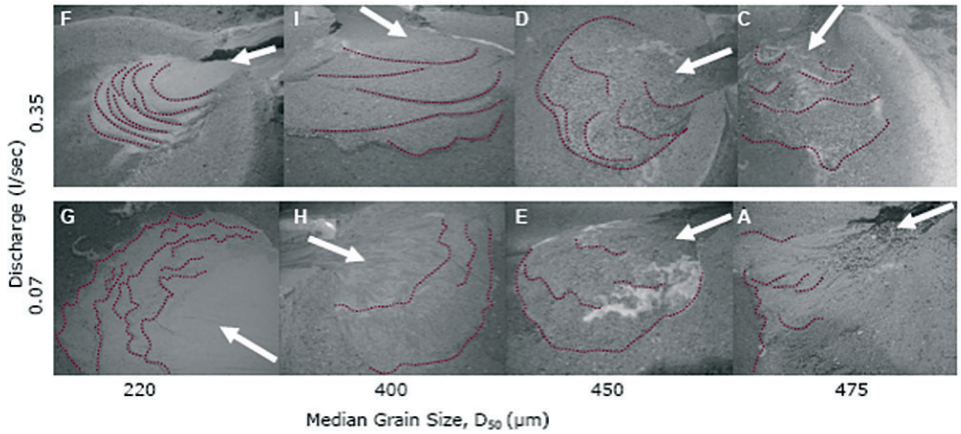

Figure 4.8: Photographs of eight retrograding back-stepping deltas formed during rising base level in a small basin (2 m), showing an increase in lobateness with increasing grain size and decreasing sorting (x-axis) and decreasing lobateness with increasing discharge (y-axis). Flow direction is indicated by white arrows.

Water loss occurred in the crater lake as a result of the permeability of the sand, especially during first event experiments (Fig. 4.9). The ratio between the volume of water entering the crater ($V_{waterinflow}$) and ponding water in the crater basin (V_{lake}) is in our experiments $V_{waterinflow}$:V_{lake} $\geq$ 1. To obtain the minimum ratio of 1 we assumed that all lakes were filled at least 55% up to a lake depth of 8 cm. A different assumption will merely shift the data points up or down in Figure 4.9. Ideally the lake water level would have been measured during the experiments which could have led to somewhat different values, but we do not expect much difference between the assumed and true maximum lake level so the trend remains the same. Figure 4.9 demonstrates that for experiments of long duration a large amount of water up to a factor of 5 of the lake volume was lost into the sub-surface through permeation. This occurred particularly when we used low discharge in long-duration experiments, because the

amount of water that was added in each time step was small. This effect is much less obvious in the large crater lake experiments.

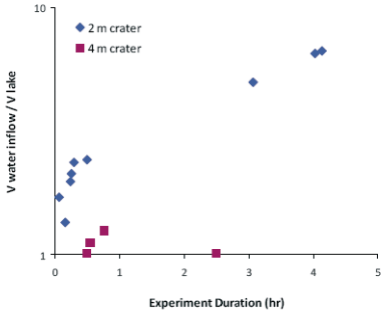

Figure 4.9: The water balance of the lake in Phase 1 experiments, showing the ratio of real water inflow and final lake volume as a function of experiment duration.

4.3.2 Phase 2 - constant and falling water level

Phase 2 experiments were initiated manually by creating a minor dent in the crater rim once the water level in the crater had reached the current height of the mouth of the feeder channel that cuts through the crater wall. The breach never occurred at the 100% full level, but always at an earlier point as the feeder channel eroded into the crater rim while filling the crater. For the small crater, we estimate that the basin was usually about 80% full. For the large crater, the basin was no more than around 50% full. This difference between the small and large crater is a reflection of the fact that it took relatively much longer to fill the large crater than it took to fill the small crater (also due to larger sub-surface lateral discharge), and during that time the stream eroded more than halfway into the rim of the crater.

Incision occurred regardless of the amount of discharge; however we observed morphological differences in the incisions based on the amount of discharge. During the breaching event, the high discharge events created deeper incisions into the delta deposit than the low discharge

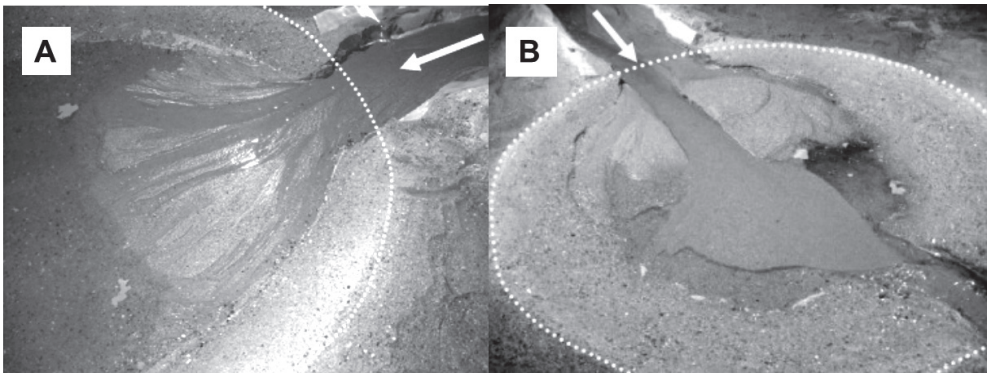

Figure 4.10: Different degrees of incision of the original delta deposit depending on the discharge. (a) Multiple channels incise in the delta plain (run H, 0.07 l/sec); (b) major channel incision on the delta plain (run I, 0.35 l/sec). Flow direction indicated by the white arrows and crater rim (2 m diameter) indicated by the white dots.

events. For example, multiple channels were formed during low discharge, and a major single channel during high discharges (runs H and I respectively; Fig. 4.10a and 4.10b).

In both discharge cases the original stepped delta was partly eroded, but during high discharge much of the original deposit remains in the form of terraces raised about 2 cm above the channel elevation and the material that was eroded by this incising channel was reworked into a new delta (Fig. 4.10b). The term "terrace" is used here solely to refer to the erosional remnant that is left after a channel has incised a delta. The deltas in these experiments were generally dominated by focussed erosion of the central parts and rapid deposition of the eroded sediment downstream. When the water level fell rapidly, the water flow destroyed parts of the original delta body, and formed deep incisions flanked by terraces. Rapid incision caused rapid abandonment of the delta plain by funnelling all the discharge through the incised valley. Especially in case of high (catastrophic) discharge (e.g. experiments D, F, I, but especially J), incision occurred very rapidly. Consequently less than 25% of the delta deposit by area was eroded by the self-confined incised channel, so that laterally more of the original deposit remained in the basin. During low discharge on the other hand, shallow incisions (e.g. experiments E, G, H) caused destruction of the delta across a larger area of the delta plain (Fig. 4.10a) due to lateral channel migration without carving such deep incisions into the delta. Thus, lateral channel shift forced by low discharge is crucial in maintaining the development of a unified delta front after crater rim breach. The formation of large terraces on the delta surface (Fig. 4.4b and 4.10b) could only be avoided if the discharge was low and the water level was constant for some time, i.e. the water left the basin at the same rate that it entered, whilst maintaining some ponding water in the basin. This was never completely the case in our experiments within the 2 m diameter crater because the crater rim continued to erode much faster than anticipated, even when cohesive material was added to the gravelly river sand. However, in the 4 m craters the rim erosion was less abrupt and nearly constant water level was maintained in most of the phase 2 experiments. Hence a more pronounced delta foreset developed, overprinting the less clearly stepped fan of phase 1. Minor erosion caused by high discharge created small terraces flanking the new channel (Fig. 4.4d). In all cases where the water level fell while the lake was still fed, the delta deposit was incised.

As in the Phase 1 experiments, coarser grain sizes resulted in more lobes on the delta front. The poorly sorted sand and silica flour mix (experiments K-N) was eroded much slower in the upstream feeder channel. The silica flour was transported in suspension further into the basin than the sediment transported as bed load (Fig. 4.11). The adhesive properties of the silica flour appeared not to have much effect on the erosion rate of the downstream crater rim (which was also constructed from poorly sorted sand with a percentage of silica flour), and thus water level dropped swiftly despite the extra adhesion. Additionally, almost no difference between 20% (experiment K) and 40% (experiment M) silica flour was observed in the erosion rates in the upstream feeder channel, on the fan itself, nor in the downstream breached crater rim.

Figure 4.11: Thin layer of fine white sediment (silica flour) draped over the delta deposit and the crater floor (run L). Flow from right to left, with low discharge, and 20% volume percentage of silica flour mixed with sand.

4.4 Quantitative approach

Since laboratory results show that the formation of delta morphologies in crater-shaped basins are similar to delta morphologies in some craters on Mars, and that these morphologies can be coupled in a simple way to discharge events and grain size, it is important to quantify the laboratory results in order to predict minimum duration of hydrological activity. This would further lead to predictions whether periods of wet climate are required on Mars or that short duration events would suffice for the formation of the Martian crater deltas.

For Martian deltas we would want to know the dominant formative processes to infer the formative flow discharge and duration of the event or multiple events. One method to do this is by calculating volumes of the water and sediment bodies and dividing these by fluxes calculated from the upstream channel dimensions (Kleinhans 2005a). In the experiments, the boundary conditions and formative duration were imposed and the dominant processes were observed. By using physics-based methods for calculation it should in principle be possible to compare small-scale experiments on Earth with full-scale examples on Mars. This requires that the proper processes at both scales are included. We will therefore combine the experiments with predictive calculations for two purposes: to assess scaling effects in the detailed flow and sediment transport processes, and to estimate relevant dimensionless parameters that allow application of our results to Martian systems.

First, detailed flow and sediment transport that could not be measured in detail in the present setup are calculated. Flow discharge is controlled, but velocity and depth measurement is inaccurate in such shallow flows. These variables are nevertheless required to assess possible scale effects and calculate dimensionless parameters to be compared to those on Mars. We therefore present a method to calculate flow friction in the laboratory. Second, the experimental data allow a basic proof of principle for the method used to calculate formative duration for Martian cases, which is sediment transport calculation from channel dimensions and formative duration estimation from deposit volume. Furthermore, we will assess to what extent the standard prediction of sediment transport under-predicts the formative time scale

because the fast initial deposition is ignored. We apply a sediment transport predictor for bed load appropriate for very steep slopes to predict slope development for a schematized experiment in a large crater to back-calculate the formative duration and the importance of hyper-concentrated flow in general. Finally, we apply the sediment transport prediction to the final measured conditions and compare predictions against measurements for all experiments to analyse the effect of the underlying assumptions as well as the independent variables. Furthermore the analysis will show whether the relevant dimensionless numbers are within the range of the calculated cases on Mars (reported in Kleinhans *et al.* 2010a). In our quantitative analysis of sediment transport as observed in the experiments we will further discuss how we apply our findings quantitatively to Martian deltas.

4.4.1 Calculation of flow resistance

Calculation of bed shear stress τ [N/m^2], the driving force per unit area for sediment transport, requires a water depth h [m] and a gradient S [m/m]:

$$\tau = \rho\, g\, h \sin(S) \tag{1}$$

where ρ is the density of water, here 1000 kg/m^3, and g is the gravitational acceleration, here 9.81 m/s^2. In the experiment, the final channel slope was measured, the channel width W [m] was measured and the flow discharge, defined as $Q=Whu$ where u [m] is flow velocity, was set. This leaves the unit discharge $q=hu$ [m^2/s] known but the values of h and u unknown. For Martian conditions these can be calculated from a semi-empirical friction relation (see Kleinhans 2005a), but for the shallow-flow experiments we must use a different approach. Three alternative assumptions about the relation between h and u are compared here.

The first possible assumption is that the flow is critical with Froude number unity, defined as:

$$\mathrm{Fr} = u/\sqrt{(g\, h)} \tag{2}$$

This condition is commonly found in natural gravel-bed rivers that are more or less in equilibrium (Grant *et al.* 1997). Steeper slopes of rapidly incising channels are however known to become supercritical temporarily (Cantelli *et al.* 2004).

The second possibility is to assume that the flow resistance is constant, or C=c, where

$$C = \sqrt{(h\, S)} / u \tag{3}$$

according to the law of Chézy (Rickenmann 1999, his equation A13). From this it follows that:

$$\mathrm{Fr} = C^2\, S / g \tag{4}$$

The third possible assumption is to use the empirically found flow resistance predictor of Ferguson (2007, equation 16b), which was designed and calibrated for shallow gravel bed rivers over a large range of channel slopes:

$$C = \sqrt{(g)}\, \alpha^{0.4}\, [q/\sqrt{(g\, (D_{90})^{0.3})}\,]^{0.6}\, S^{0.2} \tag{5}$$

where α (an empirical fitting parameter) is in the range 1-4, here chosen as 2. It is noted that this friction coefficient C does not include the extra friction due to high sediment concentration.

In our flume experiments the channel slope varied between 0.27 m/m, the slope at the first instant of flow when it entered the crater from the channel, and 0.01 m/m. We compare the Froude and Chézy numbers for the three assumptions along this range of slopes (Fig. 4.12a and 4.12b). For *C*=c and the Ferguson relation the Froude number decreases with decreasing slope from a high value (Fr~1.2-1.4) where anti-dunes are stable (Cartigny *et al.* 2013 (in press)) and which we did observe in the experiments, to a rather low value for flat bed experiments where the *C*=c assumption takes an intermediate position between the Fr=1 and Ferguson assumptions. The Chézy number depends inversely on slope for the Fr=1 assumption, and increases slowly with slope for the Ferguson predictor. The three assumptions have similar *C* for *S*≈0.1. To summarize, the assumption of constant Chézy number leads to intermediate Chézy numbers and Froude numbers between the other two methods, so for the remainder of this paper we use *C*=c for calculations on experimental data, thus following Rickenmann (1999).

4.4.2 Sediment transport rate

Two predictors for sediment transport were used: the Meyer-Peter and Mueller (MPM) (1948) predictor and the Smart (1984) predictor. The MPM predictor is valid for bed load dominated transport and was successfully calibrated and tested in the laboratory within a factor of 2-3 for the entire range from beginning of motion to high mobility (Kleinhans and van Rijn 2002; Wong and Parker 2006). Given the flat bed conditions in the experiments, total shear stress is used for transport prediction and no correction for form drag by bed-forms is applied. It was applied in the same manner to Martian deltas (Kleinhans 2005a; Kleinhans *et al.* 2010a).

MPM is calculated as:

$$\varphi = 8(\theta - 0.047)^{1.5} \quad (6)$$

where θ is the Shields mobility number defined as:

$$\theta = \tau / [(\rho_s - \rho)\, g\, D_{50}] \quad (7)$$

where ρ_s is the density of sediment, here 2650 kg/m^3. Dimensionless transport φ is defined as:

$$\varphi = q_b / \{[(\rho_s - \rho)/\rho]\, g\, D_{50}{}^3\}^{0.5} \quad (8)$$

where q_b is the dimensional transport rate in m^2/s, which is m^3/s per m channel width.
The Smart predictor is an extended version of MPM which was empirically adapted for high concentrations and steep slopes nearly up to the angle of repose, and is formulated as:

$$\varphi = 4.2\, S^{0.6}\, C\, \theta^{0.5}\, (\theta - \theta_c) \quad (9)$$

where is the critical Shields number for incipient motion, here taken at 0.047 for consistency with MPM.

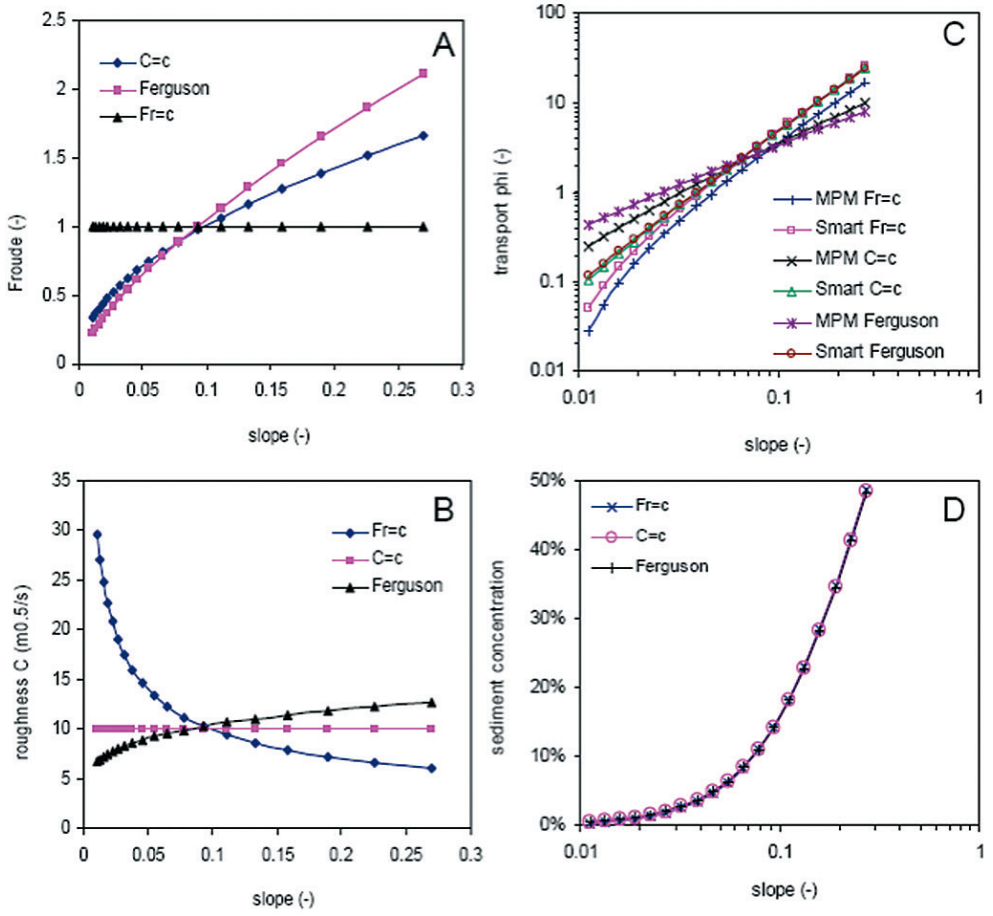

Figure 4.12: (a) Froude number (Fr) as a function of bed slope for three different assumptions for flow depth and velocity calculation where Fr is constant, C is constant or the resistance relation of Ferguson (2007) is used. (b) Chézy resistance coefficient (C) as a function of bed slope for the three different assumptions for flow depth and velocity calculation. (c) Dimensionless sediment transport rate as a function of bed slope for the Meyer-Peter and Mueller (1948) sediment transport predictor (MPM) and the Smart (1984) predictor for the three different assumptions for flow depth and velocity calculation. (d) Volumetric sediment concentration in the flow as a function of bed slope for the Smart (1984) predictor for the three different assumptions for flow depth and velocity calculation.

The prediction of transport rate is compared for all combinations of the two sediment transport predictors and the three assumptions for flow calculation (Fig. 4.12c). For steep slopes S>0.06, the Smart relation predicts higher transport rates than the MPM relation in all cases. For lower slopes, the Smart relation predicts rates intermediate between rates with MPM and Fr=c on the lower end and MPM with C=c and Ferguson on the higher end. The volumetric concentration of sediment in the flow for the Smart relation hardly depends on the assumption for flow behaviour and is less than 5% for slopes S<0.05. For channel slopes approaching the angle of repose the sediment concentration approaches that of unconsolidated sediment at rest. This behaviour is expected as avalanching will occur at such angles with such concentrations.

To summarize, the transport rate depends strongly on channel slope. The differences between the assumptions for the calculation of flow conditions are large but have a limited effect on the transport prediction. The assumption of constant Chézy number leads to intermediate Chézy number and Froude numbers between the other two methods, so for the remainder of this paper we use C=c. But the sediment transport rate may vary during formation and thus the effect of the time-dependent evolution of the eroding channel on the estimation of formative time scale based on the final slope must be investigated further.

4.4.3 Idealized model for linearly decreasing channel slope with time

Formative duration is calculated from sediment transport rate and delta volume. For Martian cases the final channel morphology has to be used for flow and sediment transport calculation, but in the experiments we observed the initiation of the channels, including the transition from initial slope failure and hyper-concentrated flow to the dilute flow that is assumed in the predictors. Real formative time scale in the laboratory is accurately determined by the experiment duration, and the real volume of the deposited delta can accurately be measured from DEMs. The channel slope was only measured after the experiment, but was much steeper during the beginning of the experiment and gradually declined as the channel eroded. This was particularly the case in the vertically exaggerated crater experiments. Therefore we can use the experiment data given in Table 4.3 to test the bias in the calculation of formative duration from final channel dimensions.

As flow is transporting sediment, the channel feeding into the lake is eroded whilst the delta grows by deposition. The initial channel was very steep at the point where it entered the lake, but rapidly became gentler and longer as it eroded. For the estimation of the formative time the final channel slope must be used because only that is observable (Kleinhans 2005a). We investigated the effect of the time-dependent slope on the formative time scale estimate by an analytical method. The idea is to calculate the duration of erosion of a series of wedges as the channel cuts backwards. The underlying assumption is that the channel slope is straight, that the base of the channel remains fixed at some point on the crater wall, and that the flow can be calculated assuming C=c and sediment transport can be calculated with Smart (1984).

Table 4.3: Initial values for the idealized model scenario.

Parameter	Value
Flow discharge [m^3/s]	$1.0x10^{-4}$
Channel width [m]	0.1
Initial slope [m/m]	0.27
Knickpoint depth [m]	0.056
Rim height [m]	0.028
Rim width [m]	0.24
D_{50} of sediment [m]	$0.45x10^{-3}$
D_{90} of sediment [m]	$1.0x10^{-3}$

A logarithmically decreasing series of slopes is predefined to represent the back-cutting channel, where S_1=0.27 (the initial slope on the large experimental crater wall) and S_{final}=0.01 (the final slope which is the minimum of the observed final slopes in all experiments reported

here). The cross-over point where the eroding channel becomes the delta deposit is the starting point for all measurements (Fig. 4.13). Based on DEM values from experiment P, a difference in height of 0.056 m between the cross-over point and the original channel elevation is used. It may have varied in reality as the lake filled, while the channel cuts back, but this could not be measured. The height (h) and the slope together define the channel bed where channel length is calculated for each slope S_i as L_i=0.056/S_i and the channel head is located at distance L_i from the crater rim. Two subsequent slopes define an obtuse triangle of sediment (a sediment wedge), of which the surface area A_i is calculated as $A_i = 0.056 (L_i\text{-}L_{i\text{-}1})/2$ where (L_i-$L_{i\text{-}1}$) is the length of the base of the obtuse triangle and 0.056 is the height. The volume of eroded sediment for each step is WA_i where W is the channel width (in this case 172 mm). The time to erode this volume of sediment is calculated as detailed above, using a staggered scheme with slopes $S_{i:(i+1)}$ in between the slopes S_i defining the obtuse triangle to better represent average conditions during the erosion of this segment.

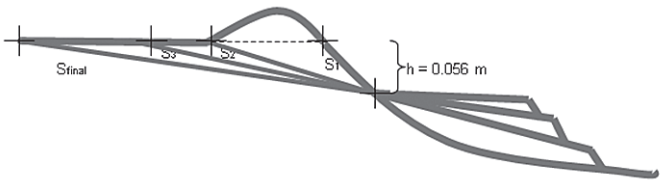

Figure 4.13: Schematic drawing of the back-cutting process that erodes sediment from the upstream channel and deposits this sediment as a delta in the downstream basin. Flow is from left to right. Compare to measured profiles in Figure 4.6. Specifically for run P, rim height is ~0.160 m, knickpoint height is ~0.087 m, rim width is ~0.180 m, and knickpoint distance is ~2.670 m from the flow starting point. The rim height and width add extra eroded sediment in the first phase of channel cutting. The slope of the eroding channel is assumed to be straight with an upstream knickpoint.

As expected from Figure 4.13, the slope decreases rapidly with time as the channel erodes backwards (Fig. 4.14a). Likewise, the knick-point or channel head migrates slower and slower as the experiment progresses and slope decreases. Consequently, a large fraction of the valley volume is eroded in a relatively short initial time period that is characterized by very large transport rates (Fig. 4.14b). From the increase of volume in the final stage, a linear under-estimate can be obtained by extrapolation (Fig. 4.14b) of the time required to erode the entire valley. Only half the volume of sediment would have been displaced by the transport rate at the end of the experiment.

In summary, this analysis shows that calculation of a formative duration based on the final slope overestimates the duration by about a factor of 2 for typical experiment settings. This bias is ascribed here to the large transport rates that occur over the initial steep slope from the channel into the crater as observed in our experiments. Furthermore the transport rate is highest immediately after the connection between water source and impact crater basin causing hyper-concentrated flows. Such a flow forms a fan-shaped deposit akin to a mass flow dominated alluvial fan without a deltaic coastline, because the water table has not yet reached the deposit. This was also observed in the Kraal *et al.* (2008b) experiments.

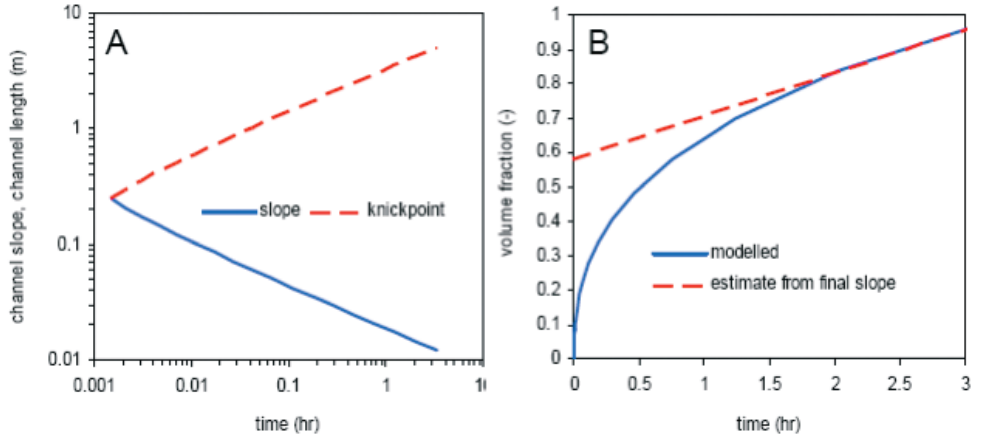

Figure 4.14: (a) Relaxation of slope over time and increase of knick point distance from the crater rim (which is the upstream channel length). (b) Normalized volume transported over time for the idealized scenario (Table 4.2) 1) showing a decline of delta volume growth rate as slope decreases over time. Extrapolation of the trend based on transport calculated for the final slope underestimates the deposit volume a factor of about 2 (intercept near 0.6).

4.4.4 Back-calculation of sediment transport rate and formative duration

The results of the experiments are interpreted based on the above analysis of appropriate flow and sediment transport predictors and the idealized model. First the volume of the delta is calculated by subtraction of the initial DEM from the final DEM for the region of interest covering the recognizable delta. The predicted experiment duration that is required for the formation of a delta is referred to as event duration and can be calculated as the measured volume of the delta divided by the predicted sediment transport rate. The predicted event duration generally matches the measured event duration (Fig. 4.15a). The formative duration of the delta is predicted within a factor of 3 for 8 out of 13 cases.

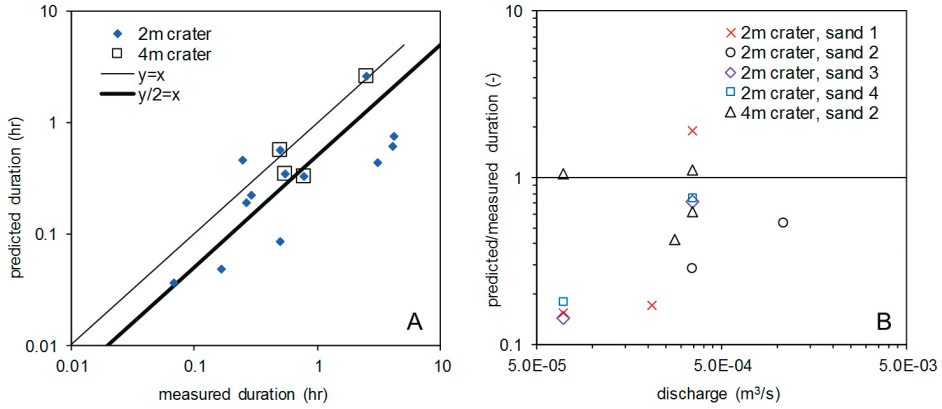

Figure 4.15: (a) Comparison of true and predicted event duration. Prediction is based on the measured delta volume divided by sediment transport rate predicted for the final slope. The y/2=x line indicates the possibility that measured delta volume is underestimated with a factor of 2, or that sediment transport rate based on final slope underestimates the transported volume with a factor of 2. (b) Lack of relation between the discrepancy ratio (predicted/measured duration) and discharge for all sediment types and crater sizes. The large crater experiments are more accurate and have predictions within a factor of 2.5.

The discrepancy ratio of predicted and measured formative duration is plotted in Fig. 4.15a, where a ratio of unity implies perfect prediction. Experiments with low flow discharge may have lower discrepancy ratios because a significant proportion of the water is lost to the subsoil (Fig. 4.9; see following subsection). Furthermore, poorly sorted sediment may form an amour layer on the channel bed surface (Kleinhans and van Rijn 2002), which we indeed observed in experiments with the largest D_{90} and poorest sorting. However, we found no significant relation between the discrepancy ratio, imposed flow discharge, and D_{90} of the mixture (Fig. 4.15b). For the smallest discharge the discrepancy ratios are indeed low for all sediments, except for the large crater experiments. We speculate that the small crater experiments have a relatively large volume of sediment to saturate below the channel and the crater rim, but this cannot be supported with observations.

Prediction of sediment transport for experiment conditions of small water depth and relatively large bottom roughness are at most within a factor of 2 of the measured values, if measured under highly controlled conditions required for accurate flow shear stress determination. However, in cases where the final slope had to be used instead of a time-dependent slope for transport calculations, the shallow flow conditions may cause a factor of 10 uncertainty in transport rate.

4.4.5 Scaling aspects

Several scaling issues have to be addressed when experiments are used to interpret full-scale prototypes, in particular with reference to the difficulty of correctly scaling flow parameters, grain size, and basin floor permeability. Analysis of scaling between prototype and experiment serves to isolate experiment scale effects from phenomena that are expected to occur in nature as in the experiment, and to calculate the possible mismatch between values of variables in prototype and experiment (Cantelli *et al.* 2004; Kleinhans *et al.* 2010b; Lajeunesse *et al.* 2010). The most important variables are the dimensionless numbers characterizing essential aspects of flow and of sediment transport. These are the 1) Reynolds number for the flow, 2) the particle Reynolds number for the boundary layer of the flow, 3) the Shields mobility number and 4) the Froude number (Paola 2000; van Heijst *et al.* 2001; Paola *et al.* 2009).

The Reynolds number of the flow assesses the occurrence of turbulence and is estimated as $Re=uh/\nu$ (-), where u (m/s) is the flow velocity, h (m) is the water depth and ν is the viscosity of water (about $1x10^{-6}$ m^2/s). For Re>500-2000, the flow is turbulent and for lower values of Re it is laminar. Flow conditions inferred for Martian channels are always far above the transition to turbulence (Kleinhans 2005a), but Reynolds numbers are always low in the experiment channels because of the limited flow depth. For a low estimate with $u\approx0.15$ m/s and $h\approx0.005$ m, the $Re\approx750$ which is in the transitional regime. This may have reduced the tendency to suspend sediment but below we show that mobility was well within ranges expected on Mars. Furthermore, Lajeunesse *et al.* (2010) argue in detail, from the physics underlying channel and bar formation, that turbulence is not important for the evolution of large-scale morphology in experiments.

The particle Reynolds number characterizes the boundary layer of the flow. Hydraulically smooth conditions occur when the laminar sub-layer at the bed is thicker than the particle size, which in our experiments (in water at about 10-20°C near the beginning of

sediment motion) is the case for sediment of 0.5 mm diameter or smaller (Kleinhans *et al.* 2010a; Lajeunesse *et al.* 2010). Hydraulic smooth conditions are conducive to the formation of unrealistically large scour holes and ripples, but to ensure sediment mobility, experiments require sediment as fine as possible without becoming cohesive, which happens for 0.06 mm or less. Our solution for the experiments described here was to use poorly sorted sand, where the small median diameter ensures high sediment mobility whilst the presence of larger particles (up to fine gravel) disrupts the laminar sub-layer (Kleinhans *et al.* 2010a). To assess the effect of different mixtures we varied sorting and also used fine sand as used in the Kraal *et al.* (2008b) experiments. The Kraal-experiments indeed showed such unrealistic scour holes, but our present comparison shows that this does not affect the general conclusions.

The Shields number characterizes sediment mobility. This depends on the flow shear stress and the particle size. In the case of Martian systems, the flow conditions of the prototype are unknown and have to be inferred from final morphology and spatial context. The particle size is even more uncertain as it can hardly be seen on imagery and usually must be inferred from locations far away from the study site of interest. However, it is much larger than in most terrestrial systems that have been scaled to laboratory experiments, and the scaling of the Martian fan deltas is therefore probably more optimal than for terrestrial deltas. Based on such limited observations and inferences, the mobility of many cases on Mars is in the transitional range between bed load dominated and suspended load dominated conditions (Kleinhans *et al.* 2010a). This was calculated assuming the final channel slope to be representative. The experiments likewise show low mobility numbers for bed load and suspended load conditions. This fact independently confirms that the method is valid, because otherwise the mobility number would have been below the threshold for motion, which would not have led to channels and deltas, or high in the suspension regime, which could not have formed the Gilbertian profiles with lee sides up to the angle of repose. But the scenario calculation demonstrated that the mobility was much higher initially - high enough to initiate hyper-concentrated flow and upper stage plane bed conditions (see Kleinhans 2005a). Given the similar range of mobility numbers of experiments and inferred prototype conditions, hyper-concentrated flows can also have occurred on Mars on the initially steep slopes. The sediment transport predictor used here for the high slopes is deemed appropriate to Mars (Parsons and Nimmo 2010) because its concentrations approach that of granular avalanches at the angle of repose, and the angle of repose on Mars is not very different from that on Earth (Kleinhans *et al.* 2011).

Flows in experiment channels like those in our experiments are generally turbulent and sub-critical. With sub-critical flow and self-forming rivers as feeder channels, exact Froude scaling was neither fully attainable nor necessary (Postma *et al.* 2008; Kleinhans *et al.* 2010a; 2010b). Flow reconstruction in Martian channels indicates that at least in the final stages the flow is sub-critical (Kleinhans 2005a). We suspect that flow into the Martian craters can well have been supercritical at first when the slope was much steeper. However, the evidence is mostly eroded so this cannot be verified from the presently known sites on Mars. In spite of scale effects in the hydraulics of flow, we maintain that these experiments are very suitable to explore large scale morphological features and formative processes in delta building, because landscape experiments reproduce these features so well (see also Paola *et al.* 2009). Due to the observation that these types of laboratory examples show more dependence on boundary

conditions and less dependence on actual sediment transport dynamics (Postma *et al.* 2008), the similarity of process approach (Hooke 1968) was deemed sufficient for our experiments.

4.5. Discussion

Our results show that the primary morphology of our experimental deltas is determined by the behaviour of the water level in the basin, and that the secondary morphology is mainly determined by other variables such as flow discharge and particle size distribution. In Figure 4.16, we illustrate the two factors that dominate the morphology of these delta deposits: water level behaviour (rising, constant and falling) and the main processes (flow discharge and sediment texture) that facilitate channelization. When there is channelization and not sheet flow, the degree to which the delta is channelized is a measure of bank stability, which is expressed by the amount of small channels on the delta surface. Low bank stability results in many short lived shallow depth channels (like on alluvial fan surfaces), while increasing bank stability results in a few single-thread channels (e.g. Leopold and Wolman 1957). In the laboratory results the degree of channelization depends on the channel width relative to delta width and on the avulsion rate at the apex of the delta (see also van Heijst and Postma 2001), which in turn are dependent on discharge, sediment texture, as well as basin size (which is directly related to the rate of water level rise/fall). These variables are all captured by the variable sediment mobility (see quantification section), which depends on flow discharge, grain size and channel slope.

4.5.1 Primary morphology: dependence on water level behaviour

As stated above, the primary morphology of the experimental deltas is determined by water level behaviour in the basin. The morphologically different types of deltas that were all formed under short period discharge conditions in the laboratory show a remarkable resemblance to many of the delta deposits that have been described for Mars (i.e. compare Fig. 4.1 to Figs. 4.4 to 4.11; see Cabrol and Grin 1999; Irwin *et al.* 2005; Di Achille *et al.* 2006a, 2006b; Kraal *et al.* 2008a; Hauber *et al.* 2009). The primary morphological features of both the laboratory and Martian deltas agree well with those of terrestrial deltas indicating that change of water level in the receiving basin is an important parameter (e.g. Schumm *et al.* 1987; Postma 1990; 1995; van Heijst and Postma 2001; Postma 1995; Muto and Steel 2004).

Morphological features of Martian deltas, such as their stepped profiles, thus illustrate that the water level history in the crater lake was dominant in determining delta shape. It means that catastrophic conditions and related rapid base level change in craters during delta formation played the dominant role in the shaping of the deltas, and that most deltas observed on Mars can form in one event (in agreement with Kraal *et al.* 2008b), simply because it is not possible to produce a stepped delta in more than one filling event without leaving evidence of surface alteration by subsequent overflow, such as incisions or terraces.

The *multiple foreset, stepped, retrograding delta* develops as a result of the rise in the water level (Fig. 4.16a) and the decrease of transport capacity of the feeder channel with decreasing gradient. Back-stepping delta lobes have been described as a feature of water-level rise (a transgressional shoreline by the original advocates of sequence stratigraphy e.g.

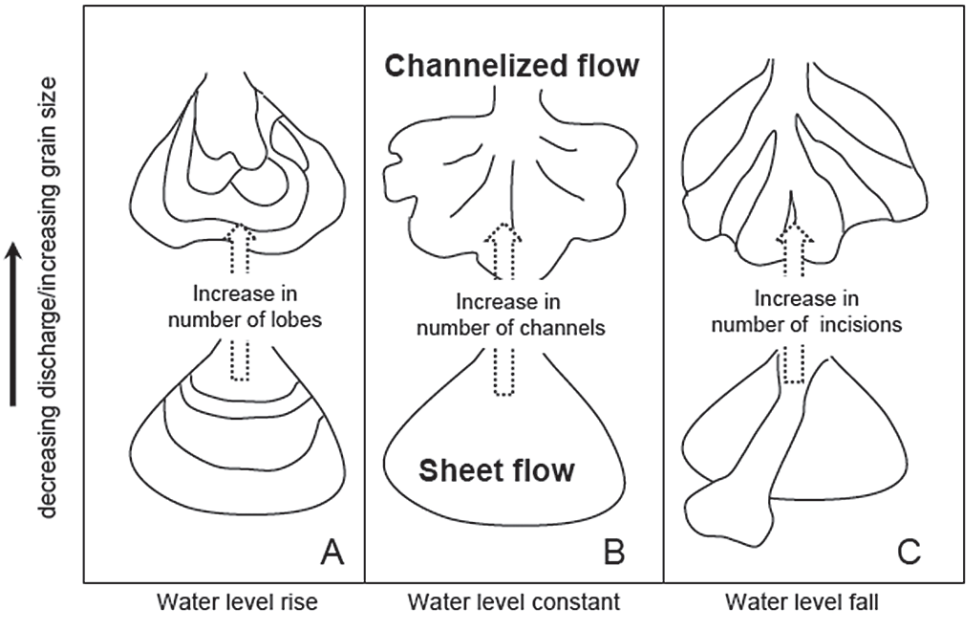

Figure 4.16: Three morphologically different types of delta deposits as a consequence of rising, steady or falling water level (shown here on x-axis). Sub-types of these deposits are formed based on the degree of channelization (shown here on y-axis) as a consequence of variation in flow discharge and sediment texture.

Posamentier *et al.* 1988; van Wagoner *et al.* 1988; van Heijst *et al.* 2001; Catuneanu *et al.* 2009).

Auto-stepping has been described by Muto and Steel (1992; 1997) as a primary process inherent to delta progradation onto a sloping basin floor during constant slow rise in water level that is responsible for stepped shorelines. The experiments by Muto and Steel (1992; 2001) were done with a constant rise in water level and a constant sediment supply. In experiments with independent base level control the sediment feed can be so high that stepped shorelines emerge without transgression of the water level. However, our experiments were done with a decreasing rate of water level rise that decreases due to the shape of the basin and a sediment supply that is not constant due to 1) the collapse of the upstream crater rim during the initial phases of the experiment, to 2) diminishing bank erosion due to widening of the feeder channel and decreasing flow velocity, and to 3) bank collapse in the upstream incising feeder channel as also observed by Kraal *et al.* (2008b). These two (constant rise in water level and constant sediment supply) factors are potentially responsible for a type of back-stepping that is strictly linked to the rise of the water level (transgression) and not necessarily an auto-cyclical process. Thus, in our experiments and by inference on Mars, the sediment supply that is decreasing with time is not nearly sufficient to fill the new accommodation space that is generated by the rapidly rising water level, and thus promotes the back-stepping morphology.

Major change in delta morphology, for instance from stepped fan to prograding fan, occurs only when the lake starts to spill over. For example, the *simple, single foreset, prograding delta* develops (Fig. 4.16b) during the breaching of the crater wall, when the

water level remains constant or is slowly falling. A *highly incised, telescopic, prograding delta* (Fig. 4.16c) develops when the water level is rapidly falling, which occurs by down-cutting of the crater rim. The rate of falling of the water level is crucial in the formation of these two different types of deltas.

A sub-type of the prograding delta, the *branched, lobate-shaped, prograding delta* (also Fig. 4.16b) is produced by reduced sediment mobility, thus in experiments with larger grain size and less well sorted sediment, or low discharge. Higher discharge maintains a more even delta plain surface because the run off is sheet-flow dominated. Lower discharge results in more channelized flow on the delta surface, which causes more lobate-shaped delta fronts (Fig. 4.16b). The depth and erosion rate of the breach would partly determine the water level, and the process is analogous to dike breaching and river bed erosion after dam removal (de Villiers *et al.* 2010) but is not further discussed here.

The erosive power of the stream always ensured that the apex of the delta was below the original rim height. We expect step-like formations visible all the way into the feeder channel if the system was left to be filled completely with water. In a few of our experiments we observed these steps retrograding all the way into the feeder channel. We never observed any step-like formations in the upstream feeder channels of the Martian deposits, and from this we infer that the Martian lakes may never have been entirely full when breaching occurred. In these few cases where the lowest part on the rim is at a higher elevation than the input stream, a breach was likely to form in the weakest part of the rim due to the pressure of the water in the lake against the rim rather than surface flow over the rim, which would not have been able to reach rim heights above that of the input stream. Numerous breached craters with both an inlet valley and an outlet valley, also known as "open basin lakes", have been identified on the surface of Mars, with more than 200 described by Fassett and Head (2008).

4.5.2 Secondary morphology: dependence on flow discharge and basin characteristics

An important aspect for the closed basin case considered here is that water level behaviour is directly influenced by discharge and basin hypsometry, which is rarely the case on Earth. Geological principles developed for terrestrial deltas cannot directly be applied to Martian deltas because on Earth the ocean acts as an infinitely large basin relative to the river discharge, and the sea level is not much affected by river inflow. But on Mars inflow is large relative to the basin size and the water level in the basin directly depends on the discharge as well as on the basin hypsometry. Thus for Mars, we propose this strong relationship between upstream flow discharge, basin hypsometry, and water level behaviour. This is in agreement with the results of Kleinhans *et al.* (2010a), who described a unique relation between delta shape and inflow discharge, given a basin hypsometry that determines the rate of lake level rise.

The extent to which lake level behaviour is influenced by discharge in closed impact crater basins also depends strongly on the permeability of the crater floor, because the relative loss of ponding water by infiltration is larger for the same final lake volume if the inflow rate is smaller. For Mars this permeability is largely unknown, but many impact craters were possibly quite permeable along the rim due to brecciation of the rock by the force of the impact itself, or due to earlier infilling of the crater by airfall fines or other fine material

brought by aeolian transport (French 1998). Large unfilled faults could also promote rapid loss of water from the crater basin, which would not lead to ponding and delta formation but alluvial fans instead. Low crater permeability is possible for craters with ice or water-rich saturated sub-surfaces, and in such cases no alluvial fans are formed since immediate ponding will lead to rapid delta formation. We argue for the formation of most of the Martian deltas, especially those in impact craters with a diameter > 5-10 km, by high discharge (catastrophic) aqueous events, thus providing enough water to fill even a somewhat permeable crater.

4.5.3 Secondary morphology: dependence on sediment texture

The large grain-sizes of Sand 1 distribution in the experiments (Table 4.2) enhance the stability of bars and channels on the delta surface producing more lobate deltas, but it also dramatically reduces the mobility of the channels by static bed surface armouring. The smaller grain size distributions of Sands 2, 3 and 4 resulted in more sheet-flow and thus a less lobate delta shape. The degree of sorting of the sediment also plays a role in the morphology; a more well-sorted sediment resulted in less channelization and vice versa. The experiments with well-sorted sand revealed better developed steps in the back-stepping delta not only due to the higher mobility of the sediment but also due to the uniform nature of the grains. Poorly sorted sediment trapped the finer part of the sediment in the pore spaces before constructing the next step, resulting in less pronounced steps in the final morphology.

The amount of fine silica flour enhanced the adhesive strength of the sediment causing somewhat more stable banks and narrower channels than in the cases without added fines. However, our experiments point out that addition of fines to the particle size distribution affects delta morphology only on a small scale leaving no detectable topographical signature in the lake (de Villiers *et al.* 2010). This could be a partial explanation for the mismatch between eroded volume of channels and deposited volume of deltas observed on Mars (Hauber *et al.* 2009), where a fraction of the sediment (mainly fines) is likely to be carried away in suspension and not deposited on the delta but elsewhere in the system, further downstream. If the original percentage of fines in the sediment source is quite high, this could be a significant fraction of the sediment that is not trapped by the delta.

The effects of different particle size distributions in the experiments point out that morphology of deltas depends partly on the smaller-scale morphodynamic processes such as channelization and sheet flow, however the causes for these processes are only partly understood (van Dijk *et al.* 2009). It may be that the smooth-topped deltas of Mars had sheet flow, or have channel dimensions beyond detection. Future high-resolution imagery may resolve questions on sediment sorting patterns and the occurrence of small channels or sheet flows.

4.5.4 Implications for Mars

We found three emergent properties of fan deltas formed in rapid discharge events that are generic and we infer them to be valid for Mars. First, an important observation in the experiments is the process of highly energetic hyper-concentrated flow in the early stages of the process. Some Martian deltas indeed show indications of having been formed on top of another deposit that may have formed from a hyper-concentrated flow (Kleinhans

et al. 2010a). Second, all experiments confirm that incision is highly focused and occurs rapidly, so that deltas without obvious incisions must have formed in one event, or must have covered an earlier delta entirely which must, therefore, have been smaller. Third, the experiments indicate that the loss of water into the subsoil may lead to under-estimation of the total volume delivered by the source as inferred from formative duration and lake level indicators, particularly the shoreline. This was referred to as the "leaky cauldron hypothesis" in Kleinhans *et al.* (2010a). Nonetheless, the overall error due to this effect in the experiments is no more than of the order of a factor of two. As for the different permeabilities of the substrate, we are inclined to argue that the time of formation of delta deposits on Mars might be shortened due to the relatively smaller permeability of the sediment or bedrock when compared to our relatively coarse and unconsolidated laboratory sands.

We conclude from the flume experiments and the numerical analyses that the most important dimensionless numbers governing the behaviour of flow and sediment are within reasonable or even narrow range of values inferred for Martian systems. The most important scale problem was crater rim incision because of the weak material and the narrow rim. The modelled crater rims were not only much more easily eroded, but were also relatively narrow when compared to natural craters (Garvin and Frawley 1998), allowing the rim to be breached and eroded very rapidly. This caused many deltas in phase 2, the overflowing lake, to be incised. This is not what we believe to be analogous to Martian conditions. On the contrary, we expect the crater rim on Mars to be substantially stronger and to resist rapid erosion and we expect the deltas to be much less incised. A much wider rim with a significant ejecta blanket simulated in the initial topography of the experiments would have largely reduced the incision processes that we observed on the deltas, particularly in the smaller craters.

Interestingly, the calculations of the formative time scale in the experiments were only somewhat less uncertain than those on Mars. This is despite the much higher control on initial and boundary conditions, and likely due to the shallowness of the flow and the dramatic transition in sediment concentration which spanned hyper-concentrated flow to dilute flow.

4.5.5 Interpretation for Martian climate

On Earth, we rarely see examples of stepped deltas because receiving basins are very large compared to the volume of hydrological input. Contrastingly, on Mars, the development of the different delta types may have often been halted during the early phase of formation because the hydrological event ended. The ending was most likely very abrupt, because any lowering of lake level whilst there still was some upstream water supply would have led to erosion of the delta shoreline. Almost all deltas on Mars show no large-scale erosion by post-formation flow over their surface, with the possible exception of the deltas in Eberswalde and Jezero Craters and other similarly complex delta complexes (which are not the topic of discussion here). The preservation of numerous deltas on Mars, mostly without indications of fluvial erosion, leads us to argue that the ancient climate on Mars may not have been warm and wet, thus not sustaining long-duration hydrological activity.

More likely, from time to time, catastrophic events led to instant production of flood waters which rapidly filled crater basins. The hydrological events that were responsible

for the delta formation ended abruptly and the crater lakes rapidly dried up, leaving the deltas exposed. The retrograding deltas on Mars are evidence of a hydrological event that ended soon after the rapid filling of the crater lake. The prograding deltas are evidence of a hydrological event that ended while the lake level was stable (either full or overflowing or slowly falling). This requires not only a trigger for the initiation of flow, but also an explanation of the abrupt ending. Brief catastrophic events can be induced by heating of the groundwater or ground-ice in the sub-surface for example through local volcanism or due to impact cratering (e.g. Head and Wilson 2007; Segura *et al.* 2008). Such processes will yield a short duration hydrological event, either through groundwater sapping or overland flow or, in exceptional cases rainfall (Kite *et al.* 2011; Jerolmack *et al.* 2004; Kleinhans 2005a). Sustained, continuous or repeated, events would imply a wet period for a longer time, on the order of hundred thousand years or more, with the possibility of multiple aqueous events that must have had much larger effects on the morphology of sedimentary deposits than observed on Mars.

In sequence stratigraphic terms (see Catuneanu *et al.* 2009), the occurrence of unaltered retrograding and prograding deltas on Mars indicates the formation of transgressive and high-stand deposits respectively, and the absence of incised deltas indicates that regressive and low-stand deposits were likely never formed. Unlike some authors (e.g. Cabrol and Grin 2001; Di Achille and Hynek 2010), we do not see evidence of cyclic discharges or a persistent hydrological cycle based on the morphologies or the mere occurrence of these deltas alone.

4.6 Conclusions

The morphology of deltas formed in closed crater basins in the laboratory show strong morphological resemblance to deltas in Martian craters. The morphologies of fan-shaped landforms on Mars and (dis)similarities with their counterparts on Earth and in the laboratory reflect the upstream (i.e. flow discharge as well as sediment availability and mobility) and downstream (water level dynamics) conditions at the time of formation. Logical combinations of these conditions resulted in three main morphological delta types with variations in sub-types (Fig. 4.16).

The behaviour of the downstream water level is the most important factor determining delta morphology. The main conditions to form the large-scale, primary delta morphology 1) stepped, retrograding delta, 2) smooth or branched, prograding delta, and 3) a telescopic, incised delta is by rising, steady and falling water level in the crater basin, respectively. Unlike in terrestrial cases, downstream conditions (rate of water level rise or fall) in the craters on Mars are entirely determined by upstream discharge, crater basin hypsometry, crater floor permeability, and the quality of the crater rim. Small-scale, secondary morphological features superimposed on the three main morphology types along the X-axis of Figure 4.16 depend on variations in flow discharge and sediment texture. Little evidence has been found for highly incised, telescopic types of delta deposits on Mars, which leads us to propose that discharge onto the delta abruptly stopped before breaching of the crater rim and never resumed again (hence it could not incise or erode the original deposit). Furthermore, breaching might not always have occurred, as sub-surface drainage and evaporation may have been important factors that reduced water level rise until the upstream discharge was halted.

Sediment transport rate is initially very high due to large amounts of available sediment in the upstream crater rim, implying the occurrence of 'en–masse' sediment transport (mass flows) in the first formative stage of delta formation. The occurrence of mass flow events shortens the overall formative time because the majority of the sediment volume is rapidly deposited after which the sediment transport rate declines as the stream gradient decreases and the availability of sediment diminishes.

Morphological evidence for episodic, short periods of intense hydrological activity is abundant and predominant in the craters of Mars. These events would flood the crater basin thus creating transgressive, retrograding delta deposits with multiple foresets. Some of these stepped deltas grew into prograding deltas with single foresets, prograding as lakes spilled over while maintaining a constant water level; however, most of these deltas do not show evidence for persistent hydrological activity. On the contrary, the smooth surfaces untouched by post-formation fluvial erosion are evidence of the abrupt end of these short, episodic events. We therefore dismiss sustained water cycles as would occur by for example periods of wet climate (rainfall), which would result in more complex water level histories along with complex sediment delivery histories and delta morphologies. We therefore conclude that rapid formation by single, high discharge events was responsible for most of these delta deposits on Mars.

4.7 Acknowledgements

The authors would like to thank all anonymous reviewers for their assistance with improving this manuscript. We also thank Dimitri van Breemen and Jan de Vries for assistance with the data collection as well as Ernst Hauber, Poppe de Boer, Steven de Jong and Wout van Dijk for interesting discussions.

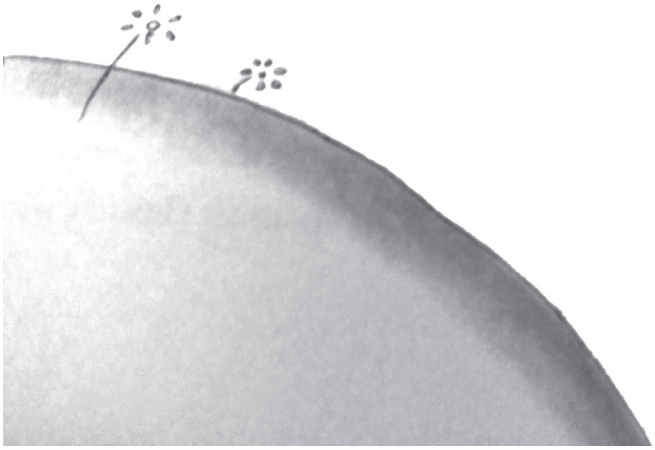

“I have always loved the desert. One sits down on a desert sand dune, sees nothing, hears nothing. Yet through the silence something throbs, and gleams ... What makes the desert beautiful,” said the little prince, “is that somewhere it hides a well.”

5 Terrestrial Alluvial Fans in the Atacama Desert

Based on:
de Villiers, G., Ventra, D., & de Boer, P. L. (n.d.). Terrestrial alluvial fan analogues for Mars – Classification and application with examples from the Atacama coast (northern Chile) (soon to be submitted). *Geological Society London - Special Publications.*

Abstract - Alluvial fans are an important depositional landform on Earth, on Mars, and perhaps on other planetary surfaces. Their morphology and associated processes are indicative of the formative conditions and may allow interpretations of the climate at the time of their formation. In order to discuss and understand alluvial fans and their processes on other planetary surfaces, understanding terrestrial analogues is essential, and a broad classification of terrestrial fan-shaped deposits is crucial for avoiding confusion and misinterpretation. We propose an elementary classification of terrestrial fans, based primarily on processes, with gradual boundaries from one type to the next, and frequently with more than one process active on the same fan at different points in space and time. We then describe a set of terrestrial coastal fans in the Atacama Desert with apparent similarities to some of the Martian alluvial fans based on satellite imagery. On the basis of detailed fieldwork, both surface sedimentology and stratigraphy are described, the latter often telling a story that is rather different from what is observable at the surface from remote sensing observations only. It shows that the majority of the Atacama coastal alluvial fans have been constructed by debris flows. With this principle of ground-truth, we then suggest that the amount of water that was necessary for the formation of similar fans on Mars, may not have been as much as generally thought and that similar fans may be merely the result of a large sediment availability during rare catastrophic floods.

5.1 Introduction

Alluvial fans represent volumetrically the most important depositional landform at the base of highland settings on Earth (Harvey 2010). They occur in a broad variety of climatic, tectonic and geomorphic settings. Though research on alluvial fans has focused classically on arid to semi-arid environments, these depositional systems can be found in regions characterized by any climate regime, from humid temperate to arctic (e.g. Beaty 1963; Bull 1968; Lecce 1990; Blair and McPherson 1994), as long as sediment supply to the base of highland settings exceeds the amount that can be transported further away to lower areas. Despite the different settings in which alluvial fans are formed, a relatively restricted range of the ratio of discharge to sediment supply is required for formation and preservation (too much precipitation will erode the fan soon after deposition, unless the sediment supply remains extremely high) and thus a relatively restricted range of primary sediment-transport processes and morphological variability is maintained. The ratio of discharge and sediment supply defines morphology which is preserved if that ratio does not alter. Precipitation should be that limited that the alluvial fan deposits (partly) remain where they are (in order to maintain the fan) and thus are not fully eroded soon after deposition. That is the reason that the bulk of alluvial fans occur in (semi/hyper) arid climate zones. In wet climates only in case of extreme sediment supply (e.g. Kosi Fan; Gohain and Prakash, 1990).

Morphological and sedimentological definitions and classifications of sub-aerial distributive, fan-shaped depositional systems have been disputed topics, due to the wide range of processes and spatial scales over which such systems develop. The possible overlap in processes and forms between the various systems has been a source of scientific debate and occasional confusion for geologists and geomorphologists. Most of the controversy is generated by the common trait of all these systems: the tendency to attain a fan-shaped depositional pattern in plan-view, related to unconfined or poorly confined aggradation of sediments issued from a stable, well-delimited source area.

Besides their occurrence on Earth, alluvial fans have been recognized on Mars (e.g. Howard *et al.* 2005; Irwin *et al.* 2005; Moore and Howard 2005; Williams and Malin 2008; Kraal *et al.* 2008a; Hauber *et al.* 2009; de Villiers *et al.*, in preparation, Chap. 3). Short- and long-range systems have been identified (from hundreds of metres to tens of kilometres), in locations all over the surface of Mars, and somewhat clustered in certain areas. Understanding the origin of these Martian landforms has increasing relevance for the characterization of surface processes and for the understanding of Martian climate and palaeoclimate. Observational interpretations are limited by the lack of direct field data, and thus rely on the quality of remotely-sensed data and on inferences on the basis of possible terrestrial analogues.

Analogue studies, i.e. comparisons of Martian alluvial fans with their terrestrial analogues, must be guided by a basic process-genetic categorization of the latter in order to be effective. This paper aims to a) propose a practical, process-based classification of alluvial fans based on field observations and reports in the literature, and b) compare examples of Martian fans to selected examples of alluvial fans surveyed in the Atacama Desert (northern Chile), deriving insights on the significance of such comparative approach, which has guided

several studies of planetary geomorphology (e.g. Baker and Milton 1974; Williams *et al.* 2006; Radebaugh *et al.* 2008, 2011; Hauber *et al.* 2010, 2011).

5.2 Reference classification of alluvial fans

Three types of fan-shaped sub-aerial landforms are most commonly discussed: a) **colluvial fans** (including talus cones and scree slopes; e.g. Blikra and Nemec 1998; Harvey 2010; 2012), formed along and at the base of slopes; b) **alluvial fans** (either dominated by sediment-gravity flows or fluid-gravity flows such as the Dolomite Fan and Anvil Spring Canyon Fan; e.g. Bull 1963; Blair and McPherson 1994); and c) **fluvial fans** (also described as megafans, dominated by distributive and avulsive fluvial processes, mostly classified as braided and/or meandering such as the Reno River Fan, northern Italy; e.g. Ori 1982; Hartley *et al.* 2010). Other prominent examples of fluvial fans include the Kosi Fan, in northern India, and the Okavango Fan, in Botswana (e.g. Gohain and Prakash 1990; Stanistreet and McCarthy 1993). In their classical review paper, Blair and McPherson (1994) considered colluvial fans as an incipient, immature stage of alluvial fans, and importantly recommended to stick to a strict genetic distinction of alluvial fans from rivers (and fluvial fans, which they considered closely related to rivers) based on hydrologic, geomorphic and sedimentological characteristics (see also McPherson *et al.* 1987). In another frequently cited review, Stanistreet and McCarthy (1993) argue for the inclusion of larger fluvial fans (e.g. the Kosi Fan) as a sub-category of alluvial fans, a position recently reinforced by Harvey (2010) as well as by new concepts on the sedimentological and geomorphical distinction of the so-called *distributive fluvial system (DFS)* (Nichols and Hirst 1998; Weissmann *et al.* 2010; Hartley *et al.* 2010). Harvey (2010) includes fluvial megafans as a type of alluvial fan, and we caution against this inclusion due to the large variation in processes that tend to occur on these two end-members. DFS as described by Hartley *et al.* 2010, includes alluvial fans, fluvial fans and megafans as equal members, but not colluvial fans. Their distinction between alluvial fans and megafans is gradual yet firm, with a category of fluvial fans separating the two end-members, i.e. deposits that are larger than alluvial fans yet smaller than megafans. It is not entirely clear from their paper whether "fluvial fans" should include only smaller megafans (still dominated by fluvial processes) or also run-off dominated alluvial fans. We caution against the unintentional mix of these two distinctly different categories, although we acknowledge that a certain degree of overlap and gradual transition between these landforms may occur.

For our discussion of Martian fans, we suggest a separation of the above three landform categories (colluvial fans, alluvial fans, and fluvial fans/megafans) as genetically distinct (Fig. 5.1) based on previous research and discussion of terrestrial systems (Ori 1982; Blair and McPherson 1994; Nichols and Hirst 1998; Smith 2000; Moscariello 2005; Harvey 2010), while acknowledging the occasional occurrence of depositional landforms of mixed origin. In particular, as mentioned briefly above, we highlight the distinction between fluvial fans *sensu stricto*, resulting from distributive patterns of properly fluvial deposition, and run-off dominated alluvial fans (or what we believe has been inaccurately referred to in the literature as "fluvially dominated" alluvial fans), which are short-radius, high-gradient landforms on which sediment deposition takes place mostly from water run-off. This minor difference is important especially when attempting to understand the environmental conditions at the

time of formation, as processes that are associated with run-off are not equivalent to fluvial distributive processes in terms of amount, temporal and spatial distribution of discharge, even though the distinction from one type to the other may be gradual.

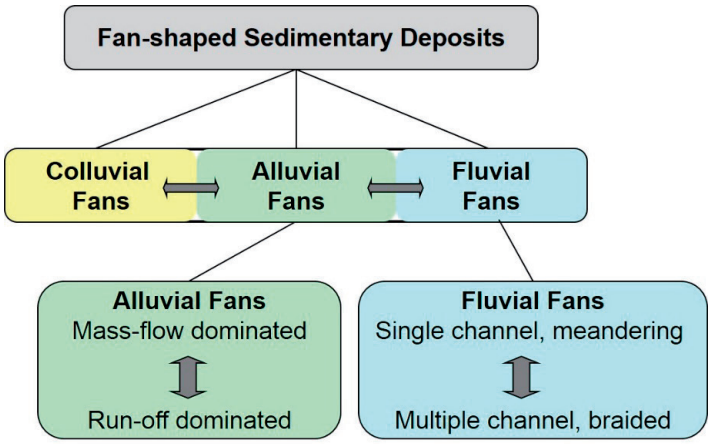

Figure 5.1: The genetic categories of fan-shaped sedimentary deposits. Note that the three categories do not have strict borders but gently grade from one to the other. Most deposits fall clearly within one of these categories but some lie on or close to the border and hence fall between two categories, strictly speaking.

The most common processes of sediment transport and aggradation on typical short-range, piedmont-type alluvial fans are sediment-gravity flows (mass flows) and fluid-gravity flows. In sediment-gravity flows, debris is mobilized by the direct action of gravity under conditions of favourable slope gradient and/or mixed fluid content. Fluid-gravity flows depend on run-off with sediment particles displaced by the action of a fluid medium, most typically water, in which they are dispersed. In terms of the mechanics of individual events, the occurrence of either process is related to the sediment/water ratio of the flowing dispersion. From the perspective of long-term fan aggradation, the dominance of either mass flows or run-off is strongly related to the morphometry and geology of the catchment in combination with the frequency and intensity of precipitation. In general, steep, mass-flow dominated fans are fed by relatively restricted catchments of high relief and with poorly integrated drainage networks, whereas larger, run-off dominated fans with relatively lesser gradients are associated with larger catchments with a more evolved drainage network (Lecce 1990; Crosta and Frattini 2004). The role of catchment geology is mostly best expressed by the character of bedrock lithology and the intensity with which rocks have been faulted. Intensely faulted rocks can provide elevated volumes of fines, preferably clay, in the regolith under local conditions of weathering and pedogenesis.

A gradation between mass-flow dominated fans and run-off dominated fans (Leeder 1999) makes that most fans are characterized by variable combinations of these two process categories. It is frequently reported that fans on which both types of processes operate are characterized by a dominance of mass-flow deposits in the proximal domain, and run-off deposits in the distal domain, due to the greater mobility of sheet floods and water flows (Bull 1977; Blair and McPherson 1994; Moore and Howard 2005).

In terms of depositional processes, and based on the observations in the following sections, we subdivide alluvial fans into four categories: a) alluvial fans built up by sediment-gravity flows only (i.e. predominantly debris flows); b) mixed-type alluvial fans dominated by mass-flow deposits and with evidence of subsequent run-off that have reworked the surface; c) mixed-type alluvial fans dominated by fluid-gravity flows (predominantly unconfined or poorly confined water flows) with an expression of these processes not only at the surface but also in stratigraphy, along with evidence of mass flows; and d) alluvial fans built by fluid-gravity flows only. Groups 'a' and 'd' correspond respectively to type 1 fans and type 2 fans of Blair and McPherson (1994), while intermediate groups 'b' and 'c' are equivalent to the mixed-flow fans described by Volker *et al.* (2007).

5.2.1 Alluvial fans dominated by sediment-gravity flows (groups a and b)

Mass-flow dominated alluvial fans form in regions where effective run-off is particularly rare or ephemeral, and where the erodibility of catchment bedrock provides sufficient sediment for elevated sediment-water ratios. Primary sediment transport processes include rockfall and debris fall in proximal domains adjacent to the relief, as well as landslides, rock avalanches and debris flows, the latter by far the most frequently documented mass-flow process on alluvial fans on all continents and in all settings (e.g. Wasson 1977; Hooke 1987; Wells and Harvey 1987; Webb and Fielding 1999; Moscariello *et al.* 2002). Debris-flow fans commonly exhibit a down-fan decrease in modal grain size, bed thickness and channel depth (Leeder 1999). Particle shape does not change significantly due to the relatively short transport distance (radial fan lengths on Earth usually range from a few hundred to a few thousand metres, rarely up to ~10 km) and especially the high viscosity of the flowing mixtures and consequently poor sorting. However, there may be a change from thick, clast-rich debris-flow lobes proximally to thinner, dominantly muddy flow lobes more distally, related to longitudinal clast segregation in rheologically composite flows. This translates into a morphological contrast between a proximal surface with coarse-grained irregular, levee-lobe elements, and a distal surface with lower relief and finer-grained, broad lobes with a high aspect ratio (e.g. Beaty 1990; Whipple and Dunne 1992; Blair and McPherson 1998; Kim and Lowe 2004). Average gradients of debris-flow fans on Earth range from 1.5º to 25º (up to 30º in extreme cases), the majority ranging between 2º and 12º (Rachocki 1981; Blair and McPherson 1994).

5.2.2 Alluvial fans dominated by fluid-gravity flows (groups c and d)

Run-off dominated alluvial fans form in areas where water flows are relatively frequent and/or protracted, and sediment yield cannot overload individual flow events (Bull 1977; Blair and McPherson 1994; Leeder 1999) while water supply is at the same time insufficient to erode the alluvial fan body. Primary processes range from fully unconfined sheet floods to shallow stream flows (e.g. Kesel and Lowe 1987; Nemec and Postma 1988; Darby *et al.* 1990; Blair 1999a; Harvey 2010). Field evidence and also models point to the importance of autocyclic dynamics in controlling shifts between channelized and unconfined run-off over fan surfaces (van Dijk *et al.* 2009; Clarke *et al.* 2010; Ventra and Nichols 2013 (in press)). Initial fan aggradation takes place mostly through unconfined flows, but as the fan surface

expands beyond a certain threshold, run-off tends to be distributed in distinct channels, as has been shown in laboratory experiments (e.g. Whipple *et al.* 1998; Pratson *et al.* 2004; van Dijk *et al.* 2009, 2012; Clarke *et al.* 2010; Reitz and Jerolmack 2012). There is a down-fan change from coarse-grained alluvium to finer-grained sediments as well as a decrease in slope, following a radial decrease in flow competence and coarse sediment load (Blair and McPherson 1994; Leeder 1999). Furthermore, the degree of longitudinal concavity increases with the dominance of run-off, which usually translates into much lower average gradients for run-off dominated fans as compared to mass-flow dominated fans (e.g. Harvey 1984; Whipple *et al.* 1998; Williams *et al.* 2006; Volker *et al.* 2007).

5.3 Alluvial fans on Mars

The Martian surface has gone through a complex and as yet not completely understood climate history. Reconstructions of the evolution of climate on Mars are uncertain and based largely upon remote sensing data (Baker 2001; Jaumann *et al.* 2002). It has been established that large valley networks formed during the Noachian Period (4.1 to ~3.7 Ga, Fig. 1.2 in Chap. 1); and that regional outflow channels, enormously wide incisions carved by outburst floods on average several to tens of kilometres across, formed mostly during the Hesperian Period (~3.7 to ~3.0 Ga, somewhat disputed) and also more recently, ~10 to 20 Ma, at Athabasca Valles (Baker and Milton 1974; Burr *et al.* 2002; Berman and Hartmann 2002). Small-scale gullying has occurred throughout the Amazonian Period (~3.0 Ga to present) and perhaps as recently as within the last million years (Dundas *et al.* 2010; McEwen *et al.* 2011; Schon and Head 2012). Although drainage densities are much lower for the Martian valley networks than for equivalent terrestrial valley networks, water must have played an important role in the sedimentary history of the planet's surface, at least during some periods and specifically during the Late Noachian (Carr 1983; Tanaka 1986; Parker *et al.* 1993; Baker 2001; Hartmann and Neukum 2001; Carr and Head 2010). Even though other options have been considered for the formation of the valleys and channels on Mars (e.g. Sagan *et al.* 1973; Zimbelman 1998; Leverington and Maxwell 2004; Leverington 2005; 2011), liquid water is still the most convincing in many cases (Stewart and Nimmo 2002; Carr and Head 2010; McEwen *et al.* 2012).

Liquid water is not likely to be stable on the surface at present due to the low atmospheric pressure combined with low temperatures. However, it evidently must have been so at some point(s) in time to sustain the formation of the older valley networks in the Noachian (Head *et al.* 1999; Mustard 2002; Carr 2003). More importantly, it may not be necessary to be stable at the surface for very long in order to produce the younger fluvial landforms (Goldspiel and Squyres 2000; Haberle *et al.* 2001; Hecht 2001). The current understanding of Mars' climate includes a thicker atmosphere during the Noachian which may have sustained a warmer climate during that time with a pulse of aqueous activity around late Noachian/early Hesperian (Craddock and Howard 2002; Irwin *et al.* 2005; Matsubara 2011), with either sustained or episodic (catastrophic) events since then being responsible for bringing liquid water to the surface from the permafrost and for creating fluvial features before this liquid water subsequently evaporated or froze (Segura *et al.* 2008; 2012; de Villiers *et al.* 2013, Chap. 4).

Besides remnants of drainage networks and other indicators of fluvial activity, gullies and alluvial fans have been identified within impact craters and other basins (e.g. Moore and Howard 2005; Kraal *et al.* 2008a; Schon *et al.* 2009; Dickson *et al.* 2007, 2009; Hauber *et al.* 2009). Martian alluvial fans have been identified at different scales, from short-range, sub-kilometre scale fans (e.g. Promethei Terra, Schon *et al.* 2009; Mojave Crater, Williams and Malin 2008) to long-range, multi-kilometre scale fans (as described by e.g. Moore and Howard 2005; Kraal *et al.* 2008a). Alluvial fans on Mars show gradients and morphometric characteristics (as observed from satellite imagery and/or calculated from digital elevation models) that are similar to those of terrestrial alluvial fans (Garvin and Frawley 1998; Howard *et al.* 2005; Kraal *et al.* 2008a). Most alluvial fans exhibit a classical cone-shaped morphology with superposed ridges, oriented radially over the surface, and these fans have short and steep, or altogether absent feeder channels. One significant difference between terrestrial and Martian alluvial fans is that Martian fan surfaces show hardly any signs of well-developed drainage networks or post-formation erosional distributary channels, as would be expected to have been created in case of subsequent rainfall and run-off events, and few signs of erosional modification by fluvial, lacustrine or marine re-working, such as wave-cut terraces on crater rims and dissected fan surfaces, have been observed (Parker and Currey 2001; Irwin *et al.* 2005). This implies that any type of aqueous event or period must have ended rather abruptly (on the order of 10's to 1000's of years), leaving no trace of major fluvial modification on the fan surface. If the morphology of the alluvial fans on Mars and their associated formative processes can be accurately placed at certain chronological points in the history of the planet, this may provide insight into Mars' climate evolution.

Early studies suggested that most Martian alluvial fans have formed at the Noachian-Hesperian boundary and during the mid-Hesperian (Howard *et al.* 2005; Moore and Howard 2005), based on the ages of the craters within which they occur. This indicates that they have been exceptionally preserved and subject to minimal reworking by fluvial, aeolian or other processes. However, recent crater-count ages suggest that many alluvial fans, for example those in the region of Margaritifer Terra, are much younger and may have formed either at the Hesperian-Amazonian boundary (Carter *et al.* 2012), or even more recently during the Amazonian (Grant and Wilson 2011). As proposed by Grant and Wilson (2011), fan development most likely occurred during a relatively short, possibly geologically late interval. Catastrophic outflow channel formation may have delivered water to the northern lowlands creating temporary oceans (Clifford and Parker 2001; Fairén *et al.* 2003) from which water may have later been redistributed by evaporation and precipitation in the southern highlands as part of a short-lived hydrological cycle, creating a run-off source for the formation of alluvial fans and other fan-shaped depositional landforms (Luo and Stepinski 2009).

Most of the large alluvial fans on Mars have been interpreted as having been deposited by fluid-gravity flows (run-off dominated) rather than by sediment-gravity flows (mass-flow dominated) (e.g. Moore and Howard 2005; Kraal *et al.* 2008a). This interpretation is commonly based on the low gradients of the fans, on their size, on apparently uniform grain sizes, on the lack of discrete lobes with significant relief, and on architectural elements at the surface that have been interpreted as scroll bars. However, with dynamic angles of repose up to 10 degrees less on Mars than on Earth due to the lower gravity on Mars (Kleinhans *et al.* 2011), care should be taken when distinction between mass-flow dominated fans and

run-off dominated fans is based primarily on gradient. In addition, weathering rates on Mars may be higher than initially estimated (de Haas *et al.* 2013), implying that the determination of formative processes based solely on visual recognition of typical morphological surface features (such as debris-flow levees and lobes) may have severe limitations resulting from the occurrence of smoothed and paved deflation surfaces even on debris-flow dominated alluvial fans.

Unfortunately, the terminology for fan-shaped depositional landforms has not been consistent and has become a major source of misunderstanding with regards to the processes that operate on the Martian fan surfaces. We underline the importance of a proper distinction between different fan types (previous section), and we propose a universal reference system so that further confusion can be avoided as we embark on higher resolution studies of the surface of Mars.

We use the catalogues by Moore and Howard (2005) and Kraal *et al.* (2008a) to study the surface expression of Martian alluvial fans. This population includes classic, cone-shaped alluvial fan deposits with relatively high gradients of roughly 3° and lengths of 5-40 km located mainly in the southern highlands. These deposits are alluvial fans in the strict sense, not colluvial fans nor fluvial fans; either debris-flow dominated or run-off dominated – to be assessed in analogy with terrestrial alluvial fan deposits with similar surface expression in satellite imagery. An exemplary list of deposits that have been considered is given in the appendix, with the location of each crater. Alluvial fans are restricted to areas where high gradients abruptly meet low gradients. On Mars this most often is the case in impact craters (where the rim is a high-gradient area that transforms relatively abruptly into a more gently sloping inner crater area; Fig. 5.2a). Alluvial fans tend to occur in the southern highlands, perhaps indicating a tendency to form in craters with less eroded rims and hence larger volumes of sediment still available at the rim as well as a significant relief to promote sediment transport. Most Martian alluvial fans are interpreted to have formed under conditions of low/short discharge and intermittent events considering that the small, closed basins within which

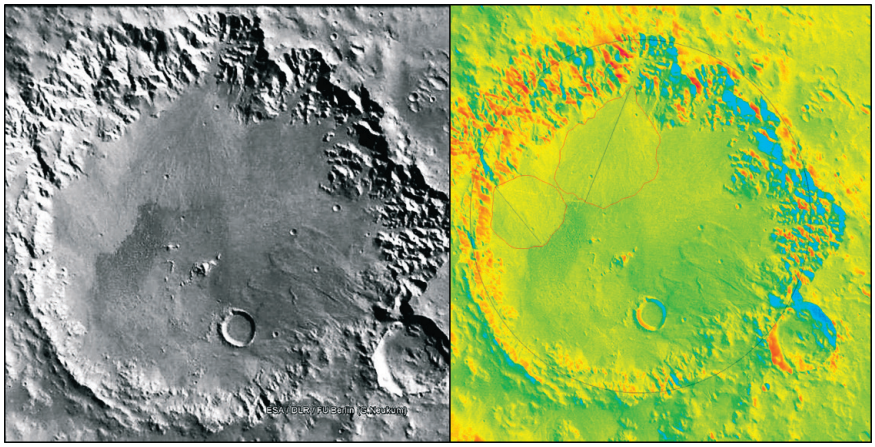

Figure 5.2: (a) An example of a crater with at least two low-gradient alluvial fan deposits (Site 1 and Crater A as referred to by Moore and Howard 2005) (b) Example of measurements taken at Site 1, background is a colour-shaded hill-slope DEM. Crater diameter is 80 kilometres and north is to the top of the images. [Image source: HRSC]

they were formed were clearly not filled with water at the time of their formation (de Villiers *et al.* 2013). Figure 5.2b shows a colour-shaded, hill-slope DEM of an impact crater and alluvial fans, initiating from the high-relief crater rim.

The data sets used in this study are primarily from the High Resolution Stereo Camera (HRSC) on board the Mars Express spacecraft which has been in orbit around Mars since December 2003 and is still functioning (Neukum *et al.* 2004b). We used both visual and topographic data from HRSC to evaluate the deposits, and visual data from other sources, including THEMIS (Thermal Emission Imaging Spectrometer), HiRISE (High Resolution Imaging Science Experiment), and MRO-CTX (Mars Reconnaissance Orbiter's Context Camera) are used where available. Figure 5.3 shows examples of satellite images that cover four alluvial fan sites in the southern highlands.

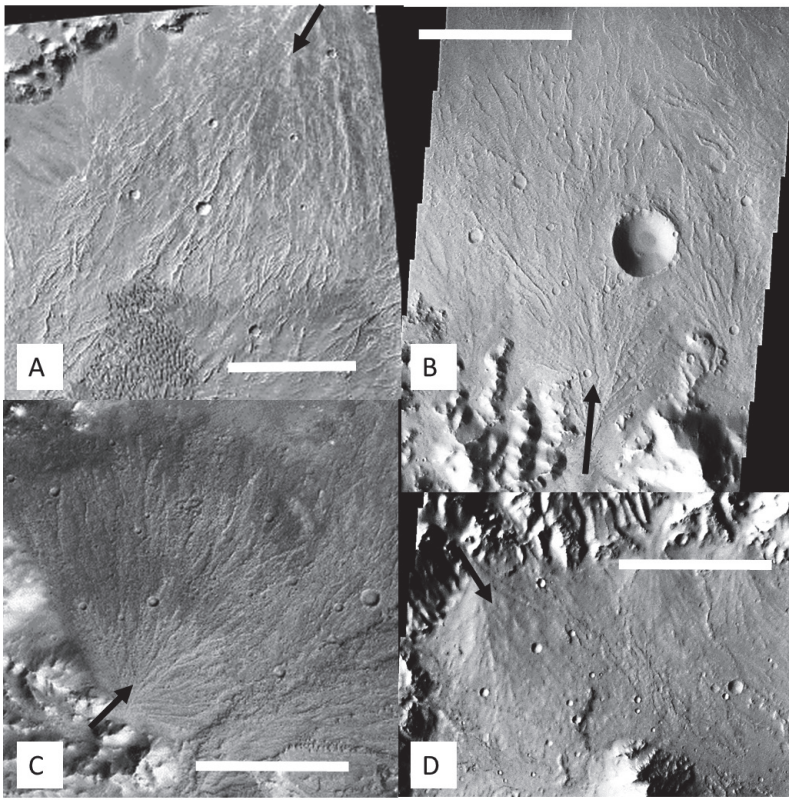

Figure 5.3: Overview of satellite imagery of Martian alluvial fans in crater basins. From left to right, top to bottom: Crater A fan at -21.39°/320.63°E, Crater S fan at -26.23°/331.52°E, Crater M fan at -21.47°/66.75°E, and Crater F at -27.00°/27.30°E (as referred to by Moore and Howard 2005; black arrow indicates direction of flow at the apex, north is towards the top). White scale bar is roughly 10 kilometres long. [Image source: MRO-CTX G19_025625_1582_XN_21S039W; THEMIS V16627004; MRO-CTX P14_006528_1583_XN_21S292W; THEMIS V18210005]

De Villiers *et al.* (in preparation, Chap. 3) discuss the morphological parameters of alluvial fans and other fan-shaped deposits, and found that alluvial fan lengths vary significantly, but do not seem related to basin diameter, and also that larger fans do not necessarily form in

larger craters (in agreement with Kraal *et al.* 2008a). Furthermore, the data shows that fan gradients are remarkably similar across the longitudinal profile (around 2-3°) and that higher fan gradients tend to be associated with shorter feeder channels and smaller fans, which is in agreement with terrestrial observations that short feeder channels usually occur in younger, smaller systems with high relief in the source area and hence high gradient deposits, while longer feeder channels are often part of established larger drainage systems which result in larger deposits with lower gradients (Bull 1964; Lecce 1990). In general, the Martian fans in our study population are long (tens of km), low-gradient, extensive alluvial fans with an inverse relation between length and gradient, as in agreement with Williams *et al.* (2006), and as established on Earth. The main question that remains is whether these large Martian fans are debris-flow dominated or run-off dominated, and to what extent the amount of discharge at the time of formation can be reconstructed.

5.4 Alluvial fans on the northern Atacama coast

The Atacama Desert extends from the Peru-Chile border in the north down to approximately 30° south latitude, bounded by the Pacific margin of South America to the west and by the Andean highlands to the east. The present climate is classified as hyperarid, and is known to have oscillated between arid and hyperarid over Neogene to Quaternary time (Miller 1976; Vargas *et al.* 2000; Hartley and Chong 2002; Hartley *et al.* 2005a); several localities in the region register no precipitation at all for many consecutive years. Morphologically, the north-Chilean coast is characterized by a prominent escarpment which extends over more than 800 km reaching altitudes up to 600-1000 m above sea level, generally referred to as *coastal cliff* or *coastal scarp* (Mortimer and Saric 1972; Hartley and Jolley 1995; Hartley *et al.* 2005b; Cembrano *et al.* 2007). As a morphotectonic feature of sub-continental scale, the escarpment represents the internal, sub-aerial boundary of the present-day Chile Trench (Flint *et al.* 1991; Allmendinger *et al.* 2005). Besides rare outcrops of Cenozoic shallow-marine deposits (e.g. Hartley and Jolley 1995), currently active sedimentary systems along the coastal scarp consist of numerous well-developed alluvial and colluvial fans, locally accompanied by accumulations of aeolian deposits and very rare, small coarse-grained deltas prograding from the mouths of ephemeral streams (e.g. Flint *et al.* 1991; Hartley and Jolley 1995; Hartley *et al.* 2005b). The coastal fans examined for this work are located between the cities of Antofagasta and Tocopilla, prograding from the seaward slopes of the Coastal Cordillera (see Fig. 5.4a).

The choice of these fans as analogues for the interpretation of Martian landforms rests on the extreme aridity of the region, which represents an environmental condition analogous to Mars' surface, and implies the absence of macroscopic vegetation and soil cover (only after very rare precipitation events some sporadic, short-lived plants may be seen), and hence a marked prevalence of physical processes of sediment transport and deposition. The whole northern Atacama region has been used in previous Martian analogue studies, including work on outcrops, geomorphology and the general environment (Cabrol *et al.* 2001; 2007; Hock *et al.* 2007; Haug *et al.* 2010; Sobron *et al.* 2013). Ten alluvial fans (hereafter referred to as fan 1, fan 2, etc.) were selected for direct field surveys, based on similarities of their surface morphologies with those of Martian fans, as observed from satellite imagery. In addition, two

entirely mass-flow dominated systems (perhaps best described as colluvial fans gradually evolving into debris-flow alluvial fans (temporally; hereafter named fans A and B) were selected to compare with the other fans in our study. The study sites are shown in Figure 5.4b, and listed in Table 5.1, along with some general morphological characteristics of fans 1-10.

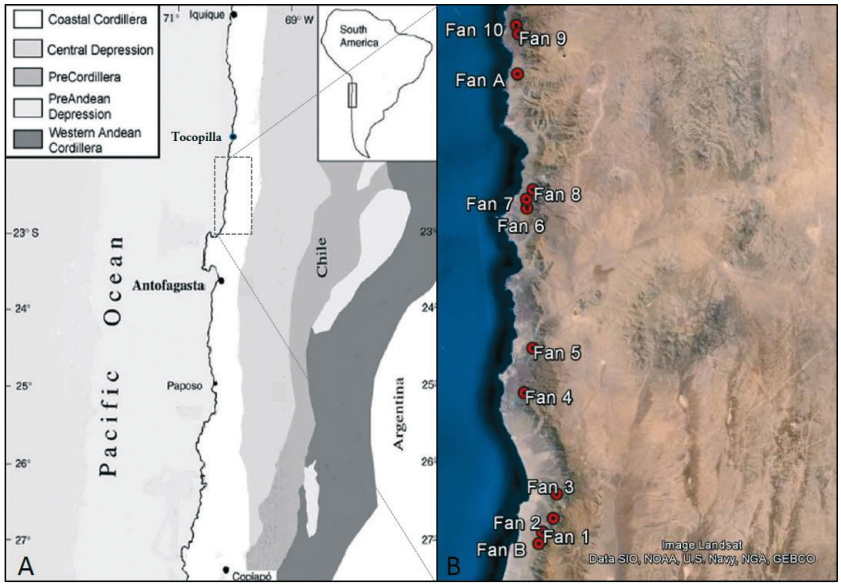

Figure 5.4: (a) The Coastal Cordillera and the associated coastal alluvial fan belt (adapted from Hock et al. 2007). (b) Locations of ten mixed-flow alluvial fan field sites between Antofagasta and Tocopilla. Two small mass-flow dominated fans (fans A and B) are located near fan 9 and fan 1 respectively. [Image source: Landsat & Google Earth]

As a result of the high quality and increased availability of satellite imagery through online geographical information programs such as Google Earth, it has become possible to effortlessly undertake regional scale morphologic studies of vast parts of our planet, especially in regions that are particularly remote or challenging to reach (e.g. Weissmann *et al.* 2010; Al-Masrahy and Mountney 2013, in press; Rodríguez-López *et al.*, in preparation). The resolution of the imagery is generally around 15 m/pixel, depending on the quality of the satellite data. Data sets from a variety of sensors in orbit around the Earth are used. One example is ASTER (Advanced Spaceborne Thermal Emission Reflection Radiometer) - a Japanese sensor on board NASA's Terra satellite launched into orbit in 1999. The Landsat Data Continuity Mission – the oldest, ongoing, Earth-observation program which was launched by NASA in the early seventies – also provides large datasets to Google Earth. For topography, Google Earth uses digital elevation model (DEM) data as acquired by NASA's Shuttle Radar Topography Mission (SRTM) with a vertical resolution of 10-16 m (Falorni *et al.* 2005). An example of satellite imagery that was used in this study is shown in Figure 5.5.

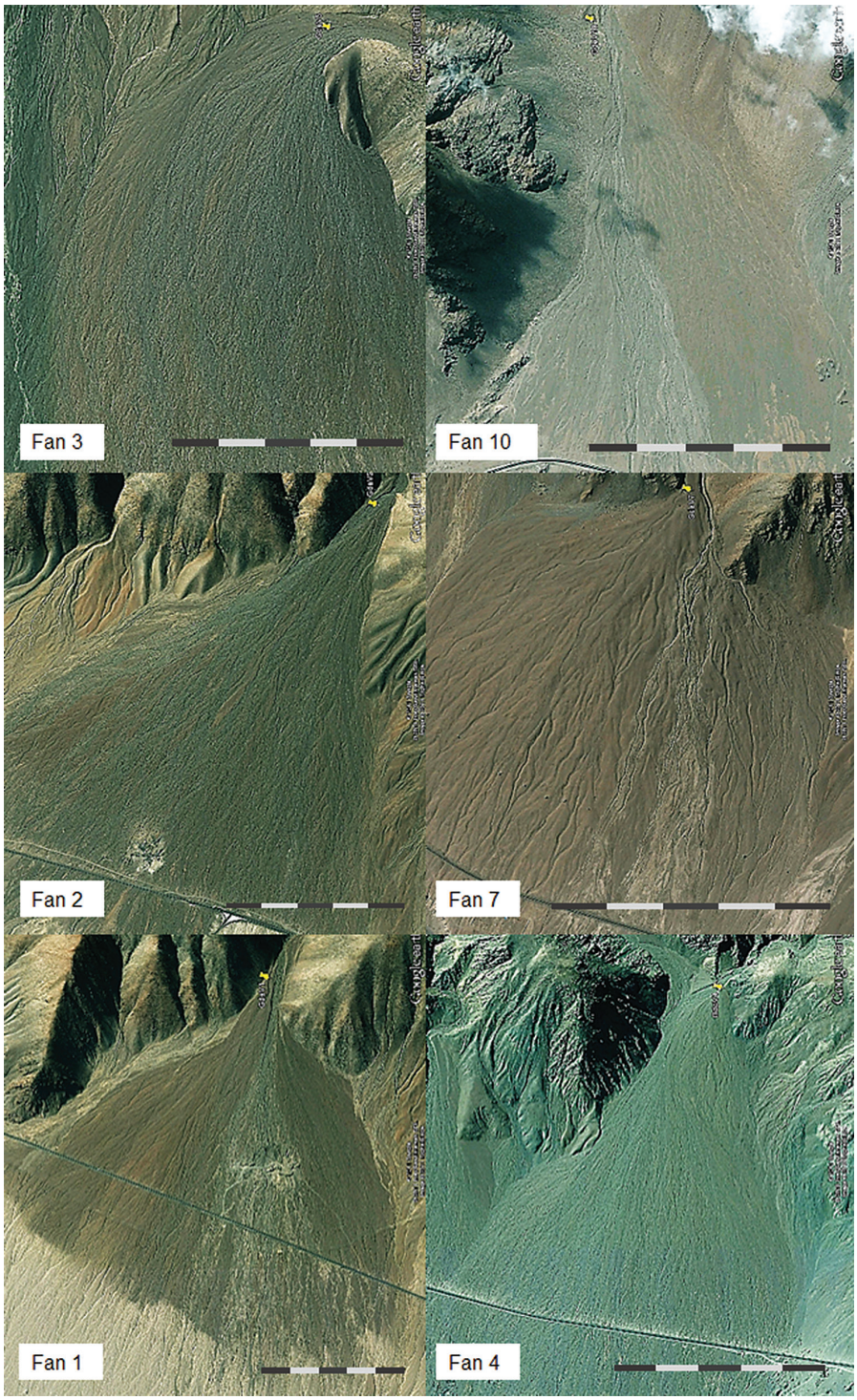

Figure 5.5: Overview of satellite imagery for some alluvial fan sites in the Atacama, fan lengths from apex to distal edge range from 1-3 km. [Image source: Google Earth]

Table 5.1: Fan site data from satellite imagery (Google Earth)

Fan	Apex Coordinates	Fan Length (km)	Fan Area (km^2)
Fan 1	22° 57.4‘ S; 70° 16.6’ W	1.5	1.9
Fan 2	22° 56.5’ S; 70° 15.6’ W	2.3	3.3
Fan 3	22° 54.7’ S; 70° 15.1’ W	1.9	2.3
Fan 4	22° 47.2’ S; 70° 16.7’ W	1.6	1.7
Fan 5	22° 44.1’ S; 70° 15.7’ W	1.2	-
Fan 6	22° 33.9’ S; 70° 14.7’ W	2.2	2.4
Fan 7	22° 33.3’ S; 70° 14.8’ W	1.1	1.0
Fan 8	22° 32.7’ S; 70° 14.3’ W	1.4	1.4
Fan 9	22° 21.3’ S; 70° 14.3’ W	2.1	-
Fan 10	22° 20.6’ S; 70° 14.0’ W	1.2	0.6
Fan A	22° 24.2’ S; 70° 14.4’ W	0.4	0.2
Fan B	22° 58.2’ S; 70° 17.0’ W	0.7	0.3

The coastal fans of the Atacama are known to be active only in the very rare occasion of particularly catastrophic precipitations concentrated on their catchments (Vargas *et al.* 2000; Hartley *et al.* 2005b). Geological evidence shows that activity rates of physical processes of primary sediment transport, responsible for fan construction, are particularly low. The exposed surfaces are subject to very long exposure (estimated times are in the order of 10^2 to 10^3 yr) and to modification by weathering and minor physical reworking which can alter the sedimentological signatures of primary depositional processes. The following sections provide an overview of the most relevant morphological features recognized over active and inactive fan surfaces as well as synthetic descriptions and process interpretations of stratigraphic facies exposed along sections incised within fan deposits. Our analysis is based on the principle that surface morphologies can provide mixed information both on the main processes of fan aggradation and on processes of surface reworking, whereas only a properly constrained stratigraphic perspective can constrain the dominant processes of fan construction.

5.4.1 Sedimentology of alluvial fan surfaces

Fan-surface deposits have been studied on eight of the ten alluvial fans (Fig. 5.6) in order to assess which processes determine specific morphological patterns. Particular attention has been paid to the contrast in genetic processes between positive relief elements (mostly gravel lobes and ridges) and negative relief elements (such as incised channels, swales, etc.). These are the two most generic categories of morphological elements identified also on Martian depositional landforms, on the base of which inferences are made about formative processes and for Martian palaeoclimates. Descriptions and interpretations of designated categories of morphological elements are reported below, and their significance for the scientific debate on Martian morphogenetic processes is discussed in a later section. The most frequent morphological elements recognized on several fans are reported here.

Figure 5.6: Overview of field sites where we collected data (site numbers refer to those in Fig. 5.5 and Tab. 5.1).

5.4.1.1 Recent Gravel Lobes (RGL) (single/amalgamated)

Recently active fan sectors (e.g. Fig. 5.7a) have surfaces characterized by topographically complex, apparently chaotic and disorganized associations of amalgamated gravel lobes and ridges (e.g. Fig. 5.7b). Some individual units can be distinguished by their textural contrast with the surrounding sediment. Sediments consist of angular to very angular, poorly sorted pebble to boulder gravel, frequently clast-supported along top surfaces while retaining significant amounts of silty to granular matrix a few centimetres below the surface. Fabrics are poorly developed in general, although domains are common with down-fan orientation of clast long axes and *ab* planes down-fan, parallel to transport direction. Outsized clasts are randomly distributed and often protruding from the surface, decreasing in abundance and grain size from proximal to distal fan sectors. Individual units may be distinguished by some or all of the following sedimentological and morphological criteria: a) plan-view patterns with down-fan-elongate gravel lobes (Figs. 5.7c, d, e, f and g) continuous over metres to tens of a metres, a few decimetres to several metres wide, commonly tapering both laterally and down-fan into b) alignments of generally coarser, matrix-free gravel with clast long axes oriented parallel to lobe margins (Figs. 5.7d and f); c) evident topographic relief, from a few centimetres to a few decimetres (Figs. 5.7d and g); d) the occasional occurrence of arcuate, transversely oriented gravel ridges within lobes, with texture and fabric similar to those signalling lobe fronts; e) more rarely, a contrast in textural mode with that of the adjacent surface (Fig. 5.7d); f) different stages of clast weathering, most commonly picked by colour contrast (Figs. 5.7d and e).

These composite surfaces most likely originated by the amalgamated stacking of cohesive debris flows (Fig. 5.7g). The poorly organized, texturally heterogeneous topography is due to the viscoplastic rheology of sediment-water mixtures (Johnson 1970; Hampton 1975), which flowed around obstacles (such as previously emplaced gravel lobes and outsized boulders) and into chutes as long as internal shear was maintained along sufficient gradients. Individual flows abruptly stopped once the shear rate dropped, for example along reduced gradients of particularly rough surfaces which slowed their propagation. The relief of the margins of the lobes of individual units relates to the strength of matrix-rich mixtures. Coarse-clast segregations along the boundaries of individual lobes correspond to the typical frontal snouts and marginal levees developed by debris flows during motion (Sharp 1942; Major 1997; 1998; Johnson *et al.* 2012). Residual gravel ridges, occasionally visible in some units, probably resulted from repeated flow surges (e.g. Sharp and Nobles 1953; Pierson 1986) in which temporary frontal snouts were breached by the continued movement of still liquefied flow bodies. Matrix-free texture upper parts of many deposits are likely due to reworking by run-off in topographic lows or due to aeolian ablation and deflation, but the most elevated lobes are perhaps due to segregation of coarse clasts at the flow top during transport (Major 1997; Johnson *et al.* 2012).

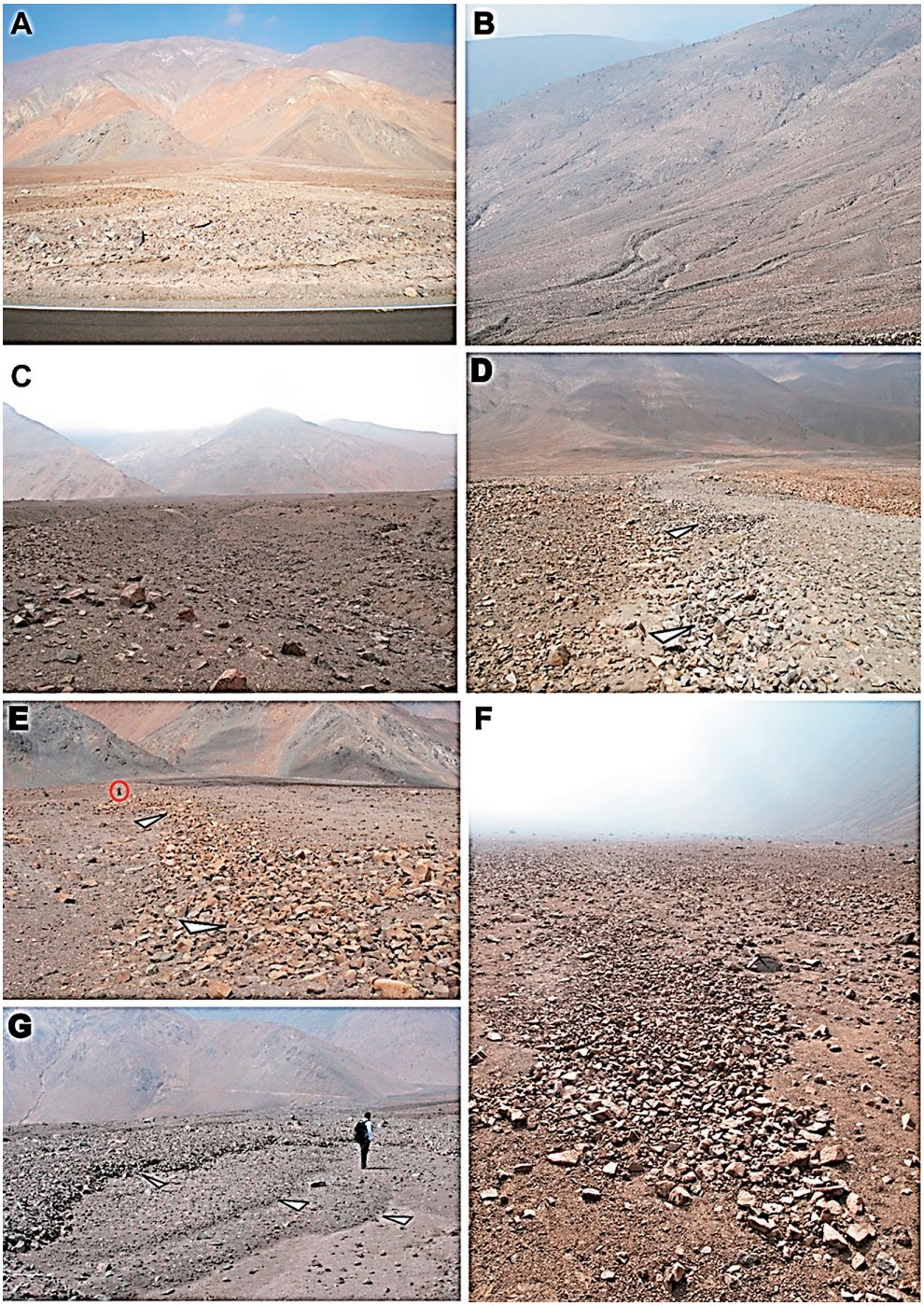
A
B
C
D
E
F
G

Figure 5.7 [Previous page]: (a) Fan 7: Morphological contrast between recently active surface (light-toned debris-flow lobes) and abandoned surface (red hue, due to rock varnish) surfaces. (b) Fan B: Typical ridge-and-channel morphology due to downslope run-out of debris flows followed in time by focused incision along levee-controlled run-off pathways. (c) Fan 8 (distal surface): Example of generally featureless, gently mounded morphology consisting of amalgamated, matrix-rich gravelly deposits (AGD); field of view at lower foreground in photo is approximately 5 m wide. (d) Fan B: Recent debris-flow lobe; field of view at lower foreground is approximately 3 m wide. Note textural segregation between coarser, matrix-free gravelly levee to the left (white pointers) and matrix-rich to matrix-supported, finer gravel of the inner-lobe deposit on the right; note also aspect difference with adjacent, varnished surface, composed of ancient, amalgamated debris-flow lobes. (e) Fan 7: Medial surface: radially oriented gravel concentrated as right levee of a large, presently degraded debris-flow lobe (left levee visible in background, top right in photo). Person for scale (circled in red) is approximately 1.7 m tall. (f) Fan 10: Residual debris-flow lobe on an abandoned fan surface, issued by larger debris-flow lobe visible in background. Note confined distribution of gravel, substantial absence of fine fractions from the gravelly framework of the deposit, and slightly coarser grain sizes distributed at the front and the margins. Field of view in foreground is approximately 2 m wide. (g) Fan 6: Recent lateral-vertical stacking and amalgamation of successive debris-flow lobes (white pointers indicate lateral margins) issued by the main incised channel; person for scale is 1.75 m tall.

5.4.1.2 Recent Incised Channels (RIC)

The recently active sectors of numerous fans are incised by low-sinuosity channels and washes which either extend individually down-fan from the apex area or form distributive networks of incisions shallowing and narrowing from the proximal to the distal domain. Depths range from a few decimetres to 2-3 m, with transverse profiles increasing in width-to-depth ratio towards the distal area. In the presence of a major incised channel (Fig. 5.8a), several secondary channels issue laterally from it or from its distal intersection point. In several instances, gravel lobes and ridges of relatively fresh and unweathered quality extend parallel to channel margins, indicating the overflow of debris flows (Fig. 5.8e).

Channel beds are invariably completely dry, showing no signs of recent run-off, and generally host poorly organized, clast-supported gravel of a similar granulometric range to that of the surrounding surface (Figs. 5.8a and b). The interstitial volume of gravel is frequently devoid of fine fractions (silt to granules) (Figs. 5.8b and c), which have been segregated into low-relief sheets and lobes downstream of inner bends or in lower-gradient channels further down-fan or blown away into the ocean through aeolian processes. Locally, lobes of poorly sorted, matrix-rich to matrix-supported gravel overlie the clast-supported beds of channels, indicating propagation along the incised fan topography.

Sporadic run-off is the dominant process reworking channel beds, as demonstrated by: a) crudely developed, gravelly side and longitudinal bars with moderate to good sorting and imbrication (Figs. 5.8a and b), indicating incipient macroform accretion at locations of reduced flow competence (Church and Gilbert 1975; Carling and Reader 1982; Zielinski 2003; Hassan 2005); b) well-developed microforms, such as gravel clusters (flow-parallel alignments of clasts upstream of an obstacle cobble or small boulder; Brayshaw 1984; Fig. 5.8c) or transverse gravel dams (alignments of coarse pebbles and cobbles transverse to channel axes, mostly along relatively steep reaches, to which they confer a stepped profile by trapping fine sediment upstream of each dam; Bowman 1977; Church and Jones 1982; Bluck 1987); c) the previously mentioned winnowing of fine sediment in proximal to medial channel reaches, accompanied by the formation of coarse sandy to fine pebbly splays and lobes down-fan, where competence and capacity were lost by flow infiltration and/or expansion (Fig. 5.8d).

Figure 5.8: (a) Fan 1: Waterlain deposits within the proximal section of the main incised channel; note relatively well-sorted gravel, run-off-controlled ridge-and-furrow morphology in the foreground (white pointers) and coarse-grained lateral bar in the background (black pointer). (b) Fan 7: Channel deposits on abandoned fan surface: note the openwork fabric and the relatively good sorting of gravelly deposits, and gravelly point bar accreted to inner side of the channel bend (white pointer). Field of view in foreground is approximately 5 m wide. (c) Fan 2 (proximal surface): tractive fabrics of waterlain gravel in secondary channel; note imbrication and transverse orientation of clast long axes. Hammer for scale is 32 cm long. (d) Fan 7 (distal surface): Terminal splay of sandy fine gravel at the mouth of a secondary incised channel. Field of view in foreground is approximately 2.5 m wide. (e) Fan 2 (distal surface): Mud-dominated texture of distal, clast-poor debris-flow lobe. Pen for scale is 12 cm long.

5.4.1.3 Mud Lobes (ML) (single/amalgamated)

Distal fan surfaces can be characterized by the presence of single or amalgamated lobes of sandy, granule- to cobble-bearing, rarely clay-rich, silty mud. The width of individual lobes varies from decimetres up to 3-4 m, and their thickness ranges from a few centimetres

up to 20-30 cm and more where several lobes have been stacked. Individual lobes have a plan-view shape characterized by distinct tapering down-fan, whereas fronts and lateral margins terminate abruptly with a marked depositional relief. Lobe surfaces are generally flat and featureless, except for protruding gravel clasts (Fig. 5.8e). Lobes can be distinguished from adjacent morphological elements by their marked depositional relief, dominantly fine texture, and occasional segregation of gravel along their margins. Where traceable upslope, mud lobes are frequently seen to merge with coarser-grained gravel units or to be issued by the distal terminations of shallow channels.

By analogy with the gravelly morphological units described above, the morphology and sedimentology point to an origin from fine-grained debris flows (i.e. mudflows) which terminated over distal fan domains, where low gradients and depletion of most of the sediment load upslope combined to reduce the internal shear of the mixture. Lateral expansion and flow halting were retarded by run-out within channels or between debris-flow levees. Although still characterized by considerable strength, as demonstrated by their stepped topography, these residual flows carried lesser gravel volumes and their lateral spreading over the distal fan thus was unhindered (Hooke 1987; Blair and McPherson 1998), except for the effects of local mesotopography or surface roughness. The frequent occurrence of these morphological elements down-fan from coarser debris-flow units and from channel terminations indicates that most mudflows spread down-fan as late-stage, relatively fluid phases of denser debris flows (Pierson 1986; Wells and Harvey 1987; Blair and McPherson 1998; Sletten *et al.* 2003).

5.4.1.4 Imbricated Gravel Lobes (IGL) (single/amalgamated)

Both recently active and abandoned surfaces of certain fans feature single or amalgamated concentrations of moderately to well-sorted gravel (Figs. 5.9a and b), ranging mostly from pebbles to coarse cobbles, a few metres in width and up to 5-10 m in radial extent, often located down-fan of the intersection points of markedly incised channels or broad, shallow washes. Most clasts have moderately to well-developed *a(t)b(i)* fabrics, and are devoid of interstitial matrix within a few centimetres from the surface (Fig. 5.9c). A relatively well-sorted, silty to sandy matrix may be abundant at depth within the deposit. Individual gravelly units have no internal organization, except for a distinctive fining upstream, with most clasts in the coarse-pebble to cobble range distributed in the distal portion (Fig. 5.9b).

Well-organized fabrics and relatively good sorting in these deposits are typical of transport from water flows. Similar depositional units have been originally described as ‘sieve lobes’ (Hooke 1967), ascribed to progressive accumulation of coarse sediments where flood waters lose competence because of fan mesotopography (channel terminations, gradient losses, obstacle vegetation, and sub-surface infiltration of water); finer sediment fractions are carried further down-fan after filtrating out of the permeable framework of the coarse gravels. While this process model has been occasionally debated and never truly ascertained in the literature (e.g. Blair and McPherson 1992; 1994; Nemec and Postma 1993; Milana 2010), the most parsimonious interpretation is probably that of rapid aggradation of coarse sediment lobes from newtonian, sediment-laden water flows with only limited ability to organize bed load during deposition (e.g. Milana 2010; Harvey 2013). Protracted run-off

during recessional flood stages was responsible for the infiltration of finer fractions in the lowermost levels of the deposit and onto the dry fan surface.

5.4.1.5 Ancient Gravel Deposits (AGD)

Most abandoned fan surfaces are characterized by a gently undulating, irregular topography of coarse and fine deposits which have been subject to prolonged exposure and weathering, as demonstrated by incipient spalling and exfoliation of gravel clasts, up to advanced stages of nearly complete disintegration, and by pervasive rock varnish. Proximal to medial surfaces are mostly occupied by a mantle of coarse angular gravel (cobbles to boulders) with little to no matrix within surface layers, but commonly with a poorly sorted silty to granular matrix evident below the topmost few centimetres. Finer gravelly domains present a continuous surface armour of fine pebbles to fine cobbles overlying a very poorly sorted, matrix- to clast-supported mixture of heterometric (silty to gravelly) sediment (Fig. 5.7c). Clear textural or geometric patterns are difficult to recognize in these sediments, but alignments and segregations of relatively coarse gravel are locally evident (Fig. 5.7e), assuming a radial orientation down-fan or a transverse, arcuate cross-fan orientation, isolated or clustered. These probably represent weathered remnants of coarse-grained debris-flow levees and snouts, as discussed above. Outsized boulders (up to 2-3 m in diameter) are common on the proximal fan, but their size and numbers generally decrease down-fan. Proximal to medial fan surfaces are characterized also by sinuous, radially-oriented segregations of openwork, relatively well-sorted gravel, a few decimetres and up to rarely 1.5-2 m wide, slightly depressed with respect to the surrounding topography and continuous over tens to hundreds of metres (Figs. 5.9d and e).

Distal surfaces within abandoned fan sectors may consist of relatively uniform mantles of fine-gravelly, silty sands to sandy silts. Lobate, longitudinally-elongate, gravelly domains are rarer over these kinds of surfaces. Topographically elevated domains have a regular, almost flat topography, although locally incised by channels (Figs. 5.9f and g). Clear evidence of prolonged weathering and deflation of the surface is given by a thin, pervasive armour of granules and pebbles (Fig. 5.10a), by the frequent occurrence of disintegrating clasts (‘clast ghosts’), by slightly hardened salt horizons directly underneath the surface, and by patterned grounds with very fine gravel segregated into reticular networks, probably related to surface disturbance by periodic mobilization of moisture and dissolved salts (Dunkerley and Brown 1997; Dixon 2009). Locally, associations of parallel, cross-fan alignments of pebble to fine cobble gravel are recognizable over fine-grained distal surfaces, with rectilinear to concave-down-fan trends in plan-view (Fig. 5.10b); these may extend laterally over several metres, at an approximately constant distance of several decimetres from each other, and with clasts featuring mostly clear *a(t)b(i)* fabrics.

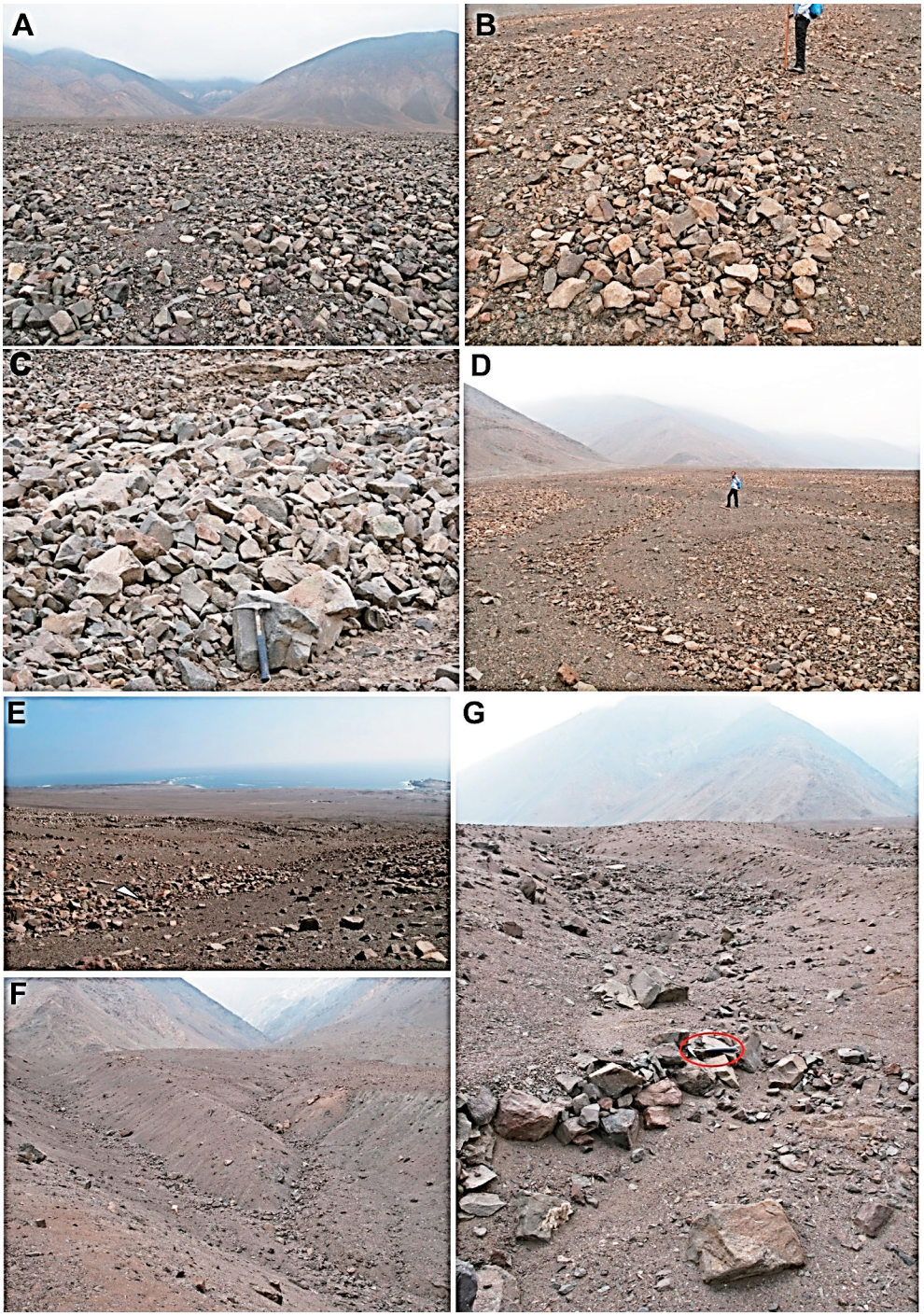
A
B
C
D
E
F
G

Figure 5.9 [Previous page]: (a) Fan 2 (medial surface): Waterlain amalgamated, well-sorted gravel lobes and splays. Field of view in foreground is approximately 4 m wide. (b) Fan 1 (proximal surface): Possible waterlain gravel lobe (sieve lobe) filling a shallow channel within the fan surface; note the abrupt frontal termination of the unit and the general decrease of grain size upstream. The complete person for scale is approximately 1.7 m tall. (c) Fan 1 (medial surface): Close-up of waterlain gravel; note generally good sorting, absence of interstitial matrix and very good imbrication (hammer for scale is 32 cm long and pointing down-fan). (d) Fan 1: Gravel lag in sinuous, shallow secondary channel reworking the medial surface. Person for scale is approximately 1.7 m tall. (e) Fan 7 (medial surface): Textural contrast between fine-rich fan surface, originally aggraded by debris flows, and coarse gravel lag filling a secondary channel (white pointer). Field of view in foreground is approximately 6 m wide. (f) Fan 8 (medial surface): Convergence of two deep incisions; note concentration of residual gravel along channel beds. Depth of both incisions is approximately 2 m. (g) Fan 8 (distal surface): Clast dam within secondary channel reworking a surface originally aggraded by debris flows; note thicker infill of fine sediment upstream of the dam, and relatively coarse texture of the channel fill as compared to the surrounding fan surface. Hammer for scale (circled in red) is 32 cm long.

Overall, the sedimentological and morphological evidence indicates that most abandoned fan surfaces consist of debris-flow deposits long exposed to weathering and deflation. Irregular topographies result from the superposition and juxtaposition of mass-flow lobes, some of which still recognizable by the remnants of levees and snouts. Intervening, sinuous gravel-filled depressions over proximal fans probably formed through run-off reworking during flash floods. The finer texture and the more subdued relief of distal areas indicate aggradation by relatively more fluidal tails of debris-flow. After most of the gravelly load has been deposited upslope, these residual flows tend to spread widely over fan surfaces, unhindered by the confinement of marginal levees and snouts. Most such distal surfaces have long been inactive and subject only to weathering and aeolian action. Sporadic alignments of gravel probably represents transverse ribs (Koster 1978; Wells and Dohrenwend 1985; Fig. 5.10a) formed by surface reworking or primary deposition during supercritical unconfined water flows, and distinguishable from debris-flow snouts because of their nearly rectilinear or concave-down-fan trends in plan-view.

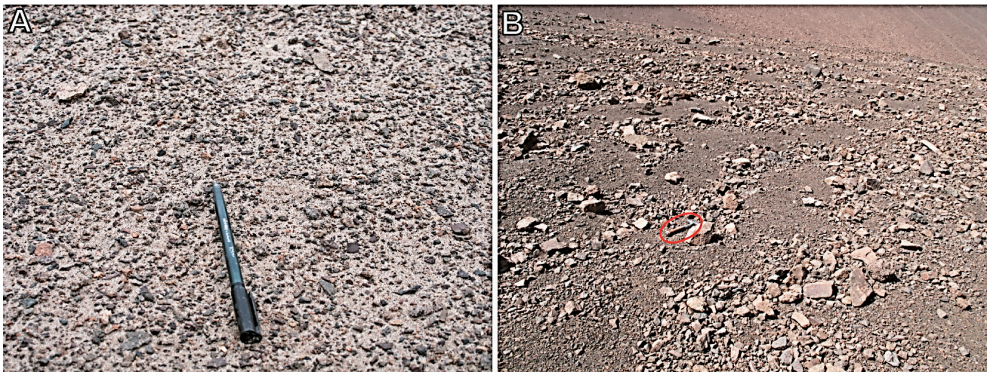

Figure 5.10: (a) Fan 10: Transverse ribs formed by supercritical unconfined waterflow over the medial fan surface; hammer for scale (circled in red) is 32 cm long. (b) Fan 2 (distal surface): Close-up of coarse sandy to fine gravelly desert pavement; pen for scale is 12 cm long.

5.4.1.6 Incised (ancient) Gravel Deposits (IGD)

Abandoned fan surfaces may be characterized by proximal to distal networks of shallow channels and washes with commonly sinuous courses and variably steep to smooth margins

(Figs. 5.9e, f and g). Channel beds are frequently occupied by deposits featuring a light tone that contrasts markedly with the darker, varnished brown to red colours of the adjacent surface. Incisions range in depth from a few decimetres to more than one metre, rarely up to a few metres, widening and shallowing down-fan to merge with the distal surface. Channel beds are invariably dry and commonly covered by moderately sorted sand to pebble gravel in low-relief sheets or in distinctly progradational splays at channel terminations. Fine channel sediments can acquire a mild degree of cohesion by salt cementation, and locally form shallow terracettes and elongate ridges. Cobble-size debris in channels is mostly concentrated in clast dams (Fig. 5.9g) and gravel clusters along channel axes, or in distinctive gravel trains along the margins of channel beds (Fig. 5.9 f).

Evidence points to run-off as the dominant factor of sediment transport and deposition within channels incised on abandoned fan surfaces. Most commonly, incisions connect up-fan to topographically depressed belts of openwork gravel, which indicates their formation from run-off over preferential pathways during several flash-flood events. Terracettes and residual gravel ridges in channel fills suggest complex phases of aggradation and degradation. Gravel concentrations at the margins of channel beds formed as lags accumulated passively where the incisions expanded or migrated laterally through alluvial-fan deposits. Clast dams and pebble clusters are due to the high energy of intense floods (Church and Jones 1982; Brayshaw 1984; Bluck 1987). The finer texture of distal channel fills and the openwork gravels of upstream channels combine to indicate gradual entrainment of fines from proximal fan deposits by run-off. Terminal splays form as floods become unconfined near channel mouths. The colour contrast of channels fills with the varnished fan surface demonstrates that most geomorphic activity occurs along fan-surface incisions, while the surrounding surface undergoes weathering and deflation.

5.4.2 Stratigraphic facies analysis of alluvial-fan outcrops

Besides examining the surface morphology of alluvial fans, the stratigraphic facies were evaluated. Exposures within the studied fans occur as a) longitudinally oriented sidewalls of incised fan channels, with depths variable from ~1.5 m to 6-8 m and a minimum extent of several hundreds of metres; as b) strike-oriented, continuous roadcut outcrops along the coastal 'Ruta Uno' between Antofagasta and Tocopilla, with depths varying from a few decimetres to a few metres; and as c) artificial trenches and large gravel pits excavated in the medial to distal fan domains for extraction of aggregate material. Stratigraphic sections provide the opportunity to examine old deposits buried below the active surface (e.g. Miall 1985). Individual beds, representing single depositional events (*sensu* Campbell 1967), can be confidently assumed to have been affected by variable degrees of reworking only in their major (upper) bounding surfaces, but not internally, thus allowing an assessment of the main processes of fan aggradation. Four gravelly facies have been observed to comprise the near totality of deposits in stratigraphic perspective (Fig. 5.11). Facies consisting mostly of sand and clay-silt represent only a minor volume of the deposits at outcrop (less than 5%), and therefore are not discussed below.

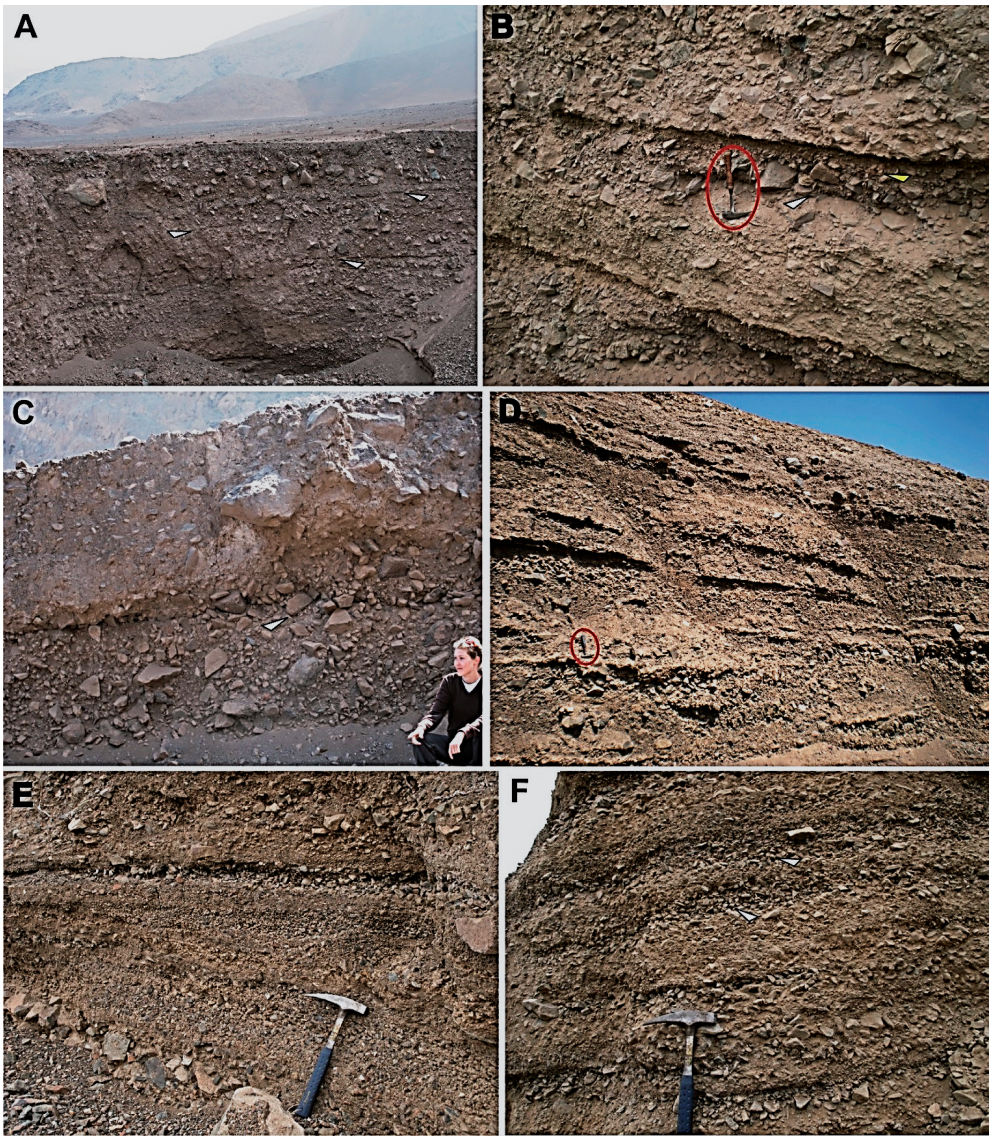

Figure 5.11: Expressions of stratigraphic facies within fan outcrops. (a) Fan 8: Stacked, amalgamated debris-flow units (facies Gmm) exposed in the main incised channel; section depth at this location is approximately 8 m. (b) Fan 6: Two debris-flow units (facies Gmm) separated by a coarse gravel lag (Gmr) and a thin unit of waterlain gravel (facies Gsc). (c) Fan 10: Debris-flow units (Gmm) separated by a discontinuous gravelly lag of facies Gmr. First author for scale. (d) Fan 3: Proximal outcrop in main incised channel; waterlain deposits represented by amalgamated lenses and planar beds of relatively well-sorted, stratified facies Gsc. Hammer for scale (circled in red) is 32 cm long. (e) Fan 1: Proximal exposure within main incised channel; waterlain deposits represented by finely stratified, well-sorted pebble to cobble gravels (facies Gsc). Hammer for scale is 32 cm long. (f) Fan 1: Exposure within medial outcrop, oriented across-fan; moderately sorted, stratified gravel deposited by confined and unconfined runoff; general flow direction toward the reader and to the left. White pointers indicate two laterally extensive lenses of openwork gravel (facies Gmo). Hammer is 32 cm long.

5.4.2.1 Facies Gmm (matrix- to clast-supported massive gravel)

Facies *Gmm* consists of structureless, very poorly sorted, matrix- to clast-supported pebble to fine boulder gravel in beds varying from a few decimetres up to 2-2.5 metres thick, laterally continuous over several metres to tens of metres in radially oriented exposures, and laterally extensive up to several metres in strike-oriented exposures (Figs. 5.11a, b and c). Beds commonly dip parallel or sub-parallel to fan surfaces (Figs. 5.11a and c), with sub-planar bases that show few signs of substrate erosion. Bed tops often are characterized by protruding outsized clasts. Depositional units are internally massive. Grading and primary sedimentary structures are absent except for occurrences of inverse grading towards the base or top of some units. Gravel clasts are generally oriented randomly in a poorly sorted, structureless matrix that varies per fan from clay-rich mud to a silty fine sand (Fig. 5.11c). Platy to oblate clasts with horizontal or sub-horizontal *ab* planes were locally found concentrated in the basal portions of some beds.

The sedimentology of facies *Gmm* indicates an origin from debris flows (e.g. Fisher 1971; Hubert and Filipov 1989; Blair and McPherson 1998; Blair 1999b) in which high-density sediment-water mixtures acquired substantial strength and plastic to pseudoplastic rheology from the substantial amounts of fine matrix. This is confirmed by the scarcity of erosion features and by the absence of clast segregation and orientation within beds, indicating essentially laminar flow behaviour in a highly concentrated sediment-water dispersion. Flows halted when reduced fan gradients or the interference of surface obstacles reduced internal shear rates below the threshold for flow mobility. Basal inverse grading in matrix-rich units is probably due to the elevated shear rate and consequent loss of matrix competence at the flow base (Hampton 1975; Naylor 1980; Hubert and Filipov 1989), whereas in clast-rich beds it is due to the higher angular momentum imparted to coarse particles in the sheared mixture, with consequent segregation of coarse clasts over smaller ones (Iverson and Denlinger 1987) and forced clast orientation sub-parallel to the flow boundaries (Rees 1968; Major 1998). The occurrence of debris flows with relatively non-cohesive, clay-poor matrix mixtures is due to the hyperarid climate of the Atacama Desert, where the scarcity of water strongly reduces the effectiveness of chemical weathering and the production of clay minerals within regolith, while clay at the surface is also easily deflated. Significant amounts of clay have been observed only in alluvial fans sourced by magmatic bedrock associations with abundant shallow intrusive rocks, originally subject to hydrothermal weathering in dyke swarms (e.g. fan 8). However, the excess pore pressures required to sustain mobility in clay-poor debris flows were temporarily provided by abundant silt and fine sand (Pérez 2001; Ventra *et al.* 2013).

5.4.2.2 Facies Gsc (clast-supported stratified gravel)

This facies consists of crudely to distinctly bedded, clast-supported, matrix-rich to openwork pebble to cobble gravel, in single or amalgamated beds and lenses, varying in thickness from a few centimetres to a few decimetres (Figs. 5.11d and e). It typically features moderate to good sorting, good imbrication and tractive fabrics in unequant clasts, and relatively thicker units are organized in planar divisions picked by textural contrasts and grading (Fig. 5.11e). Tractive structures are absent. However, some depositional units are not graded and present

sheared fabrics, with clast long *a* axes and *ab* planes oriented down-fan and sub-parallel to flow boundaries. Most beds comprise a high volume of silty to granular matrix, often normally graded, but clast-supported, matrix-free beds are also encountered. The basal surfaces of these units vary from weakly to distinctly erosive, with centimetric to decimetric relief.

Facies traits and the erosive geometry of beds indicate rapid deposition from unconfined to poorly confined water flows. Relatively good sorting, normal grading and the absence of tractive structures indicate deposition from bed load sheets (Whiting *et al.* 1988; Todd 1996) in the waning stages of flash floods. Internal layering probably relates to fluctuations in flow competence and bed load concentration during particularly protracted events. Where graded, the interstitial matrix was most likely aggraded within the coarser deposit during protracted flood recession (Frostick *et al.* 1984), but beds with abundant matrix and flow-parallel fabrics may have originated from particularly concentrated sediment dispersions (hyperconcentrated flows) in which particle density and collisions induced strong shearing and prevented grain-size segregation (Rees 1968; Todd 1989; Benvenuti and Martini 2002). Rapid deposition and relatively high sediment concentration at flow bases characterized most such events (*cf.* Nemec and Muszynski 1982; Todd 1989; Lowey 2002). The absence of tractive structures and of small macroforms probably is due also to the ephemeral duration and shallow depth of flows.

5.4.2.3 Facies Gmo (openwork massive gravel lenses)

Facies *Gco* consists of lenses of clast-supported, moderately to well sorted gravel ranging from fine pebbles to coarse cobbles, commonly characterized by prevalent openwork fabrics in coarser, cobbly units, or by the presence of a patchy, poorly sorted matrix of sand and granules in relatively finer, pebbly units. It typically occurs in lenses varying in thickness from a few clasts up to 30-40 cm, and from a few decimetres up to a couple of metres wide (Fig. 5.11f). Basal surfaces appear gently scoured into the underlying deposits. Except for some instances of crude to distinct normal grading and *a(t)b(i)* clast imbrication upcurrent in coarser-grained units, facies *Gmo* generally lacks sedimentary structures and well-developed fabrics.

The relatively good sorting of the coarsest fractions, the scarcity of finer matrix, local normal grading and clast fabrics indicate rapid deposition from ephemeral run-off in shallow channels and washes over the fan surface, confirmed also by the limited width of gravel lenses in strike-oriented outcrops. The short duration of floods did not permit the full development of tractive structures and pervasive fabrics. Some units with a more heterogeneous granulometry might have been deposited by flows with higher sediment concentrations, with transitional rheology and dynamics between hyperconcentrated flows and fluidal (non-cohesive) debris flows (Nemec and Steel 1984; Wells and Harvey 1987), in which rapid deposition of the coarsest load would have been followed by winnowing of fines during a protracted recession phase. The most extensive of these units along strike probably correspond to waterlain deposits otherwise interpreted as ‘sieve lobes’ (Hooke 1967; 1987; Blair and McPherson 1992; Milana 2010).

5.4.3.4 Facies Gmr (reworked Gmm – now clast-supported gravel layers)

The top surfaces of debris-flow beds (facies *Gmm*) are occasionally characterized by thin, discontinuous to laterally very continuous layers of clast-supported pebble to cobble gravel with weakly erosive bases (Figs. 5.11b and c). The thickness of these units varies from single clasts to a few clasts, although some lensoidal ones may attain thicknesses up to 20-30 cm. Platy and elongated clasts may feature a weak imbrication upstream. While some units present an openwork, matrix-free fabric, relatively thick units commonly contain abundant matrix concentrated towards the base.

The scarce thickness of this facies and its invariable superposition to *Gmm* beds, often accompanied by weak scouring, indicate a secondary origin through reworking of debris-flow

Table 5.2: Summary of the surface units and stratigraphic facies at each alluvial fan.

Unit Name	Notation	Fan 1	Fan 2	Fan 3	Fan 4	Fan 6	Fan 7	Fan 8	Fan 10	Fan A/B
Recent gravel lobes	RGL	-	X	X	X	X	X	X	X	X
Recent incised channels	RIC	X	X	X	X	-	X	-	-	-
Mud lobes	ML	-	-	-	-	X	X	X	X	X
Imbricated gravel layers	IGL	X	-	X	-	X	-	-	-	-
Ancient gravel deposits	AGD	X	X	X	X	X	X	X	X	X
Incised (ancient) gravel deposits	IGD	X	X	X	-	-	X	-	-	-
Matrix- to clast-supported massive gravel	*Gmm*	-	X	X	X	X	X	X	X	X
Clast-supported stratified gravel	*Gsc*	X	-	X	-	-	-	-	-	-
Open-work massive gravel lenses	*Gmo*	X	X	X	-	-	-	-	-	-
Reworked layers of massive gravel	*Gmr*	X	-	X	X	X	-	-	-	-

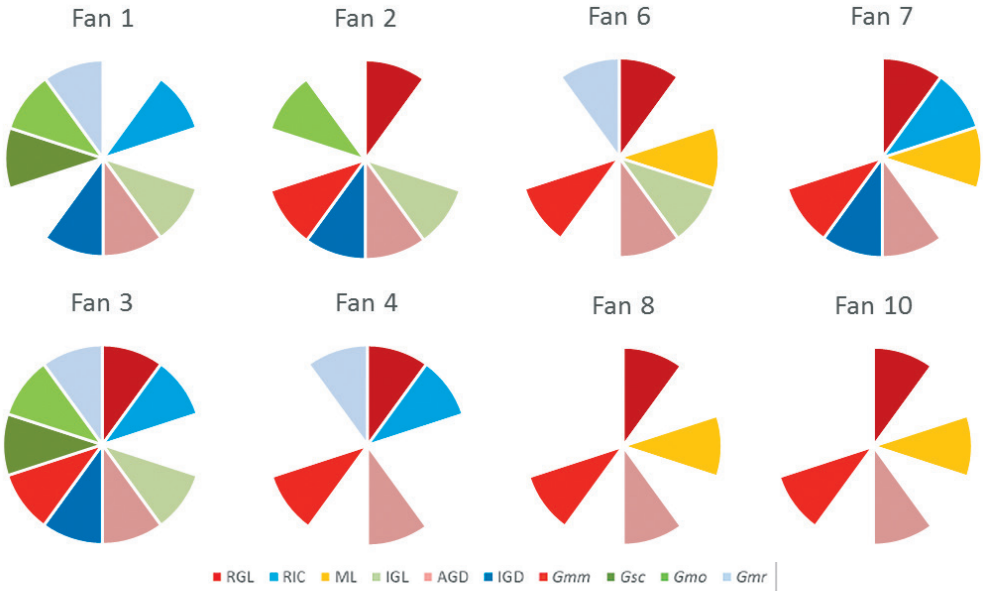

Figure 5.12: Visual representation of documented surface units and stratigraphic facies for each alluvial fan.

deposits (Blair and McPherson 1992; 1998; Moscariello *et al.* 2002): winnowing of the fine-grained, silty to sandy fractions produced a thin, stable armour of poorly structured gravel that in most instances was subject probably to only limited transport. Thicker, lenticular units were formed corresponding to shallow rills and washes which more frequently hosted run-off. Variable sorting of these thin deposits was probably related to run-off intensity and duration, whereas their frequent spatial discontinuity was due to the fractionated distribution of effective run-off on fan surfaces.

In summary, a whole suit of surface units as well as stratigraphic facies has been observed across the ten fan sites under investigation. In Table 5.2 we present a summary of the features that have been identified in association with the various fans. If a feature was not observed, that does not imply that it cannot have been present (as section views were limited), but in all likelihood the representation of features should give an indication of which processes where prevalent with regards to the construction of the particular alluvial fan. Figure 5.12 gives a visual representation of the features that have been recorded for each fan and illustrates that our observations lead to the interpretation of different processes responsible for fan formation along the Atacama coast.

From the above, it is clear that various categories of surface features and hence processes were observed. We also observe noteworthy associations between different features, for example, most fans that show evidence of recent incised channels also exhibit layers of imbricated gravel and reworked massive gravel. We notice that the different categories do not only exhibit different architectural elements on the surface or different facies in the sections, but also different gradients depending on the dominance of the processes that were responsible for the surface expression and the sub-surface stratigraphy. We use these observations to classify the coastal fans into the groups that were discussed in the introduction (a-d) and our results are listed in Table 5.3.

Table 5.3: Fan site data from field work.

Fan	Relief (m)	Gradient (°)	Group	Dominant Process
Fan 1	132	5.4	D	>90% Run-off
Fan 2	281	5.3	C	>50% Run-off
Fan 3	242	5.5	C	>50% Run-off
Fan 4	158	5.3	B	>50% Gravity-flow
Fan 6	232	6.9	B	>50% Gravity-flow
Fan 7	130	6.4	B	>50% Gravity-flow
Fan 8	188	6.4	B	>50% Gravity-flow
Fan 10	157	6.0	B	>50% Gravity-flow
Fan A	90	12.7	A	>90% Gravity-flow
Fan B	130	10.5	A	>90% Gravity-flow

The spread in the values of fan length, fan gradient, and fan area for both the population of large Martian fans in this study (50+) and the Atacama fans (8) are shown in Figure 5.13. These Martian fans are longer, larger and less steep than the Atacama fans. The population of Atacama fans is too limited to be a true representation of all terrestrial fans, and similarly the population of Martian alluvial fans in this study is not representative of all Martian alluvial

fans, but from this data there is a clear indication that Martian fans may be considerably larger than terrestrial fans and that their gradients are much lower (also observed by Moore and Howard 2005).

Profiles of the eight Atacama alluvial fans that are described here are drawn as a function of distance from the apex in Figure 5.14. We detect only small differences between the gradients of fans with more or less evidence of run-off, but that is consistent with our interpretation that these fans were all constructed predominately by debris-flows (except fan 1). It is evident from the profiles that fans A and B have distinctly higher gradients, as is expected for systems on the border between colluvial fans and mass-flow dominated alluvial fans. Note the knickpoint in the profile of fan B (Fig. 5.14), which might be seen as signifying the change from pure colluvial fan to alluvial fan. Although it has been stated that the total relief of a deposit (the height difference between fan apex and toe) is a factor that influences the gradient of this deposit, we see no relation in our data between fan relief and fan gradient and we find that both high and low relief fans can yield a high dominance in either sediment-gravity or fluid-gravity processes.

In comparison, profiles of eleven Martian alluvial fans are shown in Figure 5.15. These profiles are drawn from deposits in Crater A at -21°/320°E, Crater D at -18°/323°E, and Holden Crater at -25°/325°E (as defined by Moore and Howard, 2005) and include a range of lengths from 5 to 30 km. Profiles 1a and 1b are those that were shown in Figure 5.2. The average gradient is around 0.05 for the Martian fans, in contrast with approximately 0.1 for the Atacama fans. However, considering the much larger size of this population of Martian

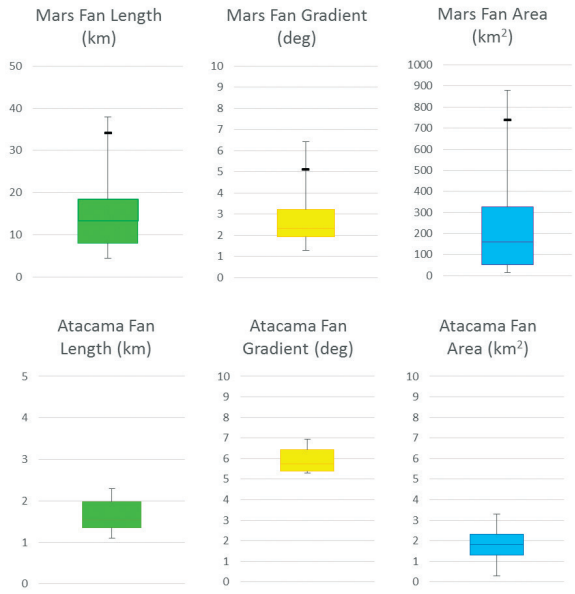

Figure 5.13: Box and whisker diagrams illustrating the minimum, maximum, median, first and third quartiles (MIN, Q1, MED, Q3, MAX) of three morphological parameters for the large alluvial fans on Mars and those in the Atacama. Note the large variation in the values for the Martian fans in comparison with the smaller variation in the values for the Atacama fans. Outliers are located outside the 1.5 IQR (interquartile range) interval, which further underlines the large spread of values recorded for the Martian fans.

alluvial fans, some degree of lower gradient is to be expected. Furthermore, as mentioned earlier, it is likely that lower run-out angles for alluvial fan deposits are to be expected on Mars due to the lower gravity.

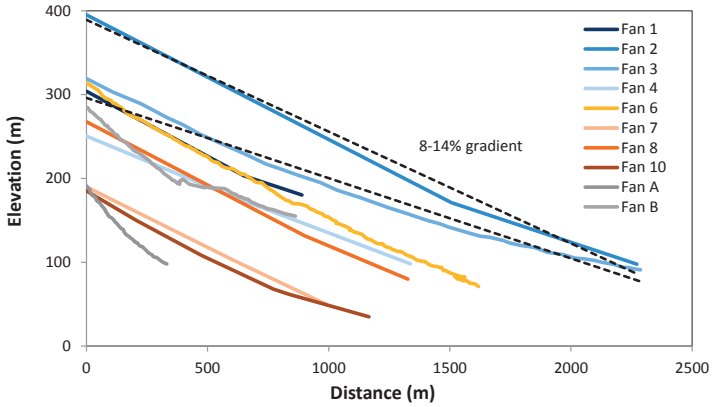

Figure 5.14: Fan profiles for twelve Atacama alluvial fans (plotted with y-values above mean sea level against metres). Trend lines indicate the range of gradients that are observed amongst these alluvial fans (thus excluding fan A and B).

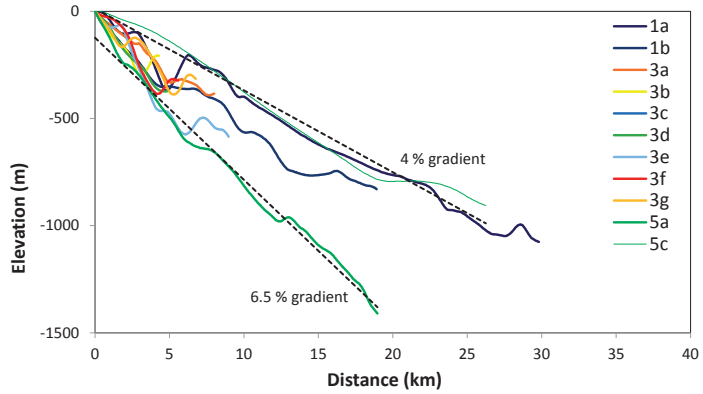

Figure 5.15: Fan profiles for eleven Martian alluvial fans (plotted with y-values showing relative elevations from the fan apex against kilometres). Trend lines indicate the range of gradients that are observed amongst these Martian alluvial fans, which is somewhat lower than the range observed for the Atacama alluvial fans.

5.5 Discussion

The Atacama coastal fans are considered valid analogues for some of the alluvial fans identified on Mars. Most of the Atacama fans described above have surface characteristics that appear similar to those of the Martian fans from remote sensing observations. The Atacama fans as well as the Martian fans have an undulating surface topography, covered by ridge-like structures that radiate from the apex towards the distal edge. The obvious difference includes the greater lengths and the lower gradients of the Martian fans, but as argued above, we still classify these fans as neither colluvial fans, nor fluvial fans; they are alluvial fans *sensu strictu* (cf. Blair and McPherson 1994).

From aerial view, most of the Atacama fans are remarkably similar in appearance to one another. However, not all these Atacama fans (that appear somewhat similar to one another from the air) are similar indeed. At the surface, we observe that some fan surfaces have been aggraded by run-off and other are merely reworked by run-off. Others have not been altered at all since primary aggradation, apart from physical weathering and deflation. The signs of erosion on the surface, and a fair amount of incised channels and other run-off related features, indicate aggradation through fluid-gravity flows.

However, based on stratigraphic indicators, we have ascertained that they range from debris-flow dominated to run-off dominated and that most are mixed-flow fans. Some of the fans show little to no construction or modification by run-off (our type a); while others show some degree of modification of the debris-flow units by later run-off but very little evidence of fan construction by means of run-off (our type b). Some of the fans have been constructed by both debris flows and run-off (our type c), while at least one fan (fan 1) has been constructed predominately by run-off with very little influence of any debris-flow processes (our type d). These origins are difficult to distinguish from satellite imagery and even at the surface in some cases, but stratigraphic sections confirm that almost all of the coastal Atacama fans have been constructed largely by debris flows. The main questions to address are whether Martian alluvial fans are debris-flow or run-off dominated and whether observed run-off features are depositional or erosional in origin. Whether debris flows or water transport dominate, depends on the quantity and the quality (e.g. amount of fines) of sediment which is produced in the catchment over a certain time interval and the amount of available discharge (incidental rainfall, snowfall, and mobilized groundwater) over such periods.

5.5.1 Sediment

In general, terrestrial alluvial fans comprise a wide range of grain sizes, from coarse gravel to clay. At least some variation can also be expected on Mars. A bimodal sediment distribution has been proposed for Mars (based on data from at least five landing sites), including a coarse, often angular, fraction in combination with fines (e.g. Herkenhoff *et al.* 2004). The coarser-grained a sedimentary deposit is, the higher its thermal inertia due to its ability to retain heat (e.g. Golombek 2003). In general, alluvial fans and other sedimentary deposits with relatively fine and loose sediment particles have a lower thermal inertia than surrounding bed-rock (Hardgrove *et al.* 2009). Martian alluvial fans have a higher thermal inertia than other sedimentary landforms such as aeolian dunes and are thus likely to be relatively coarse-grained (Moore and Howard 2005; Di Achille *et al.* 2006a).

Debris flows tend to occur in zones where catchments yield large quantities of fine sediment relative to the amount of rainfall, such as in areas where sedimentary, low-grade metamorphic, and basic igneous rocks are dominant. Run-off dominance is more easily attained where catchments are dominated by high-grade metamorphic and silica-rich igneous rocks that commonly show poorer weathering and produce a smaller fine fraction (Lecce 1990; Harvey 2010). Basaltic rocks occur throughout most of the southern highlands on Mars, and they have the potential of providing large quantities of clay and fines that contribute in acquiring and maintaining cohesive strength by debris flows. The availability of a bimodal

sediment supply with ample fine material and a higher sediment transport efficiency implies that debris flows on Mars are likely much more common than sheet flows.

Notably, it may be harder to create sediment on Mars because of the lower bedrock erosion rate related to near-absence of water as well as the lack of vegetation (Komar 1979), but it may be easier to move the sediment once created due to the higher transport efficiency resulting from lower gravity and lower friction (Bhattacharya *et al.* 2005). Due to the lower gravity on Mars (0.38g), sediment transport rate on Mars might be higher than that on Earth as a result of the lower frictional drag, but scaling laws have been applied to correctly infer sediment transport rate and other hydrological parameters on Mars and it has been shown that acceleration due to gravity is not the most significant variable (Grant and Parker 2002; Moore *et al.* 2003; Kleinhans 2005a; Hoke *et al.* 2011). In addition, it has been suggested that the dynamic angle of repose may be up to 10 degrees lower on Mars for all types of sediment (Kleinhans *et al.* 2011), implying that fans must be longer in order to accommodate the same amount of sediment.

5.5.2 Discharge and climate

Initially, fan formation in arid and semi-arid regions on Earth was believed to be linked directly to climate - i.e. higher run-off during warmer, wetter periods producing rapid growth of fan structures, and fan dissection during colder, drier periods (Blissenbach 1954; Rachocki 1981). However, it has been suggested decades ago by Lustig (1965), that alluvial fan aggradation occurs regardless of the type of climate as long as more sediment is brought to the foot of the slope than can be carried away from there. In spite of old concepts, alluvial fan deposition and aggradation in terms of processes is becoming more often considered to be not only dependent on climate but on sediment availability as well (see Ventra 2011 and references therein). Essentially, merely the relation between the amount of water (more or less) and the amount and composition of the available sediment (coarse or fine) defines a certain sediment-gravity to fluid-gravity flow ratio. This ratio is lower for run-off dominated fans than for debris-flow dominated fans, and even less for fluvial fans. The amount of available water in the catchment may locally differ, even under the same climate conditions. For example, larger catchments may produce larger amounts of discharge and thus more water-rich processes. On Mars, the catchments of most of the alluvial fans are limited to an alcove or at most a short and steep feeder channel.

As seen in the Atacama Desert, a particularly wet climate is not necessary to allow the formation of extensive alluvial fans. Occasional flash floods are the only prerequisite to mobilize significant volumes of sediment once there has been sufficient time for weathering as to produce such significant amount of sediment in the catchment. In the hyperarid context of the Atacama Desert, studies have consistently ascertained that run-off events with geomorphic effectiveness are very rare, with recurrence intervals of the order of thousands of years (Hartley *et al.* 2005a; Dunai *et al.* 2005; Nishiizumi *et al.* 2005). This confirms that alluvial fan formation is in general a poor indicator of climate conditions on Earth and that a warm and wet climate on Mars cannot be assumed based merely on the occurrence of a particular type of fan.

Long intervals with flowing surface water are not needed to explain these Martian alluvial fans or some run-off related features on their surfaces and the time of formation may have been much shorter than previously interpreted (Moore and Howard 2005; Kraal *et al.* 2008a; Armitage *et al.* 2011) based on the short formation time for sediment-rich alluvial systems.

5.6 Conclusions

Based on our insights from the Atacama fans, we suggest that the Martian fans have been constructed by debris flows and perhaps modified by run-off in cases where run-off associated surface features are described. Our terrestrial observations introduce the possibility that Martian alluvial fans were originally aggraded by mass flows to a more significant degree than previously thought and that the amount of water needed for their formation was limited and intermittent.

The formation of alluvial fans may have been the product of multiple events related to groundwater sapping and surface run-off, but even so the conditions for creating these features were either close enough to the present-day conditions and can still be referred to as cold and arid, or were merely episodically less arid with some fluvial activity driven by regional events or obliquity maxima. The intermittent occurrence of water is in agreement with suggestions of short-period, episodic hydrological cycles or flash floods as a result of widespread or regional volcanism and impact cratering events. These events induced heating of the permanent sub-surface ice layer providing enough water to form the alluvial fans on Mars without having to infer a longer period of warm and wet conditions with sustained rainfall. As such, these conditions for formation do not imply a long-term, precipitation-driven, warm and wet climate, but rather a cold climate pulsed with short-term, catastrophic, sediment-rich water pulses capable of distributing large volumes of sediment in short periods of time.

5.7 Acknowledgements

The authors acknowledge the contribution of Guillermo Chong to the organization of the fieldwork campaign, as well as Juan Pedro Rodríguez López for fruitful discussion. Stefanie de Keijzer and Wouter Hageman are thanked for their valuable input and help with data collection.

“Grown-ups like numbers. When you tell them about a new friend, they never ask questions about what really matters. They never ask: “What does his voice sound like?” “What games does he like best?” “Does he collect butterflies?” They ask: “How old is he?” “How many brothers does he have?” “How much does he weigh?” “How much money does his father make?” Only then do they think they know him.”

6 Experimental Investigation of Reservoir Dam Removal

Based on:
de Villiers, G., Kleinhans, M. G., van Breemen, D. M. O., Postma, G., & Hauber, E. (2010b). Experiments on sedimentation in wide reservoirs and erosion following dam removal. In *Proceedings of the River Flow 2010 Conference* (pp. 1147–1154). Braunschweig, Germany.

Abstract - Sedimentary deposits in reservoir lakes record the sediment transport capacity of the upstream river and past water levels of the downstream basin. Volumes and morphologies of deltas can be used to calculate flow and sediment dynamics. We constructed circular basins to which we fed constant flow discharge through a feeder channel of gravelly sand with different ratios of added silica flour. During water level rise, the longitudinal radius of the delta decreased. During water level fall, after dam removal, the deltas were partially destroyed by erosion. Surprisingly, for low discharges the channel markedly destroyed the deposit through transverse movements of the initial channel whereas for higher discharges the terraces were preserved for a longer time. Our results indicate that dam removal at wide lakes may lead to an unexpected inverse relation between discharge and erosion of the deposit, which has consequences for the subsequent sediment pulse magnitude. Point-modelling of sediment transport capacity yielded volumes in good agreement with observed volumes, proving that the time scale of activity can be inferred from feeder channel dimensions and delta volume. Our results suggest that these parameters can yield consistent reconstruction of the formative time scale also on Mars, which has consequences for the interpretation of ancient climate.

6.1 Introduction

Sediment is deposited where rivers enter plains or lakes. For plains and lakes much wider than the river, these deposits are fan-shaped because discharge spreads out as un-channelized sheet flow or channels avulse over the plain (Bull 1968; Blair and McPherson 1994; Leeder 1999; Parker 1999). We study delta formation and destruction and apply this to two completely different contexts: in crater lake sedimentation on Mars and in delta sedimentation and erosion in reservoirs following dam removal on Earth.

Deltas are found all over the Earth in several different environments, including wide hydropower reservoirs. Deltas are also found all over Mars, usually in impact craters, indicating that these must have been lakes. Some crater rims were breached, causing water to flow out of the lake. If water level remained constant then a delta built out analogous to sedimentation in reservoirs. If the water level fell then the delta was eroded in analogy to what happens in wide reservoirs on Earth upon dam removal.

Our objectives are twofold. Firstly, to understand the morphodynamics and formative time scale of deposits in a lake being filled with water, so that we can predict past hydrology in cases on Mars where this is unknown. Secondly, to understand the morphodynamics and erosive time scale of these deposits while the basin empties following dam removal or basin rim breaching, so that we can predict the fate of the deposit following dam removal on Earth and again so that we can interpret past hydrology from the morphology of Martian deltas.

As the sediment accumulates in the reservoir, the reservoir loses its potential to store water (McCully 1996; Cantelli *et al.* 2004). Trap efficiency of reservoirs depends on the ratio between storage capacity and inflow, the reservoir age and shape (related to storage capacity), the types and number of outlets, and the properties of the sediment (Brune 1953). When large amounts of catastrophic discharge are released, the sediment trap efficiency may go down with 30% as more sediment, especially fines, is washed out of the reservoir (Brune 1953). If the reservoir traps less sediment, a smaller delta deposit may therefore be formed (or erosion might take place). Using measured delta volume, sediment transport predictors and the properties of the upstream feeder channel, we can obtain a first-order estimate of the length of time required to form such a sedimentary body (Kleinhans 2005a) and hence we can speculate about the water and sediment flux and thus the environmental conditions that might have been present at the time of formation. This is relevant for Mars where we can measure the delta volume but would like to infer the amount of discharge and the implications for past climate.

On Earth, in cases of dam removal, both formative discharge and volume of the deposit are known, but sediment delivery is not well understood, especially not in the cases of wide reservoirs (Cantelli *et al.* 2004). The deposits in the reservoir provide a large source of sediment to the downstream river upon basin rim breach or dam removal. Hence, it is not only important to understand how much sediment has been trapped in the reservoir, but also what the nature of this deposit is. Fine sediments such as silt and clay can be a problem for ecosystems as they may cover vegetation, kill fish species and raise water levels (Doyle *et al.* 2002). It might also affect local downstream structures such as bridge foundations and irrigation channels. Not many experiments with fines (silt and clay particles less than 0.075 mm in diameter) in the sediment feed have been done (Cantelli *et al.* 2004), hence our

experiments also shed light on the grain size distributions and profiles for rivers that may contain significant percentages of fine material.

The longitudinal profile of a reservoir delta is characterised by a coarse-grained topset and fine-grained bottomset (Leeder 1999; Cantelli *et al.* 2004). The coarser sediments, such as gravel and sand, tend to settle out at the upper end of the reservoir, forming a "backwater" delta which gradually advances toward the dam. The lighter sediments, silt and clay, tend to be deposited nearer to the dam (McCully 1996). This longitudinal grain size profile is typical in the formation of deltas on Earth and could be similar for those formed on Mars, if the grain size distribution is at least bimodal. In systems with many narrow feeder channels (line feeders as defined by Postma 1990), this simple upward fining sequence is often displayed, but in systems with a single wide feeder channel (point feeders as defined by Postma 1990), the fining upwards cycle repeats and also intersects laterally as the channel on the surface of the delta migrates and avulses (Kleinhans 2005b). Either way, since the coarse grains occur within the delta topset and foreset, and particularly the topset and foreset are eroded by the down-cutting channel, we hypothesise that the majority of the sediment that upon breaching is delivered to the downstream system will be coarse-grained.

Thus, for prediction of reservoir lifetime it is important to understand how the delta sedimentary deposits are formed. For environmental impact it is important to understand how the deposits are modified and eroded upon dam removal. The formation of delta deposits and their subsequent modification and erosion are not mirror image processes - deposition of the delta fills the entire accommodation space whereas erosion of the delta takes place through a river channel that cuts deeply into the delta and leaves terraces that require time to be removed (Cantelli *et al.* 2004). Knowing this timescale of erosion, as well as the subsequent deposition location of the eroded sediment, is of importance for estimating possible sediment overfeeding to the downstream channel. Though narrow delta deposits (e.g. cases where the feeder channel is almost as wide as the deposit – also described as line feeder systems (Postma 1990)) have been studied experimentally, little is known about sediment terrace erosion in the case of wide delta deposits such as cases where the feeder channel is much narrower than the resulting deposit – also described as point feeder systems (Postma 1990).

By investigating the geomorphology of fan-shaped landforms (both on Earth and on Mars) one can deduce important features indicative of upstream (e.g. discharge, duration and sediment properties) and downstream (e.g. basin hypsometry) conditions at the time of formation. Furthermore, from studies of this nature, scientists can predict how rivers may react to various forcing factors as well as to changes in these conditions in real life.

6.2 Methods

The experiments were performed in the Eurotank facility at Utrecht University. The Eurotank is a 6.3x11.4x1.2 m^3 flume that can be filled with any type of sediment. Water flow to the tank is regulated with a series of calibrated valves and pumps and sediment supply (when used) is controlled with a worm screw sediment feeder. Sediment was only added to the system in two experiments; usually the channel was left to erode itself. This was done because we do not know what the sediment availability on Mars was like. It is possible that there was not a large supply of sediment available in the upstream channel and that the channel had to excavate

its own supply. We constructed circular basins with fixed diameters of two metres, (similar in shape to that of a complex impact crater) and a feeder channel leading into the basin. The basin could be breached at any point to let the water out (Fig. 6.1). Into these basins we fed constant flow discharge through a feeder channel of 1.5 metres containing gravelly sand with different ratios of bed load versus suspended load forced by the addition of silica flour.

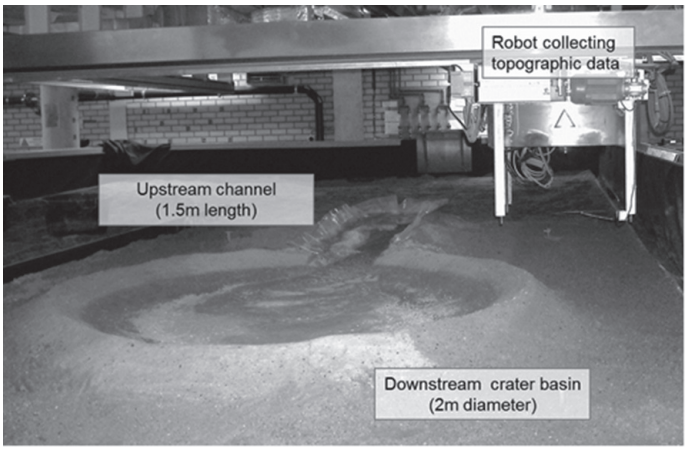

Figure 6.1: Experimental set-up of crater basin with feeder channel in the Eurotank Flume. Flow direction is towards the front. Discharge during each experiment is kept constant.

Each experimental run was performed in two stages (Fig. 6.2). During the first stage, the basin was allowed to fill with water from the upstream feeder channel (basin water level rise). During the second stage, the basin rim was breached so that some water was lost to the surrounding areas (basin water level fall, or constant in exceptional cases).

Between the two stages, the experiment was paused, the water drained and the deposit measured and photographed. In order to continue with the second stage as if no interruption has occurred, the crater lake was again filled with water (with use of an external hose pipe) after which flow in the original channel recommenced.

Important parameters such as water discharge and sediment grain size were varied systematically (Tab. 6.1). These variations were responsible for further small morphological differences in the delta deposits. However, during the experiments discharge was kept constant. Furthermore, we also varied the degree of sorting by removing the coarse tail as well as the volume percentage of fine material (silica flour) in the upstream feeder channel and in the downstream basin rim in order to experiment with bank strength.

Most of the experiments were performed with no addition of fines (0% silica flour), using only river sand or beach sand. The unsieved river sand can be classified as very coarse or even gravelly due to the presence of grains with diameters larger than 4.75 mm, even though the average grain diameter is only 0.475 mm. The sieved river sand was classified as coarse sand (D_{50} = 0.450 mm) and medium sand (D_{50} = 0.400 mm) due to the presence of grains with diameter larger than 2 mm in the first and their absence in the second. The beach sand with an average grain diameter of 0.225 mm can be classified as fine sand. Some experiments were thus performed with poorly sorted, bimodal river sand (D_{50} = 0.475 mm);

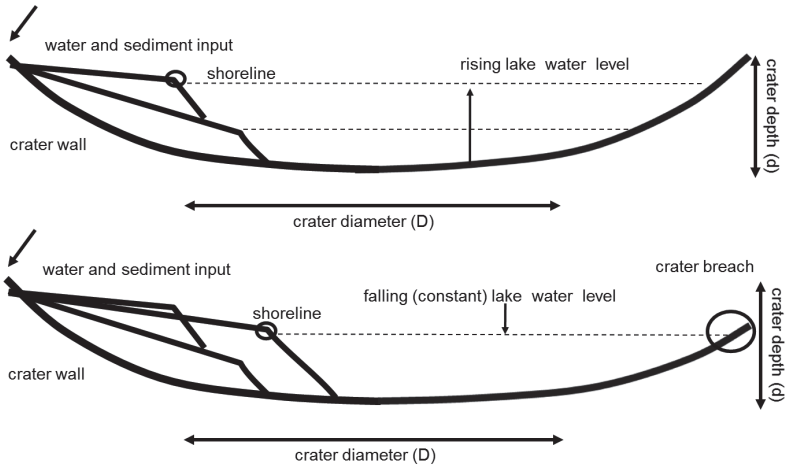

Figure 6.2: Schematic drawing of the two stages in each experimental run. Basin is constructed in the shape of a complex impact crater with diameter (D = 2 m) and depth (d = ~16 cm).

some with slightly better sorted, yet still bimodal river sand (D_{50} = 0.450 mm); some with much better sorted, almost unimodal river sand (D_{50} = 0.400 mm); and some with well sorted, unimodal beach sand (D_{50} = 0.225 mm). The sorting in the river sand was improved by dry-sieving with different sieves. Further experiments were performed with a 20% or 40% volumetric concentration of silica flour mixed into the bimodal river sand (original D_{50} = 0.450 mm, new D_{50} was not measured, but should be considerably less). We did not experiment with volumetric ratios of silica flour higher than 40% because Kleinhans *et al.* (2010b) found that above 40% silica flour the sediment either hardens completely or entirely fluidizes, as expected from the decrease in porosity due to the infilling of silica flour into the pore space of the sand.

Table 6.1: Experimental conditions and variables.

Run	Discharge (Q) (m^3/s)	Grain Size (D_{50}) (mm)	Silica (%)
A	0.07	0.475	0
B	0.21	0.475	0
C	0.35	0.475	0
D	0.35	0.450	0
E	0.07	0.450	0
F	0.35	0.225	0
G	0.07	0.225	0
H	0.07	0.400	0
I	0.35	0.400	0
J	1.08	0.450	0
K	0.35	0.450	20
L	0.07	0.450	20
M	0.35	0.450	40
N	0.35	0.450	40

Morphology before, during and after each experiment was measured by photogrammetry on an automated positioning system, designed to make high-resolution scans (0.5 mm). DEMs were created from stereo pairs using the dedicated software SANDPHOX and analysed in MATLAB.

We created fourteen delta deposits in the flume laboratory, all of which were formed as the basin filled with water (Tab. 6.1). Once full, the basin was breached by manually removing part of the crater wall (similar to dam removal) and in all cases the sedimentary deposit was at least somewhat destroyed by the incising stream. Incision into the delta deposits was more intense with higher discharge, leaving large terraces in the basin.

Sediment transport rates and volumes were calculated for all experiments using sediment transport predictors (overview in Kleinhans 2005a). We assumed that Froude number is close to unity (Fr ≈ 0.9) based on occasional observations of localised non-moving antidunes and we calculate the depth of the stream from the measured discharge and width. We also measured the channel slopes. By using a poorly sorted mixture, including coarse sand and fine gravel, the flow remained hydraulically rough or at least transitional, so that scour holes and the tendency to form ripples were prevented (Kleinhans *et al.* 2010b). Flow was transitional to turbulent in all experiments. To calculate velocity, the Chézy law was used:

$$u = C\sqrt{R\,S} \tag{1}$$

where u = flow velocity (m/s), C = Chézy roughness coefficient ($m^{0.5}/s$), R = hydraulic radius (m), calculated as Wh/(2h+W) where h = water depth and W = channel width, and S = channel gradient. Colebrook-White was used to calculate hydraulic roughness:

$$C = 18\log\left(\frac{12R}{k_s}\right) \tag{2}$$

where k_s = Nikuradse roughness length (m). The k_s can be calibrated (ranging from $k_s = D_{90}$ to $k_s = 7D_{90}$). We used Meyer-Peter and Müller (1948) for bed load transport predictions:

$$\varphi_b = \alpha\left(\theta' - \theta_c\right)^{\beta} \tag{3}$$

where φ = non-dimensional transport rate, α = 8, θ' = Shields number assuming skin friction following Van Rijn (1984) and β = 1.5. The values for α and β are non-dimensional calibration coefficients and were derived from flume experiments with well-sorted gravel, however, these values can be modified to optimise the transport prediction.

We assumed a perfect trapping of sediment in the basin and we used the Exner equation for the sediment mass balance. The volumes of all deposits were measured from DEMs (if possible) and compared to the values predicted by bed load sediment transport predictors.

6.3 Results

6.3.1 Phases of Development

Two stages of system development were created. During the first stage, the crater was allowed to fill with a constant discharge delivered through the upstream channel. This resulted in a rising water level. At the same time, sediment supply led to a delta formation, where the rising water level caused back-stepping of the delta deposit (Fig. 6.3 top). We found that all basin deposits exhibit a decreasing longitudinal length (or radius) over time during water level rise as transport capacity of the feeder channel decreased with decreasing gradient.

During the second stage, the experiment was continued after measurements and refilling by creating a breach in the crater wall and allowing the water to escape from the basin whilst maintaining upstream flow discharge. In most cases, the crater rim eroded in a short time period and the water level dropped rapidly. This resulted in a lowering water level which caused incision on the delta deposits. Deep incisions occurred on the delta surface and terraces were formed as the channel cut down rapidly into the deposit (Fig. 6.3 bottom).

Our results show most importantly that different types of deltas emerge as the result of the rising or falling of the base water level, which agrees well with the fact that it has been often stated that water level in the receiving basin is an important parameter for of delta architecture (e.g. Leeder 1999). The mere differences between rising, constant and falling water levels are responsible for large morphological differences and can be used to classify different types of deltas. Retrograding stepped deltas (with multiple steep foresets) and prograding Gilbert-type deltas (with single steep foresets) are thus created when the water level is rising (transgression) or falling (regression), respectively.

Formation of incisions and terraces on the delta surface can only be avoided if the water level is kept constant for some time, i.e. the water leaves the basin at the same rate that it enters, whilst maintaining some ponding water in the basin. This was never the case in our experiments because the crater rim was easily erodible and continued to erode much faster than expected, even when cohesive materials such as silica flour were added to the gravelly river sand. Had the rim not been eroded, a prograding delta would have formed under constant water level. We demonstrated this in a different setup, not further reported here, wherein the water level was kept constant for a certain period, resulting in a prograding delta.

6.3.2 Effect of discharge

During the ponding event (water level rise), high discharges showed much less channelization on the delta surface than low discharges. This was possibly due to the tendency for a wide sheet flow to dominate in these cases, and resulted in a more evenly distributed stepped-sheets delta with smooth edges. Low discharge experiments clearly showed channelization on the delta surface and resulted in a more erratic, lobate stacking due to nodal avulsion (Fig. 6.3). The profiles of these deposits also indicate their stepped nature.

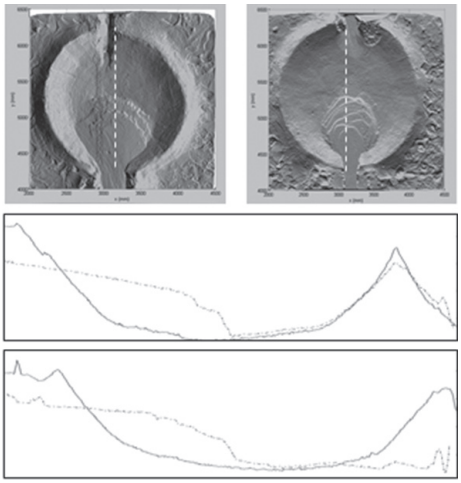

Figure 6.3: Top: Shaded DEMs of circular crater-shaped lakes (diameter 2 m) with deltas. Flow is from the bottom (breach was manually created after the first event). Left panel: low discharge (0.07 m^3/s); right panel: high discharge (0.35 m^3/s). Bottom: Profiles of the respective deltas (location of profile shown by white dashed lines in DEM). Flow is from left to right. Upper profile is of the delta in the left panel above, lower profile is of the delta in the right panel above.

During the breaching event (downstream water level fall), it seemed that the higher discharges created deeper incisions into the delta deposit. This could be due to higher transport capacity, allowing more change in a short period, and due to the higher momentum which did not allow much transverse movement. Incision occurred regardless of discharge amount; however we do observe morphological differences in the incisions based on the amount of discharge. Figure 4.10a (Chap. 4) shows the formation of a prograding delta under low discharge conditions, and Figure 4.10b (Chap. 4) shows the formation of a prograding delta under high discharge conditions. Both deltas were formed with relatively well-sorted, coarse-grained sediment with D_{50} of 0.4 mm. In both cases the original stepped delta is eroded, but in the high discharge case, much of the original deposit is preserved in the form of terraces.
Our observations show that lateral variability due to channel avulsion is crucial in the development of a wide-basin delta after dam removal, especially during low discharge events.

6.3.3 Effect of particle size

In both the ponding and the breaching events, coarser grain sizes resulted in a more lobate delta shape and exhibited less developed steps. Finer grained experiments showed better developed steps due to the higher mobility of the sediment, but the overall shape is less lobate (Fig. 6.4). Profiles of these deposits also clearly show their back-stepping morphology.

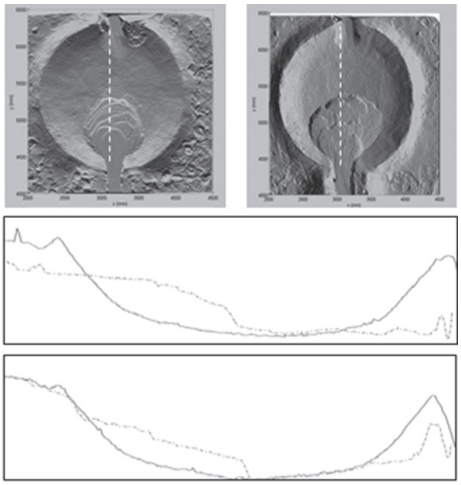

Figure 6.4: Top: Shaded DEMs of the circular crater-shaped lakes (diameter 2 m) with deltas. Flow is from the bottom (breach was manually created after the flow event). Left panel: small particle size (0.225 mm); right panel: large particle size (0.45 mm). Bottom: Profiles of the respective deltas (location of profile shown by white dashed lines in DEM). Flow is from left to right. Upper profile is of the delta in the left panel above, lower profile is of the delta in the right panel above.

Deltas formed with a clear sorting pattern in the poorly sorted sediments. The topset was coarse and often armoured. The foreset was locally fining-upward but varied strongly spatially as each lobe and avulsion formed its own foreset. The toeset, overrun by the delta to form a bottom set, consisted of very fine sand to silt (when a significant amount of fine material was supplied to the system). Upon manual crater rim breaching most of the erosion took place in the relatively coarse topset and foreset whilst the fine bottomset was commonly largely preserved.

6.3.4 Effect of silica flour

The river sand with silica flour eroded much slower in the upstream feeder channel, yet it did not have much impact in the erosion rate of the downstream crater rim that was also reinforced with silica flour. Furthermore, little difference was observed in the erosion rates between 20% and 40% silica flour (in agreement with Kleinhans *et al.* 2010b).
Figure 6.5a shows the slightly more elongate nature of the individual lobes, as derived from small channels on the delta surface. These channels are more stable than those on the previous deposits due to the added silica flour. As expected, the whole deposit was covered by sfine material from settling when the water in the crater was left to evaporate and percolate rather than overflow.

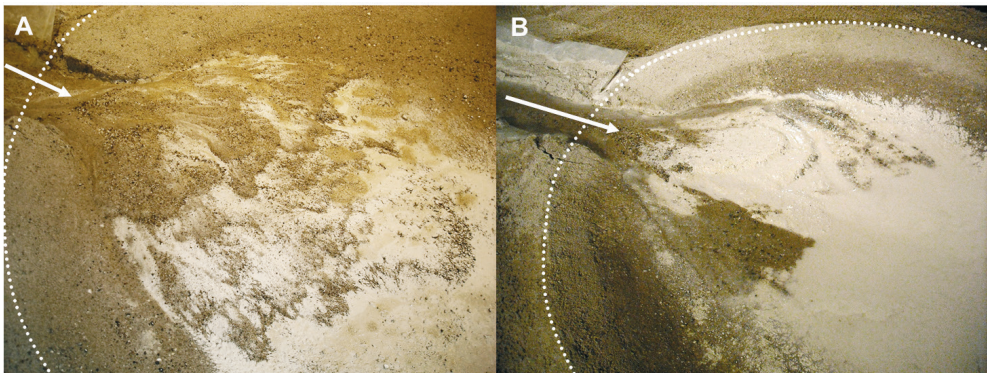

Figure 6.5: a) Thin layer of fine sediment draped over the delta deposit in the crater basin after evaporation/ percolation. Note the distinct elongate nature of the individual lobes, brought on by the increase in channel cohesion. Discharge was 0.07 m³/s with a 20% volumetric percentage of silica flour mixed with river sand. b) Same as above, however the original deposit is covered in a thicker layer of fine sediment yet partially eroded by early channel incisions on the delta front. Note the large remainder of fine sediment that is left in the basin. Discharge was 0.35 m³/s with a 40% volumetric percentage of silica flour mixed with river sand. In both figures, flow direction is indicated by the white arrow and the crater rim is outlined with a white dotted line.

In Figure 6.5b, the thin drape of fine sediment that is found throughout the basin after evaporation and percolation can be observed. If released instantaneously, these fines could potentially be a problem for downstream ecologies. However, the experiments show that most of the fine material is not removed from the basin at the time of incision due to the relatively fixed location of the incising channel. Figure 6.5b also shows partial erosion of the fine material and indicates that the fines were not completely flushed downstream but most of the fine material was left in the basin and was only slowly released back into the downstream environment with time.

6.3.5 Sediment transport

From the transport rate predictors one can estimate the volume of the delta deposit. We assumed bed load transport to be the major component. Predicted delta volumes differ from measured volumes mostly within an order of magnitude. Sediment transport values were incorrectly predicted, possibly due to armouring in the feeder channel or differences in the expected mobilities, or also possibly due to discrepancies in the time of formation.

Due to heavy armouring in run A (Tab. 6.1) and due to under-predicted mobility in run F (Tab. 6.1), these values are outside the order of magnitude boundaries. When $\alpha = 11$ in equation (3) for sediment transport and $ks = 7D_{90}$, the delta volumes are best predicted; most lie within an order of magnitude from the predicted value (Fig. 6.6). The outlier above the $y = 10x$ line can be explained by the heavy armouring that occurred in the channels in this experiments (A). Armouring inhibits sedimentation as the system is starved of sediment. The outlier below the $y = 0.1x$ line can be explained by the much higher mobility of the sediment in reality in this experiment (F). We found that mobility is less for the finer grained deltas due to the lesser effect that turbulence has on smaller grains. More mobile sediment yields more sediment in the delta than predicted. Our sediment mobility predictions may have been inaccurate due to insufficient slope measurements while active sediment transport was taking

place, or may have been affected by small errors in slope and water depth measurements (see further discussion in Chap. 4).

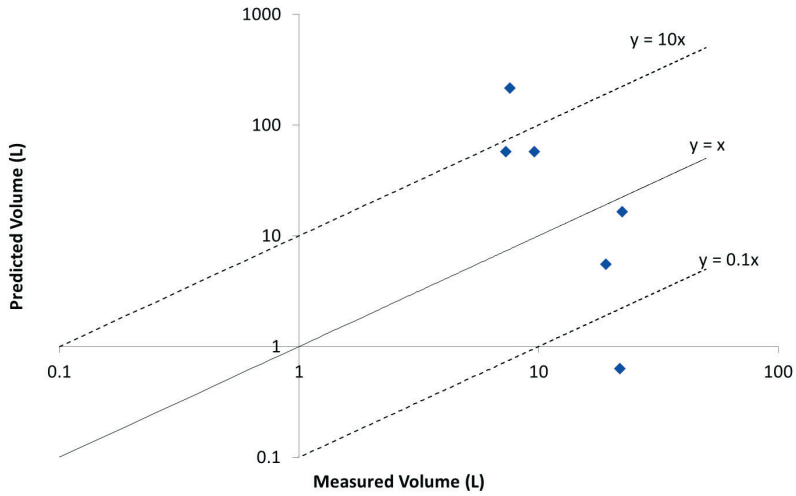

Figure 6.6: Predicted versus measured delta volumes for six delta deposits based on the calculated sediment transport rate using α = 11 and ks = 7D$_{90}$

6.4 Discussion

6.4.1 Application to hydrological reconstruction on Mars

We show that water level in the crater lake determines the overall delta shape. Variation in basin water level, caused by the different stages of crater filling and emptying, is enough to stimulate the formation of different types of deltas. They are all basically deposits arrested in a different phase of their development because the hydrological event ended, probably abruptly. Figure 4.1 (Chap. 4) shows some of the different types of delta deposits found on Mars, including retrograding, stepped deltas (from rising water levels) and smooth or branched prograding deltas (from constant or falling water levels). Further variations in morphology can perhaps be explained by channel width (discharge) relative to delta size (crater size), and by sediment properties which are basically unknown for Mars.

An interesting aspect of this study is the primary and secondary location of deposition of the fine sediment fraction. On Mars, where the quality of the sediment is still not fully understood, and where the eroded valley volumes have sometimes been shown not to balance the deposited delta volumes, the possibility of volume loss in the form of fine material is to be considered. Our experiments show that fine material is often not trapped entirely within the delta but is washed into the basin and beyond. The question of the exact quantity of fine material that may have been washed out of the Martian depositional systems is a subject for further research.

Finally, these experiments show that all these deltas can have formed in one event. Also evident is that upstream channel characteristics can be used to predict sediment transport

capacity, from which, given the relatively easily measurable delta volume, a time scale of formation can be derived. Elsewhere we have compared volumes of Martian deltas for some examples to predicted volumes, and the results indicated that these deposits formed in a very short time period, on the scale of a few months (Kleinhans *et al.* 2010a).

6.4.2 Application to dam removal

This study investigated the formation and modification of coarse-grained deltas in wide lakes and reservoirs. There are some similarities to coarse-grained deltas formed in narrow lakes (Cantelli *et al.* 2004; Kleinhans 2005b). Major differences however, include the increase in the number of channel avulsions due to a larger delta area and thus an increase in lateral variability; as well as the increase in terracing that is observed due to one large channel cutting rapidly very deeply into the deposits. This implies that the concepts of Cantelli *et al.* (2004) cannot be transplanted on wider delta cases without modification. It also implies that the former delta deposit will not deliver a large amount of sediment instantaneously to the downstream river, but this will be spread out over a longer time period (if the terraces are eroded at all).

Surprisingly, for low discharges the incising channel destroyed the deposit through transverse movements and avulsion of the initially excavated channel whereas for higher discharges the terraces were preserved for a much longer time. Our results indicate that dam removal at wide lakes may lead to an unexpected inverse relation between discharge and erosion of the deposit, which has consequences for the subsequent sediment pulse magnitude.

Furthermore, we observed a clear sorting trend in the longitudinal profile of the deltas. Coarse grains are located on the delta plain (topset) and delta front (foreset), whereas fines are located in the pro-delta (bottomset). However, the down-cutting channel only removes the fine sediment partially, hence also a large amount of fines remains behind in the sediment trap. This effect is much larger with a higher discharge due to the force of the down-cutting channel and its inclination to stick to a certain path once the surrounding terraces are too high to be crossed by an avulsing channel.

6.5 Conclusions

Our main conclusions are threefold: First, the volumes of delta deposits are predictable within an order of magnitude based on total time of formation and upstream channel and sediment characteristics. Second, coarse-grained deltas in wide lakes are mainly formed by lateral channel migration (bifurcations and avulsions). This is in contrast to the formation of coarse-grained deltas in narrow lakes, which are mainly formed by sheet flow. Most of the deltas on Mars are formed in wide lakes (impact crater basins). Lastly, in most cases a large part of the delta deposit remains in the basin after dam removal. During the period of falling water level, incision of the delta results in terraces. Comparable terraces are not observed in Martian deposits and hence we assume that the water discharge there stopped abruptly.

“All men have stars, but they are not the same things for different people. For some, who are travellers, the stars are guides. For others they are no more than little lights in the sky. For others, who are scholars, they are problems... ”

7 General Synthesis

Martian surface landforms are indicative of water-related activity in its history. The current climate on Mars is considered cold and dry, with average surface temperatures far below zero degrees (although occasionally above freezing point), and very little evidence for significant aqueous processes on the surface at this time mostly due to the low atmospheric pressure. Past climate on Mars must have been, at least on occasion, somewhat "wetter" in order to produce the many fluvial landforms of considerable size and dimensions that are observed today, but how much wetter and whether these wetter conditions were also accompanied by higher temperatures is still an open question. Temperature fluctuations may have been the result of orbital variations and/or atmosphere changes related to extreme volcanism and impact cratering. However, the extent of these fluctuations is still largely unknown. Regardless of how warm and wet it may have been, the past climate on Mars was still much more arid and with much colder and drier conditions than on Earth. The question is, how much wetter the conditions need to be to form landforms indicative of aqueous activity? We addressed this question in the preceding chapters by considering the key observations, their implications and subsequent conclusions.

7.1 Shallow-marine impact craters and the northern ocean

Exploration of impact craters on Mars is founded on the study of impact craters on Earth. The study of these geomorphological features can yield information about the climate and geology of the target surface (Barlow 2009, 2010). Specifically, impact crater studies in areas on Mars where shallow-marine impact craters are presumed to have formed (Ormö *et al.* 2004) are based upon the study of shallow-marine impact crater analogues on Earth (e.g. Wetumpka, Alabama and Chesapeake Bay, Virginia; e.g. Poag 1997; King *et al.* 2002, 2006; Horton *et al.* 2006). The processes responsible for creating indicative marine morphologies in craters, such as resurge and slumping, are thought to be similar on Mars if shallow water conditions were met in some regions, i.e. if an expansive layer of water once covered parts of the Martian surface (Ormö *et al.* 2004). Arabia Terra is a large, mid-altitude region that straddles the crustal dichotomy (McGill 1991; Watters and McGovern 2006; Fig 1.3 in Chap. 1). The dichotomy separates the cratered, southern highlands (predominantly of Noachian age) from the smooth, northern lowlands (predominately of Amazonian age) and is believed to host sedimentary rocks and evaporites (e.g. Edgett and Parker 1997; Andrews-Hanna *et al.* 2010), two potential signs of aqueous activity on the surface somewhere in the past. Ancient shorelines have been proposed in this area, most importantly the Arabia/Meridiani and Deuteronilus shorelines (Parker *et al.* 1989, 1993; Clifford and Parker 2001; Fairén *et al.* 2003). The Arabia/Meridiani shoreline is believed to be of Noachian age at around 4 Ga (Clifford and Parker 2001), and the Deuteronilus shoreline of Hesperian age around 2 Ga (Perron *et al.* 2007; Fig. 1.4). The age of these shorelines could be related to the mainly

Noachian formation of valley networks and the mainly Hesperian formation of outflow channels.

Based on the reported existence of a northern ocean(s) early in Martian history (Parker *et al.* 1989, 1993; Clifford and Parker 2001; Fairén *et al.* 2003), resurge-related and subdued morphologies are expected to be found in some of the craters in Arabia Terra. The existence of this/these northern ocean(s), referred to as Oceanus Borealis, has been disputed in the literature mainly due to the absence of coastal morphologies as well as the fact that shoreline contacts are not aligned on an equipotential surface and appear to be deformed (e.g. Ghatan and Zimbelman 2006; Malin and Edgett 1999). One of the hypotheses proposed for the lack of coastal morphologies on Mars is the possible erosion of these features especially if they were primarily of Noachian age (scenario 5 from Ghatan and Zimbelman 2006). Perron *et al.* (2007) identified the prospect of true polar wander acting as a mechanism that could have been responsible for the deformation of the proposed shorelines. They showed that the deviation of some of the prominent shorelines can be explained by the re-alignment of the surface topography to compensate for uneven mass distribution related to the creation of large, massive, volcanic provinces (Perron *et al.* 2007). Lastly, Di Achille and Hynek (2010) suggested that the majority of elevations of Noachian and Early Hesperian delta deposits delineate a planet-wide equipotential surface in the northern lowlands of Mars, without correction for polar wander.

Crater morphologies in northern Arabia Terra show notable differences from crater morphologies further southeast, which is in agreement with the hypothesis that Arabia Terra has evolved in a different manner than these other surfaces. The analysis of shallow-marine impact craters in Arabia Terra reveals some exemplary candidates for the formation in shallow-marine environments, but fewer shallow-marine crater morphologies than anticipated based on reported crater frequencies, contending the longevity of a northern ocean(s). These results sustain the hypothesis that Arabia Terra or parts thereof had been covered by water, with shallow water depths for areas within tens of kilometres from the proposed shorelines and with loose, unconsolidated sediment associated with coastal beach deposits. When comparing the locations of the exemplary candidates (craters with at least 70% water-related morphologies) to the locations of the proposed shorelines (Parker *et al.* 1989, 1993; Clifford and Parker 2001; Fairén *et al.* 2003), a slightly positive correlation is observed (Fig. 2.7). In order to investigate the nature of this correlation, further work is needed in this area as well as in other mid-altitude areas in the vicinity of the proposed shorelines.

Evidence of a northern ocean(s) was partially found (de Villiers *et al.* 2010; Chap. 2). The results do not give unequivocal evidence of a long-standing ocean in the northern lowlands, nonetheless, certain morphologies may be associated with impact crater formation in shallow water settings. These shallow-marine crater morphologies mount additional evidence that Oceanus Borealis may have existed at one or multiple points in Mars' history, albeit perhaps only for a brief geological time period(s).

7.2 Fan-shaped sedimentary deposits on Mars

The analysis of fan-shaped sedimentary deposits in Chapter 3 focuses on the relationships between morphology and the conditions at the time of formation. The relationships between

different morphological parameters on the surface of deltas and/or fans and in the upstream and downstream areas immediately adjacent to the deposits were qualified and quantified using remote sensing visual and topographic data. The morphological variety and spatial distribution of fans on Mars evoke some remarks about the duration and magnitude of surface water at the time of their formation. First, I give a brief overview of the general observations, and then I list key morphological relationships and discuss the timing of fluvial activity.

7.2.1 General observations

Different types of fan-shaped deposits including alluvial fans and fan deltas have been reported on Mars (e.g. Cabrol *et al.* 1998; Ori *et al.* 2000; Malin and Edgett 2003; Howard *et al.* 2005; Irwin *et al.* 2005; Moore and Howard 2005; Williams *et al.* 2006, 2011, 2013; Kraal *et al.* 2008a; Hauber *et al.* 2009, 2013; Di Achille and Hynek 2010; Grant and Wilson 2011). In order to constrain the amount of water that was involved in their formation, three questions were answered, where possible, for each identified deposit: a) whether the deposit is an alluvial fan or a fan delta; b) if it is an alluvial fan, whether it was dominated by run-off or by debris-flow processes; c) whether deposition occurred as a single, catastrophic and short-lived event, or during multiple episodes as part of continuous and long-lasting activity. The first question is relatively straight-forward and involves the identification of features that can be associated with either alluvial fans or with fan deltas, such as: terraces, debris-flow lobes (or sieve deposits if resolution permits), channels on the fan surface, and the nature of the feeder system. Terraces, which are erosional remnants of sedimentary deposits as a result of focussed incision or other erosion processes, indicate modification and avulsion when located on the fan or delta plain. When located on the delta front, often referred to as incisions, they indicate base-level drop while fluvial activity persisted. These terraces are not to be confused with the stepped retrograding morphologies that are a product of deposition under specific conditions. Debris-flow lobes usually are associated with alluvial fans rather than with fan deltas, if the alluvial fans are mass-flow dominated. Channels tend to occur on fan delta plains, on fluvial fans and on run-off dominated alluvial fans. However, channels may also result from secondary, post-formation, fluvial reworking, and may hide evidence of the primary depositional processes (Blair 1987; Lecce 1990; Leeder 1999). Preferential erosion by wind may have occurred, preserving only the coarser, channel-fill material as an inverted positive feature (Burr *et al.* 2009, 2010, 2012). Lastly, the nature of the feeder system and drainage pattern (if observed) could give an indication of the maturity of the system and the source and amount of water (Irwin *et al.* 2005).

Based on morphology, three important classes of fan-shaped sedimentary deposits have been identified on Mars (de Villiers *et al.,* in prep; Chap. 3) including a) *cone-shaped alluvial fans*; b) *retrograding fan deltas* with Gilbert-type profiles and multiple delta fronts stacked one upon another; and c) *prograding fan deltas* with Gilbert-type profiles and single delta fronts (Fig. 3.1). The existence of one or more delta front(s), or the lack of such features in case of alluvial fans, is considered a primary morphological feature, and is used as the basis for the classification. As further discussed in Chapter 4, the type of delta front is indicative of the amount of water in the basin at the time of formation, and more importantly, of the behaviour of the water level (de Villiers *et al.* 2013).

Within the classes of fan-shaped deposits some morphological variation, such as evidence of channels on the fan surface, is observed and documented as secondary morphological features. For example, some prograding fan deltas exhibit branched channel networks on their delta plains and others have smooth delta plains with hardly any visible relief. Additionally, the shape of the shoreline may differ between deposits. Instead of the smooth, half-circular, shape in plan view, frequently observed in Gilbert-type deltas, shorelines are more lobate or jagged, with scalloped edges in plan view (Fig. 4.8 in Chap. 4). These secondary variations are interpreted to be the result of variations in discharge and sediment character.

The types of fan-shaped deposits described above are all inferred to have been formed by liquid water. Other origins for some of these deposits, such as glacial deltas and lava deltas, have been proposed (Kargal *et al.* 1994; McMenamin and Gill 2005; Leverington 2006) but remain largely unproven (Ori *et al.* 2000; Di Achille and Hynek 2010). Furthermore, it is possible that some of the alluvial fans should rather be considered fluvial fans and also that some deposits that have been classified as deltas may rather be fluvial fans with a truncated or erosional scarp due post-depositional erosion (e.g. Schon *et al.* 2012). Lastly, at least two exceptions of fan-shaped deposits (Eberswalde and Nili Fossae) do not fall into the three major classes (Fig. 3.1), and because of their low occurrence a fourth class was not proposed (yet). More work is needed to better constrain the formative processes involved in deposits such as the Eberswalde Delta (Malin and Edgett 2003; Jerolmack 2004; Wood 2005; Pondrelli *et al.* 2011) and the Nili Fossae Delta (Fassett and Head 2005, Schon *et al.* 2012). Their inclusion or exclusion in this classification system is beyond the scope of this dissertation. However, the large majority of fan-shaped deposits can be classified in this proposed system, thereby creating some confidence that this population of deltas and fans is representative of the general Martian climate situation.

7.2.2 Morphological relationships

Analysis of the relationships between morphological parameters such as fan size, fan gradient, feeder channel geometry and basin hypsometry leads to two major observations and their implications. Firstly, fan length should correlate well with fan area, which is the case for alluvial fans and prograding fan deltas (straight line in Fig. 3.6b) – but not for retrograding fan deltas, indicating a distinctly different process for their formation. Shorter fan lengths in combination with narrow fan areas is interpreted to be a consequence of the rapid filling of the lake by catastrophic and large discharge into small, closed basins, limiting the time for progradation (and hence the length) and for radial avulsion across the fan surface as the water rises, hence limiting the width of the fan area, similar to flash flood events on Earth. This is in agreement with the proposed formation process for retrograding fan deltas on Mars (Kraal *et al.* 2008b; de Villiers *et al.* 2013). If these were wave-cut terraces on regular Gilbert-type deltas (as suggested by Ori *et al.* 2000; Williams *et al.* 2006; Di Achille *et al.* 2006b) similar to wave-modified Gilbert-type deltas on Earth (van der Straaten 1990), the distinct difference between the ratios of fan length to fan area (Fig. 3.6b) would not be observed, as the physical processes on stepped, retrograding fan deltas and regular, prograding fan deltas would be the same. Wave-cut terraces have previously been suggested to infer long-standing, stable lake levels as the product of a stable climate. However, my experiments show that the

stepped morphologies rather indicate rapidly rising lake levels as the product of catastrophic discharge (section 7.4 below).

Secondly, the type of deposit depends on the morphology of the feeder channel (e.g. Cabrol and Grin 2001), which is directly related to the quality (i.e. type, size, and degree of sorting of the sediment) and quantity of the discharge. This relationship is manifested differently for alluvial fans and fan deltas, indicating that the amount of discharge required to form these two classes of deposits differs significantly (Fig. 3.7c). Alluvial fans are widely associated with short and steep feeder channels indicative of low discharge, while fan deltas are widely associated with longer, low-gradient feeder channels indicative of higher discharge. This agrees well with the demand of a higher discharge to promote ponding in the basin so that delta fronts can develop into ponding water.

When it comes to gradients, in Figure 3.7 (b and d) we observe that alluvial fan gradients as well as prograding fan delta gradients are all very similar, but that retrograding fan delta gradients are spread somewhat widely. This interesting observation invites further analysis, but could perhaps indicate the differences in magnitudes of the different events.

Thirdly, there is a clear relationship between fan gradient and channel width/gradient for the stepped, retrograding fan deltas (Fig. 3.7 b and f), indicating a tendency of steeper deltas to be associated with larger channel widths and higher channel gradients. Larger discharges (wider and steeper channels) would fill the basin much more rapidly and hence the retrograding fan delta is formed, with limited or no time to expand and prograde. The retrograding fan delta is thus draped on the crater wall with an overall larger gradient, as shown in models by Kleinhans *et al.* (2010). This relationship is not observed between fan/delta gradient and channel width/gradient for alluvial fans and prograding fan deltas, once again indicating the fundamental difference in development of retrograding fan deltas.

In addition to these two major points, other observations include: a) that deposit type is somewhat dependent on basin size and some correlation exists (e.g. Cabrol and Grin 2001), i.e. larger fans form in larger basins due to a greater accommodation space as well as perhaps an increase in sediment supply from the crater rim, if applicable (Fig. 3.8). And b) that deposit type is dependent on the character of sediment supply, which strongly depends on lithology and the availability of sediment in the catchment.

7.3 Experimental delta formation

The Martian delta morphologies and their formative conditions were explored in flume experiments in the Eurotank, a large laboratory basin equipped with photogrammetric equipment producing high-resolution and high-quality DEMs for quantitative analysis. Results were verified against terrestrial systems and the scaling between experiment and large-scale systems was addressed using verified flow and sediment transport models that have been adapted for flow conditions on Mars. Numerical models were used to explore the different scenarios for fan/delta formation.

The experiments focused on the formation of fan deltas only, not including alluvial fans such as those created by Whipple *et al.* (1998) and van Dijk *et al.* (2012). They have shown in the laboratory that alluvial fans also capture most of their sediment similar to fan deltas, so their volume could also be indicative of formative duration. However, these alluvial fans

could also have formed by highly intermittent events so that their complete formation may be spread over longer periods than that of fan deltas. Regardless, fan deltas and alluvial fans have similar processes operating on the surface and some overlap exists between the two categories.

7.3.1 Water level behaviour and other factors

The results show that the primary morphology of the experimental fan deltas is determined by the evolution of the water level in the basin, and that the secondary morphology is mainly determined by other variables such as flow discharge and particle size distribution. Other variations include the formation of channels on the fan surface and the shape of the lobes, but these secondary variations do not alter the primary morphology to a significant extent.

The behaviour of the water level in the receiving basin affects the morphology of the fan deltas (and alluvial fans) in such a way that a continuum in development can be inferred, i.e. no ponding water, rapid water level rise, stable water level, and occasionally followed by a rapid water level fall (Fig. 4.16). The formation of an alluvial fan will always precede the formation of a fan delta unless the basin had already been (partly) filled with water before sedimentation commenced. Likewise, the formation of a retrograding fan delta will always follow the formation of an alluvial fan once ponding initiates and the water level in the basin starts to rise. This will mostly be the case for large, catastrophic discharge that cannot percolate into the subsurface or evaporate into the atmosphere fast enough. Additionally, the formation of a retrograding fan delta will precede the formation of a prograding fan delta, as long as the water level in the basin continues to rise and until an overflow point or breach is reached. If the water level would become stable at any point, caused by a balance between the water entering the basin and that leaving the basin (due to percolation, evaporation, outflow, or any combination of these), a prograding fan delta will develop. Lastly, if the aqueous activity continues while the lake level subsides, incisions are cut into the fan delta deposits. Similarly, if aqueous discharge diminishes slowly over time, fluvial erosion in the form of channels and terraces into the delta body is to be expected. These experiments support the choice of delta front (and thus water level behaviour) as the major factor in this novel classification system for Martian fan-shaped sedimentary deposits.

7.3.2 Fine material in the sediment supply

In Chapter 6 it is shown that the use of fine silica flour enhances the adhesive strength of the sediment causing somewhat different morphologies than without added fines. The addition of these fines improves the sediment cohesion and thus improves the stability of small channels on the fan surface, yielding shorelines with more jagged or scalloped edges under conditions of low discharge. Under conditions of high discharge, such small channels do not have the time to mature as the lake level rises too rapidly, and hence jagged or scalloped shorelines are not observed in that case (Figs. 6.7 and 6.8). The experiments reveal that the addition of fines to the particle size distribution affects delta morphology only on a small scale.

The thin layer of fine material that covers the experimental delta after all fines have settled from suspension and all water has dissipated leaves no detectable topographical signature. This could be a partial explanation for the mismatch between eroded volumes of

channels and deposited volumes of deltas observed on Mars (Hauber *et al.* 2009), where a fraction of the sediment (mainly fines) is likely to have been carried away in suspension, and thus was not deposited on the delta, but further downstream. If the percentage of fines in the sediment source is quite high, this could be a significant fraction of the sediment that is not trapped by the delta and thus transported out of the lake after the basin has been breached, like in the open-basin lake scenarios of Fassett and Head (2008).

7.3.3 Three key observations from sediment transport calculations

We found three emergent properties of fan deltas formed in rapid discharge events that are generic and we infer them to be valid for Mars. First, an important observation in the experiments is the process of highly energetic hyper-concentrated flow in the early stages of the process. All initial deposits were formed by high-density, hyper-concentrated flows or sheet flows until conditions stabilized. The hyper-concentrated flows are the result of higher sediment to water ratios as the crater rim is first eroded, leading to the formation of debris flows. Once enough water has reached the basin, ponding initiates if the discharge is sustained. Formation of the fan delta commenced soon afterwards, on top of the initial mass-flow alluvial fan deposits. Some Martian deltas show indications of having formed on top of a previous deposit that most likely resulted from a hyper-concentrated flow (Kleinhans *et al.* 2010a). The large number of alluvial fans in craters as compared to the smaller number of fan deltas in craters, indicates that ponding of water in the basin was a relatively rare occurrence. Furthermore, the under-estimation of sediment concentration could be a factor in over-estimating the formation time of fans and fan deltas in general.

Second, all experiments confirm that incision is highly focused and occurs rapidly, so that deltas without obvious incisions must have formed in one event that ended abruptly, whereas multiple events would have created incisions across the fan surface of the first event. Exceptions to this observation could include second events that had larger magnitudes than first ones and thus entirely covered an earlier delta which must, therefore, be smaller. Incised fans and fan deltas are not frequently observed on Mars, and large terraces on fan surfaces have not been documented at all. This indicates that fluvial episodes on Mars must have terminated as rapidly as they are believed to have started.

Third, the experiments indicate that loss of water into the subsoil may lead to under-estimation of the total water volume delivered by the source as inferred from formative duration and lake level indicators, particularly the shoreline. This was referred to as the "leaky cauldron hypothesis" in Kleinhans *et al.* (2010a). But the overall error due to this effect in the experiments is no more than a factor of two. As for the permeability of the substrate, we are inclined to argue that the time of formation of delta deposits on Mars might have been shorter than expected due to the relatively smaller permeability of the sediment or bedrock as compared to the coarse and unconsolidated laboratory sands.

7.3.4 Application to terrestrial dam removal scenarios

Chapter 6 demonstrates the terrestrial application of the laboratory work. The similarity of process between fan/delta creation and modification in closed and open (breached) basin lakes on Mars is suitable for comparative studies to dam creation and removal in active

river systems on Earth. Sedimentary deposits in reservoir lakes record the sediment transport capacity of the upstream river and past water levels in the basin, much like fan deltas do on Mars (Cantelli *et al.* 2004). As the sediment accumulates, the reservoir loses potential to store water, i.e. the trap efficiency decreases (e.g. Brune 1953; McCully 1996; Cantelli *et al.* 2004).

The removal of dams as part of river restoration for safety, ecological and environmental reasons has become a common procedure worldwide and especially in the United States where more than a thousand dams have been permanently removed in recent years (Graf 2003; Stanley and Doyle 2003; Wohl and Rathburn 2003). Upon removal of the lower boundary of the lake (i.e. the opening of either a reservoir lake on Earth or crater/rift lakes on Mars), sediment that has settled in the lake is eroded, often catastrophically, and the renewed increase in sediment load can have a negative effect downstream. Fine sediments such as silt and clay can be a problem for ecosystems as they may cover vegetation and kill fish species. The water level downstream may rise (Doyle *et al.* 2002), and may affect man-made structures such as bridge foundations and irrigation channels directly downstream.

Results show, firstly, that coarse-grained deltas in wide lakes (of which crater basins on Mars are an example) are mainly formed by lateral channel migration (bifurcations and avulsions) in contrast with coarse-grained deltas in narrow lakes, which are mainly formed by un-channelized sheet flows. Secondly, a large part of the finer sediments in suspension were washed out downstream of the observable deltas and this process could be responsible for the lack of agreement between eroded valley volume and deposited delta volume on Mars. Lastly, and most importantly, in case of dam removal in wide lakes, a counter-intuitive inverse relation between discharge and erosion of the deposits may be observed, resulting in higher discharges eroding smaller volumes of the deposits. In most high-discharge cases, a large part of the delta deposit remains in the basin after dam removal. During rapidly falling water level, incision of the delta results in terraces with large amounts of the fines still intact. This rapid erosion creates deep incisions into the deposit which prevent channel avulsions across the entire delta surface, thereby limiting the amount of sediment that is eroded and re-distributed downstream. Lower discharge results in a less rapidly falling water level, and hence in fewer terraces, which thus increases the number of channel avulsions across the delta and thus increase the overall erosion of the deposits. This observation has consequences for the subsequent sediment pulse magnitude because if applied correctly, it can lessen the amount of sediment that is delivered downstream. The implications of this observation in hydraulic engineering are that higher discharges may be considered in combination with dam removal in order to rapidly erode into the deposit and limit the amount of sediment to be eroded (de Villiers *et al.* 2010b).

7.4 Alluvial fans in the Atacama Desert

Field descriptions of a set of terrestrial coastal alluvial fans in the Atacama Desert with apparent similarities to some of the Martian alluvial fans based on satellite imagery are presented. Even though from satellite view some deposits may seem run-off dominated, surface observations reveal that these coastal alluvial fans are predominantly debris-flow dominated and merely run-off modified, and/or not influenced by run-off at all. This ground-truth forms the basis of the interpretations of Martian alluvial fan formation.

Based on insights from the Atacama fans, we suggest that the Martian fans may not have been constructed by run-off but rather constructed by debris flows and perhaps modified by run-off in cases where run-off associated surface features are described. We caution against the interpretation of long intervals of surface water based on run-off related features on the fan surfaces, and we suggest that the period of formation may have been much shorter than previously interpreted based on the short formation time for sediment-laden, debris-flow alluvial systems.

As seen in the Atacama Desert with an average precipitation of less than 5 mm per year (Rech *et al.* 2006; Bull and Asenjo 2013), a particularly wet climate is not necessary to form extensive alluvial fans. Occasional flash floods are the only prerequisite to mobilize significant volumes of sediment. In the hyper-arid context of the Atacama Desert, studies have ascertained that run-off events with geomorphic effectiveness are rare in this area, with recurrence intervals of the order of thousands of years, somewhat comparable to the obliquity cycle on Mars which may be responsible for repeated climate optima with periods of hundreds of thousands of years (Head *et al.* 2003). The orientation of the Mars axis varies up to 60°, unlike the tilt of the Earth's axis with a variation of only approximately 4°, due to the stabilizing effect of the Moon (Schorghofer 2007).

The observations in the Atacama Desert introduce the possibility that Martian alluvial fans may have aggraded by mass-flow events to a more significant degree than has been suggested (e.g. Moore and Howard 2005; Kraal *et al.* 2008a) and that the amount of water needed for their formation was relatively limited, probably intermittent. Such intermittent occurrence of water is in agreement with suggestions of short-period, episodical hydrological cycles inducing heating of the permafrost (Segura *et al.* 2008; Baker 2009b; Toon *et al.* 2010; Lasue *et al.* 2012), and providing in turn enough water to form the alluvial fans on Mars without inferring a longer period of warm and wet conditions with sustained regional rainfall.

7.5 Current state of understanding of the Martian climate

Geomorphological features on the surface of Mars, such as the alluvial fans and fan deltas studied in this dissertation, are indicative of fluvial activity and aqueous discharge. The focus in this dissertation is primarily on the interpretation of the quantity of the discharge that was responsible for the formation of these features, i.e. the amount of water that was discharged over a certain period of time; and the quality of the discharge, i.e. the episodic or sustained nature of the flow. Four key observations from this dissertation and their implications for climate are briefly considered below.

7.5.1 Key observations and implications

Firstly, observations with regards to some (although not much) evidence of shallow-marine impact crater morphologies indicate the possible, brief existence of a northern ocean at one or several different periods in Martian history (perhaps during both the Noachian and Hesperian), and agrees well with Fairen *et al.* (2003) that the flooding of the northern lowlands was episodic at most (de Villiers *et al.* 2010a). Physical evidence of shorelines (Parker *et al.* 1989; Baker *et al.* 1991; Clifford and Parker 2001; Fairen *et al.* 2003, Di Achille and Hynek 2010) is questionable (Malin and Edgett 1999; Carr and Head 2002; Ghatan and Zimbelman 2006)

and reasons for the lack of extensive coastal morphology have been proposed by Ghatan and Zimbelman (2006), but their reasoning does not include the possibility that a northern ocean(s) might never have been long-lasting. This explanation could perhaps provide an interesting solution for the lack of coastal morphology.

Secondly, observations with regards to fan-shaped sedimentary deposits illustrate that these deposits vary in age, morphology and volume throughout Mars' history (Hauber *et al.* 2013; de Villiers *et al.*, in prep.; Chap. 3). Different morphologies are described as different phases of development of the sedimentary system, i.e. an alluvial fan precedes a retrograding fan delta, which in turn is followed by a prograding fan delta, if continuous discharge flows into and fills an empty basin. The preservation of these three types of fans in basins on Mars indicates that the hydrological cycle was immature throughout the Martian history and did not provide enough discharge to fill all basins across the surface with prograding fan deltas (a clear sign of a full basin for an extended period of time). The evolution of these fans and fan deltas was often paused or fully stopped at different points in time for different deposits, resulting in the preservation of alluvial fans and retrograding fan deltas, instead of presenting only prograding fan deltas as the end product in all cases. Furthermore, the distinct difference between the fan length to fan area ratios of retrograding and prograding fan deltas, which argues for the rapid, single-event formation of retrograding fan deltas, is indicative of their short formation times and catastrophic origin. Additionally, the range of ages of these deposits illustrates that their formation is not linked to a specific, warm and wet period at the end of the Noachian (Hauber *et al.* 2013).

Thirdly, experimental delta formation illustrates the formation of fan deltas in a short period, and numerical models calculate short formation times for many Martian fan deltas. Experiments demonstrate that such deltas preferentially formed during one aqueous event, which parsimoniously argues for short-term hydrological activity (Kraal *et al.* 2008b; de Villiers *et al.* 2013). The simple retrograding and prograding fan delta morphologies formed during single, short-lived events cannot be reconciled with long-term hydrological activity, because that would imply lake-level fluctuations resulting from complex water level histories along with complex sediment delivery histories. Numerical verifications support the hypothesis that simple delta morphologies on Mars (lengths of 2-10 km) can only be associated with single, short-lived events of the order of single years or decades at most (Kleinhans *et al.* 2010a; de Villiers *et al.* 2013). Some deltas such as Eberswalde are large and complex, and have sediment volumes that seem greater than what can be transported in a single event, which allows for other mechanisms such as sapping, mass-flow and perhaps even multiple events (Goldspiel and Squyres 1991; Pondrelli *et al.* 2008; Mangold *et al.* 2012). In the case of more complex deltas such as Eberswalde, a variety of minimum formation times have been calculated by different authors, ranging from 50 years by Jerolmack *et al.* (2004), to several 100's of years by Lewis and Aharonson (2006), to a range of 7-900 years by Orofino *et al.* (2009) to 1.5 x 10^5 years by Bhattacharya *et al.* (2005). Orofino *et al.* (2009) calculated the time of formation using Bagnold's sediment transport model in combination with grain sizes calculated from thermal inertia measurements as well as from the mean grain size as measured by NASA' Opportunity rover. These formation times, although orders of magnitude longer, are still geologically short (with the exception of the period proposed by Bhattacharya *et al.* (2005) which is believed to be an over-estimation) and therefore cannot

be used to imply a sustained, hydrologically active climate. Furthermore, Postma and Kraal (2008) and Mangold *et al.* (2012) have suggested that dense flows with sediment to water ratios of 3:10 to 1:100 (as opposed to ratios of 1:30 – 1:300 of more fluid flows; Orofino *et al.* 2009) can also explain the formation of Eberswalde, and thus would prove once more that a warm and wet climate is not necessary for the formation of fan deltas on Mars.

Lastly, the observations in the Atacama Desert of terrestrial alluvial fans that are debris-flow dominated despite their run-off-dominated surface morphologies, indicate that alluvial fans on Mars may have been subject to the same inaccurate interpretation, with a bias towards a stable and long-lived hydrological cycle (de Villiers *et al.*, submitted; Chap. 5). The formation of alluvial fans may have been the product of multiple events related to sapping and surface run-off, but even so the conditions for creating these features were either close enough to the present-day conditions and can still be referred to as cold and arid, or were merely episodically less arid with some fluvial activity driven by regional events or obliquity cycles (de Villiers *et al.*, submitted; Chap. 5). These formative conditions do not imply a long-term, precipitation-driven, warm and wet climate.

In short, clear evidence for extensive and sustained water on Mars does not appear from the features studied in this dissertation. Instead, observations in this dissertation support a predominantly cold and hyper-arid history on Mars, while somewhat wetter at certain points in time with intermitted pulses of hydrological activity and with perhaps a higher frequency of such pulses during early Martian history. In order to verify this interpretation, other hydrological features observed on Mars and the possibility of their formation under similar arid conditions with intermittent hydrological events is addressed below.

7.5.2 Re-evaluation of formation hypotheses of other surface features

Gullies are formed under current climate conditions (Dundas *et al.* 2010), although most likely at a much slower rate than perhaps was the case during previous maximum obliquity conditions (Schon and Head 2011). The processes that could be responsible for the formation of gullies include surface run-off related to melting of snow or sub-surface ice (Costard *et al.* 2002; Christensen 2003; Schon and Head 2011), groundwater sapping (Malin and Edgett 2000; Mellon and Phillips 2001) and sediment-laden debris flows or dry, granular mass flows (Costard *et al.* 2002; Shinbrot *et al.* 2004). Examples of gully systems that were created by more than one event have been shown (e.g. Schon *et al.* 2009), and Parsons and Nimmo (2010) concluded that multiple fluvial discharge events ranging from debris flows to stream flows with intermediate sheet flows are the most likely formative mechanism for these gullies. Gully activity has been linked to orbital-driven climate cycles (Schon and Head 2011) which importantly signifies that their formation is not related to a potential persistent warm and wet climate during early Mars.

The formation of outflow channels has been shown to relate to catastrophic aquifer release, mostly during the Hesperian and also during the Amazonian (Baker 1982; Carr 1983; Andrews-Hanna and Phillips 2007; Zegers *et al.* 2010). Andrews-Hanna and Phillips (2007) demonstrated with the use of flow modelling that the outflow channels were carved by numerous flood events over a long period of time, but Bargery and Wilson (2011) have shown that many outflow channels could also have formed in single events that lasted 24-48 hours

instead of previously suggested periods of 1-3 months (Ghatan *et al.* 2005). Specifically, we underline the hypothesis that massive, short-lived outflow events are the result of the collapse of a buried ice-lake, providing an instant source of high discharge (Zegers et al. 2010). Furthermore, these outflow channels may have formed under present climate conditions and are thus not an indication of warmer pulses during the Hesperian (Zegers *et al.* 2010; Bargery and Wilson 2011; Schumacher and Zegers 2011). It thus is possible that the outflow channels were created in short time periods, and that their formation took place throughout Martian history, irrespective of orbital-driven climate cycles.

Masursky *et al.* (1977), Malin and Carr (1999), and several other studies have suggested that the valley networks were created by surface run-off, and some authors (e.g. Craddock and Howard 2002) have suggested that precipitation caused this run-off. During the Noachian, frequent impact crater formation may have led to an increase in atmospheric water vapour (Howard *et al.* 2005; Irwin *et al.* 2005) and in combination with volcanic outgassing and the presence of the magnetic field (Fassett and Head 2011), a thicker atmosphere sustaining such a precipitation-driven hydrological cycle may have existed (Jakosky and Phillips 2001). Due to clear differences in the population of Noachian valley networks, a two-fold mechanism has been proposed: Older, degraded valleys are interpreted to have been formed by precipitation-generated run-off, and younger, more pristine valleys by groundwater sapping (Baker and Partridge 1986; Harrison and Grimm 2005). Howard *et al.* (2005), Irwin *et al.* (2005) and others have proposed that late-stage fluvial activity occurred at or near the boundary between the Noachian and Hesperian (around 3.7 Ga), creating incised channels within the valleys as well as large alluvial fans and fan deltas, features which are not observed in association with the older Noachian deposits.

Precipitation is not the only mechanism for creating the surface run-off that is required for the formation of the valley. Other mechanisms for the formation of the valley networks have been proposed. Goldspiel and Squyres (2000) suggested that the valley networks may not be as strongly linked to a warm early climate as suggested by some (e.g. Sagan *et al.* 1973; Craddock and Howard 2002; Malin and Edgett 2003) and that many of the valley networks may have formed as a result of localized groundwater sapping under cold and arid conditions much like those on Mars today (Pieri 1980; Gulick 2001). Sapping does not require atmospheric temperatures to be higher than at present, as long as there is enough geothermal heat supply and a high regolith permeability, for example, resulting from widespread volcanism or impacts. In fact, Schuster and Weiss (2005) have shown in their calculations based on meteorite thermochronology, that Martian surface temperatures may have been similar to present day temperatures for the last billion years. Other advocates of alternative primary mechanisms for the creation of the valley networks include Aharonson *et al.* (2002), who showed that the characteristics of the valley network drainage basins are inconsistent with surface run-off and more likely related to groundwater sapping; and Toon *et al.* (2010) who showed that large impact processes ultimately may have been responsible for the formation of valley networks by heating the subsurface sufficiently to melt the ice layers and thus creating temporary hydrological cycles. Impacts, especially during early Mars history (Mid to Late Noachian), were frequent events that could have catastrophically generated large amounts of atmospheric volatiles, which in turn would condensate into precipitation that drained into temporary lakes and seas while creating the valley networks observed

today, before subsequently freezing again (Segura *et al.* 2008, 2012; Toon *et al.* 2010; Lasue *et al.* 2012). This shows that a long-lived hydrological cycle is not necessarily required to produce the valley networks of the Noachian and these alternatives add to the evidence that a sustained, warm and wet climate may not have occurred on Mars. Furthermore, as suggested by Cabrol and Grin (2001), the signs of aqueous activity are spread throughout all Martian chronological periods and are thus not indicative of a single, warm and wet climate in early Martian history.

7.5.3 Conclusions

Fans and fan deltas have not only been formed in the Noachian, but instead throughout the history of Mars. Their occurrence points to a formation process that can operate under cold and dry conditions – which may temporarily have been less dry or slightly "wetter". Triggers for the heating of ground ice and the creation of a temporary hydrological cycle include magmatism, volcanism and impact cratering on both small (i.e. regional events that occurred throughout Martian history) and large scales (i.e. global conditions related to increased volcanism and impact cratering during the Late Noachian and Early Hesperian, which then were more frequent than during the Amazonian). On a more local scale, obliquity cycles may have been responsible for temporary changes of atmospheric conditions, allowing the formation of smaller scale, local features. During the global and large regional events, water catastrophically modified the surface of the planet as it drained into the proposed large temporary oceans or seas in the northern lowlands. The more recent aqueous activity on Mars is evidence that it was not limited to the Late Noachian or Early Hesperian, although it may have been more prevalent during these early periods.

As satellite data continue to increase in quantity and quality, continued work on the morphology of fan-shaped deposits on Mars may shed more light on how much fluvial erosion has shaped the surface of Mars. Planned scientific missions to Mars include more in-situ research and sampling for aqueous minerals and biological material as well as the potential of sample return missions. Future work could be aimed at a) better constraining the ages of known deposits, b) better understanding the morphodynamic behaviour of salty brines and other liquids besides water, for example, the methane on Titan, and c) at better comprehending the processes that form the outlier deposits such as Nili Fossae and Eberswalde.

Even though water has played a crucial role in shaping the landscape of Mars, there is limited evidence of a long-term, stable hydrological cycle able to support long-lived oceans. Features such as alluvial fans and fan deltas are not clear indicators of a warm and wet climate early during Martian history. A much more likely scenario entails a predominately cold and dry climate history for the planet Mars, with intermittent pulses of hydrological activity capable of producing the landforms studied in this dissertation.

“The recitals of explorers are put down first in pencil. One waits until the explorer has furnished proofs, before putting them down in ink.”

8 References

Aharonson, O., Zuber, M. T. & Rothman, D. H. (2001). Statistics of Mars' topography from the Mars Orbiter Laser Altimeter: Slopes, correlations, and physical Models. *Journal of Geophysical Research: Planets*, *106*(10), 23723–23735. doi:10.1029/2000JE001403

Aharonson, O., Zuber, M. T., Rothman, D. H., Schorghofer, N. & Whipple, K. X. (2002). Drainage basins and channel incision on Mars. *Proceedings of the National Academy of Sciences of the United States of America*, *99*(4), 1780–3.

Allmendinger, R. W., Gonzalez, G., Yu, J., Hoke, G. & Isacks, B. (2005). Trench-parallel shortening in the Northern Chilean Forearc: tectonic and climatic implications. *Geological Society of America Bulletin*, *117*, 89–104. doi:10.1130/B25505.1

Al-Masrahy, M. A. & Mountney, N. P. (2013). Remote sensing of spatial variability in aeolian dune and interdune morphology in the Rub' Al-Khali, Saudi Arabia. *Aeolian Research*. doi:10.1016/j.aeolia.2013.06.004

Andrews-Hanna, J. C. & Phillips, R. J. (2007). Hydrological modeling of outflow channels and chaos regions on Mars. *Journal of Geophysical Research: Planets*, *112*(8), 1–14. doi:10.1029/2006JE002881

Andrews-Hanna, J. C., Zuber, M. T., Arvidson, R. E., Wiseman, S. M. & Hanna, J. C. (2010). Early Mars hydrology: Meridiani playa deposits and the sedimentary record of Arabia Terra. *Journal of Geophysical Research: Planets*, *115*(6), 1–22. doi:10.1029/2009JE003485

Armitage, J. J., Warner, N. H., Goddard, K. & Gupta, S. (2011). Timescales of alluvial fan development by precipitation on Mars. *Geophysical Research Letters*, *38*(17), L17203. doi:10.1029/2011GL048907

Artemieva, N. A. & Shuvalov, V. V. (2002). Shock metamorphism on the ocean floor (numerical simulations). *Deep Sea Research Part II: Topical Studies in Oceanography*, *49*(6), 959–968. doi:10.1016/S0967-0645(01)00136-9

Arzani, N. (2012). Catchment lithology as a major control on alluvial megafan development, Kohrud Mountain range, central Iran. *Earth Surface Processes and Landforms*, *37*(7), 726–740. doi:10.1002/esp.3194

Assine, M. L. (2005). River avulsions on the Taquari megafan, Pantanal wetland, Brazil. *Geomorphology*, *70*(3-4), 357–371. doi:10.1016/j.geomorph.2005.02.013

Baker, V. R. (1982). *The Channels of Mars* (p. 204). Austin: University of Texas Press.

Baker, V. R. (2001). Water and the martian landscape. *Nature*, *412*, 228–36. doi:10.1038/35084172

Baker, V. R. (2006). Geomorphological Evidence for Water on Mars. *Elements*, *2*(3), 139–143. doi:10.2113/gselements.2.3.139

Baker, V. R. (2009a). The Channeled Scabland: A Retrospective. *Annual Review of Earth and Planetary Sciences*, *37*(1), 393–411. doi:10.1146/annurev.earth.061008.134726

Baker, V. R. (2009b). Megafloods and global paleoenvironmental change on Mars and Earth. In M. G. Chapman & L. Kesthelyi (ds.), *Preservation of Random Mega-scale Events on Mars and Earth: Influence on Geologic History* (pp. 25–36). Geological Society of America Special Paper 453. doi:10.1130/2009.453

Baker, V. R., Dohm, J. M., Fairén, A. G., Ferré, T. P. A., Ferris, J. C., Miyamoto, H. & Schulze-Makuch, D. (2005). Extraterrestrial hydrogeology. *Hydrogeology Journal*, *13*(1), 51–68. doi:10.1007/s10040-004-0433-2

Baker, V. R. & Milton, D. J. (1974). Erosion by Catastrophic Floods on Mars and Earth. *Icarus*, *41*, 27–41. doi:10.1016/0019-1035(74)90101-8

Baker, V. R. & Partridge, J. B. (1986). Small Martian Valleys: Pristine and Degraded Morphology. *Journal of Geophysical Research*, *91*(3), 3561–3572. doi:10.1029/JB091iB03p03561

Baker, V. R., Strom, R. G., Gulick, V. C., Kargal, J. S., Komatsu, G. & Kale, V. S. (1991). Ancient oceans, ice sheets and the hydrological cycle on Mars. *Nature*, *352*(August), 589–594.

Bandfield, J. L., Hamilton, V. E. & Christensen, P. R. (2000). A global view of Martian surface compositions from MGS-TES. *Science (New York, N.Y.), 287*(3), 1626–1630. doi:10.1126/science.287.5458.1626

Bargery, A. S. & Wilson, L. (2011). Erosive flood events on the surface of Mars: Application to Mangala and Athabasca Valles. *Icarus*, *212*(2), 520–540. doi:10.1016/j.icarus.2011.01.001

Barlow, N. G. (1990). Constraint on Early Events in Martian History as Derived from the Cratering Record. *Journal of Geophysical Research*, *95*, 191–201. doi:10.1029/JB095iB09p14191

Barlow, N. G. (1993). Depth-diameter rations for Martian inpact craters: implications for target properties and episodes of degradation. *LPI Technical Report 93-06 Part 1*.

Barlow, N. G. (1995). The degradation of impact craters in Maja Valles and Arabia, Mars. *Journal of Geophysical Research*, *100*, 307–316. doi:10.1029/95JE02492

Barlow, N. G. (2005). A review of Martian impact crater ejecta structures and their implications for target properties. *Geological Society of America Special Papers*, *384*, 433–442. doi:10.1130/0-8137-2384-1.433

Barlow, N. G. (2009a). Martian Central Pit Craters: Summary of Northern Hemisphere Results. In *LPSC*.

Barlow, N. G. (2009b). Effect of impact cratering on the geologic evolution of Mars and implications for Earth. *Geological Society of America Special Papers*, *453*, 15–24. doi:10.1130/2009.453(02)

Barlow, N. G. (2010). What we know about Mars from its impact craters. *Geological Society of America Bulletin*, *122*(5-6), 644–657. doi:10.1130/B30182.1

Barlow, N. G. & Perez, C. (2003). Martian impact crater ejecta morphologies as indicators of the distribution of subsurface volatiles. *Journal of Geophysical Research: Planets*, *108*(8), 5085. doi:10.1029/2002JE002036

Beaty, C. B. (1963). Origin of alluvial fans, White Mountains, California and Nevada. *Annals of the Association of American Geographers*, *53*(4), 516–535.

Beaty, C. B. (1990). Anatomy of a White Mountains debris-flow – The making of an alluvial fan. In A. H. Rachocki & M. Church (Eds.), *Alluvial Fans: A Field Approach* (pp. 69–89). John Wiley & Sons Ltd.

Benvenuti, M. & Martini, I. P. (2002). Analysis of terrestrial hyperconcentrated flows and their deposits. In I. P. Martini, V. R. Baker, & G. Garzon (Eds.), *Flood and Megaflood Processes and Deposits: Recent and Ancient Examples* (pp. 167–193). IAS Special Publication.

Berman, D. C. & Hartmann, W. K. (2002). Recent Fluvial, Volcanic, and Tectonic Activity on the Cerberus Plains of Mars. *Icarus*, *159*(1), 1–17. doi:10.1006/icar.2002.6920

Beuthe, M., Le Maistre, S., Rosenblatt, P., Pätzold, M. & Dehant, V. (2012). Density and lithospheric thickness of the Tharsis Province from MEX MaRS and MRO gravity data. *Journal of Geophysical Research: Planets*, *117*(4), n/a–n/a. doi:10.1029/2011JE003976

Bhattacharya, J. P., Payenberg, T. H. D., Lang, S. C. & Bourke, M. C. (2005). Dynamic river channels suggest a long-lived Noachian crater lake on Mars. *Geophysical Research Letters*, *32*(10), 2–5. doi:10.1029/2005GL022747

Bibring, J.-P., Langevin, Y., Gendrin, A., Gondet, B., Poulet, F., Berthé, M., … Drossart, P. (2005). Mars surface diversity as revealed by the OMEGA/Mars Express observations. *Science (New York, N.Y.), 307*, 1576–81. doi:10.1126/science.1108806

Bibring, J.-P., Langevin, Y., Mustard, J. F., Poulet, F., Arvidson, R. E., Gendrin, A., … Neukum, G. (2006). Global mineralogical and aqueous Mars history derived from OMEGA/Mars Express data. *Science (New York, N.Y.), 312*, 400–4. doi:10.1126/science.1122659

Blair, T. C. (1987). Sedimentary Processes, Vertical Stratification Sequences, and Geomorphology of the Roaring River Alluvial Fan, Rocky Mountain National Park, Colorado. *SEPM Journal of Sedimentary Research*, *57*(1), 1–18. doi:10.1306/212F8A8A-2B24-11D7-8648000102C1865D

Blair, T. C. (1999a). Cause of dominance by sheet flood vs debris-flow processes on two adjoining alluvial fans, Death Valley, California. *Sedimentology*, *46*, 1015–1028.

Blair, T. C. (1999b). Sedimentology of the debris-flow-dominated Warm Spring Canyon alluvial fan, Death Valley, California. *Sedimentology*, *46*, 941–965.

Blair, T. C. & McPherson, J. G. (1992). The Trollheim alluvial fan and facies model revisited. *Geological Society of America Bulletin*, *104*, 762–769.

Blair, T. C. & McPherson, J. G. (1994). Alluvial fans and their natural distinction from rivers based on morphology, hydraulic processes, sedimentary processes, and facies assemblages. *Journal of Sedimentary Research*, *64*, 450–489.

Blair, T. C. & Pherson, J. G. M. C. (1998). Recent Debris-Flow Processes and Resultant Form and Facies of the Dolomite Alluvial Fan, Owens Valley, California. *Journal of Sedimentary Research*, *68*(5), 800–818. doi:10.1306/D426887E-2B26-11D7-8648000102C1865D

Blikra, L. H. & Nemec, W. (1998). Postglacial colluvium in western Norway: depositional processes, facies, and palaeoclimatic record. *Sedimentology*, *45*, 909–959.

Blissenbach, E. (1954). Geology of Alluvial Fans in Semi-Arid Regions. *Geological Society of America Bulletin*, (2). doi:10.1130/0016-7606(1954)65

Bluck, B. J. (1987). Bed forms and clast size changes in gravel-bed rivers. In K. S. Richards (Ed.), *River Channels: Environment and Processes* (pp. 159–178). Blackwell Scientific Publications.

Bowman, D. (1977). Stepped bed morphology in arid gravelly channels. *Geological Society of America Bulletin*, (77), 291–298.

Boyce, J. M. & Garbeil, H. (2007). Geometric relationships of pristine Martian complex impact craters, and their implications to Mars geologic history. *Geophysical Research Letters*, *34*(16), 1–5. doi:10.1029/2007GL029731

Boyce, J. M., Mouginis-Mark, P. J. & Garbeil, H. (2005). Ancient oceans in the northern lowlands of Mars: Evidence from impact crater depth/diameter relationships. *Journal of Geophysical Research: Planets*, *110*(3), E03008. doi:10.1029/2004JE002328

Brayshaw, A. C. (1984). Characteristics and Origin of Cluster Bedforms in Coarse-Grained Alluvial Channels. *Sedimentology of Gravels and Conglomerates*, *10*, 77–85.

Brune, G. M. (1953). Trap Efficiency of Reservoirs. *American Geophysical Union*, *34*(3), 407–418.

Bull, A. T. & Asenjo, J. A. (2013). Microbiology of hyper-arid environments: recent insights from the Atacama Desert, Chile. *Antonie van Leeuwenhoek*, *103*(6), 1173–9. doi:10.1007/s10482-013-9911-7

Bull, W. B. (1963). Alluvial fan deposits in western Fresno County, California. *Journal of Geology*, *71*, 243–251.

Bull, W. B. (1964). Relation of alluvial fan size and slope to drainage basin size and lithology in western Fresno County, California. *U.S. Geological Survey Professional Paper*, *450-B*, 51–53.

Bull, W. B. (1968). Alluvial Fans. *Journal of Geologic Education*, *17*(3), 101–106.

Bull, W. B. (1977). The alluvial fan environment. *Progress in Physical Geography*, *1*(2), 222–270. doi:10.1177/030913337700100202

Burr, D. M. (2002). Repeated Aqueous Flooding from the Cerberus Fossae: Evidence for Very Recently Extant, Deep Groundwater on Mars. *Icarus*, *159*(1), 53–73. doi:10.1006/icar.2002.6921

Burr, D. M., Enga, M.-T., Williams, R. M. E., Zimbelman, J. R., Howard, A. D. & Brennand, T. A. (2009). Pervasive aqueous paleoflow features in the Aeolis/Zephyria Plana region, Mars. *Icarus*, *200*(1), 52–76. doi:10.1016/j.icarus.2008.10.014

Burr, D. M., Williams, R. M. E., Wendell, K. D., Chojnacki, M. & Emery, J. P. (2010). Inverted fluvial features in the Aeolis/Zephyria Plana region, Mars: Formation mechanism and initial paleodischarge estimates. *Journal of Geophysical Research: Planets*, *115*(7), E07011. doi:10.1029/2009JE003496

Cabrol, N. A. (1998). Duration of the Ma'adim Vallis/Gusev Crater Hydrogeologic System, Mars. *Icarus*, *133*(1), 98–108. doi:10.1006/icar.1998.5914

Cabrol, N. A., Chong-Diaz, G., Stoker, C. R., Gulick, V. C., Landheim, R., Lee, P., … Witzke, B. (2001). Nomad Rover Field Experiment, Atacama Desert, Chile: 1. Science results overview. *Journal of Geophysical Research: Planets*, *106*(4), 7785. doi:10.1029/1999JE001166

Cabrol, N. A. & Grin, E. A. (1999). Distribution, classification, and ages of Martian impact crater lakes. *Icarus*, *172*, 160–172.

Cabrol, N. A. & Grin, E. A. (2001). The Evolution of Lacustrine Environments on Mars: Is Mars Only Hydrologically Dormant? *Icarus*, *149*(2), 291–328. doi:10.1006/icar.2000.6530

Cabrol, N. A., Wettergreen, D. S., Warren-Rhodes, K., Grin, E. A., Moersch, J. E., Diaz, G. C., … Wyatt, M. B. (2007). Life in the Atacama: Searching for life with rovers (science overview). *Journal of Geophysical Research: Biogeosciences*, *112*(4), G04S02. doi:10.1029/2006JG000298

Campbell, C. V. (1967). Lamina, laminaset, bed and bedset. *Sedimentology*, *8*, 7–26.

Cantelli, A., Paola, C. & Parker, G. (2004). Experiments on upstream-migrating erosional narrowing and widening of an incisional channel caused by dam removal. *Water Resources Research*, *40*(3), 1–12. doi:10.1029/2003WR002940

Carling, P. A. & Reader, N. A. (1982). Structure, composition and bulk properties of upland stream gravels. *Earth Surface Processes and Landforms*, *7*, 349–365.

Carr, M. H. (1979). Formation of Martian flood features by release of water from confined aquifers. *Journal of Geophysical Research: Solid Earth*.

Carr, M. H. (1983). Stability of streams and lakes on Mars. *Icarus*, *56*(3), 476–495. doi:10.1016/0019-1035(83)90168-9

Carr, M. H. (2003). Oceans on Mars: An assessment of the observational evidence and possible fate. *Journal of Geophysical Research: Planets*, *108*(5), 5042. doi:10.1029/2002JE001963

Carr, M. H. & Head, J. W. (2010). Geologic history of Mars. *Earth and Planetary Science Letters*, *294*(3-4), 185–203. doi:10.1016/j.epsl.2009.06.042

Carter, J., Poulet, F., Bibring, J.-P., Mangold, N. & Murchie, S. (2013). Hydrous minerals on Mars as seen by the CRISM and OMEGA imaging spectrometers: Updated global view. *Journal of Geophysical Research: Planets*, *118*(4), 831–858. doi:10.1029/2012JE004145

Carter, J., Poulet, F., Mangold, N., Ansan, V., Dehouck, E., Bibring, J.-P. & Murchie, S. L. (2012). Composition of Alluvial Fans and Deltas on Mars. *Lunar and Planetary Science Conference Abstracts*.

Cartigny, M., Ventra, D., Postma, G. & van den Berg, J. H. (2013). Morphodynamics and sedimentary structures of bedforms under supercritical-flow conditions: new insights from flume experiments (in press). *Sedimentology*.

Catuneanu, O., Abreu, V., Bhattacharya, J. P., Blum, M. D., Dalrymple, R. W., Eriksson, P. G., … Winker, C. (2009). Towards the standardization of sequence stratigraphy. *Earth-Science Reviews*, *92*(1-2), 1–33. doi:10.1016/j.earscirev.2008.10.003

Cembrano, J., Lavenu, A., Yañez, G., Riquelme, R., Garcia, M., Gonzalez, G. & Herail, G. (2007). Neotectonics. In T. Moreno & W. Gibbons (Eds.), *The Geology of Chile* (pp. 231–261). The Geological Society, London.

Christensen, P. R., Bandfield, J. L., Bell, J. F., Gorelick, N., Hamilton, V. E., Ivanov, A. B., … Wyatt, M. B. (2003). Morphology and composition of the surface of Mars: Mars Odyssey THEMIS results. *Science (New York, N.Y.), 300*, 2056–61. doi:10.1126/science.1080885

Christensen, P. R., Jakosky, B. M., Kieffer, H. H., Malin, M. C., McSween, H. Y., Nealson, K. H., … Ravine, M. A. (2004). The Thermal Emission Imaging System (THEMIS) for the Mars 2001 Odyssey Mission. *Space Science Reviews*, *110*(1-2), 85–130.

Church, M. & Gilbert, R. (1975). Proglacial fluvial and lacustrine sediments. In A. V. Jopling & B. C. Macdonald (Eds.), *Glaciofluvial and Glaciolacustrine Sedimentation* (pp. 22–100). SEPM Special Publication, 23.

Church, M. & Jones, D. (1982). Channel bars in gravel bed rivers. In R. D. Hey, J. C. Bathurst, & C. R. Thorne (Eds.), *Gravel Bed Rivers* (pp. 291–338). John Wiley & Sons Ltd.

Clark, B. C. (1978). Implications of Abundant Hygroscopic Minerals in the Martian Regolith. *Icarus*, *34*, 645–665.

Clarke, L., Quine, T. A. & Nicholas, A. (2010). An experimental investigation of autogenic behaviour during alluvial fan evolution. *Geomorphology*, *115*, 278–285.

Clifford, S. M. & Parker, T. J. (2001). The Evolution of the Martian Hydrosphere: Implications for the Fate of a Primordial Ocean and the Current State of the Northern Plains. *Icarus*, *154*(1), 40–79. doi:10.1006/icar.2001.6671

Collins, G. S., Melosh, H. J., Morgan, J. V. & Warner, M. R. (2002). Hydrocode Simulations of Chicxulub Crater Collapse and Peak-Ring Formation. *Icarus*, *157*(1), 24–33. doi:10.1006/icar.2002.6822

Collins, G. S. & Wünnemann, K. (2005). How big was the Chesapeake Bay impact? Insight from numerical modeling. *Geology*, *33*(12), 925. doi:10.1130/G21854.1

Collinson, J. D. (1996). Alluvial Sediments. In H. G. Reading (Ed.), *Sedimentary Environments: Processes, facies and stratigraphy* (3rd ed., p. 688). Blackwell Publishing Ltd.

Costa, J. E. (1988). Rheologic, geomorphic, and sedimentologic differentiation of water floods, hyperconcentrated flows, and debris flows. In V. R. Baker, R. C. Kochel, & P. C. Patton (Eds.), *Flood Geomorphology* (pp. 113–122). New York: Wiley & Sons.

Costard, F., Forget, F., Mangold, N. & Peulvast, J. P. (2002). Formation of recent martian debris flows by melting of near-surface ground ice at high obliquity. *Science (New York, N.Y.), 295*, 110–3. doi:10.1126/science.1066698

Craddock, R. A. & Howard, A. D. (2002). The case for rainfall on a warm, wet early Mars. *Journal of Geophysical Research: Planets*, *107*(11), 5111. doi:10.1029/2001JE001505

Craddock, R. A., Maxwell, T. A. & Howard, A. D. (1997). Crater morphometry and modification in the Sinus Sabaeus and Margaritifer Sinus regions of Mars. *Journal of Geophysical Research: Planets*, *102*(6), 13321–13340.

Crosta, G. B. & Frattini, P. (2004). Controls on modern alluvial fan processes in the central Alps, northern Italy. *Earth Surface Processes and Landforms*, *29*, 267–293.

Darby, D. A., Whittecar, G. R., Barringer, R. A. & Garrett, J. R. (1990). Alluvial lithofacies recognition in a humid-tropical setting. *Sedimentary Geology*, *67*, 161–174.

De Haas, T., Hauber, E. & Kleinhans, M. G. (2013). Local late Amazonian boulder breakdown and denudation rate on Mars. *Geophysical Research Letters*, *40*(May), n/a–n/a. doi:10.1002/grl.50726

De Villiers, G., Hauber, E., Kleinhans, M. G. & Postma, G. (n.d.). Fan-shaped sedimentary deposits on Mars - morphology, classification, distribution, and implications for climatic evolution (in preparation).

De Villiers, G., King, D. T. & Marzen, L. J. (2007). Shallow Marine Impact Craters on Mars. In *Lunar and Planetary Science Conference Abstracts*.

De Villiers, G., King, D. T. & Marzen, L. J. (2010a). A study of candidate marine target impact craters in Arabia Terra, Mars. *Meteoritics & Planetary Science*, *45*(6), 947–964. doi:10.1111/j.1945-5100.2010.01068.x

De Villiers, G., Kleinhans, M. G. & Postma, G. (2013). Experimental delta formation in crater lakes and implications for interpretation of Martian deltas. *Journal of Geophysical Research: Planets*, *118*(4), 651–670. doi:10.1002/jgre.20069

De Villiers, G., Kleinhans, M. G., Postma, G., Hauber, E., de Jong, S. & de Boer, P. L. (2009). Types of Martian Fan-shaped Sedimentary Deposits. In *LPSC*. doi:10.1029/2005GL025435.

De Villiers, G., Kleinhans, M. G., van Breemen, D. M. O., Postma, G. & Hauber, E. (2010b). Experiments on sedimentation in wide reservoirs and erosion following dam removal. In *Proceedings of the River Flow 2010 Conference* (pp. 1147–1154). Braunschweig, Germany.

De Villiers, G., Ventra, D. & de Boer, P. L. (n.d.). Terrestrial alluvial fan analogues for Mars – Classification and application with examples from the Atacama coast (northern Chile) (in preparation). *Geological Society, London, Special Publications*.

Di Achille, G. & Hynek, B. M. (2010). Ancient ocean on Mars supported by global distribution of deltas and valleys. *Nature Geoscience*, *3*(7), 459–463. doi:10.1038/ngeo891

Di Achille, G., Marinangeli, L., Ori, G. G., Hauber, E., Gwinner, K., Reiss, D. & Neukum, G. (2006). Geological evolution of the Tyras Vallis paleolacustrine system, Mars. *Journal of Geophysical Research: Planets*, *111*(4), 1–19. doi:10.1029/2005JE002561

Di Achille, G., Ori, G. G., Reiss, D., Hauber, E., Gwinner, K., Michael, G. G. & Neukum, G. (2006). A steep fan at Coprates Catena, Valles Marineris, Mars, as seen by HRSC data. *Geophysical Research Letters*, *33*(7), 2–5. doi:10.1029/2005GL025435

DiBiase, R. A., Limaye, A. B., Scheingross, J. S., Fischer, W. W. & Lamb, M. P. (2013). Deltaic deposits at Aeolis Dorsa: Sedimentary evidence for a standing body of water on the northern plains of Mars. *Journal of Geophysical Research: Planets*, *118*, 1285–1302. doi:10.1002/jgre.20100

Dickson, J. L., Fassett, C. I. & Head, J. W. (2009). Amazonian□aged fluvial valley systems in a climatic microenvironment on Mars: Melting of ice deposits on the interior of Lyot Crater. *Geophysical Research Letters*, *36*(8), 2–6. doi:10.1029/2009GL037472

Dickson, J. L., Head, J. W. & Kreslavsky, M. A. (2007). Martian gullies in the southern mid-latitudes of Mars: Evidence for climate-controlled formation of young fluvial features based upon local and global topography. *Icarus*, *188*(2), 315–323. doi:10.1016/j.icarus.2006.11.020

Diniega, S., Byrne, S., Bridges, N. T., Dundas, C. M. & McEwen, A. S. (2010). Seasonality of present-day Martian dune-gully activity. *Geology*, *38*(11), 1047–1050. doi:10.1130/G31287.1

Dixon, J. C. (2009). Aridic soils, patterned ground, and desert pavements. In A. J. Parsons & A. A. D. (Eds.), *Geomorphology of Desert Environments* (pp. 101–122). Springer Science.

Doyle, M. W., Harbor, J. M. & Stanley, E. H. (2003). Toward policies and decision-making for dam removal. *Environmental management*, *31*(4), 453–65. doi:10.1007/s00267-002-2819-z

Doyle, M. W., Stanley, E. H. & Harbor, J. M. (2002). Geomorphic Analogies for Assessing Probable Channel Response To Dam Removal. *Journal of the American Water Resources Association*, *38*(6), 1567–1579. doi:10.1111/j.1752-1688.2002.tb04365.x

Dunai, T. J., González López, G. A. & Juez-Larré, J. (2005). Oligocene–Miocene age of aridity in the Atacama Desert revealed by exposure dating of erosion-sensitive landforms. *Geology*, *33*(4), 321. doi:10.1130/G21184.1

Dundas, C. M., McEwen, A. S., Diniega, S., Byrne, S. & Martinez-Alonso, S. (2010). New and recent gully activity on Mars as seen by HiRISE. *Geophysical Research Letters*, *37*(7), n/a–n/a. doi:10.1029/2009GL041351

Dunkerley, D. L. & Brown, C. J. (1997). Desert soils. In D. S. G. Thomas (Ed.), *Geomorphology - Process, Form and Change in Drylands* (pp. 55–68). John Wiley & Sons Ltd.

Dypvik, H., Burchell, M. J. & Claeys, P. (2004). Impacts into Marine and Icy Environments – A Short Review. In *Cratering in marine environments and on ice* (pp. 1–20).

Dypvik, H., Gudlaugsson, S. T., Tsikalas, F., Attrep, M., Ferrell, R. E., David, H., … Jr, R. E. F. (1996). Mjølnir structure : An impact crater in the Barents Sea. *Geology*, *24*(April 2009), 779–782. doi:10.1130/0091-7613(1996)024<0779:MLSAIC>2.3.CO;2

Dypvik, H. & Jansa, L. F. (2003). Sedimentary signatures and processes during marine bolide impacts: a review. *Sedimentary Geology*, *161*(3-4), 309–337. doi:10.1016/S0037-0738(03)00135-0

Edgett, K. S. & Parker, T. J. (1997). Water on early Mars : Possible subaqueous sedimentary deposits covering ancient cratered terrain in western decade. *Geophysical Research Letters*, *24*(22), 2897–2900.

El Maarry, M. R., Dohm, J. M., Marzo, G. A., Fergason, R., Goetz, W., Heggy, E., … Markiewicz, W. J. (2012). Searching for evidence of hydrothermal activity at Apollinaris Mons, Mars. *Icarus*, *217*(1), 297–314. doi:10.1016/j.icarus.2011.10.022

Fairén, A. G., Dohm, J. M., Baker, V. R., de Pablo, M. A., Ruiz, J., Ferris, J. C. & Anderson, R. C. (2003). Episodic flood inundations of the northern plains of Mars. *Icarus*, *165*(1), 53–67. doi:10.1016/S0019-1035(03)00144-1

Falorni, G. (2005). Analysis and characterization of the vertical accuracy of digital elevation models from the Shuttle Radar Topography Mission. *Journal of Geophysical Research: Earth surface*, *110*(2), F02005. doi:10.1029/2003JF000113

Fassett, C. I. & Head, J. W. (2005). Fluvial sedimentary deposits on Mars: Ancient deltas in a crater lake in the Nili Fossae region. *Geophysical Research Letters*, *32*(14), 1–5. doi:10.1029/2005GL023456

Fassett, C. I. & Head, J. W. (2007). Layered mantling deposits in northeast Arabia Terra, Mars: Noachian-Hesperian sedimentation, erosion, and terrain inversion. *Journal of Geophysical Research: Planets*, *112*(8), 1–19. doi:10.1029/2006JE002875

Fassett, C. I. & Head, J. W. (2008). Valley network-fed, open-basin lakes on Mars: Distribution and implications for Noachian surface and subsurface hydrology. *Icarus*, *198*(1), 37–56. doi:10.1016/j.icarus.2008.06.016

Fassett, C. I. & Head, J. W. (2011). Sequence and timing of conditions on early Mars. *Icarus*, *211*(2), 1204–1214. doi:10.1016/j.icarus.2010.11.014

Ferguson, R. (2007). Flow resistance equations for gravel- and boulder-bed streams. *Water Resources Research*, *43*(5), n/a–n/a. doi:10.1029/2006WR005422

Fisher, R. V. (1971). Features of coarse-grained, high-concentration fluids and their deposits. *Journal of Sedimentary Petrology*, *41*, 916–927.

Flint, S., Turner, P. & Jolley, E. J. (1991). Depositional architecture of Quaternary fan-delta deposits of the forearc: relative sea-level changes as a response to aseismic ridge subduction. In D. I. M. Macdonald (Ed.), *Sedimentation, Tectonics, and Eustasy: Sea-Level Changes at Active Margins* (pp. 91–103). IAS Special Publication 12.

French, B. M. (1998). *Traces of Catastrophe: A Handbook of Shock-Metamorphic Effects in Terrestrial Meteorite Impact Structures* (p. 120). LPI Contribution.

Frostick, L. E., Lucas, P. M. & Reid, I. (1984). The infiltration of fine matrices into coarse-grained alluvial sediments and its implications for stratigraphical interpretation. *Journal of the Geological Society of London*, *141*, 955–965.

Gaidos, E. & Marion, G. (2003). Geological and geochemical legacy of a cold early Mars. *Journal of Geophysical Research: Planets*, *108*(6), 5055. doi:10.1029/2002JE002000

Galloway, W. E. (1975). Process framework for describing the morphologic and stratigraphic evolution of deltaic depositional systems. In M. L. Broussard (Ed.), *Deltas: Models for Exploration* (pp. 87–98). Houston: Houston Geological Society.

Garvin, J. B. & Frawley, J. J. (1998). Geometric properties of Martian impact craters: Preliminary results from the Mars Orbiter Laser Altimeter. *Geophysical Research Letters*, *25*(24), 4405–4408.

Garvin, J. B., Sakimoto, S. E. H., Frawley, J. J. & Schnetzler, C. (2000). North Polar Region Craterforms on Mars: Geometric Characteristics from the Mars Orbiter Laser Altimeter. *Icarus*, *144*(2), 329–352. doi:10.1006/icar.1999.6298

Gasnault, O., Jeffrey Taylor, G., Karunatillake, S., Dohm, J., Newsom, H., Forni, O., Pinet, P. & Boynton, W. (2010). Quantitative geochemical mapping of martian elemental provinces, *Icarus*, 207(1), 226-247. doi:10.1016/j.icarus.2009.11.010

Gault, D. E. & Sonett, C. P. (1982). Laboratory simulation of pelagic asteroidal impact: Atmospheric injection, benthic topography, and the surface wave radiation field. In *Geological Society of America Special Papers* (Vol. 190, pp. 69–92). doi:10.1130/SPE190-p69

Geleynse, N., Storms, J. E. A., Stive, M. J. F., Jagers, H. R. A. & Walstra, D. J. R. (2010). Modeling of a mixed-load fluvio-deltaic system. *Geophysical Research Letters*, *37*(5), n/a–n/a. doi:10.1029/2009GL042000

Gersonde, R., Deutsch, A., Ivanov, B. A. & Kyte, F. T. (2002). Oceanic impacts—a growing field of fundamental geoscience. *Deep Sea Research Part II: Topical Studies in Oceanography*, *49*(6), 951–957. doi:10.1016/S0967-0645(01)00134-5

Ghatan, G. J., Head, J. W. & Wilson, L. (2005). *Mangala Valles, Mars: Assessment of Early Stages of Flooding and Downstream Flood Evolution*. *Earth, Moon, and Planets* (Vol. 96, pp. 1–57). doi:10.1007/s11038-005-9009-y

Ghatan, G. J. & Zimbelman, J. R. (2006). Paucity of candidate coastal constructional landforms along proposed shorelines on Mars: Implications for a northern lowlands-filling ocean. *Icarus*, *185*(1), 171–196. doi:10.1016/j.icarus.2006.06.007

Gilbert, G. K. (1890). Lake Bonneville. US Geological Survey Monograph (Vol. 1, p. 438).

Gohain, K., & Prakash, B. (1990). Morphlogy of the Kosi Megafan. In A.H. Rackchoki & M. Church (Eds.), *Alluvial Fans: A Field Approach* (pp. 151-178). John Wiley and Sons Ltd.

Goldspiel, J. M. & Squyres, S. W. (1991). Ancient aqueous sedimentation on Mars. *Icarus*, *89*(2), 392–410. doi:10.1016/0019-1035(91)90186-W

Goldspiel, J. M. & Squyres, S. W. (2000). Groundwater Sapping and Valley Formation on Mars. *Icarus*, *148*(1), 176–192. doi:10.1006/icar.2000.6465

Golombek, M. P., Haldemann, A. F. C., Forsberg-Taylor, N. K., DiMaggio, E. N., Schroeder, R. D., Jakosky, B. M., … Matijevic, J. R. (2003). Rock size-frequency distributions on Mars and implications for Mars Exploration Rover landing safety and operations. *Journal of Geophysical Research: Planets*, *108*(12), 8086. doi:10.1029/2002JE002035

Gooding, J. L. (1992). Soil Mineralogy and Chemistry on Mars: Possible Clues from Salts and Clays in SNC Meteorites. *Icarus*, *99*(1), 28–41.

Goudge, T. A., Head, J. W., Mustard, J. F. & Fassett, C. I. (2012). An analysis of open-basin lake deposits on Mars: Evidence for the nature of associated lacustrine deposits and post-lacustrine modification processes. *Icarus*, *219*(1), 211–229. doi:10.1016/j.icarus.2012.02.027

Grant, J. A. & Parker, T. J. (2002). Drainage evolution in the Margaritifer Sinus region, Mars. *Journal of Geophysical Research*, *107*(9), 1–19. doi:10.1029/2001JE001678

Grant, J. A. & Wilson, S. A. (2011). Late alluvial fan formation in southern Margaritifer Terra, Mars. *Geophysical Research Letters*, *38*(8), L08201. doi:10.1029/2011GL046844

Grieve, R. A. F. (1987). Terrestrial Impact Craters. *Annual Review of Earth and Planetary Sciences*, *15*, 245–270.

Gudlaugsson, S. T. (1993). Large impact crater in the Barents Sea. *Geology*, *21*(April 2009), 291–294. doi:10.1130/0091-7613(1993)021<0291

Gulick, V. C. (2001). Origin of the valley networks on Mars: a hydrological perspective. *Geomorphology*, *37*(3-4), 241–268. doi:10.1016/S0169-555X(00)00086-6

Gupta, S. (1997). Himalayan drainage patterns and the origin of fluvial megafans in the Ganges foreland basin. *Geology*, *25*(1), 11–14. doi:10.1130/0091-7613(1997)025<0011:HDPATO>2.3.CO;2

Gwinner, K., Scholten, F., Spiegel, M., Schmidt, R., Giese, B., Oberst, J., … Neukum, G. (2009). Derivation and Validation of High-Resolution Digital Terrain Models from Mars Express HRSC Data. *Photogrammetric Engineering and Remote Sensing*, *75*(9), 1127–1142.

Haberle, R. M., Mckay, C. P., Schaeffer, J., Cabrol, N. A., Grin, E. A., Zent, A. P. & Quinn, R. (2001). On the possibility of liquid water on present-day Mars. *Journal of Geophysical Research: Planets*, *106*(10), 23317–23326. doi:10.1029/2000JE001360

Hampton, M. A. (1975). Competence in fine-grained debris flows. *Journal of Sedimentary Petrology*, *45*, 834–844.

Hardgrove, C. J., Moersch, J. E. & Whisner, S. (2009). Thermal imaging of alluvial fans: A new technique for remote classification of sedimentary features. *Earth and Planetary Science Letters*, *285*(1-2), 124–130. doi:10.1016/j.epsl.2009.06.004

Harrison, K. P. & Grimm, R. E. (2005). Groundwater-controlled valley networks and the decline of surface runoff on early Mars. *Journal of Geophysical Research: Planets*, *110*(12), 1–17. doi:10.1029/2005JE002455

Hartley, A. J. & Chong, G. (2002). Late Pliocene age for the Atacama Desert: Implications for the desertification of western South America. *Geology*, *30*(1), 43. doi:10.1130/0091-7613(2002)030<0043:LPAFTA>2.0.CO;2

Hartley, A. J., Chong, G., Houston, J. & Mather, A. E. (2005a). 150 million years of climatic stability: evidence from the Atacama Desert, northern Chile. *Journal of the Geological Society*, *162*(3), 421–424. doi:10.1144/0016-764904-071

Hartley, A. J. & Jolley, E. J. (1995). Tectonic implications of Late Cenozoic sedimentation from the Coastal Cordillera of northern Chile (22°-24° S). *Journal of the Geological Society of London*, *152*, 51–63.

Hartley, A. J., Mather, A. E., Jolley, E. J. & Turner, P. (2005b). Climatic controls on alluvial fan activity, Coastal Cordillera, northern Chile. In A. M. Harvey, E. Mather, Anne, & M. Stokes (Eds.), *Alluvial Fans: Geomorphology, Sedimentology, Dynamics* (pp. 95–115). Geological Society of London, Special Publication 251.

Hartley, A. J., Weissmann, G. S., Nichols, G. J. & Warwick, G. L. (2010). Large Distributive Fluvial Systems: Characteristics, Distribution, and Controls on Development. *Journal of Sedimentary Research*, *80*(2), 167–183. doi:10.2110/jsr.2010.016

Hartmann, W. K. (1966). Martian Cratering. *Icarus*, *5*(1-6), 565–576. doi:10.1016/0019-1035(66)90071-6

Hartmann, W. K. (1977). Relative Crater Production Rates on Planets. *Icarus*, *31*(2), 260–276.

Hartmann, W. K. & Neukum, G. (2001). Cratering chronology and the evolution of Mars. *Space Science Reviews*, *96*(1-4), 165–194.

Harvey, A. M. (1984). Debris flows and fluvial deposits in Spanish Quaternary alluvial fans: Implications for fan morphology. In E. H. Koster & R. J. Steel (Eds.), *Sedimentology of Gravels and Conglomerates* (pp. 123–132). Canadian Society of Petroleum Geologists Memoir 10.

Harvey, A. M. (2010). Local buffers to the sediment cascade: debris cones and alluvial fans. In T. Burt & R. Allison (Eds.), *Sediment Cascades: An Integrated Approach* (pp. 153–180). Wiley & Sons.

Harvey, A. M. (2012). The coupling status of alluvial fans and debris cones: a review and synthesis. *Earth Surface Processes and Landforms*, *37*(1), 64–76. doi:10.1002/esp.2213

Harvey, A. M. (2013). Processes of sediment supply to alluvial fans and debris cones. In M. Schneuwly-Bollschweiler, M. Stoffel, & F. Rudolf-Miklau (Eds.), *Dating Torrential Processes on Fans and Cones* (pp. 15–32). Springer Science.

Hassan, M. A. (2005). Characteristics of gravel bars in ephemeral streams. *Journal of Sedimentary Research*, *75*, 29–42.

Hauber, E., Grott, M. & Kronberg, P. (2010). Martian rifts: Structural geology and geophysics. *Earth and Planetary Science Letters*, *294*(3-4), 393–410. doi:10.1016/j.epsl.2009.11.005

Hauber, E., Gwinner, K., Kleinhans, M. G., Reiss, D., Di Achille, G., Ori, G. G., … Neukum, G. (2009). Sedimentary deposits in Xanthe Terra: Implications for the ancient climate on Mars. *Planetary and Space Science*, *57*(8-9), 944–957. doi:10.1016/j.pss.2008.06.009

Hauber, E., Platz, T., Reiss, D., Le Deit, L., Kleinhans, M. G., Marra, W. A., … Carbonneau, P. (2013). Asynchronous formation of Hesperian and Amazonian-aged deltas on Mars and implications for climate. *Journal of Geophysical Research: Planets*, n/a–n/a. doi:10.1002/jgre.20107

Hauber, E., Reiss, D., Ulrich, M., Preusker, F., Trauthan, F., Zanetti, M., … Olvmo, M. (2011). Landscape evolution in Martian mid-latitude regions: insights from analogous periglacial landforms in Svalbard. *Geological Society, London, Special Publications*, *356*(1), 111–131. doi:10.1144/SP356.7

Haug, E. W., Kraal, E. R., Sewall, J. O., Van Dijk, M. & Diaz, G. C. (2010). Climatic and geomorphic interactions on alluvial fans in the Atacama Desert, Chile. *Geomorphology*, *121*(3-4), 184–196. doi:10.1016/j.geomorph.2010.04.005

Head, J. W., Hiesinger, H., Ivanov, M. A., Kreslavsky, M. A., Pratt, S. & Thomson, B. J. (1999). Possible ancient oceans on Mars: evidence from Mars Orbiter Laser Altimeter data. *Science (New York, N.Y.), 286*(5447), 2134–7.

Head, J. W., Kreslavsky, M. A., Hiesinger, H., Ivanov, M. A., Smith, D. E. & Zuber, M. T. (1998). Oceans in the Past History of Mars: Tests for their Presence Using Mars Orbiter Laser Altimeter (MOLA) data. *Geophysical Research Letters*, *24*, 4401–4404.

Head, J. W., Marchant, D. R. & Kreslavsky, M. A. (2008). Formation of gullies on Mars: link to recent climate history and insolation microenvironments implicate surface water flow origin. *Proceedings of the National Academy of Sciences of the United States of America*, *105*(36), 13258–63. doi:10.1073/pnas.0803760105

Head, J. W. & Wilson, L. (2007). Heat transfer in volcano–ice interactions on Mars: synthesis of environments and implications for processes and landforms. *Annals of Glaciology*, *45*(1), 1–13. doi:10.3189/172756407782282570

Hecht, M. H. (2002). Metastability of Liquid Water on Mars. *Icarus*, *156*(2), 373–386. doi:10.1006/icar.2001.6794

Heldmann, J. L. & Mellon, M. T. (2004). Observations of martian gullies and constraints on potential formation mechanisms. *Icarus*, *168*(2), 285–304. doi:10.1016/j.icarus.2003.11.024

Heldmann, J. L., Toon, O. B., Pollard, W. H. & Mellon, M. T. (2005). Formation of Martian gullies by the action of liquid water flowing under current Martian environmental conditions. *Journal of Geophysical Research: Planets*, *110*(5), E05004. doi:10.1029/2004JE002261

Herkenhoff, K. E., Squyres, S. W., Arvidson, R. E., Bass, D. S., Bell, J. F., Bertelsen, P., … Wang, A. (2004). Textures of the soils and rocks at Gusev Crater from Spirit's Microscopic Imager. *Science (New York, N.Y.)*, *305*(5685), 824–6. doi:10.1126/science.1100015

Hock, A. N., Cabrol, N. A., Dohm, J. M., Piatek, J. L., Warren-Rhodes, K., Weinstein, S., … Glasgow, J. (2007). Life in the Atacama: A scoring system for habitability and the robotic exploration for life. *Journal of Geophysical Research: Biogeosciences*, *112*(4), G04S08. doi:10.1029/2006JG000321

Hoffman, N. (2000). White Mars: A New Model for Mars' Surface and Atmosphere Based on CO^2, *Icarus*, 146(2), 326-342.

Hoffman, N. (2002). Active polar gullies on Mars and the role of carbon dioxide. *Astrobiology*, *2*(3), 313–23. doi:10.1089/153110702762027899

Hoke, M. R. T., Hynek, B. M. & Tucker, G. E. (2011). Formation timescales of large Martian valley networks. *Earth and Planetary Science Letters*, *312*(1-2), 1–12. doi:10.1016/j.epsl.2011.09.053

Hooke, R. (1967). Processes on arid-region alluvial fans. *Journal of Geology*, *75*, 438–460.

Hooke, R. (1968). Model Geology : Prototype and Laboratory Streams : Discussion. *Geological Society of America Bulletin*, *79*(3), 391–394. doi:10.1130/0016-7606(1968)79

Hooke, R. (1987). Mass movement in semi-arid environments and the morphology of alluvial fans. In M. G. Anderson & K. S. Richards (Eds.), *Slope Stability* (pp. 505–529). John Wiley & Sons Ltd.

Horton, B. K. & DeCelles, P. G. (2001). Modern and ancient fluvial megafans in the foreland basin system of the central Andes, southern Bolivia : implications for drainage network evolution in fold- thrust belts. *Basin Research*, *13*, 43–63.

Horton, J. W., Ormö, J., Powars, D. S. & Gohn, G. S. (2006). Chesapeake Bay impact structure: Morphology, crater fill, and relevance for impact structures on Mars. *Meteoritics & Planetary Science*, *41*(10), 1613–1624. doi:10.1111/j.1945-5100.2006.tb00439.x

Howard, A. D., Moore, J. M. & Irwin, R. P. (2005). An intense terminal epoch of widespread fluvial activity on early Mars: 1. Valley network incision and associated deposits. *Journal of Geophysical Research: Planets*, *110*(12), 1–20. doi:10.1029/2005JE002459

Hubert, J. F. & Filipov, J. A. (1989). Debris-flow deposits in alluvial fans of the west flank of the White Mountains, Owens Valley, California, U.S.A. *Sedimentary Geology*, *61*, 177–205.

Hynek, B. M., Beach, M. & Hoke, M. R. T. (2010). Updated global map of Martian valley networks and implications for climate and hydrologic processes. *Journal of Geophysical Research: Planets*, *115*(9), 1–14. doi:10.1029/2009JE003548

Hynek, B. M., Phillips, R. J. & Arvidson, R. E. (2003). Explosive volcanism in the Tharsis region: Global evidence in the Martian geologic record. *Journal of Geophysical Research*, *108*(9), 1–16. doi:10.1029/2003JE002062

Irwin, R. P., Watters, T. R., Howard, A. D. & Zimbelman J. R. (2004). Sedimentary resurfacing and fretted terrain development along the crustal dichotomy boundary, Aeolis Mensae, Mars. *Journal of Geophysical Research: Planets*, *109(9)*. doi:10.1029/2004JE002248.

Irwin, R. P., Howard, A. D., Craddock, R. A. & Moore, J. M. (2005). An intense terminal epoch of widespread fluvial activity on early Mars: 2. Increased runoff and paleolake development. *Journal of Geophysical Research: Planets*, *110*(12). doi:10.1029/2005JE002460

Iverson, R. M. & Denlinger, R. P. (1987). The physics of debris flows - a conceptual assessment. In R. L. Beschta, T. Blinn, G. E. Grant, G. G. Ice, & F. J. Swanson (Eds.), *Erosion and Sedimentation in the Pacific Rim* (pp. 155–165). IAHS Publication 165.

Jakosky, B. M., Pepin, R. O., Johnson, R. E. & Fox, J. L. (1994). Mars Atmospheric Loss and Isotopic Fractionation by Solar-Wind-Induced Sputtering and Photochemical Escape. *Icarus*, *111*(2), 271–288. doi:http://dx.doi.org/10.1006/icar.1994.1145

Jakosky, B. M. & Phillips, R. J. (2001). Mars' volatile and climate history. *Nature*, *412*(6843), 237–44. doi:10.1038/35084184

Jaumann, R., Hauber, E., Lanz, J., Hoffmann, H. & Neukum, G. (2002). Geomorphological Record of Water-Related Erosion on Mars. In *Astrobiology - The Quest for the Conditions of Life* (pp. 89–109). Springer Berlin Heidelberg. doi:10.1007/978-3-642-59381-9_7

Jaumann, R., Neukum, G., Behnke, T., Duxbury, T. C., Eichentopf, K., Flohrer, J., … Wählisch, M. (2007). The high-resolution stereo camera (HRSC) experiment on Mars Express: Instrument aspects and experiment conduct from interplanetary cruise through the nominal mission. *Planetary and Space Science*, *55*(7-8), 928–952. doi:10.1016/j.pss.2006.12.003

Jaumann, R., Reiss, D., Frei, S., Neukum, G., Scholten, F., Gwinner, K., … Carr, M. H. (2005). Interior channels in Martian valleys: Constraints on fluvial erosion by measurements of the Mars Express High Resolution Stereo Camera. *Geophysical Research Letters*, *32*(16), L16203. doi:10.1029/2005GL023415

Jerolmack, D. J., Mohrig, D., Zuber, M. T. & Byrne, S. (2004). A minimum time for the formation of Holden Northeast fan, Mars. *Geophysical Research Letters*, *31*(21), 1–5. doi:10.1029/2004GL021326

Johnson, A. M. (1970). *Physical processes in geology: A method for interpretation of natural phenomena* (p. 577). Freeman, Cooper & Co., San Francisco, USA.

Johnson, C. G., Kokelaar, B. P., Iverson, R. M., Logan, M., LaHusen, R. G. & Gray, J. M. N. T. (2012). Grain-size segregation and levee formation in geophysical mass flows. *Journal of Geophysical Research: Earth surface*, *117*(1), F01032. doi:10.1029/2011JF002185

Johnston, A. K., Reiss, D., Hauber, E., Zanetti, M., Hiesinger, H., Johansson, L. & Olvmo, M. (2012). Periglacial mass-wasting landforms on Mars suggestive of transient liquid water in the recent past: Insights from solifluction lobes on Svalbard. *Icarus*, *218*(1), 489–505. doi:10.1016/j.icarus.2011.12.021

Kargal, J. S., Kirk, R. L., Fegley, B. & Treiman, A. H. (1994). Carbonate-Sulfate Volcanism on Venus? *Icarus*, *112*, 219–252.

Kenkmann, T. & Schönian, F. (2005). Impact Craters on Mars and Earth: Implications by Analogy. In *LPSC*.

Kennett, J. P. (1982). *Marine Geology* (p. 813). Englewood Cliffs: Prentice Hall.

Kereszturi, A. & Rivera-Valentin, E. G. (2012). Locations of thin liquid water layers on present-day Mars. *Icarus*, *221*(1), 289–295. doi:10.1016/j.icarus.2012.08.004

Kesel, R. H. & Lowe, D. R. (1987). Geomorphology and sedimentology of the Toro Amarillo alluvial fan in a humid tropical environment, Costa Rica. *Geografiska Annaler*, *69*, 85–99.

Kim, B. C. & Lowe, D. R. (2004). Depositional processes of the gravelly debris flow deposits, South Dolomite alluvial fan, Owens Valley, California. *Geosciences Journal*, *8*, 153–170.

King, D. T., Neathery, T. L., Petruny, L. W., Koeberl, C. & Hames, W. E. (2002). Shallow-marine impact origin of the Wetumpka structure (Alabama, USA). *Earth and Planetary Science Letters*, *202*(3-4), 541–549. doi:10.1016/S0012-821X(02)00803-8

King, D. T., Ormö, J., Petruny, L. W. & Neathery, T. L. (2006). Role of water in the formation of the Late Cretaceous Wetumpka impact structure, inner Gulf Coastal Plain of Alabama, USA. *Meteoritics & Planetary Science*, *41*(10), 1625–1631. doi:10.1111/j.1945-5100.2006.tb00440.x

Kite, E. S., Rafkin, S., Michaels, T. I., Dietrich, W. E. & Manga, M. (2011). Chaos terrain, storms, and past climate on Mars. *Journal of Geophysical Research: Planets*, *116*(10), E10002. doi:10.1029/2010JE003792

Kleinhans, M. G. (2005a). Flow discharge and sediment transport models for estimating a minimum timescale of hydrological activity and channel and delta formation on Mars. *Journal of Geophysical Research: Planets*, *110*(12), E12003. doi:10.1029/2005JE002521

Kleinhans, M. G. (2005b). Autogenic cyclicity of foreset sorting in experimental Gilbert-type deltas. *Sedimentary Geology*, *181*(3-4), 215–224. doi:10.1016/j.sedgeo.2005.09.001

Kleinhans, M. G., Hauber, E. & van de Kasteele, H. E. (2010a). Palaeoflow reconstruction from fan delta morphology on Mars. *Earth and Planetary Science Letters*, *294*(3-4), 378–392. doi:10.1016/j.epsl.2009.11.025

Kleinhans, M. G., van Dijk, W. M., van de Lageweg, W. I., Hoendervoogt, R., Markies, H. & Schuurman, F. (2010b). From nature to lab : scaling self-formed meandering and braided rivers. In *Proceedings of the River Flow 2010 Conference*. Braunschweig, Germany.

Kleinhans, M. G., Markies, H., de Vet, S. J., Veld, A. C. & Postema, F. N. (2011). Static and dynamic angles of repose in loose granular materials under reduced gravity. *Journal of Geophysical Research: Planets*, *116*(November), 1–13. doi:10.1029/2011JE003865

Kleinhans, M. G. & van Rijn, L. C. (2002). Stochastic Prediction of Sediment Transport in Sand-Gravel Bed Rivers. *Journal of Hydraulic Engineering*, *128*(4), 412–425.

Kodama, Y. (1994). Downstream Changes in the Lithology and Grain Size of Fluvial Gravels, The Watarase River, Japan: Evidence of the Role of Abrasion in the Downstream Fining. *Journal of Sedimentary Research*, *64*(1), 68–75.

Komar, P. D. (1979). Comparisons of the hydraulics of water flows in Martian outflow channels with flows of similar scale on earth. *Icarus*, *37*(1), 156–181. doi:10.1016/0019-1035(79)90123-4

Koster, E. H. (1978). Transverse ribs: their characteristic, origin, and paleohydraulic significance. In A. D. Miall (Ed.), *Fluvial Sedimentology* (pp. 161–186). Canadian Society of Petroleum Geologists, Memoir 5.

Kraal, E. R., Asphaug, E., Moore, J. M., Howard, A. D. & Bredt, A. (2008a). Catalogue of large alluvial fans in martian impact craters. *Icarus*, *194*(1), 101–110. doi:10.1016/j.icarus.2007.09.028

Kraal, E. R., van Dijk, M., Postma, G. & Kleinhans, M. G. (2008b). Martian stepped-delta formation by rapid water release. *Nature*, *451*, 973–6. doi:10.1038/nature06615

Kraal, E. R., Asphaug, E., Moore, J. M. & Lorenz, R. D. (2006). Quantitative geomorphic modeling of Martian bedrock shorelines. *Journal of Geophysical Research: Planets*, *111*(3), 1–13. doi:10.1029/2005JE002567

Kring, D. A. (2005). Hypervelocity collisions into continental crust composed of sediments and an underlying crystalline basement: comparing the Ries (□24km) and Chicxulub (□180km) impact craters. *Chemie der Erde - Geochemistry*, *65*(1), 1–46. doi:10.1016/j.chemer.2004.10.003

Kuang, W., Jiang, W. & Wang, T. (2008). Sudden termination of Martian dynamo?: Implications from subcritical dynamo simulations. *Geophysical Research Letters*, *35*(14), L14204. doi:10.1029/2008GL034183

Lajeunesse, E., Malverti, L., Lancien, P., Armstrong, L., Mã‰Tivier, F., Coleman, S., … Parker, G. (2010). Fluvial and submarine morphodynamics of laminar and near-laminar flows: a synthesis. *Sedimentology*, *57*(1), 1–26. doi:10.1111/j.1365-3091.2009.01109.x

Lasue, J., Mangold, N., Hauber, E., Clifford, S., Feldman, W., Gasnault, O., … Mousis, O. (2012). Quantitative Assessments of the Martian Hydrosphere. *Space Science Reviews*, *174*(1-4), 155–212. doi:10.1007/s11214-012-9946-5

Lecce, S. A. (1990). The Alluvial Fan Problem. In A. H. Rachocki & M. Church (Eds.), *Alluvial Fans: A Field Approach* (pp. 3–24). John Wiley & Sons Ltd.

Lecce, S. A. (1991). Influence of lithologic erodibility on alluvial fan area, western white mountains, California and Nevada. *Earth Surface Processes and Landforms*, *16*(1), 11–18. doi:10.1002/esp.3290160103

Leeder, M. (1999). *Sedimentology and Sedimentary Basins. From Turbulence to Tectonics* (p. 592). Massachusetts: Blackwell Science.

Leier, A. L., DeCelles, P. G. & Pelletier, J. D. (2005). Mountains, monsoons, and megafans. *Geology*, *33*(4), 289. doi:10.1130/G21228.1

Leopold, L. B. & Wolman, M. G. (1957). *River Channel Patterns: Braided, Meandering and Straight*. *US Geological Survey Professional Paper 282-B* (p. 85). Washington.

Leshin, L. A. & Vicenzi, E. (2006). Aqueous Processes Recorded by Martian Meteorites: Analyzing Martian Water on Earth. *Elements*, *2*(3), 157–162. doi:10.2113/gselements.2.3.157

Leverington, D. W. (2004). Volcanic rilles, streamlined islands, and the origin of outflow channels on Mars. *Journal of Geophysical Research: Planets*, *109*(10), 1–14. doi:10.1029/2004JE002311

Leverington, D. W. (2006). Volcanic processes as alternative mechanisms of landform development at a candidate crater-lake site near Tyrrhena Patera, Mars. *Journal of Geophysical Research: Planets*, *111*(11), E11002. doi:10.1029/2004JE002382

Leverington, D. W. (2011). A volcanic origin for the outflow channels of Mars: Key evidence and major implications. *Geomorphology*, *132*(3-4), 51–75. doi:10.1016/j.geomorph.2011.05.022

Leverington, D. W. & Maxwell, T. A. (2004). An igneous origin for features of a candidate crater-lake system in western Memnonia, Mars. *Journal of Geophysical Research: Planets*, *109*(6), 1–17. doi:10.1029/2004JE002237

Lewis, K. W. & Aharonson, O. (2006). Stratigraphic analysis of the distributary fan in Eberswalde crater using stereo imagery. *Journal of Geophysical Research: Planets*, *111*(6), 1–7. doi:10.1029/2005JE002558

Lillis, R. J., Frey, H. V. & Manga, M. (2008). Rapid decrease in Martian crustal magnetization in the Noachian era: Implications for the dynamo and climate of early Mars. *Geophysical Research Letters*, *35*(14), L14203. doi:10.1029/2008GL034338

Lillisand, T. M., Kiefer, R. W. & Chipman, J. W. (2007). *Remote Sensing and Image Interpretation* (6th ed.). New York: John Wiley & Sons.

Lindström, M., Sturkell, E. F. F., Ormö, J. & Törnberg, R. (1996). The Lockne Marine Impact in the Ordovician of Central Sweden. *Geologiska Föreningens Förhandlingar*, *118*, 193–206.

Lowey, G. W. (2002). Sedimentary processes of the Kusawa Lake torrent system, Yukon, Canada, as revealed by the September 16, 1982 flood event. *Sedimentary Geology*, *151*, 293–312.

Luo, W. & Stepinski, T. F. (2009). Computer-generated global map of valley networks on Mars. *Journal of Geophysical Research: Planets*, *114*(11), 1–11. doi:10.1029/2009JE003357

Lustig, L. K. (1965). Clastic sedimentation in Deep Springs Valley, California. *Erosion and sedimentation in a semiarid environment*, *352-F*, 131–192.

Mahaffy, P. R., Webster, C. R., Atreya, S. K., Franz, H., Wong, M., Conrad, P. G., … Trainer, M. (2013). Abundance and isotopic composition of gases in the martian atmosphere from the Curiosity rover. *Science (New York, N.Y.)*, *341*, 263–6. doi:10.1126/science.1237966

Major, J. J. (1997). Depositional processes in large-scale debris-flow experiments. *Journal of Geology*, *105*, 345–366.

Major, J. J. (1998). Pebble orientation on large, experimental debris-flow deposits. *Sedimentary Geology*, *117*, 151–164.

Malin, M. C., Danielson, G. E., Ingersoll, A. P., Masursky, H., Veverka, J., Ravine, M. A. & Soulanille, T. A. (1992). Mars Observer Camera. *Journal of Geophysical Research*, *97*(5), 7699–7718.

Malin, M. C. & Edgett, K. S. (1999). Oceans or seas in the Martian northern lowlands: High resolution imaging tests of proposed coastlines. *Geophysical Research Letters*, *26*(19), 3049–3052. doi:10.1029/1999GL002342

Malin, M. C. & Edgett, K. S. (2000). Evidence for Recent Groundwater Seepage and Surface Runoff on Mars. *Science (New York, N.Y.)*, *288*, 2330–5. doi:10.1126/science.288.5475.2330

Malin, M. C. & Edgett, K. S. (2003). Evidence for persistent flow and aqueous sedimentation on early Mars. *Science (New York, N.Y.), 302*, 1931–1934. doi:10.1126/science.1090544

Malin, M. C., Edgett, K. S., Cantor, B. A., Caplinger, M. A., Danielson, G. E., Jensen, E. H., … Supulver, K. D. (2010). An overview of the 1985-2006 Mars Orbiter Camera science investigation. *The Mars Journal*, *5*, 1–60. doi:10.1555/mars.2010.0001

Mangold, N., Kite, E. S., Kleinhans, M. G., Newsom, H., Ansan, V., Hauber, E., … Tanaka, K. (2012). The origin and timing of fluvial activity at Eberswalde crater, Mars. *Icarus*, *220*(2), 530–551. doi:10.1016/j.icarus.2012.05.026

Masursky, H., Boyce, J. M., Dial, A. L., Schaber, G. G. & Strobell, M. E. (1977). Classification and Time of Formation of Martian Channels Based on Viking Data. *Journal of Geophysical Research*, *82*(28), 4016–4038.

Matsubara, Y., Howard, A. D. & Drummond, S. A. (2011). Hydrology of early Mars: Lake basins. *Journal of Geophysical Research: Planets*, *116*(4), E04001. doi:10.1029/2010JE003739

McCarthy, T. S. (1993). The great inland deltas of Africa. *Journal of African Earth Sciences*, *17*(3), 275–291. doi:10.1016/0899-5362(93)90073-Y

McCully, P. (1996). *Silenced Rivers: The Ecology and Politics of Large Dams* (p. 350). London: Zed Books.

McEwen, A. S., Keszthelyi, L. P. & Grant, J. A. (2012). Have there been large, recent (mid-late Amazonian) water floods on Mars? In *Lunar and Planetary Science Conference Abstracts* (Vol. 85721).

McEwen, A. S., Ojha, L., Dundas, C. M., Mattson, S. S., Byrne, S., Wray, J. J., … Gulick, V. C. (2011). Seasonal flows on warm Martian slopes. *Science (New York, N.Y.), 333*, 740–3. doi:10.1126/science.1204816

McGill, G. E. & Squyres, S. W. (1991). Origin of the Martian crustal dichotomy: Evaluating hypotheses. *Icarus*, *93*(2), 386–393. doi:10.1016/0019-1035(91)90221-E

McGill, G. E. (2002). Geologic map transecting the highland/lowland boundary zone, Arabia Terra, Mars: Quadrangles 30332, 35332, 40332, and 45332, scale 1:1M. *United States Geological Survey* Geologic Investigations Series Map I-2736.

McMenamin, D. S. & McGill, G. E. (2005). Processes involved in the formation of martian fan-shaped deposits. In *Lunar and Planetary Science Conference Abstracts*.

McPherson, J. G., Shanmugam, G. & Moiola, R. J. (1987). Fan-deltas and braid deltas: varieties of coarse-grained deltas. *Geological Society of America Bulletin*, *99*, 331–340.

McSween, H. Y. (2006). Water on Mars. *Elements*, *2*(3), 135–137. doi:10.2113/gselements.2.3.135

Mellon, M. T. & Phillips, R. J. (2001). Recent gullies on Mars and the source of liquid water. *Journal of Geophysical Research: Planets*, *106*(10), 23165–23179. doi:10.1029/2000JE001424

Melosh, H. J. (1980). Cratering Mechanics-Observational, Experimental, and Theoretical. *Annual Review of Earth and Planetary Sciences*, *8*(1), 65–93. doi:10.1146/annurev.ea.08.050180.000433

Melosh, H. J. (1989). *Impact Cratering: A Geologic Process* (p. 245). New York: Oxford University Press.

Melosh, H. J. (2011). *Planetary Surface Processes* (p. 520). Cambridge University Press.

Melosh, H. J. & Vickery, A. M. (1989). Impact erosion of the primordial atmosphere of Mars. *Nature*, *338*, 487–489.

Meyer-Peter, E. & Müller, R. (1948). Formulas for Bed-Load Transport. In *Proceedings of the 2nd Meeting of the International Association for Hydraulic Structures Research* (pp. 39–64).

Miall, A.D. (1985). Architectural-element analysis: a new method of facies analysis applied to fluvial deposits. *Earth Science Reviews*, 22, 261-308.

Milana, J. P. (2010). The sieve lobe paradigm: observations of active deposition. *Geology*, *38*, 207–210.

Miller, A. (1976). The Climate of Chile. In W. Schwerdtfeger (Ed.), *Climates of Central and South America* (pp. 113–145). Elsevier Ltd.

Molina-Cuberos, G. (2001). Cosmic Ray and UV Radiation Models on the Ancient Martian Surface. *Icarus*, *154*(1), 216–222. doi:10.1006/icar.2001.6658

Moore, D. (1966). Deltaic Sedimentation. *Earth Science Reviews*, *1*(2-3), 87–104.

Moore, J. M. & Howard, A. D. (2005). Large alluvial fans on Mars. *Journal of Geophysical Research: Planets*, *110*(4), 1–24. doi:10.1029/2004JE002352

Moore, J. M., Howard, A. D., Dietrich, W. E. & Schenk, P. M. (2003). Martian Layered Fluvial Deposits: Implications for Noachian Climate Scenarios. *Geophysical Research Letters*, *30*(24), 2292–2295. doi:10.1029/2003GL019002

Mortimer, C. & Saric, N. (1972). Landform evolution in the coastal region of Tarapaca Province. *Revue de Geómorphologie Dynamique*, *21*, 162–170.

Moscariello, A. (2005). Exploration potential of the mature Southern North Sea basin margins: some unconventional plays based on alluvial and fluvial fan sedimentation models. In A. G. Doré & B. A. Vining (Eds.), *Petroleum Geology: Northwest Europe and Global Perspectives - Proceedings of the 6th Petroleum Geology Conference* (pp. 595–605). Geological Society, London.

Moscariello, A., Marchi, L., Maraga, F. & Mortara, G. (2002). Alluvial fans in the Italian Alps : sedimentary facies and processes. In I. P. Martini, V. R. Baker, & G. Garzón (Eds.), *Flood and Megaflood Processes and Deposits: Recent and Ancient Examples* (pp. 141–166). IAS Special Publication 32.

Mustard, J. F. (2002). A wet and altered Mars. *Nature*, *417*(May), 5–6.

Muto, T. & Steel, R. J. (1992). Retreat of the front in a prograding delta. *Geology*, *20*(11), 967–970. doi:10.1130/0091-7613(1992)020<0967:ROTFIA>2.3.CO;2

Muto, T. & Steel, R. J. (1997). Principles of regression and transgression : the nature of the interplay between accommodation and sediment supply. *Journal of Sedimentary Research*, *67*(6), 994–1000.

Muto, T. & Steel, R. J. (2001). Autostepping during the transgressive growth of deltas: Results from flume experiments. *Geology*, *29*(9), 771–774. doi:10.1130/0091-7613(2001)029<0771:ADTTGO>2.0.CO;2

Muto, T. & Steel, R. J. (2004). Autogenic response of fluvial deltas to steady sea-level fall: Implications from flume-tank experiments. *Geology*, *32*(5), 401–404. doi:10.1130/G20269.1

Naylor, M. A. (1980). The origin of inverse grading in muddy debris flow deposits - a review. *Journal of Sedimentary Petrology*, *50*, 1111–1116.

Nemec, W. & Muszynsky. (1982). Volcaniclastic alluvial aprons in the Tertiary Sofia District (Bulgaria). *Annales Societatis Geologorum Poloniae*, *52*, 239–303.

Nemec, W. & Postma, G. (1993). Quaternary alluvial fans in southwestern Crete: sedimentation processes and geomorphic evolution. *Alluvial sedimentation*, 235–276.

Nemec, W. & Steel, R. J. (1984). Alluvial and coastal conglomerates: their significant features and some comments on gravelly mass-flow deposits. In E. H. Koster & R. J. Steel (Eds.), *Sedimentology of Gravels and Conglomerates* (pp. 1–31). Canadian Society of Petroleum Geologists Memoir 10.

Nemec, W. & Steel, R. J. (1988). *Fan Deltas - Sedimentology and Tectonic Settings* (p. 444). Glasgow: Blackie.

Neukum, G., Jaumann, R. & the HRSC Co-Investigator and Experiment Team. (2004b). *HRSC: the High Resolution Stereo Camera of Mars Express*. (A. Wilson & A. Chicarro, Eds.)*Mars Express - The Scientific Payload* (pp. 17–35). Noordwijk, The Netherlands: ESA Special Publication.

Neukum, G., Jaumann, R., Hoffmann, H., Hauber, E., Head, J. W., Basilevsky, A. T., … McCord, T. B. (2004a). Recent and episodic volcanic and glacial activity on Mars revealed by the High Resolution Stereo Camera. *Nature*, *432*, 971–9. doi:10.1038/nature03231

Nichols, G. J. & Fisher, J. (2007). Processes, facies and architecture of fluvial distributary system deposits. *Sedimentary Geology*, *195*(1-2), 75–90. doi:10.1016/j.sedgeo.2006.07.004

Nichols, G. J. & Hirst, J. P. (1998). Alluvial fans and fluvial distributary systems, Oligo-Miocene, northern Spain: contrasting processes and products. *Journal of Sedimentary Research*, *68*, 879–889.

Nichols, G. J. & Thompson, B. (2005). Bedrock lithology control on contemporaneous alluvial fan facies, Oligo-Miocene, southern Pyrenees, Spain. *Sedimentology*, *52*(3), 571–585. doi:10.1111/j.1365-3091.2005.00711.x

Nishiizumi, K., Caffee, M. W., Finkel, R. C., Brimhall, G. & Mote, T. (2005). Remnants of a fossil alluvial fan landscape of Miocene age in the Atacama Desert of northern Chile using cosmogenic nuclide exposure age dating. *Earth and Planetary Science Letters*, *237*, 499–507.

Nummedal, D. & Prior, D. B. (1981). Generation of Martian chaos and channels by debris flows. *Icarus*, *45*(1), 77–86. doi:10.1016/0019-1035(81)90007-5

Ori, G.G. (1982). Braided to meandering channel patterns in humid-region alluvial fan deposits, River Reno, Po Plain (northern Italy). *Sedimentary Geology*, 31, 231-248.

Ori, G. G., Marinangeli, L. & Baliva, A. (2000). Terraces and Gilbert-type deltas in crater lakes in Ismenius Lacus and Memnonia (Mars). *Journal of Geophysical Research: Planets*, *105*(7), 17629–17641. doi:10.1029/1999JE001219

Ormö, J., Dohm, J. M., Ferris, J. C., Lepinette, A. & Fairén, A. G. (2004). Marine-target craters on Mars? An assessment study. *Meteoritics & Planetary Science*, *39*(2), 333–346. doi:10.1111/j.1945-5100.2004.tb00344.x

Ormö, J. & Lindström, M. (2000). When a cosmic impact strikes the sea bed. *Geological Magazine*, *137*(1), 67–80. doi:10.1017/S0016756800003538

Ormö, J. & Muinonen, P. (2000). Impact Craters as Indicators for Oceanic Phases on Mars. In *LPSC*.

Ormö, J., Shuvalov, V. V. & Lindström, M. (2002). Numerical modeling for target water depth estimation of marine-target impact craters. *Journal of Geophysical Research: Planets*, *107*(12), 5120. doi:10.1029/2002JE001865

Ormö, J., Sturkell, E. F. F. & Lindström, M. (2007). Sedimentological analysis of resurge deposits at the Lockne and Tvären craters: Clues to flow dynamics. *Meteoritics & Planetary Science*, *42*(11), 1929–1943. doi:10.1111/j.1945-5100.2007.tb00551.x

Orofino, V., Goldspiel, J. M., Carofalo, I., Blanco, A., Fonti, S. & Marzo, G. A. (2009). Evaluation of carbonate abundance in putative martian paleolake basins. *Icarus*, *200*(2), 426–435. doi:10.1016/j.icarus.2008.11.020

Orton, G. J. & Reading, H. G. (1993). Variability of deltaic processes in terms of sediment supply, with particular emphasis on grain size. *Sedimentology*, *40*(3), 475–512.

Paige, D. A. (2005). Ancient Mars: wet in many places. *Science (New York, N.Y.)*, *307*(5715), 1575–6. doi:10.1126/science.1110530

Paola, C. (2000). Quantitative models of sedimentary basin filling. *Sedimentology*, *47*, 121–178. doi:10.1046/j.1365-3091.2000.00006.x

Paola, C., Straub, K. M., Mohrig, D. & Reinhardt, L. (2009). The "unreasonable effectiveness" of stratigraphic and geomorphic experiments. *Earth-Science Reviews*, *97*(1-4), 1–43. doi:10.1016/j.earscirev.2009.05.003

Parker, G. (1999). Progress in the modeling of alluvial fans. *Journal of Hydraulic Research*, *37*, 805–825.

Parker, T. J. & Currey, D. R. (2001). Extraterrestrial coastal geomorphology. *Geomorphology*, *37*(3-4), 303–328. doi:10.1016/S0169-555X(00)00089-1

Parker, T. J., Gorsline, D. S., Saunders, R. S., Pieri, D. C. & Schneeberger, D. M. (1993). Coastal geomorphology of the Martian northern plains. *Journal of Geophysical Research: Planets*, *98*(6), 11061–11078. doi:10.1029/93JE00618

Parker, T. J., Saunders, R. S. & Schneeberger, D. M. (1989). Transitional morphology in the west Deuteronilus Mensae region of Mars: Implications for modification of the lowland/upland boundary. *Icarus*, *82*, 111–145.

Parsons, R. A. & Nimmo, F. (2010). Numerical modeling of Martian gully sediment transport: Testing the fluvial hypothesis. *Journal of Geophysical Research: Planets*, *115*(6), 1–13. doi:10.1029/2009JE003517

Pérez, F. L. (2001). Matrix granulometry of catastrophic debris flows (December 1999) in central coastal Venezuela. *Catena*, *45*, 163–183.

Perron, J. T., Mitrovica, J. X., Manga, M., Matsuyama, I. & Richards, M. A. (2007). Evidence for an ancient martian ocean in the topography of deformed shorelines. *Nature*, *447*(7146), 840–3. doi:10.1038/nature05873

Pieri, D. C. (1980). Geomorphology of Valleys on Mars: A summary of morphology, distribution, age and origin. *Science (New York, N.Y.), 210*(4472), 895–897.

Pierson, T. C. (1986). Flow behavior of channelized debris flows, Mount St. Helens, Washington. In A. D. Abrahams (Ed.), *Hillslope Processes* (pp. 269–296). Allen & Unwin.

Plaut, J. J., Picardi, G., Safaeinili, A., Ivanov, A. B., Milkovich, S. M., Cicchetti, A., … Edenhofer, P. (2007). Subsurface radar sounding of the south polar layered deposits of Mars. *Science (New York, N.Y.), 316*, 92–5. doi:10.1126/science.1139672

Poag, C. W. (1997). The Chesapeake Bay bolide impact: a convulsive event in Atlantic Coastal Plain evolution. *Sedimentary Geology*, *108*(1-4), 45–90. doi:10.1016/S0037-0738(96)00048-6

Pondrelli, M., Rossi, a. P., Platz, T., Ivanov, a., Marinangeli, L. & Baliva, a. (2011). Geological, geomorphological, facies and allostratigraphic maps of the Eberswalde fan delta. *Planetary and Space Science*, *59*(11-12), 1166–1178. doi:10.1016/j.pss.2010.10.009

Pondrelli, M., Rossi, A. P., Marinangeli, L., Hauber, E., Gwinner, K., Baliva, A. & Di Lorenzo, S. (2008). Evolution and depositional environments of the Eberswalde fan delta, Mars. *Icarus*, *197*(2), 429–451. doi:10.1016/j.icarus.2008.05.018

Porebski, S. J. & Steel, R. J. (2006). Deltas and Sea-Level Change. *Journal of Sedimentary Research*, *76*(3), 390–403. doi:10.2110/jsr.2006.034

Posamentier, H. W., Jervey, M. T. & Vail, P. R. (1988). Eustatic controls on clastic deposition I—conceptual framework. *Soc. Econ. Paleontol. Mineral*, (42), 109–124.

Postma, G. (1990). Depositional architecture and facies of river and fan deltas: a synthesis. In A. Colella & D. B. Prior (Eds.), *Coarse-Grained Deltas: Special Publication 10 of the IAS* (pp. 13–27).

Postma, G. (1995). Sea-level-related architectural trends in coarse-grained delta complexes. *Sedimentary Geology*, *98*(1-4), 3–12. doi:10.1016/0037-0738(95)00024-3

Postma, G. (2001). Physical climate signatures in shallow- and deep-water deltas. *Global and Planetary Change*, *28*(1-4), 93–106. doi:10.1016/S0921-8181(00)00067-9

Postma, G., Kleinhans, M. G., Meijer, P. T. & Eggenhuisen, J. T. (2008). Sediment transport in analogue flume models compared with real-world sedimentary systems: a new look at scaling evolution of sedimentary systems in a flume. *Sedimentology*, *55*(6), 1541–1557. doi:10.1111/j.1365-3091.2008.00956.x

Postma, G. & Kraal, E. R. (2007). Alternative origin for the point bars of the Martian Eberswalde delta. In *European Mars Science and Exploration Conference*.

Poulet, F., Bibring, J.-P., Mustard, J. F., Gendrin, A., Mangold, N., Langevin, Y., … Forget, F. (2005). Phyllosilicates on Mars and implications for early martian climate. *Nature*, *438*, 623–7. doi:10.1038/nature04274

Pratson, L., Swenson, J., Kettner, A., Fedele, J., Postma, G., Niedoroda, A., … Das, H. (2004). Modeling Continental Shelf Formation in the Adriatic Sea and Elsewhere. *Oceanography*, *17*(4), 118–131. doi:10.5670/oceanog.2004.09

Rachocki, A. H. (1981). *Alluvial Fans : An Attempt at an Empirical Approach*. *Earth Surface Processes and Landforms* (Vol. 7, pp. 162–172). John Wiley & Sons. doi:10.1002/esp.3290070312

Radebaugh, J., Lorenz, R. D., Lunine, J. I., Wall, S. D., Boubin, G., Reffet, E., … Spencer, C. (2008). Dunes on Titan observed by Cassini Radar. *Icarus*, *194*, 690–703.

Radebaugh, J., Lorenz, R. D., Wall, S. D., Kirk, R. L., Wood, C. A., Lunine, J. I., … West, R. D. (2011). Regional geomorphology and history of Titan's Xanadu province. *Icarus*, *211*, 672–685.

Reading, H. G. & Levell, B. K. (1996). Controls on the sedimentary rock record. In H. G. Reading (Ed.), *Sedimentary Environments: Processes, facies and stratigraphy* (3rd ed., p. 688). Cambridge: University Press.

Rech, J. a., Currie, B. S., Michalski, G. & Cowan, A. M. (2006). Neogene climate change and uplift in the Atacama Desert, Chile. *Geology*, *34*(9), 761. doi:10.1130/G22444.1

Rees, A. I. (1968). The production of preferred orientation in a concentrated dispersion of elongated and flattened grains. *Journal of Geology*, *76*, 457–465.

Reitz, M. D. & Jerolmack, D. J. (2012). Experimental alluvial fan evolution: Channel dynamics, slope controls, and shoreline growth. *Journal of Geophysical Research: Earth surface*, *117*(2), F02021. doi:10.1029/2011JF002261

Rickenmann, D. (1999). Empirical Relationships for Debris Flows. *Natural Hazards*, *19*, 47–77.

Ritchie, B. D., Gawthorpe, R. L. & Hardy, S. (2004). Three-Dimensional Numerical Modeling of Deltaic Depositional Sequences 1: Influence of the Rate and Magnitude of Sea-Level Change. *Journal of Sedimentary Research*, *74*(2), 203–220. doi:10.1306/091303740203

Rodríguez López, J. P., de Villiers, G., Melendez, N., Soria, A. R. & de Boer, P. L. (n.d.). Multiannual changes in coastal and interior dune fields in Baluchistan (Pakistan) analysed using Google Earth (in preparation).

Russell, C. T. (1978). The magnetic field of Mars: Mars 3 evidence reexamined. *Geophysical Research Letters*, *5*(1), 81–84. doi:10.1029/GL005i001p00081

Sagan, C., Veverka, J., Fox, P., Dubisch, R., French, R., Gierasch, P., … Pollack, J. B. (1973). Variable features on Mars, 2, Mariner 9 global results. *Journal of Geophysical Research*, *78*(20), 4163–4196. doi:10.1029/JB078i020p04163

Schon, S. C. & Head, J. W. (2011). Keys to gully formation processes on Mars: Relation to climate cycles and sources of meltwater. *Icarus*, *213*(1), 428–432. doi:10.1016/j.icarus.2011.02.020

Schon, S. C., Head, J. W. & Fassett, C. I. (2009). Unique chronostratigraphic marker in depositional fan stratigraphy on Mars: Evidence for ca. 1.25 Ma gully activity and surficial meltwater origin. *Geology*, *37*(3), 207–210. doi:10.1130/G25398A.1

Schon, S. C., Head, J. W. & Fassett, C. I. (2012). An overfilled lacustrine system and progradational delta in Jezero crater, Mars: Implications for Noachian climate. *Planetary and Space Science*, *67*(1), 28–45. doi:10.1016/j.pss.2012.02.003

Schorghofer, N. (2007). Dynamics of ice ages on Mars. *Nature*, *449*(7159), 192–194. doi:10.1038/nature06082

Schumacher, S. & Zegers, T.E. (2011). Aram Chaos and its constraints on the surface heat flux of Mars. *Icarus*, 211, 305-315.

Schumm, S. A. (1987). Alluvial Fans. In S. A. Schumm, M. P. Mosley, & W. E. Weaver (Eds.), *Experimental Fluvial Geomorphology* (p. 413). New York: Wiley & Sons.

Scott, W. E. (1989). Volcanic and Related Hazard. In *US Geological Survey (USGS)* (pp. 9–23). American Geophysical Union. doi:10.1029/SC001p0009

Segura, T. L., McKay, C. P. & Toon, O. B. (2012). An impact-induced, stable, runaway climate on Mars. *Icarus*, *220*(1), 144–148. doi:10.1016/j.icarus.2012.04.013

Segura, T. L., Toon, O. B. & Colaprete, A. (2008). Modeling the environmental effects of moderate-sized impacts on Mars. *Journal of Geophysical Research: Planets*, *113*(11), E11007. doi:10.1029/2008JE003147

Selby, M. J. (1982). *Hillslope materials and processes* (p. 466). Oxford, UK: Oxford University Press.

Senft, L. E. & Stewart, S. T. (2007). Modeling impact cratering in layered surfaces. *Journal of Geophysical Research: Planets*, *112*(11), 1–18. doi:10.1029/2007JE002894

Sharp, R. P. (1942). Mudflow levees. *Journal of Geomorphology*, *5*, 222–227.

Sharp, R. P. (1973). Mars: Fretted and chaotic terrains. *Journal of geophysical research*, *78*(20), 4073–4083.

Sharp, R. P. & Malin, M. C. (1975). Channels on Mars. *Geological Society Of America Bulletin*, *86*(5), 593–609. doi:10.1130/0016-7606(1975)86<593

Sharp, R. P. & Nobles, L. H. (1953). Mudflow of 1941 at Wrightwood, Southern California. *Geological Society of America Bulletin*, *64*(5), 547–560. doi:10.1130/0016-7606(1953)64[547:MOAWSC]2.0.CO;2

Shinbrot, T., Duong, N.-H., Kwan, L. & Alvarez, M. M. (2004). Dry granular flows can generate surface features resembling those seen in Martian gullies. *Proceedings of the National Academy of Sciences of the United States of America*, *101*(23), 8542–6. doi:10.1073/pnas.0308251101

Shuster, D. & Weiss, B. (2005). Martian surface paleotemperatures from thermochronology of meterorites. *Science*, 309, 594-597.

Shuvalov, V. V. & Trubestkaya, I. A. (2002). Numerical Modeling of Marine Target Impacts, *36*(5), 450–463.

Sletten, K., Blikra, L. H., Ballantyne, C. K., Nesje, A. & Dahl, S. O. (2003). Holocene debris flows recognized in a lacustrine sedimentary succession: sedimentology, chronostratigraphy, and cause of triggering. *The Holocene*, *13*, 907–920.

Smart, G. M. (1984). Sediment Transport Formula for Steep Channels. *Journal of Hydraulic Engineering*, *110*(3), 267–276. doi:10.1061/(ASCE)0733-9429(1984)110:3(267)

Smith, D. E., Zuber, M. T., Frey, H. V., Garvin, J. B., Head, J. W., Muhleman, D. O., … Sun, X. (2001). Mars Orbiter Laser Altimeter: Experiment summary after the first year of global mapping of Mars. *Journal of Geophysical Research*, *106*(23), 689–722.

Smith, G. A. (2000). Recognition and significance of streamflow-dominated piedmont facies in extensional basins. *Basin Research*, *12*, 399–411.

Sobron, P., Lefebvre, C., Leveille, R., Koujelev, A., Haltigin, T., Du, H., … Craft, J. (2013). Geochemical profile of a layered outcrop in the Atacama analogue using laser-induced breakdown spectroscopy: Implications for Curiosity investigations in Gale. *Geophysical Research Letters*, *40*(10), 1965–1970. doi:10.1002/grl.50261

Solomon, S. C., Aharonson, O., Aurnou, J. M., Banerdt, W. B., Carr, M. H., Dombard, A. J., … Zuber, M. T. (2005). New perspectives on ancient Mars. *Science (New York, N.Y.), 307*, 1214–1220. doi:10.1126/science.1101812

Sonett, C. P., Pearce, S. J. & Gault, D. E. (1991). The oceanic impact of large objects. *Advances in Space Research*, *11*(6), 77–86. doi:10.1016/0273-1177(91)90234-B

Squyres, S. W., Grotzinger, J. P., Arvidson, R. E., Bell, J. F., Calvin, W. M., Christensen, P. R., … Soderblom, L. A. (2004). In situ evidence for an ancient aqueous environment at Meridiani Planum, Mars. *Science (New York, N.Y.), 306*, 1709–14. doi:10.1126/science.1104559

Stanistreet, I. G. & McCarthy, T. S. (1993). The Okavango Fan and the classification of subaerial fan systems. *Sedimentary Geology*, *85*, 115–133.

Stewart, S. T. & Nimmo, F. (2002). Surface runoff features on Mars: Testing the carbon dioxide formation hypothesis. *Journal of Geophysical Research: Planets*, *107*(9), 5069. doi:10.1029/2000JE001465

Stewart, S. T. & Valiant, G. J. (2006). Martian subsurface properties and crater formation processes inferred from fresh impact crater geometries. *Meteoritics & Planetary Science*, *41*(10), 1509–1537. doi:10.1111/j.1945-5100.2006.tb00433.x

Sun, T., Paola, C., Parker, G. & Meakin, P. (2002). Fluvial fan deltas: Linking channel processes with large-scale morphodynamics. *Water Resources Research*, *38*(8), 26–1–26–10. doi:10.1029/2001WR000284

Tanaka, K. L. (1986). The stratigraphy of Mars. *Journal of Geophysical Research: Solid Earth*, *91*(13), E139–E158. doi:10.1029/JB091iB13p0E139

Tanaka, K. L. (1999). Debris-flow origin for the Simud/Tiu deposit on Mars. *Journal of Geophysical Research: Planets*, *104*(4), 8637–8652. doi:10.1029/98JE02552

Tanaka, K. L., Skinner, J. A. & Hare, T. M. (2005). Geologic Map of the Northern Plains of Mars - Scientific Investigations Map 2888.

Todd, S. P. (1989). Stream-driven, high-density gravelly traction carpets: possible deposits in the Trabeg Conglomerate Formation, SW Ireland and some theoretical considerations of their origin. *Sedimentology*, *36*, 513–530.

Todd, S. P. (1996). Process Deduction from Fluvial Sedimentary Structures. In P. A. Carling & M. R. Dawson (Eds.), *Advances in Fluvial Dynamics and Stratigraphy* (pp. 299–350). John Wiley & Sons Ltd.

Toon, O. B., Segura, T. L. & Zahnle, K. (2010). The Formation of Martian River Valleys by Impacts. *Annual Review of Earth and Planetary Sciences*, *38*(1), 303–322. doi:10.1146/annurev-earth-040809-152354

Tsikalas, F., Gudlaugsson, S.T., Eldholm, O., and Faleide, J.I. (1998). Integrated geophysical analysis supporting the impact origin of the Mjølnir Structure, Barents Sea. *Tectonophysics*, 289, 257-280.

Tye, R. S. & Coleman, J. M. (1989). Depositional processes and stratigraphy of fluvially dominated lacustrine deltas; Mississippi delta plain. *Journal of Sedimentary Research*, *59*(6), 973–996.

Van den Berg van Saparoea, A. P. H. & Postma, G. (2008). Control of climate change on the yield of river systems. *SEPM, Special Publication*, *90*, 1–26.

Van der Straaten, H. C. (1990). Stacked Gilbert-type deltas in the marine pull-apart basin of Abaran, late Serravallian-early Tortonian, southeastern Spain. In A. Colella & D. B. Prior (Eds.), *Coarse-grained Deltas* (Vol. 10, pp. 199–222). International Association of Sedimentologists.

Van Dijk, M., Kleinhans, M. G., Postma, G. & Kraal, E. R. (2012). Contrasting morphodynamics in alluvial fans and fan deltas: effect of the downstream boundary. *Sedimentology*, *59*(7), 2125–2145. doi:10.1111/j.1365-3091.2012.01337.x

Van Dijk, M., Postma, G. & Kleinhans, M. G. (2009). Autocyclic behaviour of fan deltas: an analogue experimental study. *Sedimentology*, *56*(5), 1569–1589. doi:10.1111/j.1365-3091.2008.01047.x

Van Heijst, M. W. I. M. & Postma, G. (2001). Fluvial response to sea-level changes: a quantitative analogue, experimental approach. *Basin Research*, *13*(3), 269–292. doi:10.1046/j.1365-2117.2001.00149.x

Van Heijst, M. W. I. M., Postma, G., Meijer, X. D., Snow, J. N. & Anderson, J. B. (2001). Quantitative analogue flume-model study of river shelf systems : principles and verification exemplified by the Late Quaternary Colorado river delta evolution. *Basin Research*, *13*, 243–268.

Van Rijn, L. (1984). Sediment transport, part III: bed forms and alluvial roughness. *Journal of Hydraulic Engineering*, *110*(12), 1733–1754.

Van Wagoner, J. C. V., Posamentier, H. W., Mitchum, R. M., Vail, P. R., Sarg, J. F., Loutit, T. S. & Hardenbol, J. A. N. (1988). An Overview of the Fundamentals of Sequence Stratigraphy and Key Definitions. In *Sea-Level Changes: An Integrated Approach*.

Vargas, G., Ortlieb, L. & Rutllant, J. (2000). Aluviones históricos en Antofagasta y su relación con eventos El Niño/Oscilación del Sur. *Revista Geológica de Chile*, *27*, 157–176.

Ventra, D. (2011). *Basement and climate controls on proximal depositional systems in continental settings*.PhD Dissertation, Utrecht University, ISBN: 978-90-6266-285-2

Ventra, D., Diaz, G. C. & de Boer, P. L. (2013). Colluvial sedimentation in a hyperarid setting (Atacama Desert, northern Chile): Geomorphic controls and stratigraphic facies variability. *Sedimentology*, *60*(5), 1257–1290. doi:10.1111/sed.12029

Ventra, D. & Nichols, G. J. (2013). Autogenic dynamics of alluvial fans in endorheic basins: outcrop examples and stratigraphic significance (in press). *Sedimentology*.

Volker, H. X., Wasklewicz, T. & Ellis, M. A. (2007). A topographic fingerprint to distinguish alluvial fan formative processes. *Geomorphology*, *88*(1-2), 34–45. doi:10.1016/j.geomorph.2006.10.008

Von Dalwigk, I. & Ormö, J. (2001). Formation of resurge gullies at impacts at sea: The Lockne crater, Sweden. *Meteoritics & Planetary Science*, *36*, 359–369.

Wasson, R. J. (1977). Last-glacial alluvial fan sedimentation in the Lower Derwent Valley, Tasmania. *Sedimentology*, *24*, 781–799.

Watters, T. R., Campbell, B. A., Carter, L. M., Leuschen, C. J., Plaut, J. J., Picardi, G., … Stofan, E. R. (2007). Radar sounding of the Medusae Fossae Formation Mars: equatorial ice or dry, low-density deposits? *Science*, *318*, 1125–8. doi:10.1126/science.1148112

Watters, T. R. & McGovern, P. J. (2006). Introduction to special section: The Hemispheric Dichotomy of Mars. *Geophysical Research Letters*, *33*(8). doi:10.1029/2006GL025755

Webb, J. A. & Fielding, C. R. (1999). Debris flow and sheetflood fans of the northern Prince Charles Mountains, East Antarctica. In A. J. Miller & A. Gupta (Eds.), *Varieties of Fluvial Form* (pp. 317–341). John Wiley & Sons.

Weissmann, G. S., Hartley, A. J., Nichols, G. J., Scuderi, L. A., Olson, M., Buehler, H. & Banteah, R. (2010). Fluvial form in modern continental sedimentary basins: Distributive fluvial systems. *Geology*, *38*(1), 39–42. doi:10.1130/G30242.1

Weitz, C. M., Irwin, R. P., Chuang, F. C., Bourke, M. C. & Crown, D. A. (2006). Formation of a terraced fan deposit in Coprates Catena, Mars. *Icarus*, *184*(2), 436–451. doi:10.1016/j.icarus.2006.05.024

Wells, S. G. & Dohrenwend, J. C. (1985). Relic sheetflood bed forms on late Quaternary alluvial-fan surfaces in the southwestern United States. *Geology*, *13*, 512–516.

Wells, S. G. & Harvey, A. M. (1987). Sedimentologic and geomorphic variations in storm-generated alluvial fans, Howgill Fells, northwest England. *Geological Society of America Bulletin*, *98*, 182–198.

Whipple, K. X. & Dunne, T. (1992). The influence of debris-flow rheology on fan morphology, Owens Valley, California. *Geological Society of America Bulletin*, *104*(March 2009), 887–900. doi:10.1130/0016-7606(1992)104<0887

Whipple, K. X., Parker, G., Paola, C. & Mohrig, D. (1998). Channel Dynamics, Sediment Transport, and the Slope of Alluvial Fans: Experimental Study. *The Journal of Geology*, *106*(6), 677–694. doi:10.1086/516053

Whiting, P. J., Dietrich, W. E., Leopold, L. E., Drake, T. G. & Shreve, R. L. (1988). Bedload sheets in heterogeneous sediment. *Geology*, *16*, 105–108.

Williams, R. M. E., Deanne Rogers, a., Chojnacki, M., Boyce, J. M., Seelos, K. D., Hardgrove, C. J. & Chuang, F. C. (2011). Evidence for episodic alluvial fan formation in far western Terra Tyrrhena, Mars. *Icarus*, *211*(1), 222–237. doi:10.1016/j.icarus.2010.10.001

Williams, R. M. E., Grotzinger, J. P., Dietrich, W. E., Gupta, S., Sumner, D. Y., Wiens, R. C., … Deen, R. G. (2013). Martian fluvial conglomerates at Gale crater. *Science (New York, N.Y.), 340*, 1068–72. doi:10.1126/science.1237317

Williams, R. M. E. & Malin, M. C. (2008). Sub-kilometer fans in Mojave Crater, Mars. *Icarus*, *198*(2), 365–383. doi:10.1016/j.icarus.2008.07.013

Williams, R. M. E., Zimbelman, J. R. & Johnston, A. K. (2006). Aspects of alluvial fan shape indicative of formation process: A case study in southwestern California with application to Mojave Crater fans on Mars. *Geophysical Research Letters*, *33*(10), 2–5. doi:10.1029/2005GL025618

Wilson, S. A., Grant, J. A. & Howard, A. D. (2013). INVENTORY OF EQUATORIAL ALLUVIAL FANS AND DELTAS ON MARS. In *Lunar and Planetary Science Conference Abstracts*. doi:10.1029/2011

Winsemann, J., Brandes, C. & Polom, U. (2011). Response of a proglacial delta to rapid high-amplitude lake-level change: an integration of outcrop data and high-resolution shear wave seismics. *Basin Research*, *23*(1), 22–52. doi:10.1111/j.1365-2117.2010.00465.x

Winsemann, J., Hornung, J. J., Meinsen, J., Asprion, U., Polom, U., Brandes, C., … Weber, C. (2009). Anatomy of a subaqueous ice-contact fan and delta complex, Middle Pleistocene, North-west Germany. *Sedimentology*, *56*(4), 1041–1076. doi:10.1111/j.1365-3091.2008.01018.x

Withers, P., Fallows, K., Girazian, Z., Matta, M., Häusler, B., Hinson, D., … Witasse, O. (2012). A clear view of the multifaceted dayside ionosphere of Mars. *Geophysical Research Letters*, *39*(18), n/a–n/a. doi:10.1029/2012GL053193

Wohl, E. & Rathburn, S. (2003). Mitigation of sedimentation hazards downstream from reservoirs. *International Journal of Sediment Research*, *18*(2), 97–106.

Wohletz, K. H. & Sheridant, M. F. (1983). Martian Rampart Crater Ejecta : Experiments and Analysis of Melt-Water Interaction ~, *37*, 15–37.

Wolman, M. G. & Miller, J. P. (1960). *Magnitude and Frequency of Forces in Geomorphic Processes*.

Wong, M. & Parker, G. (2006). Reanalysis and Correction of Bed-Load Relation of Meyer-Peter and Müller Using Their Own Database. *Journal of Hydraulic Engineering*, (November), 1159–1168.

Wood, L. J. (2005). Geomorphology of the Mars Northeast Holden Delta. *Search and Discovery*, *110027*.

Wright, L. D. & Coleman, J. M. (1973). Variations in Morphology of Major River Deltas as Functions of Ocean Wave and River Discharge Regimes. *AAPG Bulletin*, *57*(2), 370–398.

Wyatt, M. B. & McSween, H. Y. (2006). The Orbital Search for Altered Materials on Mars. *Elements*, *2*(3), 145–150. doi:10.2113/gselements.2.3.145

Yen, A. S., Gellert, R., Schröder, C., Morris, R. V., Bell, J. F., Knudson, A. T., … Zipfel, J. (2005). An integrated view of the chemistry and mineralogy of martian soils. *Nature*, *436*, 49–54. doi:10.1038/nature03637

Zegers, T.E., Oosthoek, J.H., Rossi, A.P., Blom, J.K. & Schumacher, S. (2010). Melt and collapse of buried water ice: An alternative hypothesis for the formation of chaotic terrains on Mars. *Earth and Planetary Science Letters*, 297, 496-504.

Zielinski, T. (2003). Catastrophic flood effects in alpine/foothill fluvial system (a case study from the Sudetes Mts, SW Poland). *Geomorphology*, *54*, 293–306.

Zimbelman, J. R. (1998). Emplacement of long lava flows on planetary surfaces. *Journal of Geophysical Research: Solid Earth*, *103*(11), 27503–27516. doi:10.1029/98JB01123

“It's a question of discipline,” the little prince told me later on, “when you’ve finished washing and dressing each morning, you must tend your planet. But sometimes, there is no harm in putting off a piece of work until another day.”

9 Appendix

Selected Retrograding Deltas:
Number and coordinates given above picture; basin name and diameter below.

#20: 12.0; 307.3 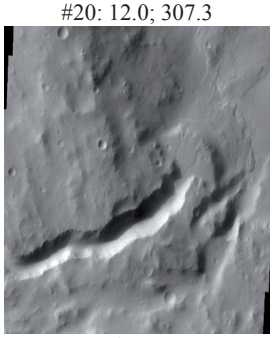 Subur; 42	#22: -15.7; 204.8 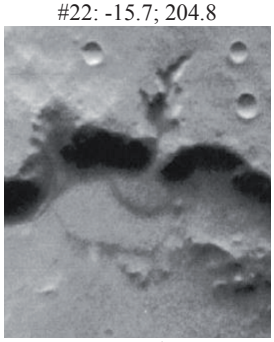 Unnamed; 39	#23: -8.6; 200.7 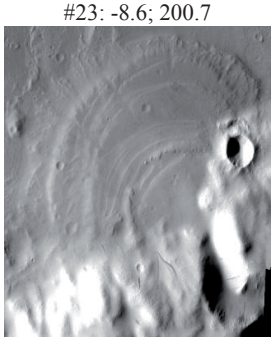 Unnamed; 72
#24: -8.0; 213.4 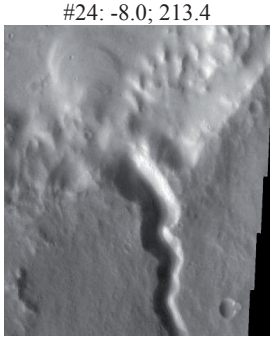 Unnamed; 33	#50: 8.2; 310.7 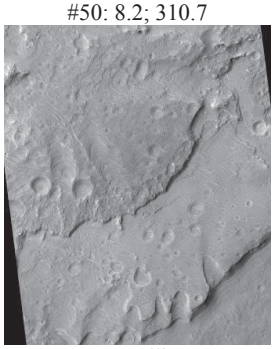 Tyras Vallis; 66	#52: 2.7; 308.3 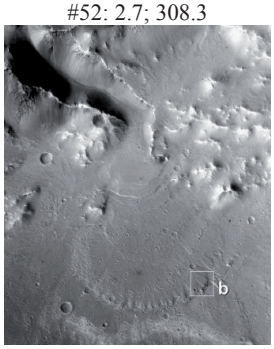 Unnamed; 63
#55: -15.0; 299.7 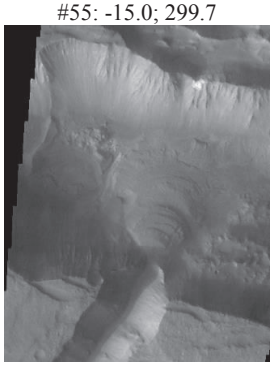 Coprates Catena	#61: -10.9; 306.6 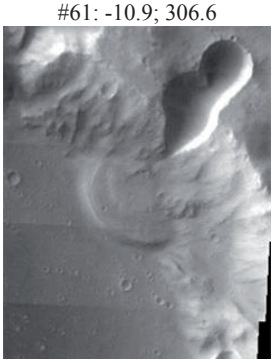 Ophir Planum; 39	#65; 20.0; 11.7 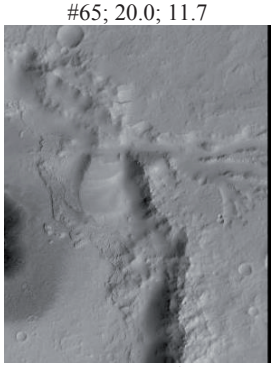 Unnamed

Selected Alluvial Fans:
Number and coordinates given above picture; basin name and diameter below.

#1: -21.1; 320.7 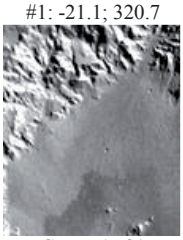 Crater A; 81	#2: -20.3; 324.2 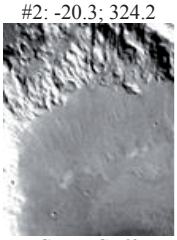 Crater C; 69	#3: -18.1; 322.9 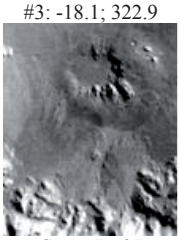 Crater D; 37	#4: -23.3; 27.1 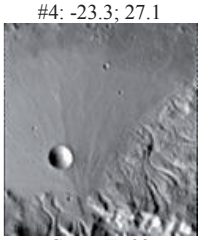 Crater E; 92
#5: -26.4; 324.8 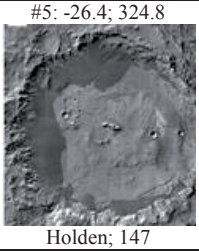 Holden; 147	#7: -21.3; 72.7 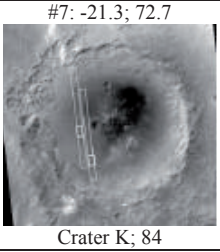 Crater K; 84	#8: -22.7; 74.5 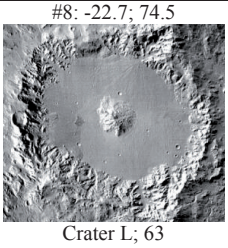 Crater L; 63	#9: -21.5; 67.2 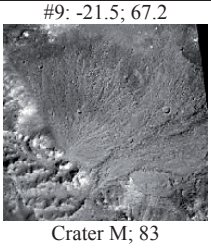 Crater M; 83
#11: -26.2; 331.5 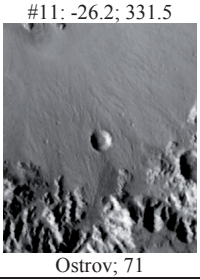 Ostrov; 71	#12: -23.2; 320.5 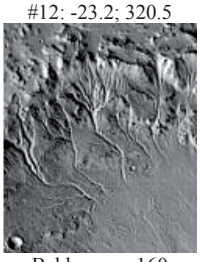 Bakhuysen; 160	#13: -27.0; 27.3 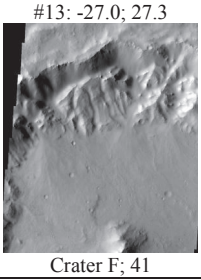 Crater F; 41	#14: -27.6; 83.3 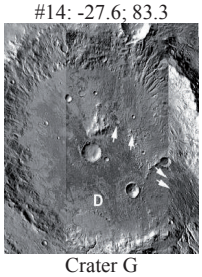 Crater G
#41: -49.6; 113.6 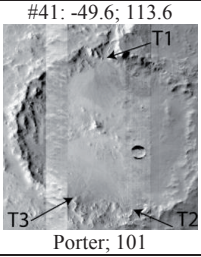 Porter; 101	#42: -7.3; 356.2 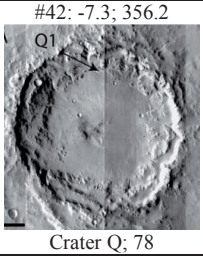 Crater Q; 78	#44: -33.0; 84.3 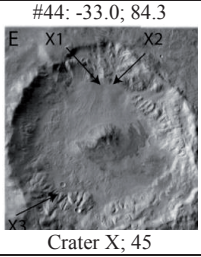 Crater X; 45	#45: -1.4; 58.3 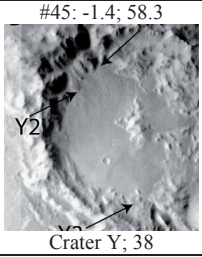 Crater Y; 38
#46: -20.1; 123.2 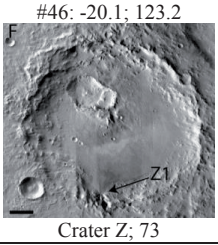 Crater Z; 73	#48: 11.9; 313.2 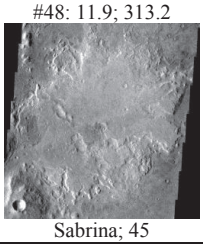 Sabrina; 45	#49: 11.6; 315.1 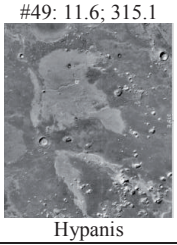 Hypanis	#60: -7.0; 173.0 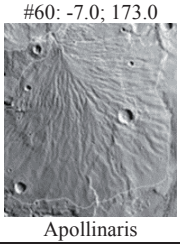 Apollinaris

Selected Prograding Deltas:
Number and coordinates given above picture; basin name and diameter below.

<table>
<tr>
<td>#5: -26.4; 324.8
 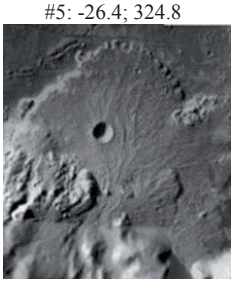
Holden; 147</td>
<td>#17: 30.9; 12.3
 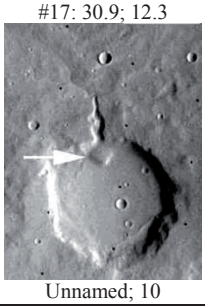
Unnamed; 10</td>
<td>#18: 33.9; 17.5
 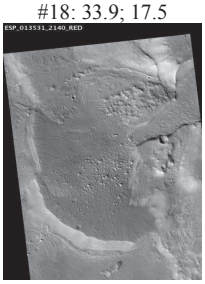
Unnamed; 62</td>
<td>#19: 34.3; 18.1
 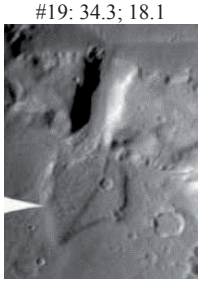
Unnamed; 33</td>
</tr>
<tr>
<td>#21: -6.2; 210.5
 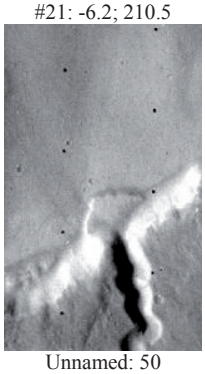
Unnamed: 50</td>
<td>#25: -5.8; 137.3
 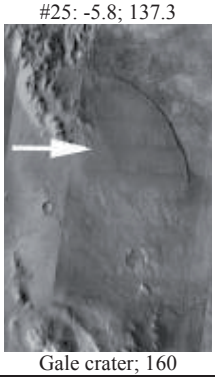
Gale crater; 160</td>
<td>#26: 5.1; 301.4
 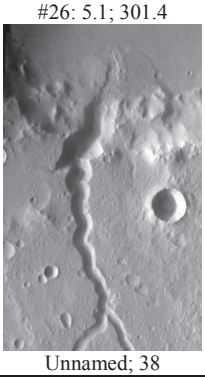
Unnamed; 38</td>
<td>#27: 28.0; 26.7
 
Unnamed; 13</td>
</tr>
<tr>
<td>#28: 28.1; 27.2
 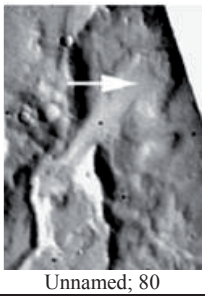
Unnamed; 80</td>
<td>#29: 29.5; 25.7
 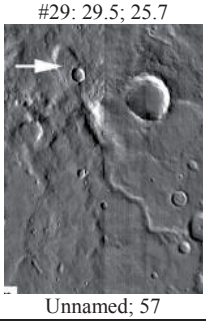
Unnamed; 57</td>
<td>#30: 35.5; 26.3
 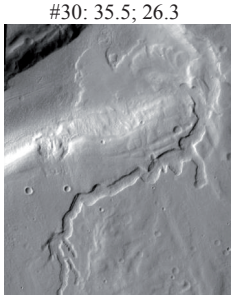
Unnamed</td>
<td>#32: -27.9; 83.1
 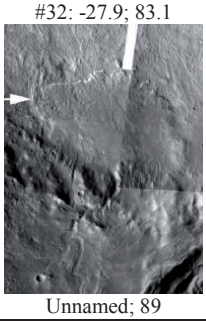
Unnamed; 89</td>
</tr>
<tr>
<td>#33a: -3.65; 132.7
 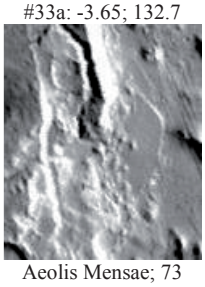
Aeolis Mensae; 73</td>
<td>#33b: -5.15; 132.9
 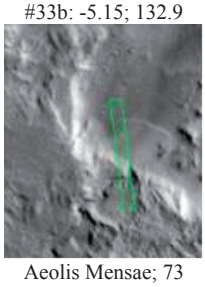
Aeolis Mensae; 73</td>
<td>#34: -6.8; 151.1
 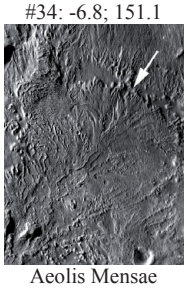
Aeolis Mensae</td>
<td>#35: 18.4; 77.6
 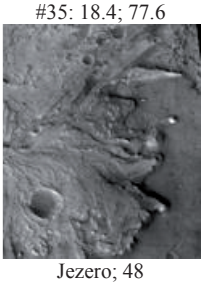
Jezero; 48</td>
</tr>
</table>

More Selected Prograding Deltas:
Number and coordinates given above picture; basin name and diameter below.

#37: 2.1; 121.6 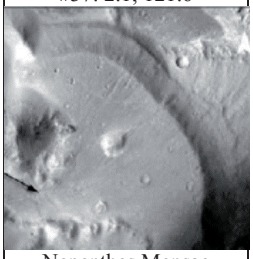 Nepenthes Mensae	#38: -23.5; 347.9 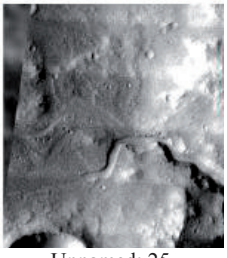 Unnamed; 25	#39: -19.1; 353.6 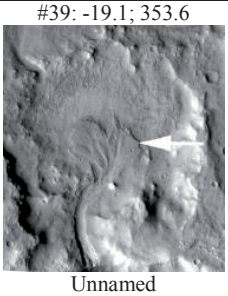 Unnamed	#40: 27.9; 11.6 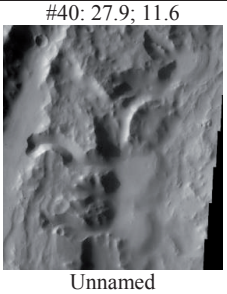 Unnamed
#47: 8.5; 312.0 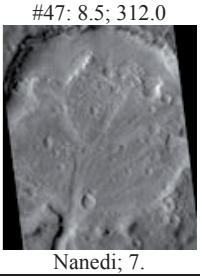 Nanedi; 7.	#58: -13.6; 308.3 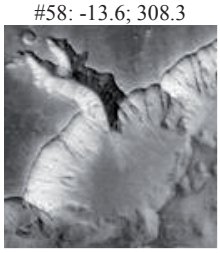 Unnamed	#59: -15.5; 175.6 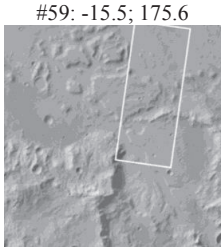 Gusev Crater	#62: 11.4; 308.7 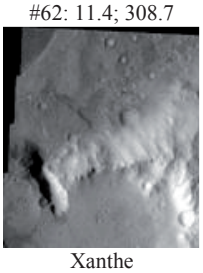 Xanthe
#64: -22.4; 336.3 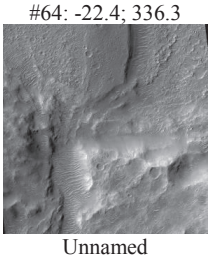 Unnamed	#66: 2.5; 341 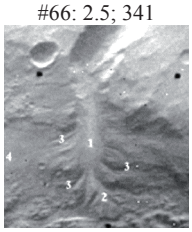 Aram Chaos	#67: 3.1; 316.6 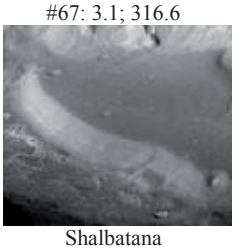 Shalbatana	#81: 35.1; 304.5  Tempe Terra: n.a.
#86: -26.6; 75.8 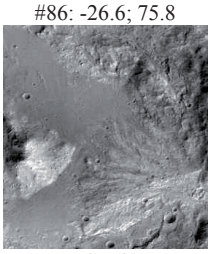 CIF4	#88: 6.3; 38.7 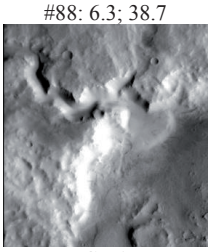 CIF1	#89: 7.9; 333.8 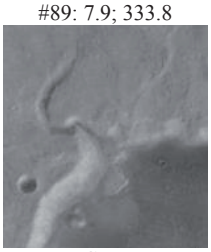 CIF5	#90: 30.2; 345.7 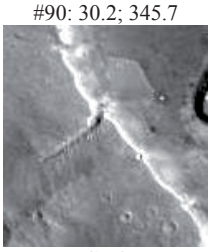 CIF3

“Goodbye, said the fox. And now here is my secret, a very simple secret. It is only with the heart that one can see rightly. What is essential is invisible to the eye.”

10 Acknowledgements

Exactly 17 years ago, my journey into space commenced. We celebrated my 13th birthday in true stellar style with the theme "2013". I remember well how we dressed as astronauts, robots, aliens, and various spaceship residents, believing completely that by the time this "distant future" would arrive, we might actually all be familiar with space travel. Only three years later, I wrote a fictional essay that documented my future autobiography in the year 2013, as an astronaut who had just returned from outer space. That same essay subsequently launched me to the other side of the planet to start my life abroad and finally led me to undertake this PhD degree in Utrecht.

Over the past five years I received highly-valued assistance, strong moral support, and continuous encouragement from a great number of individuals whom I acknowledge here. The journey has been extremely challenging, but the unwavering support around me has led to the completion of this chapter in my life. This dissertation is the fruit of years of patience and prayer of those around me and it belongs as much to them as to myself.

First, I would like to express my sincere thanks and deepest appreciation to my four internal committee members for their endless patience and from whom I learned infinite amounts during my time at Utrecht University. **Maarten**, my daily co-supervisor from the Physical Geography Department, you have the attitude and the substance of a trailblazer. You always conveyed a spirit of adventure in your research and a spirit of excitement in your teaching, both which served to inspire me tremendously. Your vision in securing the grant and your persistence greatly contributed to my completion of this project. **George**, my daily co-supervisor from the Earth Science Department, you inspired me to take pride in my research and to do the best that I can. Your unceasing questioning about each individual step in my project has led me to delve deeper into the theory behind every observation and has resulted in my much deeper understanding of the subject matter and will hopefully continue to lead me to produce better research. **Steven**, my supervisor from the Physical Geography Department, you gave direction when it was most needed, both in my academic and personal life. Your sound and steady advice throughout this process, and specifically your example, has kept me focused on what is truly important during my project as well as in my life and has helped me to remain standing throughout several tough periods. **Poppe**, my supervisor from the Earth Science Department, you embody the figure of a kind and constantly available professor. You provided continuous support during the hardest of times and you poured endless amounts of much-needed and greatly-appreciated red ink into my paragraphs at all times of day and night. Your guidance has made this a rewarding journey and your principles will remain with me for many more years to come. I also sincerely thank my external dissertation committee members, **Alexander Dunsmore**, **Ernst Hauber**, **Hans Middelkoop**, **Gian Ori**, and **Tanja Zegers** for your valuable suggestions and for the time that you spent in evaluating my work.

A few people were a strong inspiration and contributed to this dissertation in a fundamental way. **Ernst Hauber**, thank you for sharing your vast knowledge and experience in planetary science in such a comprehensible manner and for arranging my multiple visits to the DLR in Berlin. **Erin Kraal**, thank you for letting me build on your pilot experiments and for sharing your thoughts with me on more than one occasion. **Gian Ori**, thank you for including me in two extremely interesting field work excursions to the Sahara (Tunisia for the Sahara Oriental in 2009 and Western Sahara and Morocco for the Sahara Occidental in 2012). You helped me remember to always stay firmly grounded with our extra-terrestrial hypotheses. **Jelmer Oosthoek**, thank you for for teaching me volumes about data processing and for the energetic enthusiasm that you poured into Mars science. I will remember our feverish and fanatical discussions about the Mars Trilogy and other interesting books for many years to come – may this passion for science and its benefit to humanity always remain deep in our hearts.

A large component of this project was the laboratory work that was done in the Eurotank (and based upon pilot lab work that was done in the FG stroomgoot), and I can safely say that the success of the experiments can be mainly attributed to the valuable assistance of several key persons, including **Bas van Dam**, **Thony van der Gon-Netscher**, **Marcel van Maarseveen**, **Henk Markies**, **Henk van der Meer**, and **Chris Roosendal**, as well as a group of dedicated students including **Jochem Bijkerk**, **Dimitri van Breemen**, **Joost Mulder**, **Wouter Poos**, **Jan de Vries**, and **Jeffrey Walet**. To the students that I had the pleasure to work with more closely: **Dimitri van Breemen**, **Steffie de Keijzer**, and **Jan de Vries**, thank you for your curiosity and your questions, for your patience and your persistence, and above all for your contribution to science. A couple of colleagues also deserve special thanks for their impact on my work in the Eurotank: **Maurits**, you introduced me to the tank and taught me everything you knew about the fickly robot. You immediately included me as a colleague even when I still felt like I had no idea what I was doing (and I was right at the time!). **Matthieu**, you kept me company during many days in the tank and you always showed genuine interest in my unearthly experiments and made me feel welcome in an environment where I did not quite feel at ease at first. Thank you to you both for helping me make the Eurotank my second home.

This project could never have been started had it not been for the flawless administrative support provided by the department and faculty, and specifically by **Carla, Juul, Marjan**, and **Wendy**. Your ever-smiling faces and your friendly efficiency made many a critical administrative moment turn into a nothing more than a pleasant side-step. The more technical support provided by **Arno, Gerlach, Maarten Z., Rob**, and other IT staff members was as efficient and extremely valuable, especially during the very numerous occurrences of "technical difficulties" but also during conference preparation with regards to poster preparations. A very big thank-you goes out to each one of you for this often overlooked, yet immensely appreciated service.

To the large bunch of colleagues who became friends during my years in Utrecht – thank you for the breaks, the small talk and the numerous cups of tea in the coffee corner. Especially in the FG department, thanks to **Wiebe, Wietse, Willem, Wim, Wout, Wouter**, and also a few folks with names starting with other initials: **Annelies**, **Anouk**, **Arien, Ate, Ayi, Derek, Edwin, Elisabeth, Esther, Filip, Florent, Frans, Frederiek, Geert, Gerben,**

Gilles, Hans D., Hans M., Ingwer, Janrik, Jasper, Kim, Leo, Liesbeth, Loes, Marc, Marcel, Marieke, Maarten K., Maarten V., Maarten Z., Marjolein, Martin, Nelleke, Niko, Noemi, Nynke, Oliver, Paul, Piet, Renske, Roy, Sanneke, Sibren, Steven, Tim, Tjalling, Ton, Top, Yoshi and all others for their interest in my research and my South African stories but also for keeping me in touch with reality and for giving me the opportunity to share some laughs along the way, especially at the hysterical promotie-cabarets. From the other side, in the sedimentology group, thanks to **Daniel, Dario, Joao, Joris, Juan Pedro,** and **Manuela** (in addition to **Matthieu** and **Maurits** from the Eurotank, and **George** and **Poppe** in my committee) for the lunches and the dinners and all the talk of food that went with it. We sure were a bunch with good taste! Also the geological excursions and field work with students were a welcome diversion from daily work and I really appreciate the wealth of wisdom that was shared on these trips – including the multiple open-ended questions. To **Dario** and **Poppe**, specifically, thank you for the adventures that we shared in Chile in 2011 as well as in the Emirates in 2012. Once more, these excursions helped to remind me that the best way to look at geological questions on Mars is to venture out into the field and have a look at what we see in nature on Earth. This particular lesson is infinitely valuable and will influence all research I may do in future.

I am grateful to my expat (and expat-minded) friends in the lowlands: **Bram, Fenneke, Joyce, Juliana, Leslie, Linda, Marco, Margarida, Nikolas, Pieter, Riana, RinaMae, Ron, Rosalie, Sanne, Tanya**, and **Tom**, thank you for helping me tremendously in dealing with the unavoidable culture shock in the Netherlands and for contributing to my healthy balance of work and play. I wish to thank especially my Cambridgelaan neighbours **Ayu, Indah, Miek**, and **Susan** for the innumerable dinners that helped me to remember to eat, and for the feeling of family that we allowed to be created amongst us. To my faithful friends back home or elsewhere: **Alta, Gloria, Karabo, Maria,** and **Marjorie**, thanks for your continuous friendship despite the distance and for the often well-timed messages of encouragement and even a few visits. A special word of thanks to Dr. **Bas Oldenburg**, Dr. **Lou Pistorius**, and the team of care-givers at UMC who ensured that I am in the position to finish this endeavour today.

A special note of thanks to **Giovanna della Porta** from the University of Milan, who arranged for me to be a visitor in the UNIMI Earth Science Department while I complete my dissertation during the last year. The friendly faces of **Alessia, Antonella, Federica, Francesca, Gaia, Irene**, and several others made the transition and relocation to yet another foreign city much more pleasant and enjoyable.

Two very special people that have already been mentioned were particularly supportive during my years in Utrecht, and I am honoured that they are willing to stand by my side as my paranymphs as I face the final hurdle in this race. **Frans**, you were my very first point of reference at Utrecht University, and you remain one of the closest friends I have made during my time here. Your kind personality and strong work ethics uplifted and inspired me. Thanks for sharing your office and life with me. **Margarida**, you have been my best friend during these PhD-years and we have shared so much that trying to write down a few sentences is basically impossible. Thank you for the crazy parties, the unforgettable dinners, the sleep-overs and the morning-afters, the holidays and the sightseeing, and for all the discussions about life, love and everything else.

Many, many thanks go to my large family who have carried me through this journey through prayer and by constantly reminding me of their love. To my Italian family, **Babbo Armando** and **Mamma Mirella**: "Grazie mille per tutto che avete fatto per me e state facendo ancora per me - siete due grande tifosi e vi tengo molto". To my American family, **Larry, Becky, Granny, Page, Lia**, and all the others: thanks for the ways in which you contributed to grant me the opportunity to attain a doctorate degree – "ya'll" are a huge inspiration to me. I know **Larry** would be proud that this moment has arrived and I am delighted to dedicate this dissertation to him, reminding myself and those around me of his philosophy that the true thing that counts in life is not our qualifications nor our background nor our status nor our wealth, but the genuine curiosity into the intricate beauty around us in this universe with a humble attitude towards all living creatures combined with an intense gratitude for all the good things that come our way in life. To my dearest and most cherished family in South Africa, **Pappa** and **Mamma**, **Lorida** and **Obus**, **Marina** and **Waldo**, and all the others who have left deep footprints in my heart: "Baie, baie dankie vir alles wat julle vir my doen en is. Dankie dat julle my geleer het om te droom, dat julle my gewys het om hard te werk, dat julle my toegelaat het om my vlerke so wyd te sprei, dat julle my styf vashou in jul harte al is ek so ver, dat julle so baie vir my kom kuier en gereeld vir my skryf, en dat julle aanhoudend vir my bid. Julle is kosbaar en meer as werd as al die skatte van die hemelruim. Veral **Mamma** se eindelose liefde en ondersteuning was die ruggraat in hierdie groot avontuur – so duisend dankies vir al die groot en klein opofferinge wat hierdie oorwinning moontlik gemaak het."

Last but obviously not least, I genuinely thank **Filippo**, my husband, for your innumerable sacrifices that allowed me to pursue this degree, for the countless moments of disaster-management when I found it hard to keep standing, and for the endless guidance and support you gave me. Thank you for loving me and for letting me be your crazy geoscientist. You are my rock and I love you to infinity and beyond. And finally, I thank my Heavenly Father for showing me once again that all things are possible through Him.

PS: I did not make it to Mars (yet), but if I had gone, this might have been the postcard that I would have sent home.

Curriculum Vitae

Germari de Villiers, daughter of Gerard and Gerda de Villiers, was born on 28 February, 1983, in Pretoria, South Africa, as the first of three daughters. She grew up in Johannesburg, South Africa, and attended Laerskool Unika and Hoërskool Randburg. Since an early age she had a keen interest in all things related to science: an immense love for the skies (mostly when star-studded, but watching the clouds has often been a favourite pass-time also), a healthy interest in the outdoors and everything related to hiking and camping, a vast rock collection with some fossils (and a few more recent mammal bones much to her mother's delight), a slightly less vast but still significant stamp collection, a particular curiosity relating to maps of all sorts, and a profound love for books ranging from science fiction to legal mysteries to historical biographies and also a few chemistry textbooks. She graduated from Reeltown High School, Alabama, in 2001 and matriculated from Greenside High School, Johannesburg, in 2002. Her interest in Mars exploration first led her to enrol for a degree in Aeronautical Engineering at the University of Witwatersrand but her love for rocks and clouds instead led her to graduate with a Bachelor of Science in Geology (with Chemistry and Meteorology as minors) from the University of Pretoria, South Africa, in 2005. She soon realized with dismay that South Africa did not offer enough possibilities in planetary science and thus proceeded to graduate with a Master of Science in Geology (cum laude) from Auburn University, United States of America, in 2007. Germari commenced her PhD studies at Utrecht University in April 2008. Her favourite extra-curricular activity during her stay in Utrecht was her participation in the "Utrecht Klokkenluider Gilde" as a certified bell ringer in the Dom Tower and various other church towers in Utrecht. She is married to Filippo Bianchi and currently resides in Milan, Italy where she has been a guest at the University of Milan since her relocation from Utrecht.

List of Publications

Peer-reviewed publications

de Villiers G., Hauber E., Kleinhans M.G., and Postma G. (in preparation). *Fan-shaped deposits on Mars - morphology, distribution, and implications for climatic evolution.*

de Villiers G., Ventra D., and de Boer P. (soon to be submitted). *Alluvial Fans on Mars – Atacama Desert fans as analogues.*

de Villiers G., Kleinhans M.G., and Postma G. (2013). *Martian delta morphologies and analogue laboratory experiments.* Journal of Geophysical Research: Planets 118, DOI: 10.1002/jgre.20069.

de Villiers G., Kleinhans M.G., van Breemen D.M.O., Postma G., and Hauber E. (2010). *Experiments on sedimentation in wide reservoirs and erosion after dam removal*. Proceedings from RIVERFLOW 2010; p 1147-1154.

de Villiers G., King D.T. Jr, and Marzen L.J. (2010). *A study of candidate marine target impact craters in Arabia Terra, Mars.* Meteoritics and Planetary Science 45(6), DOI: 10.1111/j.1945-5100.2010.01068.x .

Selected conference abstracts

de Villiers G., Ventra D., and de Boer P. (2012). *Fan-shaped Sedimentary Deposits in the Atacama Desert and Elsewhere in the Solar System.* 4th International Conference on Alluvial Fans, Ras-Al-Kaimah, United Arab Emirates.

de Villiers G., Ventra D., and de Boer P. (2012). *Alluvial Fans on Mars – Atacama Desert fans as analogues.* 3rd Conference on Terrestrial Mars Analogues, Marrakech, Morocco.

de Villiers G., Hauber E., Kleinhans M.G., and Postma G. (2011). *Fan-shaped Deposits on Earth, Mars and in the laboratory.* 42nd Lunar and Planetary Science Conference, Houston, TX.

de Villiers G., Kleinhans M.G., and Hauber E. (2010). *Palaeoflow reconstruction from delta morphology on Mars*. AGU Fall Meeting 2010, San Francisco, CA.

de Villiers G., Kleinhans M.G., and Postma G. (2010). *Interpretation of processes in Martian deltas based on experimental work.* 18th International Sedimentological Congress, Mendoza, Argentina.

de Villiers G., Postma G, and Kleinhans M.G. (2010). *Different types of fan-shaped sedimentary deposits on Earth, on Mars, and in the laboratory.* 18th International Sedimentological Congress, Mendoza, Argentina.

de Villiers G., Kleinhans M.G., and Postma G. (2009). *Deltas on Mars – Experiments in the Eurotank.* 27th Meeting of Sedimentology, Alghero, Italy.

de Villiers G., Hauber E., Postma G., and Kleinhans M.G. (2009). *Fan-Shaped Sedimentary Deposits on Earth and Mars*. 27th Meeting of Sedimentology, Alghero, Italy.

de Villiers G., Kleinhans M.G., Postma G., Hauber E., De Jong S., and De Boer P.L. (2009). *Types of Martian Fan-Shaped Sedimentary Deposits*. 40th Lunar and Planetary Science Conference, Houston, TX.

de Villiers G., King D.T., and Marzen L.J. (2007). *Shallow-marine Impact Crater Candidates on Mars.* Geological Society of America Annual Meeting & Exposition, Denver, CO.

de Villiers G., King D.T., and Marzen L.J. (2007). *Shallow-Marine Impact Craters on Mars?* 38th Lunar and Planetary Science Conference, Houston, TX.

de Villiers G. and King D.T. (2006). *Lunar and Planetary Geology: Laboratory Exercise on Geologic Mapping on Mars*. On The Cutting Edge – Discoveries from Mars, Phoenix, AZ.

"What place would you advise me to visit now?" he asked.
"The planet Earth," replied the geographer. "It has a good reputation."